UNIVERSITÀ DEGLI STUDI DI MILANO

DIPARTIMENTO DI CHIMICA

Doctorate School in Chemical Sciences and Technologies

***Curriculum* Industrial Chemistry**

XXVII Cycle

Peptide-Polymer Conjugates as Tools to Selectively Target EGFR

PhD Thesis of
Marco Biagiotti
R09635

Tutor: Prof.ssa Giovanna Speranza

Coordinator: Prof.ssa Dominique Roberto

Academic Year: 2013/2014

INDEX

1. Introduction

"I would like to describe a field, in which little has been done, but in which an enormous amount can be done in principle. This field is not quite the same as the others in that it will not tell us much of fundamental physics (in the sense of, "What are the strange particles?") but it is more like solid-state physics in the sense that it might tell us much of great interest about the strange phenomena that occur in complex situations. Furthermore, a point that is most important is that it would have an enormous number of technical applications.

What I want to talk about is the problem of manipulating and controlling things on a small scale."

This is an extract from the talk entitled "There's Plenty of Room at the Bottom", performed by physicist Richard Feynman at an American Physical Society meeting at the California Institute of Technology (CalTech) on December 29 in 1959, that is now commonly considered the first enunciation of the ideas and concepts behind what are now called nanoscience and nanotechnology, that is the possibility for scientists to manipulate and control individual atoms and molecules. The term nanotechnology was coined over ten years later by Norio Taniguchi, while it was studying ultraprecisions machines (Taniguchi, **1974**), but it was only with the development of the scanning tunneling microscope that could "see" individual atoms (1981) that modern nanotechnology really began.

A good definition of nanotechnology was given by Bawa: Nanotechnology can be considered "the design, characterization, production, and application of structures, devices, and systems by controlled manipulation of size and shape at the nanometer scale (atomic, molecular, and macromolecular scale) that produces structures, devices, and systems with at least one novel/superior characteristic or property" (Bawa, **2005**).

1.1. Polymeric nanoparticulate systems

Recently, a lot of important results have been achieved applying nanotechnology concepts in the field of electronics, photonics, supramolecular assemblies, material science and drug delivery. Notably, nanomedicine (ie the medical application of nanotechnologies) drove to the development of nanosized structures able to load drugs and to deliver them to their site of action; among these so called nanocarriers, liposomes, micelles and above all nanoparticles are the most important (Nicolas, **2013**; Farokhzad, **2009**; Brambilla, **2011**; Brigger, **2002**; Sanhai, **2009**; Riehemann K., **2009**). Now a lot of studies are dedicated to

the engineering of nanoparticulate systems with the aim to create effective tools to use as diagnostic or in the treatment of pathologies such as infectious and neurodegenerative diseases and cancer.

Nanoparticulate systems are colloidal-sized particles, with diameters ranging from 1 to 1000 nm; they can be composed of many different materials including inorganic materials, lipids (Al-Jamal, **2011**; Muller, **2004**) and polymers that confer to the system different physicochemical properties making them suitable for different applications. Among the others, polymer based colloidal systems are particularly interesting thanks to the almost infinite number of polymers, that differ in terms of nature and properties, that are at disposal. Moreover, it is possible to load them with drugs and to functionalize them with specific ligands, intended to be recognize by surface receptors overexpressed by abnormal cells, thus opening the way to active targeting application (Elsabahy, **2012**; Kamaly, **2012**; Lee, **2012**).

To design a successful targeted nanocarrier, it is necessary to consider the nature of the polymer and the ligand but also to choose a proper coupling reaction, taking into account organic chemistry, macromolecular synthesis, physical-chemistry and pharmaceutical science; so far a great number of ligation strategies have been proposed, each of them having its own benefits and drawbacks.

1.1.1. Morphology

Polymeric nanocarriers can be divided in three main classes with regard to their morphology: polymersomes, polymeric micelles and nanoparticles. Each of these systems is highly tunable in terms of drug loading, release mechanism, surface charge, size etc.

1.1.1.1. Polymersomes

Polymersomes can be considered “reservoir” systems: they are formed of a core space delimitated and isolated by a membrane that is composed, in that case, by amphiphilic block copolymers. They can be considered biomimetic analogues of phospholipids and have been prepared with sizes ranging from tens of nanometers to tens of micrometers having a relatively good control on the size distribution (LoPresti, **2009**). In a typical polymersome the formation of the membrane is due to the hydrophobic blocks of each

copolymer that tend to associate in order to minimize the direct exposure to water, consequently hydrophilic blocks face the inner and outer aqueous environment. The result is a typical bilayer membrane (Discher, **1999**) delimitated by two interfaces that represents the key feature of this nanocarriers. Such membrane confers the system some interesting properties; for example, it can, depending on its permeability to hydrophobic or hydrophilic molecules, partition aqueous volumes with different compositions and concentrations. Moreover, this kind of structure allows the incapsulation of both hydrophobic molecules within the membrane either hydrophilic ones in the inner aqueous cave.

1.1.1.2. Polymeric micelles

Even polymeric micelles are formed by self-assembly of amphiphilic block copolymers in aqueous solution and can be considered reservoir-like systems (Peer, **2007**). In this case the morphology can be indicated as core-shell: hydrophobic drugs can be stored in the core, whereas the hydrophilic shell stabilizes the system; the average diameters of such structures usually are between 5-100 nm (Oerlemans, **2010**). A typical feature of micelles based systems is the existence of a critical micelle concentration (CMC), value that represents the threshold below which the micelles disassembles in unimers (Torchilin, **2007**); polymeric micelles usually exhibit low CMC values and so resulted to be relatively insensitive to diluition with positive effects on properties such as circulation time (Adams, **2003**). Till now, micelles appear to be the most advanced polymeric based nanoparticulate system for clinical trials and gave good results in delivering hydrophobic drugs and DNA (Orlemans, **2010**).

1.1.1.3. Nanoparticles

Polymeric nanoparticles (NPs) are solid colloidal systems in which the drug is physically dispersed, dissolved or chemically bounded to the polymer chains (Hillaireau, **2006**). They can have the form of nanosphere or nanocapsule, depending on the method used for their preparation. The first can be described as matrix-like systems and the drug are usually dispersed within them; on the other hand, nanocapsules are more similar to already described polymersomes and micelles: they are vesicular systems formed by a single polymeric membrane that defines a core formed by an aqueous or lipophilic liquid in which the drug is dissolved (Letchford, **2007**). Polymeric NPs offer two great advantage:

first of all using them it is possible to load hydrophobic drugs at concentrations greater than their intrinsic solubility (Liu, **2004**). Moreover, these structures are highly tunable in terms of composition, surface properties and derivatization, circulation time and drug release rate (Elsabahy, **2012**).

1.1.2 Preparation (Pinto Reis, **2006**)

Many methods exist to prepare polymeric nanostructures; they can be divided into two big groups depending whether the formulation involves a polymerization reaction or requires a preformed polymer or macromolecule (Couvreur, **1995**).

1.1.2.1. Nanostructures obtained by polymerization of monomers

All methods based on the template polymerization of monomers can be used to prepare nanoparticles but are not useful for micelles and polymersomes. Among such methods the most important are by far emulsion polymerization and interfacial polymerization.

1.1.2.1.1. Emulsion polymerization

This method is one of the fastest at disposal, is readily scalable (Kreuter, **1990**), and it is suitable only for the preparation of nanoparticles. It can be applied to organic or aqueous continuous phases. In the first case the monomer is dispersed into an emulsion (or an inverse microemulsion) in which it is not soluble (nonsolvent) along with surfactants or protective polymers useful to prevent aggregation in the first stages of polymerization (Kreuter, **1991**). The method has been widely used in the past but now has lost importance because it is difficult to remove the residues of the toxic organic solvents, surfactants, monomers and initiators used during the preparation from the formed nanoparticles. When an aqueous continuous phase is used, surfactants and emulsifiers are usually not necessar and phase separation and formation of solid particles can take place before or after termination of the polymerization reaction (Kreuter, **1982**). With these two methods structures based on polymers such as poly(methylmethacrylate) (PMMA) and poly(alkylcyanoacrylate)s (PACAs) that have been loaded with drugs or tracers such as fluorescein (El-Samaligy, **1986**), pilocarpine (Harmia-Pulkkinen, **1989**), timolol (ibidem) etc has been prepared.

1.1.2.1.2. Interfacial polymerization

In this method the monomer and the drug are dissolved into an organic solvent and slowly added, for example extruding it through a needle, in a well-stirred aqueous solution containing surfactants and initiators. The polymerization occurs forming a membrane at the interface of the formed oil/water or water/oil emulsion (Couvreur, **2002**). The method allows a very efficient drug encapsulation and the main disadvantage is represented by the presence of organic solvents that must be carefully removed. With this method various PACAs have been prepared and used to encapsulate insulin (Watnasirichaikul, **2000**), calcitonin (Lowe, **1994**), darodipine (Hubert, **1991**) etc.

1.1.2.2. Nanostructures obtained by preformed polymers

With a few exceptions most of the techniques described above lead to slowly biodegradable or nonbiodegradable polymers that must be carefully purified from solvents and residual molecules (monomers, oligomers, surfactants etc.). Methods based on preformed polymers permits to overcome these limitations and, as a consequence, are now usually preferred; moreover they permit the preparations not only of nanoparticles but also of polymersomes and polymeric micelles.

1.1.2.2.1. Emulsification/solvent evaporation

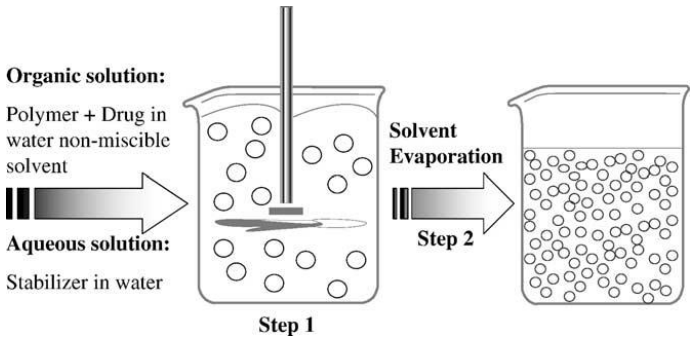

Figure 1: Schematic representation of the emulsification-evaporation technique (Pinto Reis, 2006).

This method requires three steps: first of all, the polymer must be dissolved along with the drug in a suitable non-water miscible solvent. With the aid of a dispersing agent, it is subsequently emulsified into a stirred aqueous phase in form of nanodroplets, that constitute the templates for the self-assembly process. Then, organic solvent is evaporated

causing the precipitation of polymeric nanostructures. Size of products can be controlled varying the stir rate, the type and the amount of dispersing agent, the viscosity of organic and aqueous phase and temperature (Tice, **1985**). The use of oil/water emulsion is preferred over water/oil ones because using water as non solvent eliminates the need for recycling, facilitate washing steps and minimize agglomeration (Aftabrouchard, **1992**). The method, however, can be applied only to liposoluble drugs and is difficult to scale up. This approach has been applied to many polymers, for example poly(lactic acid) (PLA) (Gurny, **1981**), poly(lactic-*co*-glycolic acid) (PLGA) (Ueda, **1997**), ethylcellulose (EC) (Bodmeier, **1990**), poly(ε-caprolactone) (PCL) (Gref, **1994**) etc. Among drugs that have been encapsulated, we can cite testosterone (Gurny, **1981**), texanus toxoid (Tobío, **1998**), cyclosporine A (Jaiswal, **2004**) etc.

1.1.2.2.2. Solvent displacement and interfacial deposition

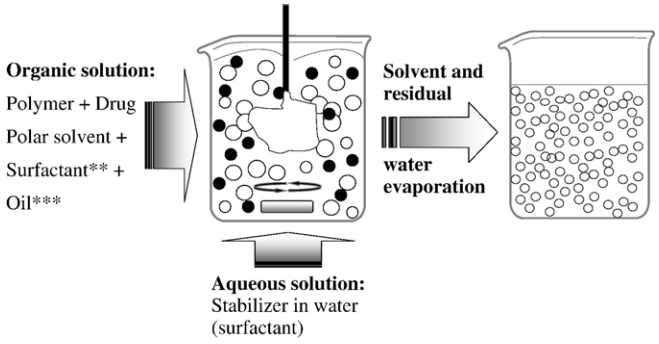

Figure 2: Schematic representation of the solvent displacement technique. **Surfactant is optional. ***In interfacial deposition method, a fifth compound was introduced only on preparation of nanocapsules (Pinto Reis, 2006).

These are two similar methods based on the spontaneous emulsification of a water-miscible organic phase (containing the polymer and the drug) in an aqueous phase (sometimes containing a surfactant). When applied to the preparation of nanoparticles, solvent displacement can be used to form both nanospheres and nanocapsules, interfacial deposition, on the other hand, leads only to the latter. In solvent displacement method the solution containing the polymer is injected into the water solution: if the diffusion of the organic solvent is fast enough, a spontaneous emulsification takes place and the colloidal polymer particles immediately form at the interface, encapsulating the drug (Quintanar-Guerrero, **1998**). This technique was applied to various polymers, such as PLA (Némati, **1996**) and PLGA (Barichello, **1999**), and revealed particularly efficient in encapsulating cyclosporine A (Allémann, **1998**).

Interfacial deposition is based on the same principle but introduce a compound of oil nature, miscible with the solvent of the polymer but immiscible with its mixture with water. In this case the polymer deposit at the interface between the finely dispersed oil droplets and the aqueous phase, forming nanocapsules (Couvreur; **1995**).

1.1.2.2.3. Emulsification/solvent diffusion

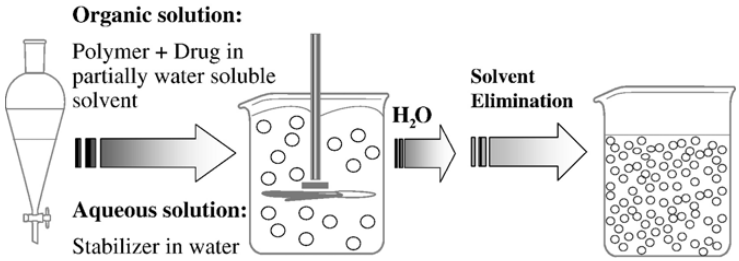

Figure 3: Schematic illustration of the ESD technique (Pinto Reis, 2006).

The polymer is dissolved in a partially water soluble solvent (e.g. propylene carbonate) that is then saturated with water to promote diffusion. Subsequently, the polymer-water saturated solvent is emulsified in an aqueous solution containing stabilizer and diffuse to the external phase thus leading to the formation of the nanostructures. Finally the solvent is eliminated and the products recovered. This technique has very high efficiency in encapsulating lipophilic drugs and it is also very advantageous for many other reasons (no need for homogenization, high batch to batch reproducibility, ease of scale up and narrow size distribution among others); the main disadvantage is the high volumes of water required and the scarce encapsulation efficiency for water-soluble drugs that tend to leak into the saturated-aqueous external phase during emulsification (Quintanar-Guerrero, **1998**). With this method doxorubicin-loaded nanoparticles (Yoo, **1999**), plasmid DNA-loaded PLA nanoparticles (Perez, **2001**) and many other structures were produced.

1.1.2.2.4. Nanoprecipitation technique

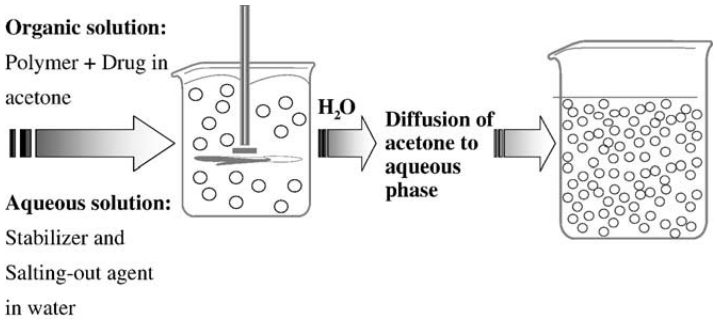

Figure 4: Schematic of the nanoprecipitation technique (Pinto Reis, 2006).

This method, sometimes indicated as salting-out, directly derives from the previous one and is based on the separation of a water-miscible solvent from an aqueous solution *via* a salting-out effect. Polymer and drug are dissolved in a suitable organic solvent (usually acetone or DMSO) that is then slowly added to an aqueous solution containing the salting-out agent(e.g. electrolytes such as magnesium or calcium chloride or non-electroliytes such as sucrose) and a colloidal stabilizer. If the polymer is not water soluble, the diffusion of the organic solvent into aqueous phase lead to the formation of drug loaded nanostructures that can be recovered and purified from solvents and other contaminating agents by means of centrifugation or cross-flow filtration (Quintanar-Guerrero; **1998**). Method doesn't require the use of harmful solvents and is very mild and so it is extremely useful to encapsulate sensitive drugs.

1.2. Design of targeted drug delivery systems

The concept of "magic bullet", i.e. a drug that selectively destroys diseased cells without harming healthy ones, was suggested for the first time by Paul Ehrlich, Nobel Prize for Medicine in 1908 (Shi, **2011**) and since then has been the center of intense reaserch, especially in the field of the treatment of cancer.

The first real advancement in this direction was obtained with the discovery of the enhanced permeability and retention (EPR) effect (Dreher, **2006**; Maeda, **2000**; Iyer, **2006**; Greish, **2007**), that allows passive tumor targeting by means of suitably designed nanostructures and opened the way to many new design strategies. Among them PEGylation, which bestows on nanostructures a prolonged circulation time, can be

considered by far the most successful, so that in 1995 FDA approved the use of DOXIL, PEGylated liposomes loaded with doxorubicin, that has been the first therapeutic nanomedicine to reach the market (Gabizon, **1994**).

However, EPR effect cannot be used to target all types of cancer (for example is not suitable for low vascular permeability ones) and, moreover, it was discovered that repeated injections of PEGylated nanostructures induce the production of anti-PEG IgM which dramatically reduce the circulation time of such constructs (Accelerated Blood Clearance Effect). Consequently the researchers focus started to shift toward active targeting and therefore to the development of targeted drug delivery systems able to selectively recognize specific cells or tissues (Elsabathy, **2012**; Peer, **2007**; Shi, **2011**; Gullotti, **2008**).

Active targeting can be achieved inducing recognition of the carrier by signature molecules, overexpressed at the disease site, either *via* ligand-receptor, antigen-antibody or aptamer mediated interactions. To this aim it is necessary to position at the periphery of the polymeric nanoconstruct a suitable biologically active ligand.

Ligands can be linked to the scaffold before or after the self-assembly of the desired nanostructure. The choice of the synthetic strategy is influenced by many variables; first of all must be considered the size of the ligand that has to be linked: for small ligands (e.g. small organic molecules or peptides) both options are suitable, on the other hand bulky ligands can be attached, with few exception (Zeng, **2006**), only at the surface of preformed nanocarriers both for self-assembly either hydrophilic/lipophilic balance reasons (Gindy, **2008**).

Conjugating the ligand before the nanocarrier formation offers some inherent advantages, such as the possibility to control the coupling reaction yield and to characterize the resulting conjugates by routine methods. Moreover, by mixing ligand-conjugated and bare polymer during the nanostructure preparation, it is possible to tune the density of the ligand on the surface of the carrier thus controlling the binding efficiency for the target (Jule, **2003**). The main drawback of this method is that conjugation with the ligand can change the physicochemical properties (mainly the hydrophilic/lipophilic balance and the charge) of the polymer, resulting in the need to adapt the self-assembly conditions to these new situation.

On the other hand, the conjugation of the ligand after the nanocarrier formation may complicate the purification and chemical characterization of the final construct. Indeed, many of the purification procedure applicable, such as centrifugation, dialysis or filtration, can degrade/modify the nanocarriers. Besides, since NMR is not suitable, advanced surface characterization methods (e.g. XPS, TOF-SIMS) must be applied to prove the formation of the desired covalent linkages (Patil, **2009**).

1.2.1. Epidermial Growth Factor Receptor (EGFR)

The epidermial growth factor receptor family comprises four receptors (EGFR/ErbB-1, HER2/ErbB-2, HER3/ErbB-3 and HER4/ErbB-4) which represent the starting point of a complex signal transduction cascade that has great influence on important cellular processes such as cell proliferation, adhesion, migration and differentiation; an abnormal activities of these receptors produce responses that have been demonstrated to play a key role in the development and growth of many tumor cells.

EGFR family ligands are mainly peptides and can be divided in three groups on the basis of their receptor specificity. The first includes epidermial growth factor (EGF), tranformig growth factor (TGF)-α, amphiregulin (AR) and epigen (EPG) that bind specifically to EGFR. The second group members have a dual specificity for both EGFR and ErbB-4, among them betacellulin (BTC), heparin-binding EGF (HB-EGF) and epiregulin (EPR) can be found. Finally the third group includes the neuregulins (NGRs) that can be divided on the basis of their ability to bind EErbB-3 and ErbB-4 (eg. NRG-1 and NRG-2) or only ErbB-4 (eg. NRG-3 and NRG-4). These ligands are expressed as integral membrane proteins and are cleaved by metalloproteinases (typically members of a disintegrin and metalloproteinase family of membraneous proteases) to release soluble mature ligand and this represents a crucial point in regulation of EGFR signaling (Daub, **1996**; Mill, **2009**).

The EGFR signaling module has been highly conserved during evolution. All receptors of EGFR family have an extracellular ligand-binding domain, a hydrophobic transmembrane domain and an intracellular tyrosine-rich domain with tyrosine kinase activity (Ullrich,**1990**). When a ligand binds to the extracellular domain, EGFR is stabilized in an extended conformation inducing the formation of receptor homo or heterodimers (Klein, **2004**): one of the two members has a regulatory role and stabilize the tyrosine kinase domain on the other monomer; catalytic monomer can now phosphorylate exposed

tyrosine residues on the regulatory monomer: it must be noticed that different ligands cause the phosphorylation of distinct groups of usally 10 residues following still unclear mechanisms (Schulze, **2005**). These modified tyrosines represent docking sites for a number of cytosolic proteins containing Src homology 2(SH2) domains (McCune, **1989**) or phospho-tyrosine binding (PTB) motifs. The subsequent dissociation of these complexes releases activated effectors and adaptor proteins into the cytoplasm where they induce many different signal transduction cascades (eg. Mitogenic- activated protein kinase pathway, phosphoinositol kinase, apoptotica kinase, transcriptional regulators etc.) (Lemmon, **2010**; Bianco, **2006**). The EGFR signal is switched off by endocitosys of the original receptor-ligand complex followed by degradation or recycle to the cell surface; also this mechanism is usually modulated by the ligand (Wells, **1999**). For example, phosphorylation of EGFR Tyr974 triggers EGFR endocytosis while phosphorylation of EGFR Tyr1045 triggers Cbl-dependent EGFR ubiquitination and proteosomal degradation (Wilson, **2009**; Sorkin, **1996**). All the cycle is summarized in Figure 5.

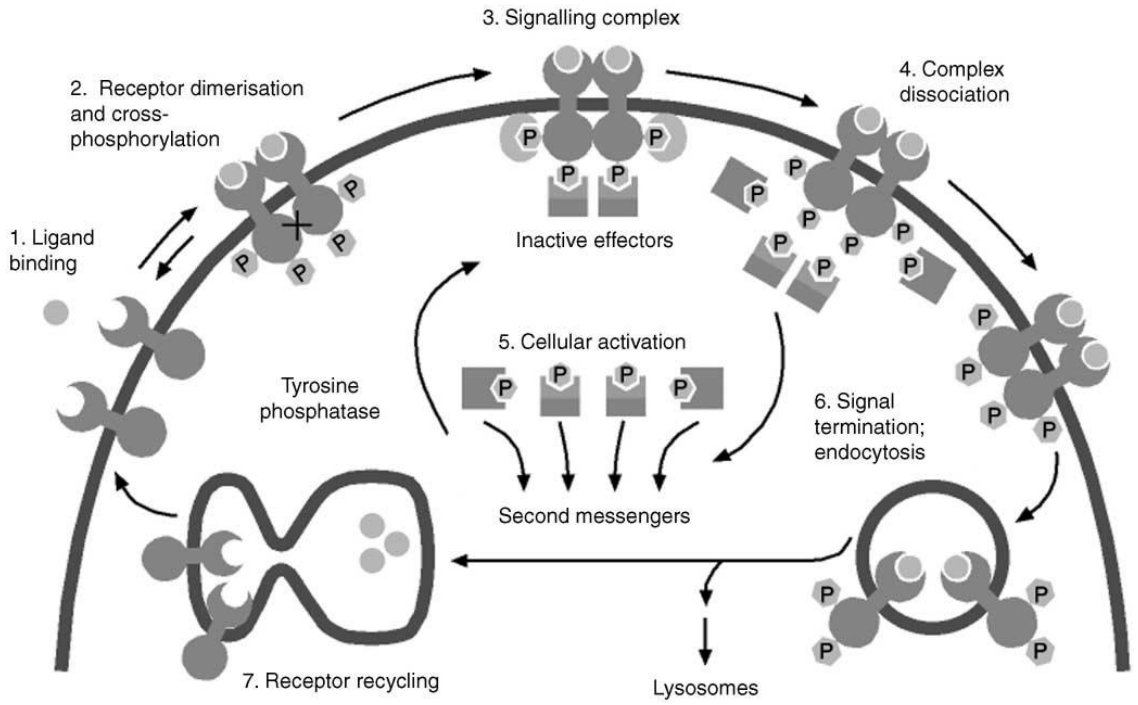

Figure 5: the epidermial growth factor signal trasduction model (Yarden, 1991)

Different couples of receptors activate different responses (Figure 6). Among all, EGFR-HER2 complexes produce by far the most potent signals and induce a more prolonged activation of the signaling network. There are many reasons for this: first of all, EGFR activated heterodimeric complexes containg HER2 are more stable at cell surface

(Lenferink, **1998**) and last for more time before undergoing internalization; moreover HER2 is able to stabilize EGFR in a conformation required for dimerization and tyrosine phosphorylation even in the absence of ligand, resulting in ligand-independent EGFR signaling and increased ligand affinity for EGFR (Riese,**1998**; Earp, **1995;** Wada, **1990**). Finally after internalization, while EGFR homodimers are degraded, HER2-EGFR heterodimers are recycled and returned to the cell surface ready for another cycle of activation.

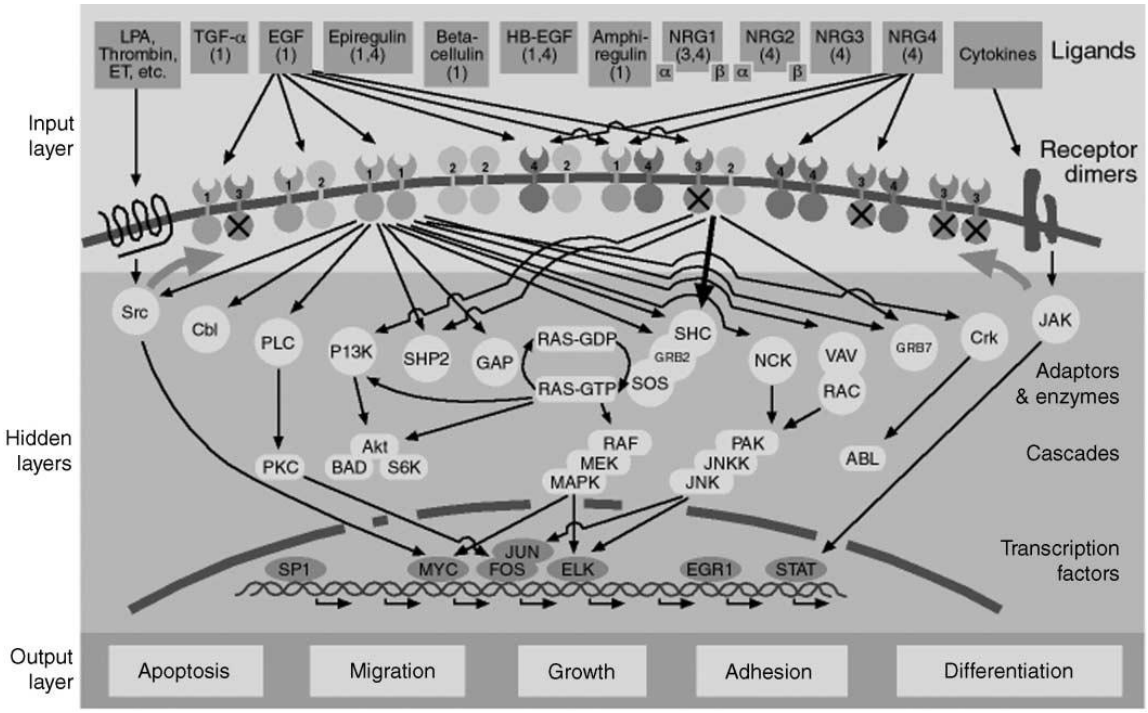

Figure 6: EGFR signalling network (Yarden, 2001b)

The endocytic receptor downregulation mechanism is considered to play a key role in determinate EGFR output. EGFR dimerization and activation of intrinsic kinase following ligand bond to the extracellular domain, lead to signaling and relocation of invaginating clathrin-coated pits (CCPs) on the plasma membrane and to the subsequent formation of clathrin-coated endocytic vesicles that can be released from the membrane and fused with endosomes. From here the receptor is processed either back to the cell surface by recycling or to the multivesicular bodies for eventual delivery of EGFR to late endosomes and lysosomes for degradation, resulting in temporary EGFR downregulation. Also clathrin independent pathways are possible as alternative mechanism for EGFR internalization (Orth, **2006**; Sigismund, **2005**; Yamazaki, **2002**). It must be noticed that, even in the absence of ligands, each EGFR receptor is internalized constitutively after an half-life of

30 min on the cell surface and usually recycled many times before degradation (in tumor cell lines EGFR has a metabolic half-life of about 20 h) (Sundvall, **2008**; Suo, **2002**). This continuous EGFR trafficking is a key point to understand how antibody drugs that bind to the receptor can be internalized and released into the cell.

Since EGFR activation leads to cellular growth and this can provide substantial advantage to tumor cells, it was the first receptor which was directly associated to human cancer (deLarco, **1978**) and an abnormal regulation of the receptor has been observed in a wide variety of carcinomas including breast, renal, ovarian, head and neck, colon, bladder, non-small-cell lung carcinoma, etc. (Yarden, **2001**). EGFR related pathways malfunctioning can be due to a receptor overexpression (normal cells express from $4*10^4$ to $1*10^5$ receptors while tumor cells can show more than $2*10^6$ receptors), to autocrine signaling or to mutations (Herbst, **2002**; Franovic, **2007**; Sizeland, **1992**; Citri, **2006**).

Some oncogenic viruses use EGFR signaling network to express their virulence, altering both receptor tyrosine kinase activity and gene expression (Figure 7). For example, hepatitis B and Epstein-Barr viruses activate EGFR expression during invasion, avian erythoblastosys virus encodes a modified version of EGFR that is constitutively active and human papilloma virus E5 block the degradation of activated receptors; all of these events result in an abnormal stimulation of proliferative pathways (Miller, **1999**). Poxviruses encode soluble forms of growth factors that bind to EGFR, although with lower affinity that corresponding mammalian homologues and induce substained EGFR phosphorylation and signaling (Tzahar,**1998**).

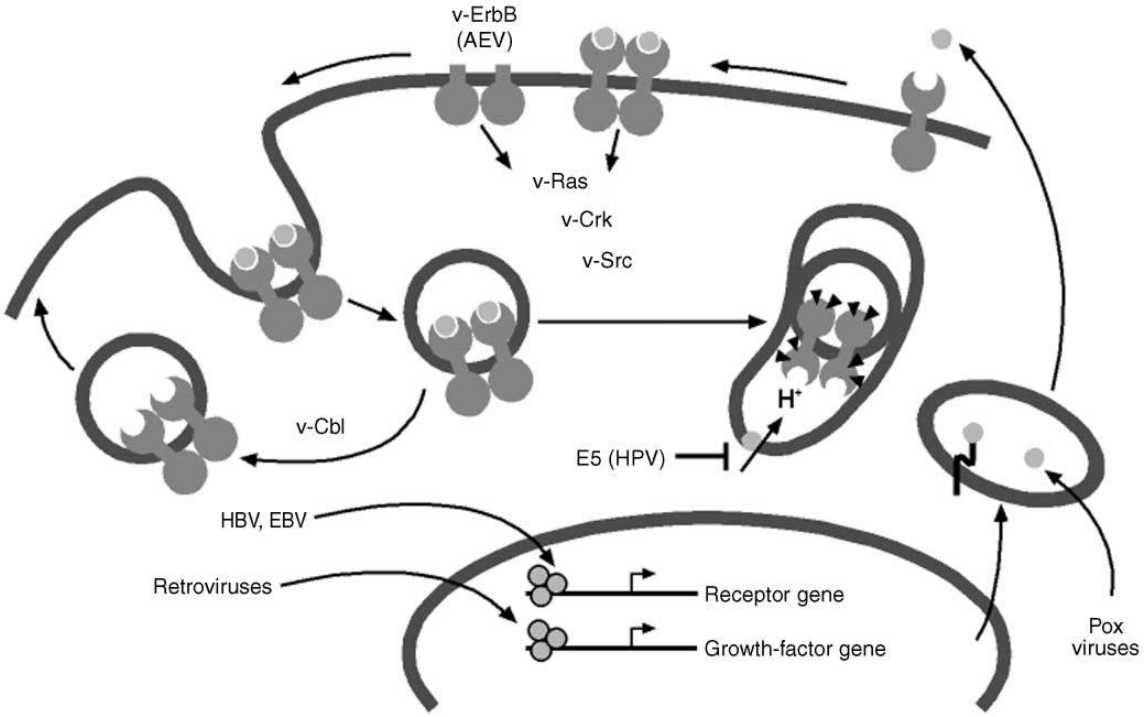

Figure 7: Action of oncogenic viruses over EGFR receptor; EBV = Epstein-Barr virus; HPV = human papilloma virus; HBV = Hepatitis B virus (Yarden, 2001b)

1.2.1.1. EGFR targeting

In the last 20 years a lot of therapeutic agents for treatment of EGFR overexpressing cells have been developed and some of them have obtained interesting results against several human malignancies. These agents can be roughly divided in the subsequent classes:

- **Monoclonal antibodies** (Garrett, **2002**; Ogiso, **2002**): mAbs for cancer therapy have been developed for the first time to target EGFR overexpressing cells. Anti-EGFR mAbs bind with high selectivity to the extracellular domain of EGFR and compete with endogenous ligands to block the ligand induced EGFR tyrosine kinase activation. Presently, two anti-EGFR mAbs, Cetuximab and Panitumumab are widely used in the treatment of metastatic colorectal and head and neck cancer.
- **Tyrosine kinase Inhibitors (TKIs)** (Azemar, **2000**)**:** As already said, EGFR tyrosine kinases activity is fundamental in the regulation of growth factor signaling; these enzymes are activated by the autophosphorylation of cytoplasmic domains of EGFR induced by dimerization of the receptor. TKIs are small molecules able to compete reversibly with adenosine 5' triphosphate to bind to the intracellular catalytic domain of EGFR tyrosine kinase and inhibit the EGFR

autophosphorylation and, consequently downstream signalling. Different TKIs are available for clinical use, among them must be cited Gefitinib (Iressa), Erlotinib (OSI-1774; Tarceva), Lapatinib (GW-572016), and Canertinib (CI-1033).

- **Antisense oligodeoxynucleotides (AS ODNs)** (Ciardiello, **2001**)**:** this kind of agent (among which must be cited GEM 231) decreases the expression of EGFR and regulates the cell proliferation. However, this therapeutics lack of effective delivery systems and it is very difficult to obtain the desired bio-activity from them; all these difficulties have hindered AS ODNs clinical development so far**.**

Apart from this anti-EGFR strategies, in last years have been developed various strategies based on the use of molecules able to bind EGFR to target EGFR overexpressing cells. The first try was made using antibody-drug conjugates which were made with clinically useful anti-cancer drugs, such as doxorubicin, methotrexate, cisplatin and vinca alkaloids but was largely unsuccessful (Goldmacher, **2002**; Hu, **1996**). In recent years the attention shifted towards nanotechnology based applications of EGFR ligands: a suitable nanocarrier designed for drug delivery, photodynamic therapy or gene therapy can be lead to abnoramal cells by molecules such as antibodies, affibodies and peptides able to bind to EGFR with good affinity. Moreover, the nature itself of the receptor permits the internalization of the carrier and so favor the therapeutic action of the delivered molecules.

Among all possible targeting agents for such kinds of applications, peptides, till now widely undertaken, are gaining increasing popularity mainly because they can be relatively easily synthesized by using recombinant or chemical synthesis techniques, moreover they can be simply grafted to the scaffold. Most natural ligands of EGFR are peptides and so a lot of such molecules show a very high affinity for the receptor.

The most important of this ligand is by far epidermal growth factor (EGF). EGF is a 53-aa polypeptide, with a molecular weight of 6045 Da, that derive by proteolysis, catalyzed by one or more still not identified metalloproteinases, of a transmembrane precursor (named prepro-EGF) composed of 1207 aa in humans or 1217 aa in rodents (Carpenter G., **1979**; Carpenter, **1987**). It was isolated for the first time by Stanley Cohen from mice submaxillary glands and immediately its abilities to stimulate precocious tooth eruption and eyelid opening in newborn mice was demonstrated (Cohen S., **1962**). Other peptidic growth factors, similar to EGF but encoded by distinct genes, exist; among them must be cited TGFα, the poxvirus growth factors, and amphiregulin (Carpenter, **1990)**. All these

EGF-like molecules have high affinity binding to EGFR, produce mitogenic responses in EGF-sensitive cells, and have a primary structure composed of approximately 50-60 residues, containing 6 half-cystines in the general sequence $X_nCX_7X_{2\text{-}3}GXCX_{10\text{-}13}CXCX_3YXGXRCX_4LX_n$. It is interesting to observe that this motif of half-cystine residues is also found in a lot of cell surface and extracellular proteins that are not agonists for the EGF receptor but have roles in processes such as development, cell adhesion and protein-protein interactions; moreover site-directed mutagenesis experiments have been used to demonstrated that all half-cystine residues are necessary for biological activity of EGF and related growth factors (Carpenter, **1990**).

As obvious full EGF and related polypeptides have a strong mitogenic and neoangiogenic activity and so can't be used as they are to target nanocarriers toward EGFR; in addition all attempts made to find out biologically active peptides corresponding to various portions of the EGF molecule had no significant successes. To identify a peptidic substitute for EGF, Gu and coworkers (Li, **2005**) has performed a phage display libraries screening and isolated a novel peptide clone, that named GE11, with high binding capacity to EGFR but low mitogenic activity.

1.2.1.2. GE11 peptide

Gu (**2005**) individuated GE11, whose sequence is YHWYGYTPQNVI, screening Ph.D.-12 Phage Display Peptide Library. He discovered that the number of GE11 displaying phages bound to EGFR was 1000-fold higher than to Bovine Serum Albumin (BSA, used as negative control) and that the binding could be inhibited by both EGF and synthetic GE11 (Figure 8).

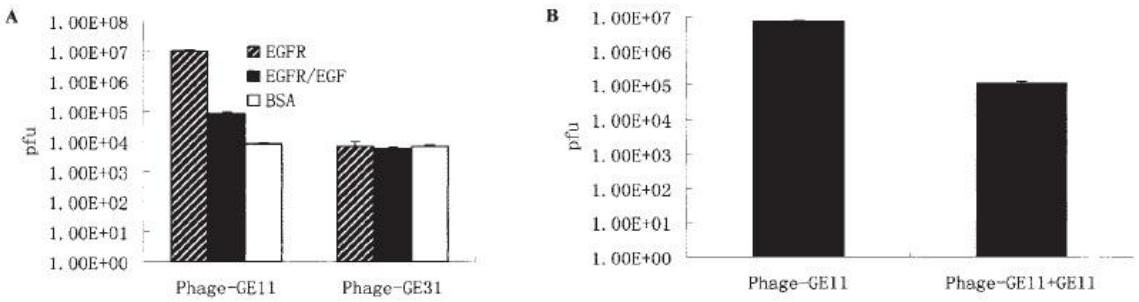

Figure 8: Binding specificity of phage-GE11 to EGFR. *A)* Phage binding to EGFR. *B)* Competitive binding of Phage-GE11 in the absence or presence of GE11 peptides (Li, 2005).

To confirm the binding specificity of GE11, Gu prepared a ^{125}I labeled version of the peptide and used it to treat EGFR and EGFR overexpressing cells. This experiments (Figure 9) demonstrated that the presence of unlabeled GE11 or free EGF efficiently inhibit the binding; reciprocally ^{125}I-EGF binding was also blocked by GE11. So it was possible to conclude that GE11 can specifically bind to EGFR and that its binding site on the receptor and that of EGF are probably partly overlapped. Using the same data Gu could calculate for GE11 a binding affinity at least 10-fold less than that of EGF; this lower affinity can be easily comprehended considering that EGF bound both the domain I and the domain III of EGFR (Ogiso, **2002**) while GE11, that contains only 12 residues, might bind only one region of the receptor.

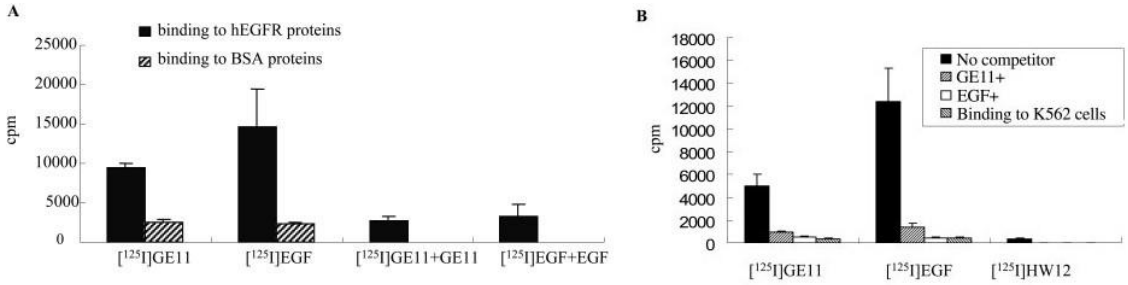

Figure 9: Binding specificity and affinity of GE11 to EGFR. *A)* [125I]GE11 or [125I]EGF bound hEGFR proteins or BSA proteins. In a competition assay; *B)* [125I]GE11, [125I]EGF or [125I]HW12, an irrelevant peptide, bound SMMC-7721 or K562 cells in the absence or presence of 0.5 mM unlabeled peptide (Li, 2005).

Li studied also *in vivo* biodistribution of ^{125}I-labeled GE11 in mice implanted with xenograft EGFR overexpressing tumors (Figure 10). Half an hour after the injections of the petide *via* tail vein, the radioactivity in the tumor was lower than those in kidney, liver or blood and represented the ~5.85 % of the given dose; after 4 hours, however, it was the highest among the tissue examinated, corresponding to 3.18% of the injected peptide. When unlabeled GE11 was coinjected with labeled one, the radioactivity in tumor dropped by 5-fold at 0.5 h and 4.5-fold at 4 h, thus confirming GE11 affinity toward EGFR overexpressing cells also *in vivo*.

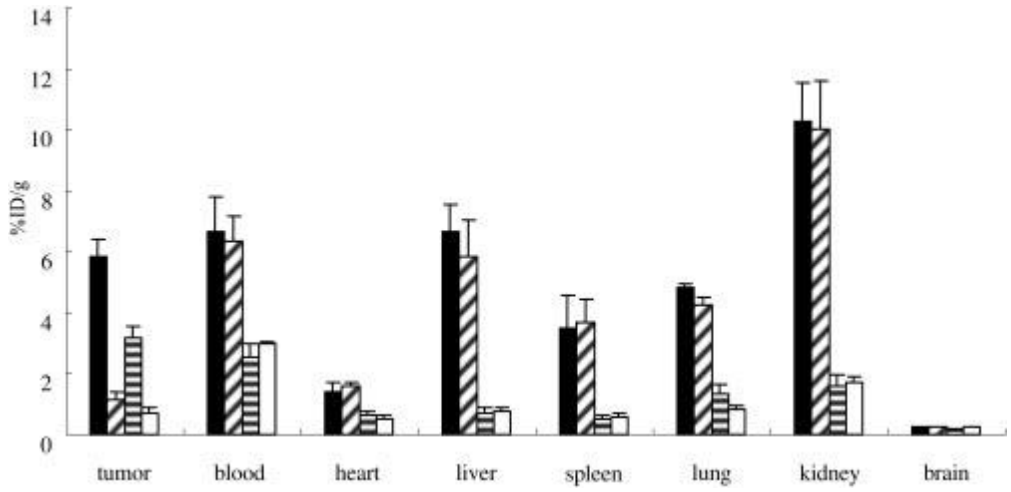

Figure 10: In vivo biodistribution assay (Li, 2005)

Using FITC-labeled GE11, Gu demonstrated also that the peptide can be taken up efficiently only by EGFR overexpressing cell (Figure 11).

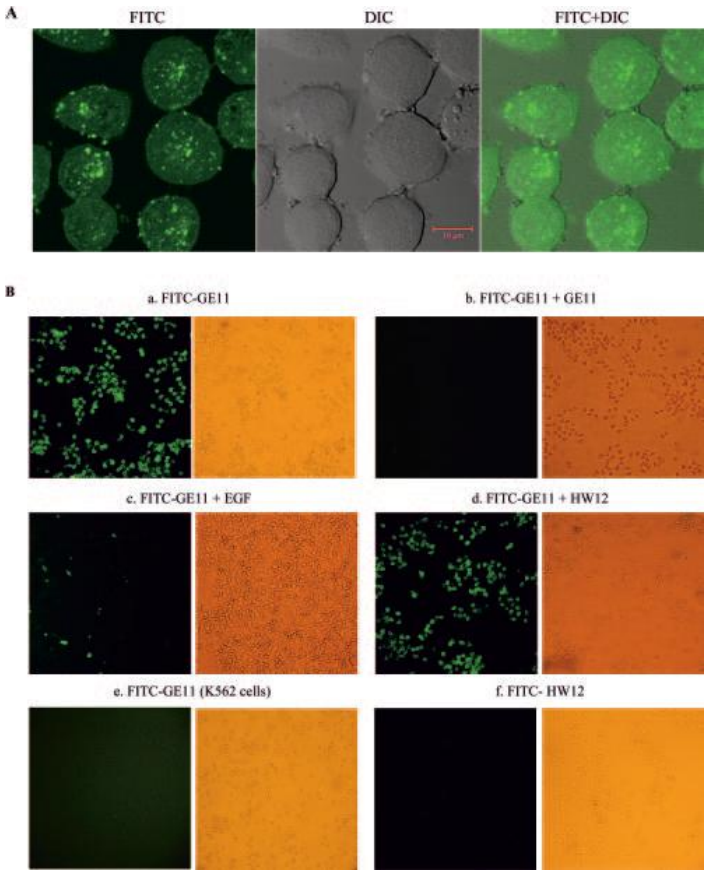

Figure 11: Internalization of peptide GE11. *A)* Internalization of FITC-labeled GE11 viewed with FITC visualization and differential interference contrast (DIC) *B)* The block of binding of FITC-labeled GE11 viewed under fluorescence microscope (Li, 2005).

To evaluate GE11 ability to inhibit or stimulate cell proliferation, standard MTT assay was used (Fiigure 12). At the concentration of 1 μg/mL, GE11 stimulates the growth of EGFR overexpressing cells by ~10% while EGF induced a ~50% increase of cell growth. Moreover, no significant increase of stimulation by GE11 was found with concentrations up to 10 μg/mL.

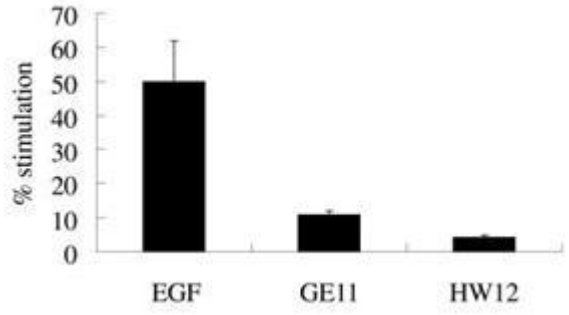

Figure 12: Activity of the GE11 peptide of SMMC-7721 cells studied in a MTT assay (Gu, 2005).

1.2.2 The Material: poly(γ-glutamic acid) (γ-PGA)

Naturally occurring polymers have recently attracted considerable interest in many scientific areas (bioremediation, agriculture, food, pharmaceuticals, etc) due to the growing demand of industrial processes based on safe procedures and biodegradable raw materials (Rehm 2010). In medicine and pharmaceutics, interest in polymers arises as a result of the search for increasingly innovative and higher performing materials to assist in the achievement of more efficient, selective and safer therapies. Polymers play an important role in drug delivery since they can tailor the performances of drugs according to the therapy needs, by controlling drug release in a predictable manner, minimizing drug degradation, contributing to mitigation of drug toxicity and improving drug bioavailability. However, polymers should be biocompatible, non-toxic, non-immunogenic, biodegradable, stable upon sterilization/sanitization for a convenient use in medicine.

Recent advances in the knowledge of bacterial polymer biosynthesis and the use of new molecular genetic strategies has opened the way to the production of tailor-made biopolymers suitable for industrial and medical applications.

Poly(γ-glutamic acid) (γ-PGA, Figure 13) is a biopolymer of bacterial origin. belonging to the class of bacterial polyamides, with molecular weights of up to millions of daltons

produced by several members of the genus *Bacillus* (Rehm, **2010**). It is composed of D- and/or L-glutamic acid monomers, connected by amide bonds between α-amino and γ-carboxyl groups (Shih, **2009**). This unusual anionic, water-soluble homopolyamide was first identified by Ivánovic as a component of *Bacillus anthracis* capsule, a major virulence factor which disguises *B. anthracis* from immune surveillance and allows its unimpeded growth in the host (Shih, **2001**, **2009**). Some years later it was found that the same biopolymer was freely secreted into the growth medium of *Bacillus subtilis* as a product of fermentation (Bovarnich, **1942**) and up to the present, a number of species from all three domains (Archaea, bacteria and eukaryotes) have been shown to produce γ-PGA (Shih, **2009**; Sung, **2005)**.

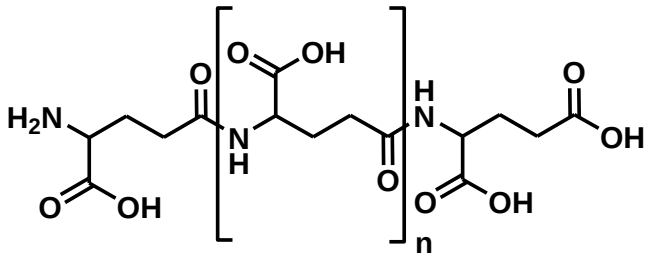

Figure 13: γ-PGA structure

The reason why γ-PGA is produced *in vivo* is not well known. Its presumptive biological functions depend on the species synthesizing it and are believed to consist in contributing to microbial adaptation to adverse conditions e.g. by increasing resistance to starvation, pollution and drought or by creating a physical barrier against phagocytosis in pathogens such as *B. anthracis* and *Staphylococcus epidermidis*, in which the polymer is anchored to the cell surface (Bajaj, **2011**).

As regards the stereochemistry of the monomeric units, three stereochemically different types of γ-PGA are known: a homopolymer composed only of D-glutamic acid, a homopolymer composed of L-glutamic, and a stereocopolymer containing both D-and L-glutamic acid units in variable amounts depending on the microorganism and fermentation condition. Although it has been suggested that D- and L-isomeric units are not lined up at random but distributed in a blocky microstructure with an average numbers of D- and L-repeating units for-each stereoblock between 7 and 11, the stereochemical structure of the bacterial copolymer needs to be further investigated (Martinez de Ilarduya, **2002**; Wang, **2008**)

Organism	Configuration
Bacillus anthracis	D
B. mesentericus (probably B. subtilis)	D
B. licheniformis	D and L
B. megaterium	D and L
B. pumilus	D and L
B. subtilis	D and L
Planococcus halophilus	D
Sporosarcina halophila	D
Staphylococcus epidermidis	D and L
Natrialba aegyptiaca	L
Hydra	nd*
Fusobacterium nucleatum	nd*

Table 1: Organisms reported to produce γ-PGA; * nd: not determined"

The chemical synthesis of γ-PGA is very arduous and costly and therefore unfeasible for the production of large amounts of the product (Muñoz-Guerra, **2013**). γ-PGA cannot be obtained by direct polycondensation of glutamic acid because intramolecular cyclization predominantly proceeds to form a stable five-membered lactam, pyroglutamic acid (Scheme 1). Ring-opening polymerization of an amino acid anhydrides (NCAs) is the most popular and economic process for the preparation of long polypeptides (e.g. α-PGA). Unfortunatly, the ring-opening polymerization of the corresponding seven membered ring carboxyanhydride, as opposed to α-PGA synthesis, is not practicable because the compound easily releases CO_2 to give again pyroglutamate without forming γ-PGA (Mori, **2007**). Samples of γ-PGA of varying stereochemical composition (either stereopure, or with different degrees of D/L tacticities) were obtained by polycondensation of glutamic acid dimers, suitable protected at the carboxylic acid termini as methyl esters in rather poor yield (Sanda, **2001**).

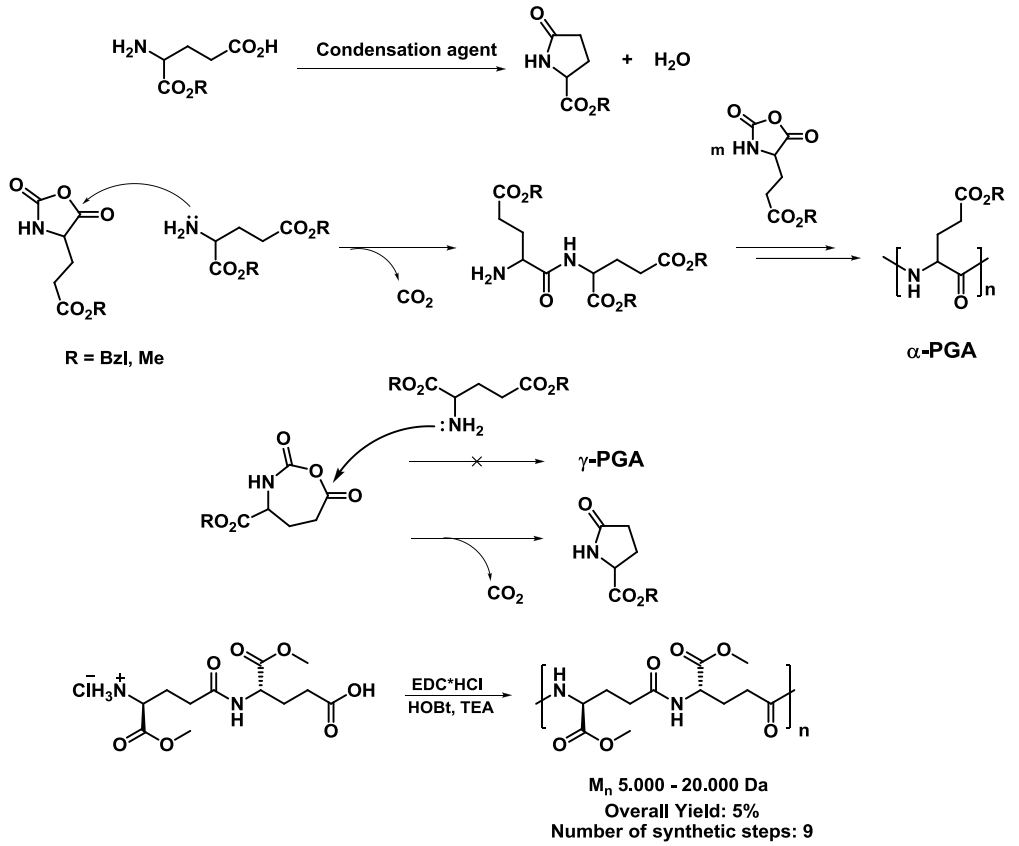

Scheme 1: Chemical synthesis of γ-PGA

At present, bacterial fermentation of organic substrates is the only practicable route for γ-PGA production at the industrial level. Generally, γ-PGA is produced by a number of microbial species, most prominently various *Bacilli*, recently including laboratory strains of *Bacillus subtilis*. For each specific producer strain, the culture conditions used, in particular nutritional requirements, can have a great impact on the production yield, average molecular weight as well as stereochemical composition of the γ-PGA produced and enormous efforts have been devoted to identify those which are useful to obtain the maximum productivity (Shih, **2009**; Poo, **2010**). As the knowledge of the genetics and physiology of *Bacillus subtilis* is highly advanced, it is now possible to intervene also at the genetic and metabolic level to optimize the biochemical processes responsible for γ-PGA production increasing the polymer yield and controlling its size and monomer composition. Generally γ-PGA is produced in *Bacillus Sub.* in a ribosome-independent manner through the membrane-associated PGA synthase complex (PgsBCA) which has been described in great detail. However, it could not been isolated in an active state because it is strongly hydrophobic and highly instable (Candela, **2006**; Buescher; **2007**; Ashiuchi, **2010**).

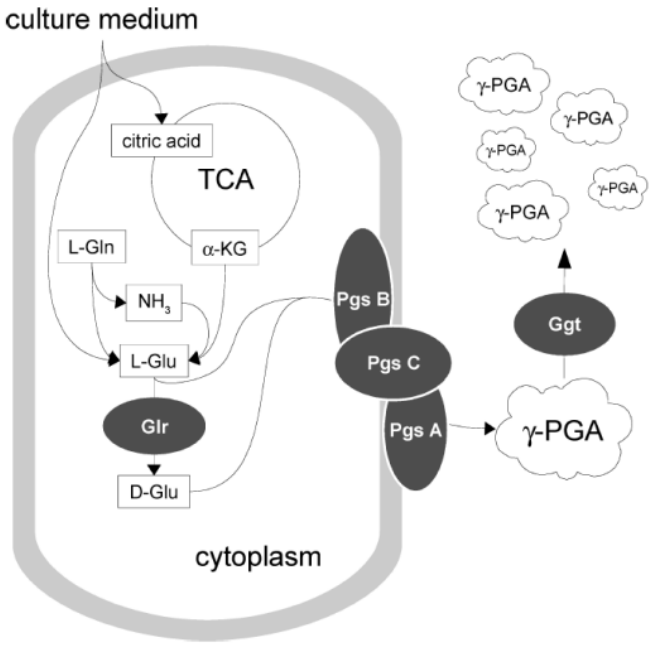

Figure 14: A proposed pathway for the synthesis of γ–PGA in *Bacilli* (Buescher, 2007).

Depending on pH, γ-PGA can be either in the acid or anionic form (usually as sodium carboxylate). It is hygroscopic and water soluble, leading to highly viscous solutions even at low concentrations, and in the salt form is able to generate gels containing water in more than 3000 times its weight. γ–PGA is fairly resistant to hydrolysis at the amide bond although it is readily degraded in basic medium at high temperature. It is also biodegraded by a good number of bacteria but appears to be insensitive to common proteases such as pepsin or trypsin. Perhaps the most outstanding feature of γ-PGA is its being completely innocuous and edible and as such non-toxic towards human and environment. The traditional food known as *natto* in Japan or *dan-douchi* in China, consisting of fermented soybeans contains between 0.1 and 1% of γ-PGA, and has formed part of the daily diet of Asian people for hundreds of years (Sung, **2005**; Bajaj, **2011**).

The whole of these characteristics, in particular its biodegradability and its intrinsic absence of toxicity, as well as the availability of GRAS (Generally Regarded As Safe) producer bacterial strains have raised a tremendous interest in γ-PGA as a novel material for many industrial and biotechnological applications. γ-PGA has been proposed as flocculant absorber of heavy metals in waste water treatments, cryoprotectant, humectant, moisturizer in cosmetic products, thickener, curable biological adhesive, drug carrier in

medicine, and as food and feed additive (Oppermann-Sanio, **2002**; Buescher, **2007**; Bajaj, **2011**) .

Even more interesting perspectives arise from the possibility of chemical modification of the material to modulate its chemical-physical properties and create new materials suitable for technological as well as biomedical purpose (Buescher, **2007**; Oppermann-Sanio, **2002**; Kubota, **1993**; Morillo, **2001**; Pérez-Camero, **2001**).

In spite of its great potential and high biocompatibility, γ-PGA appears to be still unexploited and underdeveloped. This might be basically ascribed to several reasons including the still high costs of gamma-PGA production since it easily achieved by chemical synthesis (Buescher, **2007**; Poo, **2010**) and the extreme variability in molecular weight and stereochemical composition of the naturally produced biopolymer, that can obviously affect its physical and chemical properties result in batch-to-batch variations in targeted applications (Shih, **2001**; Shih, **2009**). But the main cause is certainly the difficult handling of the natural biopolymer due to its high viscosity, its scarcesolubility in organic solvents and the low reactivity on the α-carboxylic side groups that are highly hindered by the presence of the polypeptide main chain.

The above considerations prompted us to investigate the possibility of both enhancing the reactivity of γ-PGA and facilitating its manipulation.

2. Aim of the thesis

As described in introduction, EGFR targeted polymer based nanostructures are promising tools for selective treatment of EGFR overexpressing cells. A lot of works have been reported in literature on the topic and a lot of strategies have been explored, while only few of them demonstrated to have the potential for a real clinical application. Among others, particularly important has been the identification of a peptide, named GE11, able to selectively bind to EGFR with high efficiency but with no evident mitogenic or toxic activity (Li, **2005**): this molecule seems to be the ideal EGFR targeting agent and so research shifted towards the design of suitable scaffolds to exploit it.

Our attention has been attracted by polymeric nanostructures, in particular those made of biodegradable polymers, i.e. polymeric materials that can be degraded *in vivo* and can be further eliminated by normal metabolic pathways. A lot of such polymers, both of synthetic and natural origin, are commercially available, each with its own qualities and drawbacks. Among them we chose to focus on γ-PGA; this interesting but little known biomaterial, spontaneously produced by many microorganisms, has a lot of properties that seem to suit very well to nanomedical application; γ-PGA is biodegraded by a good number of bacteria but appears to be insensitive to common proteases (Oppermann-Sanio, **2002**), it is non-immunogenic, completely innocuous and even edible. Moreover it bears, in the α- position of each monomer, a carboxylic group, which is available for chemical derivatization allowing the modification of its molecular properties and, more importantly the attachment of GE11.

γ-PGA has also some intrinsic drawbacks: first of all it is very expensive. It can't be chemically synthesized in an efficient manner and its bioproduction is nowadays far to be efficient; this is due to many reasons but for sure one very important problem is that the biosynthetic pathway by which it is formed *in vivo* has not been clarified yet.

Moreover, γ-PGA in aqueous media tends to degrade and it is not very thermally stable. Derivatization can partially solve these problems but unfortunately γ-PGA is quite unreactive in standard conditions, partially because of its own structure (derivatizable carboxyles are narrow to the polymeric backbone and so highly hindered) but mainly because of its very poor solubility in organic solvents. Consequently a lot of work had to be done in order to tame this material before starting to use it efficiently for nanotechnological purposes.

With this background, my PhD work had two main goals: on one hand we started the study of EGFR-targeted nanostructures using a more “docile”, even if less original, material; our purpose in this field was to find out good experimental conditions for the preparation of both GE11 peptide and polymer-peptide conjugates, and eventually to make some preliminary studies on the preparation and characterization of corresponding nanostructures.

On the other hand we worked a lot on studying γ-PGA reactivity in processes, such as amidation and esterification, useful for the preparation of peptide decorated scaffolds for targeted drug delivery.

Moreover, also the problem of γ-PGA conformation and degradation was tackled. The results obtained on these topics will be exposed in the two appendices of this thesis.

3. Results and Discussion

3.1. Peptide synthesis

Peptide synthesis has been a challenge for organic chemists since the discovery of the biological role of these molecules. In fact the isolation, structure and synthesis (Vigenaud, **1954**) of the lactogenic nonapeptide amide hormone oxytocin by du Vigneaud in the early 1950's initiated a new era in both biology and chemistry and made strong the request of natural peptides and their analogues.

The classical methods of solution peptide synthesis demonstrated to be inadequate to meet this explosives increase in demand: even in skilful hands, yields in peptide bonds formation were often only modest, giving low overall yields and contamination with side products that resulted difficult to remove using the techniques at disposal at time. This was the background for the search in the 1950's for workable accelerated procedures of which solid phase synthesis has proved to be by far the most successful.

Solid phase peptide synthesis (SPPS) was born thanks to the work of R.B. Merrifield that in 1963 proposed the solid phase (Merrifield, **1963**) as a really revolutionary tool in peptide synthesis. The principle of all solid phase synthesis is quite simple: the target oligomeric chain is prepared attached to a solid particle, easy to separate from all soluble reagents and from solvents, and is detached from it only at the end of the synthesis for the purification and characterization of the final product. This origin a number of immediate advantages:

1. Separation processes are quick and simple and can be machine aided.
2. Much of the product losses deriving from the operations of the classical solution synthesis (solvent extraction, filtration end crystallization) can be avoided.
3. Large excess of reagents can be used thanks to the easiness of separation procedures.
4. The process can be automated.

However the technique has also some inbuilt disadvantages, that limit its diffusion and cased hostility among many peptide chemists:

1. Very high reaction efficiencies are needed.

2. All by product deriving from incomplete reactions can be separated only at the end of the synthesis.
3. The use of large excess of reagents imply higher costs and so limit the applicability on large scale.

In the original Merrifield protocol, the solid support used was a styrene-divinylbenzene co-polymer, funtionalized by chloromethylation. The resulting benzyl chloride derivative is known as Merrifield resin and can be used to anchor the first amino acid *via* an ester linkage. The peptide bond is then formed using a carbodiimide as coupling reagent to link a *N*-Boc protected amino acid to the free amine of the first residue. Boc can now be removed leaving a free amine that can be used to attach the third member of the sequence. This cycle of coupling and deprotection can be reiterated until the completion of the sequence. The peptide could finally be cleaved from then resin, with concurrent deprotection of side-chain protecting groups (mainly benzyl), using liquid hydrogen fluoride.

In 1970, a totally innovative protecting-group strategy was introduced (Carpino, **1970**): 9-fluorenylmethyloxycarbonyl (Fmoc) group, that is removed in presence of secondary amines (e.g. piperidine) but is stable in presence of tertiary amines and in acidic condition, substituted Boc as protective group for the α-amino moiety, thereby allowing the orthogonal protection of the side chains using acid labile groups. In brief Fmoc strategy allowed a general mildening of the reaction conditions and enhanced the importance of orthogonality in SPPS, with a consequent development of new reagents and resins that allowed more selective cleavages and the introduction of functional diversities (Aerthon, **1989;** Kimmerlin, **2005**).

Nowadays a lot of different resins are available for SPPS, each with specific characteristics suitable for different applications. In this work for the synthesis of GE11 and related peptides two different resins were used, hereafter are reported the main feature of this two supports:

1. Wang Resin

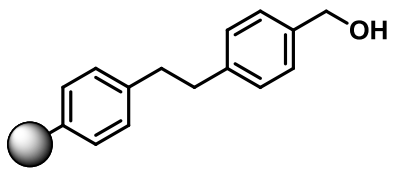

Linker: p-benzyloxybenzyl alcohol

Polymeric matrix: Copoly(styrene-1%DVB)

Mesh: 100-200

Characteristics: cleaved only in strong acidic condition (95% TFA) and consequently orthogonal also with very acid labile side chain protective groups (e.g. Mtt); the *C*-terminal is released as free carboxylic acid.

2. 2-Chlorotrytilchloride resin

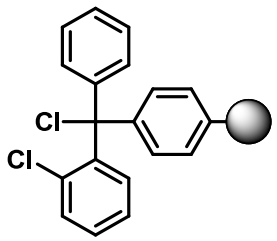

Polymeric matrix: Copoly(styrene-1%DVB)

Mesh: 200-400

Characteristics: cleaved in very mild acidic condition (1% TFA in DCM) and consequently orthogonal with the most commonly used acid labile protective groups (e.g. *t*-butyl esters); the *C*-terminal is released as free carboxylic acid.

A protective group is used temporarily to block some reactive sites in a multifunctional molecule and to carry out selectively reaction at only one of them. A protective group must fulfill certain requirements (Greene, **1999**):

1. It must react selectively and in high yield to give a protected substrate.
2. It must be selectively removed in quantitative yield by reagents that do not harm the regenerated functional group.

3. The protective group should form a derivative that can be readily separated by side product formed during its removal.
4. It should have a minimum of functionality to avoid side reactions.

During this PhD work AAs protected with the subsequent groups were used:

Protective Group	Used for	Cleavage conditions
 *t*-Bu	Thr, Tyr side chains	Strong acidic condition: TFA 50% minimum
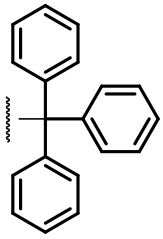 Trt	Asn, His, Gln side chains	Strong acidic condition: TFA 50% minimum
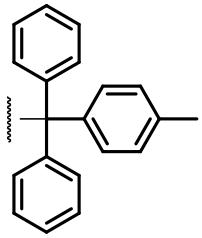 Mtt	Lys side chain	Very mild acidic condition: 1% TFA in dichloromethane
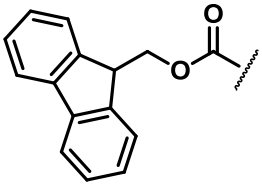 Fmoc	All amino acids α-amines	20% Pyp in DMF
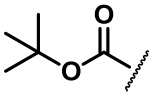 Boc	Trp side chain	Strong acidic condition: TFA 50% minimum

As coupling agents were used the subsequent molecules:

Coupling Agent	Characteristics
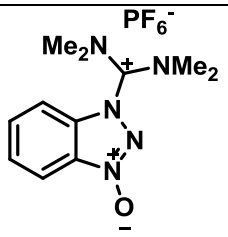 HBTU	Coupling agent with reactivity similar to symmetrical anhydrides and Bop based reagents
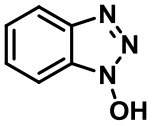 HOBt	Used for *in situ* activation of carboxylic functions avoiding racemization. It is always used in combination with other agents (HBTU) to improve reaction rate
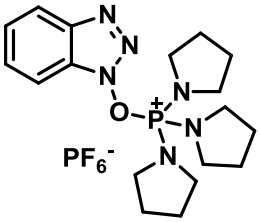 PyBop	Coupling agents stronger than HBTU, often used in a combination with HOBt

First of all we synthesized a short peptide with sequence FQPV (Figure 15) to use as a model compound to tune the coupling reaction with scaffold. FQPV was synthesized using 2-Chlorotrytilchloride resin as solid support; the first AA was loaded on resin using DIPEA in anhydrous DCM. All the synthesis were performed using a semiautomated microwave peptide synthesizer (Biotage SP Wave Initiator+); each Fmoc deprotection was carried out at RT treating two times the resin with an adequate amount of a 20% pyperidine in DMF solution for 5 and 15 minutes respectively, and then washing the resin with DMF. Each AA was dissolved in DMF along with a 3 fold excess coupling agents (HOBt and HBTU) and a 6 fold excess of DIPEA as base 15 minutes before each coupling reaction that was carried out under MW irradiation (50 °C) for 20 minutes; after each coupling a DMF washing step was performed. After last coupling, resin was washed with DCM and the peptide was finally cleaved from resin support using a mixture of TFA and scavenging agents (85% TFA, 5% PhOH, 5% water and 2% TIPS). The raw product was purified by semipreparative HPLC, using 0.1% TFA in water as base eluent and performing a gradient

of a 80:20 acetonitrile/0.1% TFA in water solution. The final product was analyzed by MALDI-TOF mass spectrometry and his purity was verified using analytical HPLC in the same condition already described for the purification.

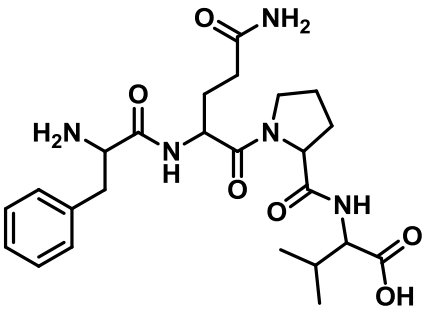

Figure 15: FQPV peptide

Then we synthesized GE11 peptide (Figure 16) using 2-Chlorotrytilchloride resin as a solid support and following the same strategy already described for the synthesis of FQPV. Also in this case the final peptide was analyzed by MALDI-TOF mass spectrometry and his purity was checked using analytical HPLC.

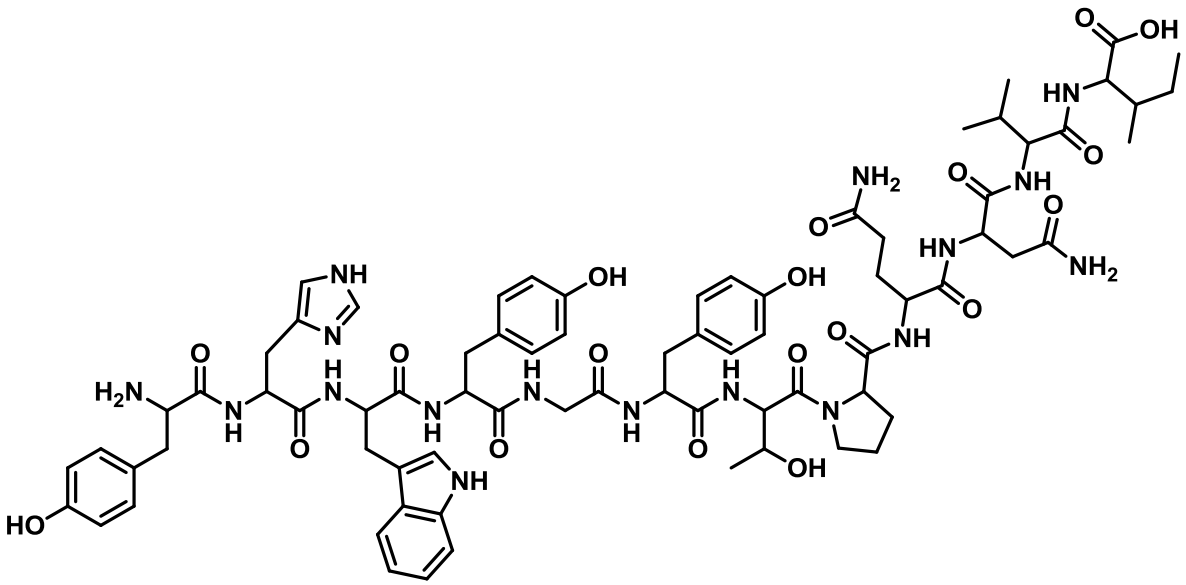

Figure 16: GE11 peptide

Fluorescent derivatives of GE11 peptide (FluoGE12) were synthesized using a slightly different protocol that needed careful studies. We chose 5(6)-carboxyfluoresceine as fluorescent molecule and we decide to link it at the peptide through an aminoacidic spacer

in order to create a certain distance between the bulky fluoresceine core and the peptide chain. As a spacer we decided to use 6-aminohexanoic acid and as ligation strategy the formation of an amide bond. Since the *N*-terminal amine is necessary to attach the peptide to the scaffold, we had to introduce at the end of the sequence an amino acid bearing an amine on the side chain: to this aim we chose to use lysine orthogonally protected on α- and ε-amine. The first strategy we used is depicted in Scheme 2.

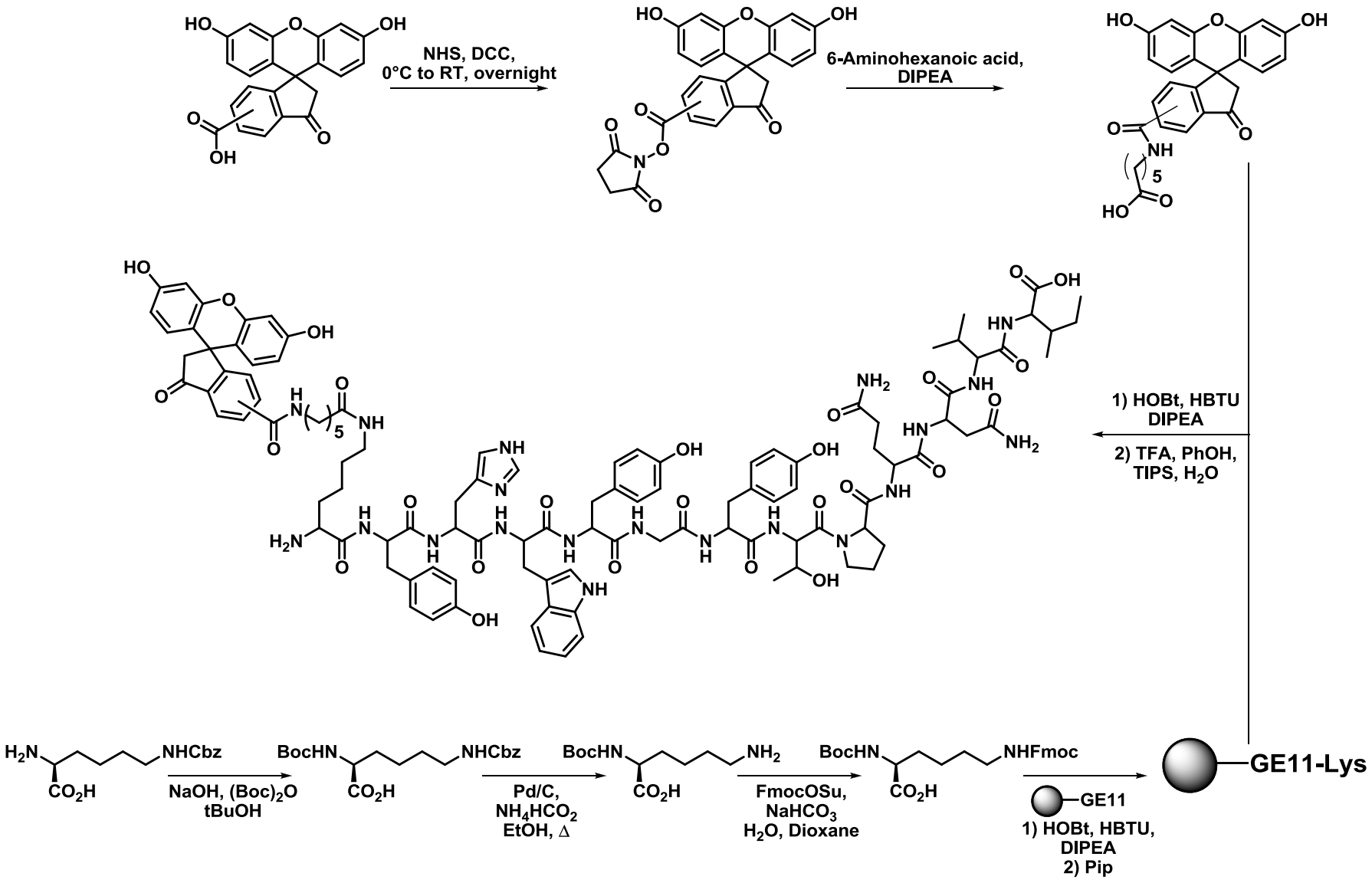

Scheme 2: FluoGE12 peptide preparation, strategy A

In this strategy first of all we prepared 6-[Fluorescein-5(6)-carboxyamido]hexanoic acid, through a coupling between NHS ester of 5(6)-carboxyfluoresceine and 6-aminohexanoic acid; for this reaction we used standard conditions. Then we synthesized GE11 on solid phase using the same condition described before and introduced as last amino acid of the sequence a Lysine protected as Boc on α-amine and as Fmoc on amine (also this amino acid was prepared following very consolidated reactions); we removed Fmoc using piperidine cleavage and we condensed to ε position the preformed 5(6)-carboxyfluoresceinen working at RT with HOBt/HBTU (3 fold excess each) as coupling agents. For this coupling we tried the same coupling conditions used for all other couplings but it was impossible to obtain the desired product, probably because of the emergence of side reaction induced by fluorescein decomposition due to MW heating; so the coupling reaction was carried out for 2 hours at RT without MW irradiation. Then the peptide was cleaved from resin using the same mixture already described for FQPV, purified through semipreparative HPLC and analyzed using MALDI-TOF and analytical HPLC. The peptide was obtained in a good yield and purity; however the procedures were quite tedious since requires the synthesis of the suitabily protected Lysine; moreover the procedure for the preparation of 6-[Fluorescein-5(6)-carboxyamido]hexanoic acid through activation of 5(6)-carboxyfluoresceine was far to be efficient having not very good yield and producing not extremely pure products.

So we decided to optimize the methos changing both the Lysine protections either the synthetic route to the probe (Scheme 3). In this second strategy 6-[Fluorescein-5(6)-carboxyamido]hexanoic acid was prepared on solid phase: Fmoc protected 6-aminohexanoic acid was loaded on 2-Cl-Trytil resin and condensed to fluorescein using HOBt, HBTU and DIPEA. The reaction outcome was very good and the desired product was reached in shorter time and with less trouble than in the previously described preparation. For peptide synthesis we decided to use a Lysine residue protected with Mtt, that is, as already noticed, very acid labile protective group, on ε-amine and with a Fmoc group on α amine; this choice forced us to shift from 2-Cl-Trytil resin to Wang Resin that, as already noticed, requires harsh acidic condition for peptide cleavage, and so it is suitable when a selective removal of acid labile side chain protective groups is needed. Wang resin was loaded with first AA following the procedures proposed by Sandhya (Sandhya, **2008**; Raju, **1997**): resin was activated with thionyl chloride in anhydrous DCM, washed with DCM and MeOH and finally treated with the first AA in DMF in presence of potassium

iodide and DIPEA. The synthesis was carried out as described for GE11 adding at *N*-terminus one additional. Mtt protection was then selectively removed using a DCM/TFA/TIPS (94:1:5) mixture and, subsequently, previously prepared 6-[Fluorescein-5(6)-carboxyamido]hexanoic acid was condensed to ε-amine using HOBt (3 fold excess) and PyBop (3 fold excess) as coupling agents and DIPEA as base (6 fold excess) working at RT without MW irradiation and prolonging the reaction time up to 2 hours. Fmoc protection on the α amine was then removed in standard conditions and the cleavage and purification were performed as already described for previous peptides.

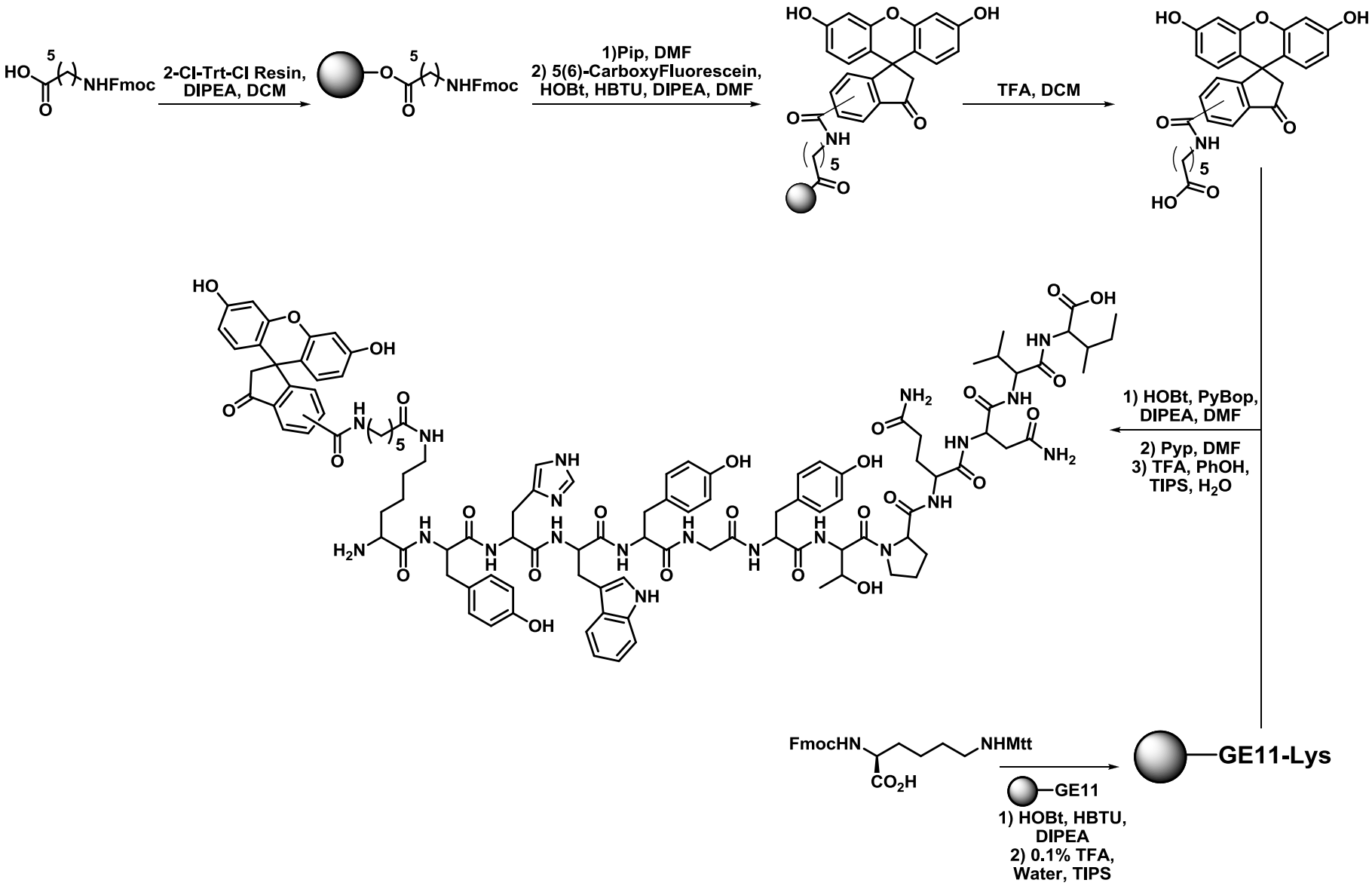

Scheme 3: FluoGE12 peptide preparation, strategy B

3.2. Preparation and characterization of polymer-peptide conjugates

3.2.1. Choice of the material

A material is defined biodegradable when it can be degraded *in vivo*, not necessary by the action of enzymes, giving biocompatible by-products that can be further eliminated by normal metabolic pathways. In recent years a lot of such materials have been proposed as interesting tools in the field of controlled drug delivery, roughly they can be divided in (Ulrich, **1999**; Nair, **2007**; Anderson, **1997**):

1. Synthetic biodegradable polymers such as α-hydroxy acids (e.g. PLGA), polyanhydrides, and others that are relatively hydrophobic.
2. Naturally occurring polymers, such as complex sugars (hyaluronan, chitosan), polyamino acids (PGA, ply-lysine) and inorganics (hydroxyapatite).

It is important to observe that biocompatibility is not an intrinsic property of a material but it depends on the biological environment and the tolerability that exists with respect to specific drug-polymer-tisssue interactions (Anderson, **1997**).

As already evidenced our first intent was to use γ-PGA as scaffold; however this material is far to be easy to derivatize and manage, mainly due to its already evidenced scarce solubility in organic solvents and its inactivity toward many classical derivatization methodologies. So we decided to look for a more commonly used material that could be used to set up with more ease experimental strategies for peptide conjugation to polymers and for the preparation of nanoparticles.

3.2.1.2. Poly(lactic-*co*-glycolic acid)

Among all biomaterials, poly(lactic-*co*-glycolic acid) (Figure 17) has drawn particular attention because of its long clinical experience, its strength, its favourable degradation characteristics and possibilities for sustained drug delivery. The use of PLGA has already been approved by FDA in parenteral microspheres, imolants and periodontal drug-delivery systems (eg Lupron Depot, Zoladex, Vivitrol, OsteoScaf, Atridox, Sandostatin LAR Depot, Arestin and Risperdal Costa).

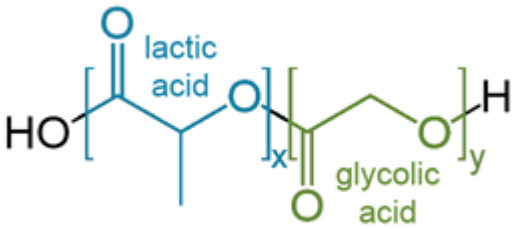

Figure 17: PLGA structure

From a chemical point of view PLGA is a polyester and a copolymer of poly lactic acid (PLA) and poly glycolic acid (PGA). Poly lactic acid contains an asymmetric α-carbon and so can be found in enantiopure forms poly D-lactic acid (PDLA) and poly L-lactic acid (PLLA); however PLGA lactic acid is not enantiopure but can be found as poly D,L-acid where D- and L- are in equal ratio.

PLGA is soluble in a wide range of commonly used solvents including chlorinated solvents, tetrahydrofuran, acetone or ethyl acetate. It is not very water-soluble and degrades by hydrolysis of its ester bonds. Since PLA is more hydrophobic than PGA, lactide rich PLGA copolymers are less hydrophilic, absorb less water and, subsequently, degrades more slowly. Due to its tendency to hydrolysis, parameter that are typically considered invariant descriptor of a solid formulation (glass transition temperature, moisture content, molecular weight etc.) can change in time in the case of PLGA and this consideration is very important to understand and tune the performances of the material. Mechanical strength, swelling behaviour and biodegradation rate of the polymer are strictly linked to the degree of crystallinity of PLGA, which is further dependant on the type and molar ratio of the individual monomer components in the copolymer chain as well as to the molecular weight. The T_g of PLGA copolymers are reported to be above the physiological temperature of 37°C and hence are glassy in nature, thus exhibiting fairly rigid chain structure. It has been further reported that T_g of PLGA decrease with a decrease of lactide content in the copolymer composition and with a decrease in molecular weight (Passerini, **2001**).

PLGA based nanostructures are considered a promising carrier, however they have some intrinsic drawbacks:

1. They are prone to opsonisation, consequently they don't have a long life in systemic circulation.
2. PLGA alone allows only the formation of microsphere or nanoparticles; other formulation such as micelles and polyplexes are not permitted.
3. PLGA nanoparticles lack of versatile functional groups that could favour surface derivatization.
4. Bare PLGA nanoparticles are negatively charged and this is often a disvantage in term of cellular uptaking; moreover, they can't pass through blood-brain barrier.

To overcome the limitations of bare PLGA nanoparticles and thus improve their functionality and *in vivo* performances, strategies have been elaborated that are mainly based on the surface modification of the structure (eg PEGylation, lipid- or surfactant-coating, conjugation with cell-targeting ligands etc.). Such modifications have a lot of beneficial effects on the system effectiveness: minimize opsonine absorption, lengthen blood residence time, reduce drug side effects, permit targeted drug delivery and synergistic drug combination strategies and improve cellular uptake (Maeda, **2000**; Davis, **2008**).

PLGA characteristics are controlled by the stereochemistry of lactic acid (D, L or DL), by the degree of crystallinity, lactic acid/glycolic acid ratio and molecular weight. PLGA end groups could be modified to tune the material properties; the most common among these modification are esterification of the free carboxylic end group (as lauryl or methyl ester) that augment the polymer stability and PEGylation. PEGylation contributes to (Vonarbourg, **2006**):

1. Reducing intramolecular aggregation.
2. Increase aqueous solubility and stability.
3. Decreasing immunogenicity.
4. Prolonging the systemic circulation time.

PEGylation also makes possible the preparation of self assembling mycelles based on PLGA.

Functional PLGA nanostructures can be classified in various groups Among them, the most significant are the following:

1. PEGylated/ non-PEGylated micelles (Yasugi, **1999**; Nam, **2003**).
2. Polyplexes (Mishra, **2011**).
3. PEGylated nanoparticleas (Yamamoto, **2001**; Verrecchia, **1995**; Gref, **1998**).
4. Polymerosomes (Discher, **1999**; Meng, **2003**).
5. Core-shell type hybrid nanoparticles/nanocelles (Chan, **2009**; Zhang, **2010**; Zhang, **2008**).
6. Cell-mimiking nanoparticles (Hu, **2011**).
7. Surface derivatized PLGA nanoparticles.

3.2.2. PLGA-peptide conjugates

Our effort have been focused on the preparation of PLGA nanoparticles functionalized with GE11 peptide as a cell targeting agent. As already noticed in the introduction generally speaking about functionalized nanoparticles, also in the case of PLGA the desired ligands can be attached either to the surface of a preformed nanoparticles or to the polymer chain before the formation of the structure; in the first case both a simple physical association, driven for example by electrostatic interactions or hydrophobica association, either a real conjugation reaction are eligible, in the latter case only a chemical coupling to the chain is possible. The functionalization can involve the carboxyl terminus of a bare PLGA or the end group of a suitably modified PEG in PEGylated-PLGA (commonly a carboxyl, an aldehyde, a maleimide or a thiol).

Many strategies for the formation of such kind of bonds have been reported so far; the most commonly used are reported in Figure 18.

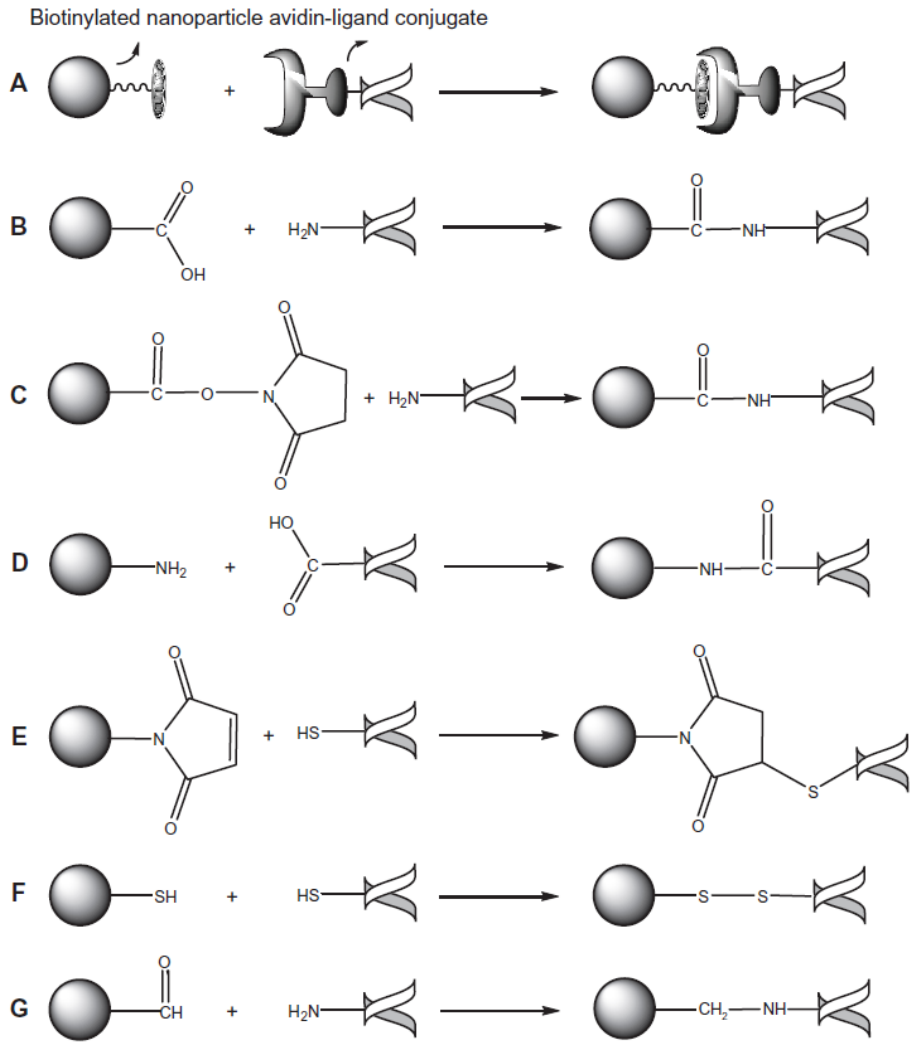

Figure 18: Strategies for the formation of PLGA-cell-recognizable ligands conjugates: (A) physical association driven by the specific avidin-biotin binding affinity; (B–D) amide coupling reactions using carbodiimide reagents; (E) maleimide-thiol reaction; (F) thiol-thiol reaction (G) aldehyde-amine reaction (Sah, 2013).

Our intent is to create PLGA nanoparticles decorated with cell targeting peptide, in particular with GE11 peptide described in introduction; we decided to perform the conjugation reaction before the formation of the nanoparticles to maximize the number of peptide decorated chains and to have the opportunity to obtain a better quantification of the linked peptide. On the other hand, as already evidenced in introduction, the method offers a very poor control over the surface concentration and distribution of peptide chains

For the coupling reaction we decided to follow an amide bond formation strategy based on the use of water soluble carbodiimide reagents such as EDC and NHS. EDC reacts with the carboxyl group in PLGA forming an amine-reactive *O*-acylisourea intermediate and subsequently NHS is added to transform the intermediate into its NHS ester derivative that is more stable and could eventually be isolated. The rapid reaction of this last compound

with the primary amine group at *N*-terminus of the peptide and the subsequent liberation of NHS lead to the formation of a PLGA-ligand conjugate through an amide bond.

This method is usually preferred over other alternatives because it is quite simple and take advantage only of the native functional groups of both PLGA and peptides to achieve the coupling, this resulting in a lower probability to loose ligand specific activity (Nobs, **2004**). However, the presence of multiple functional groups in the ligand can result in the possibility of multi-site attachment, thus making difficult the control of the ligand orientation at the surface of the nanocarrier. In our case, the model peptide and GE11 related peptides bring only one group, the *N*-terminal amine, prone to the formation of an amide bond with PLGA *via* carbodiimide activation, therefore this method appear to be extremely suitable to the formation of the desired conjugates.

For our experiments we used PLGa supplied by Lahkeshore Biomaterials with a nominal composition of 75% D,L-Lactide/25% Glycolide and a average molecular weight of 30 kDa. First of all, we performed the activation of PLGA using EDC/NHS in DCM, then we isolated the active ester and performed the coupling reaction with model peptide and GE11 based peptides in a mixture of water and acetonitrile (Scheme 4). The isolation of the activated polymer and the change of solvent, although not convenient in term of synthetic efficiency, were necessary to conciliate the different solubility of PLGA (soluble in organic solvents but unsoluble in water) and peptides (soluble in water and barely soluble in only few organic solvents).

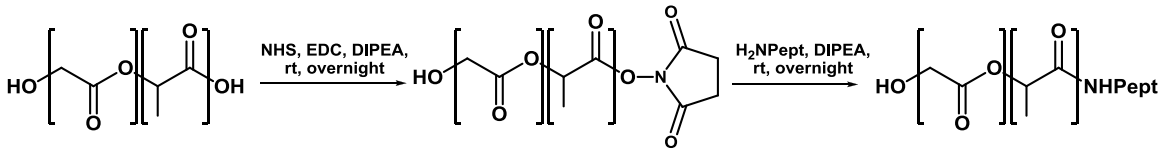

Scheme 4: Conjugation of peptides to PLGA

PLGA-peptide conjugates were characterised using different techniques. DSC allowed to observe a change in the thermal behaviour of the material. Figure 19 reported DSC responses for FQPV-PLGA and GE11-PLGA respectively along with the signal of bare PLGA as reference compound.

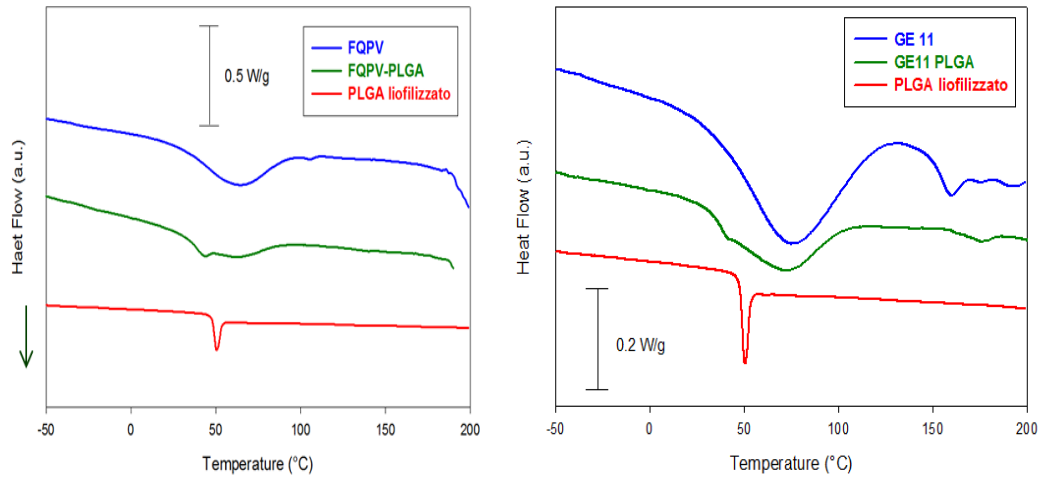

Figure 19: DSC responses for FQPV-PLGA and GE11-PLGA

Also IR spectra of GE11, PLGA and PLGA-GE11 conjugates were registered (Figure 20). It can be observed that the spectra of the product deriving from the coupling reaction, shows signal both from the polymer and the peptide. This is particularly clear in the region between 1500 and 1700 cm^{-1}; this region is flat in PLGA spectrum while presents two evident peaks (at 1515 and 1652 cm^{-1} respectively) in GE11 one; these peaks are also present, although slightly shifted at 1517 and 1684 cm^{-1} respectively and decisively weaker, in the conjugate spectra along with a peak at about 1746 cm^{-1} that clearly derives from PLG;, thus indicates the success of the coupling reaction.

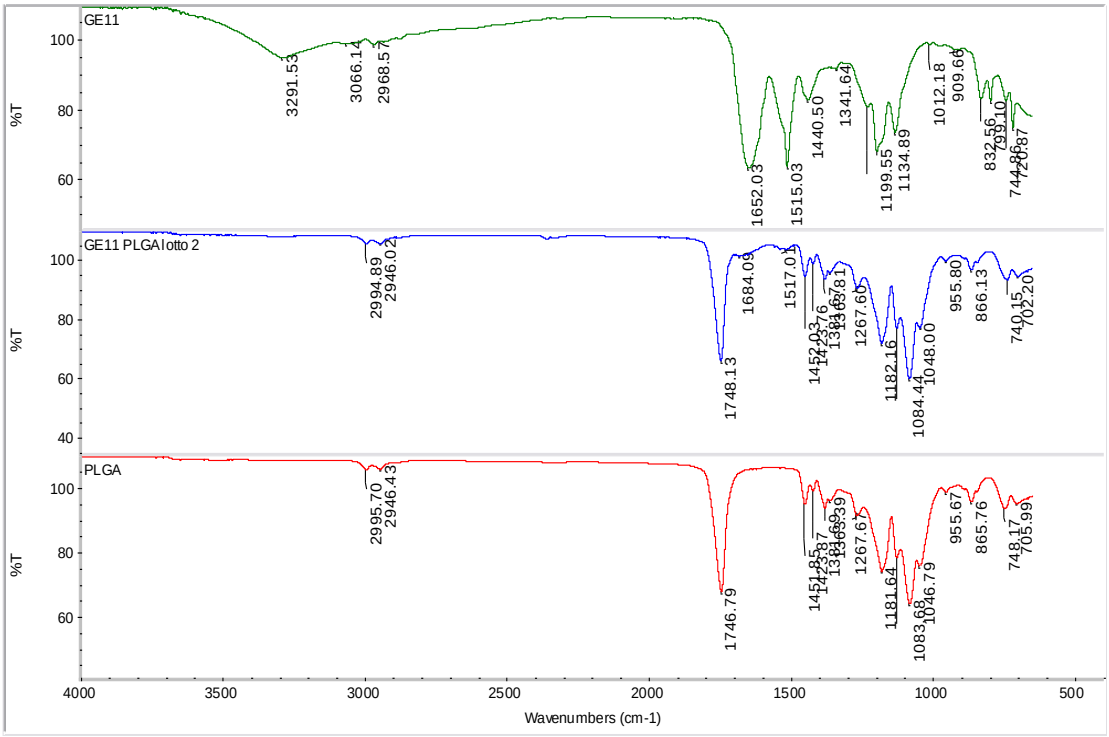

Figure 20: IR Spectra of PLGA (red), PLGA-GE11 (blue), GE11 (green)

Finally, we used ^{1}H NMR spectroscopy (Figure 21, 22, 23) to confirm the formation of the peptide polymer bond and to give a rough estimation of the peptide-functionalization of the recovered polymer. To this last purpose, we compare the integration area values of peaks clearly assignable to known groups in the peptide sequence with other that can be ascribed to the polymer; knowing both the lactic acid/glycolic acid ratio (75/25) and the average Mw (30 KDa) of the polymer it was possible to calibrate integrals, thus obtaining a good estimation of the functionalization degree.

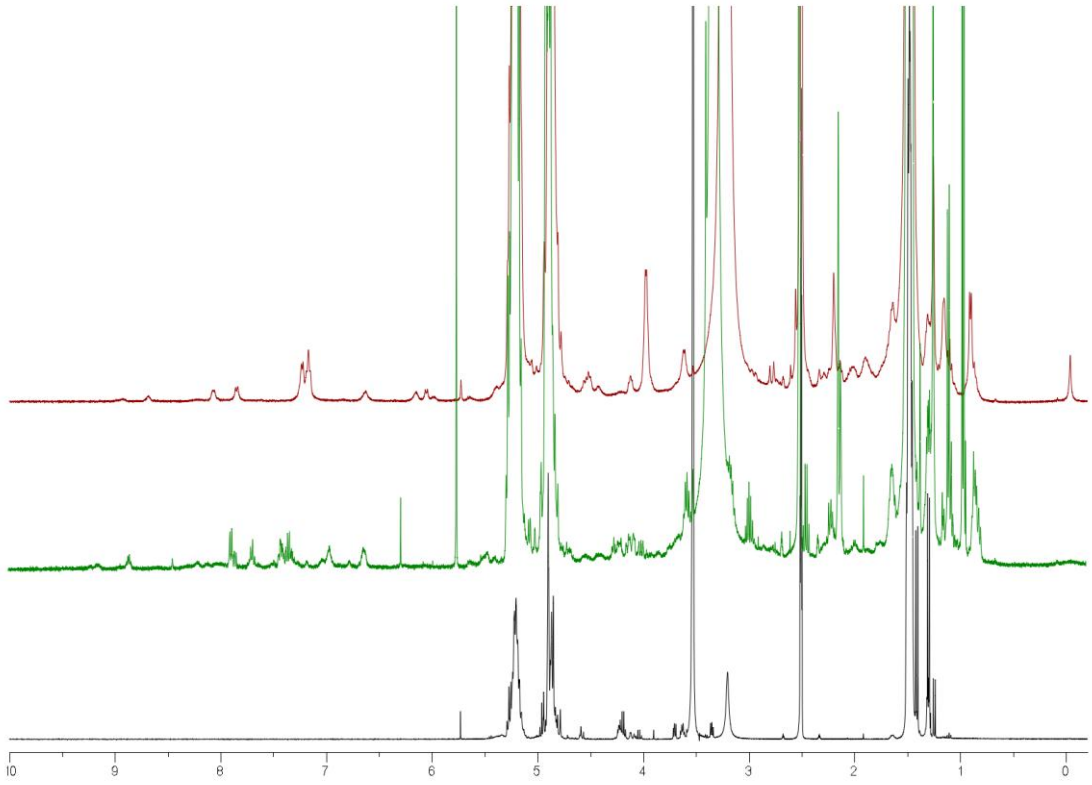

Figure 21: ^{1}H NMR spectra registered in DMSO-d_6: black PLGA, red FQPV peptide, green PLGA-FQPV conjugate.

In the case of PLGA-FQPV conjugate (Figure 21), we used the peak at about 0.9 ppm for the peptide and the peak at about 5.3 ppm for the polymer as reference signals to quantify functionalization degree. A 95% functionalization degree was calculated.

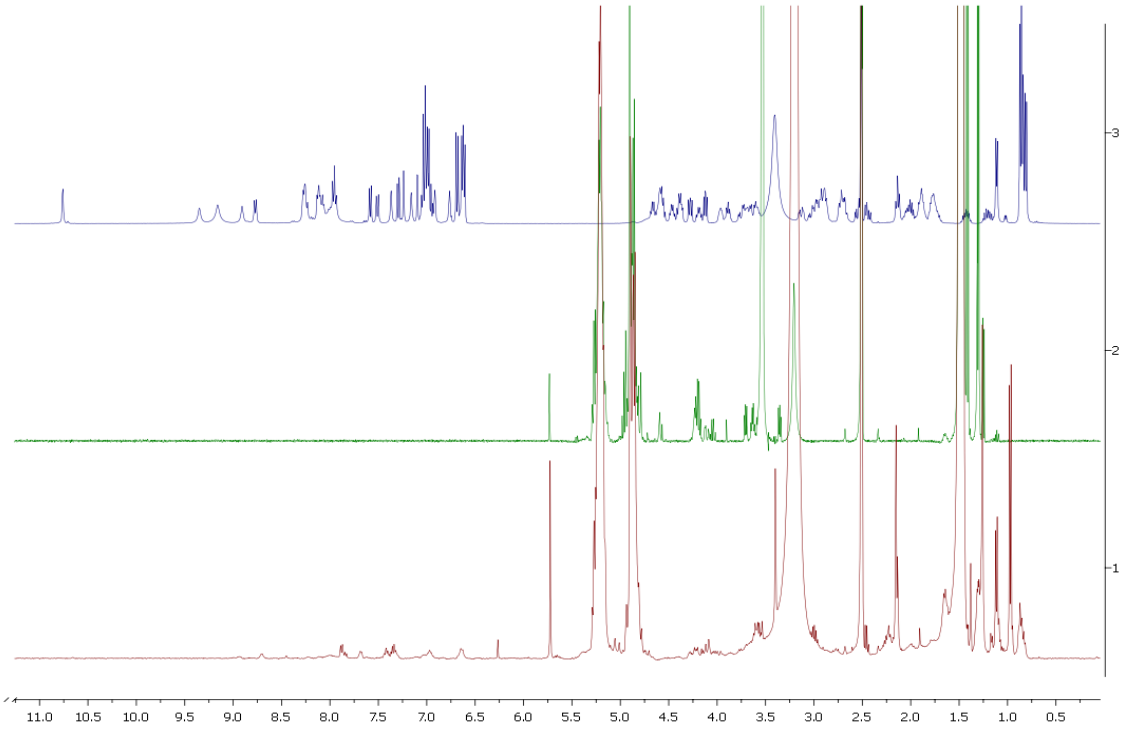

Figure 22: ^{1}H NMR spectra registered in DMSO-d_6: green PLGA, blue GE11 peptide, red PLGA-GE11 conjugate.

In the case of PLGA-GE11 conjugate (Figure 22), we used the peak at about 0.85 ppm for the peptide and the peak at about 5.2 ppm for the polymer as reference signals to quantify functionalization degree. A 98% functionalization degree was calculated.

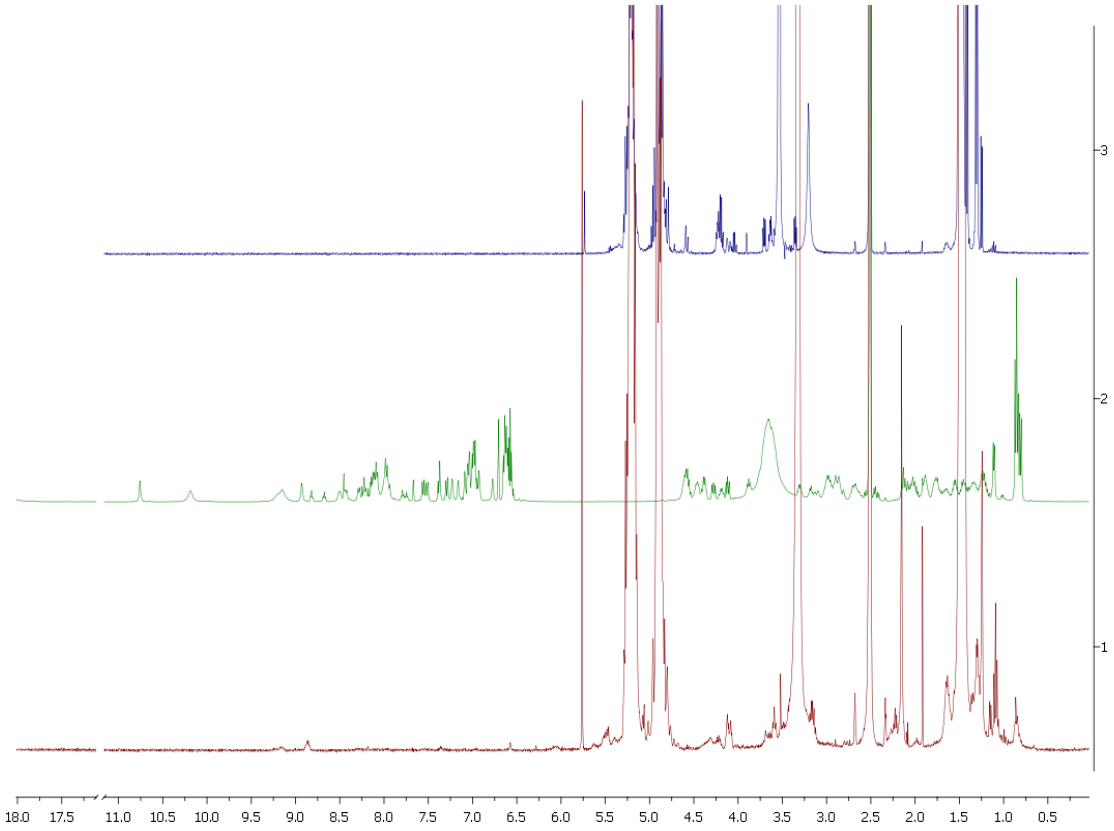

Figure 23: ^{1}H NMR spectra registered in DMSO-d_6: blue PLGA, green FluoGE12 peptide, red PLGA-FluoGE12 conjugate.

In the case of PLGA-FluoGE12 conjugate (Figure 23), we used the peak at about 0.84 ppm for the peptide and the peak at about 5.3 ppm for the polymer as reference signals to quantify functionalization degree. A 75% functionalization degree was calculated.

3.2.3. Nanoparticles preparation

Given that FQPV-PLGA conjugate is not soluble in acetone, the model FQPV-PLGA NPs were prepared, following nanoprecipitation technique, using DMSO. The nanoparticles were recovered by high speed ultracentrifugation and characterized with respect to their morphology (TEM) (Figure 24), showing proper dimensions for the intended applications as well as a regular round shape and an homogeneous dimensional distribution even after freeze drying thanks to the addition of a proper crioprotectant.

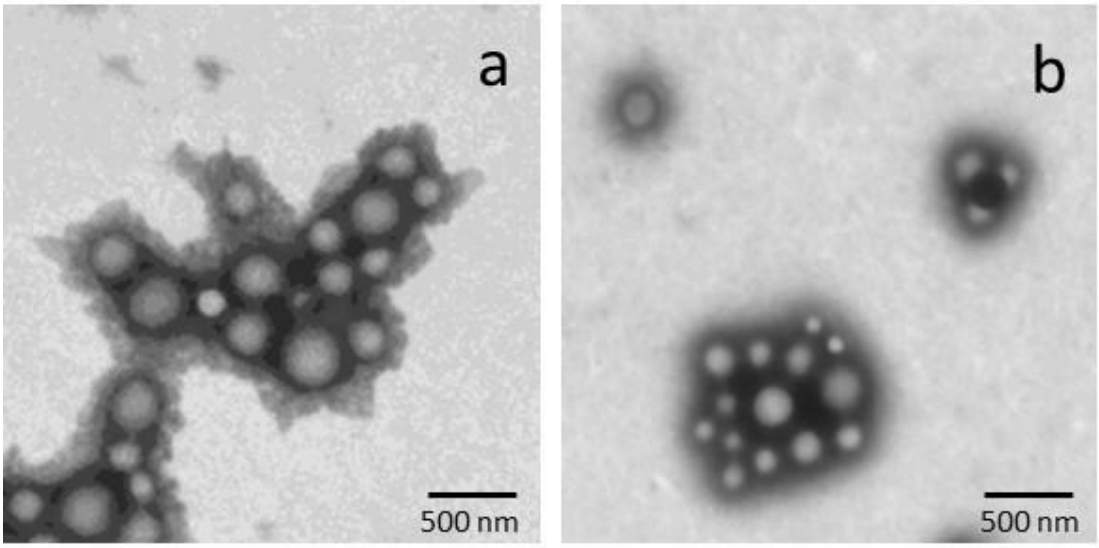

Figure 24: TEM images of fresh PLGA NP (a) and freeze dried PLGA NP with cryoprotectant(b).

A "hybrid method", based on the use of a mixture of CH_2Cl_2:Acetone 20:80 v:v, was also tested and proved to be quite effective: even using this technique were produced NPs with good dimensional properties. We also prepared NPs made of bare PLGA and charged with FQPV by absorption or encapsulation in order to compare different techniques for peptide loading to the polymer.

Table 1 summarize all data recovered from the analysis of FQPV-PLGA NPs, prepared with different protocols.

Table 2: FQPV-PLGA nanoparticles characterization

Batch #	Solvent	Dimensions		Zeta Potential (mV)	Process Yield (% v/v)	FQPV loaded (FQPV: PLGA, w:w)
		nm	PI			
#1 PLGA	Acetone	140.8±54.5	0.150	-0.76	44.28	/
#2 PLGA	DMSO	143.7±62.3	0.188	-0.65	45.56	/
#3 FQPV-PLGA	DMSO	202.3±73.8	0.133	-0.15	40.36	1:61.47 (0.0163)
#4 FQPV-PLGA	CH_2Cl_2/Acetone	241.7±89.4	0.199	-0.20	41.25	1:61.47 (0.0163)
#5 PLGA + FQPV encapsulated	Acetone	353.8±104.0	0.080	-0.70	65.98	1:150 (0.0067)
#6 PLGA + FQPV adsorbed	Acetone	244.1±65.7	0.072	-0.30	40.15	1:29.9 (0.033)

Some considerations have to be done on entry #5 and #6 of the table. Due to the low molecular weight and the high hydrophilicity of the peptide, the method selected to encapsulate the FQPV into PLGA NP (entry #5) demonstrated not to be valid, as can be observed by the low FQPV:PLGA ratio (FQPV:PLGA w:w 1:150). A second observation can be done on the method of FQPV adsorption; it allows good FQPV loading (FQPV:PLGA ratio w:w 1:29.9), reaching the highest FQPV loading after 60 minutes of incubation in a FQPV aqueous solution (Figure 25). As expected the polymer/peptide interaction does not lead to a stable compound, as demonstrated by the reduction of the amount of FQPV adsorbed after 90 minutes (Figure 25). NP batches and their characterization. Z-potential was measured using (NICOMP 380ZLS apparatus)

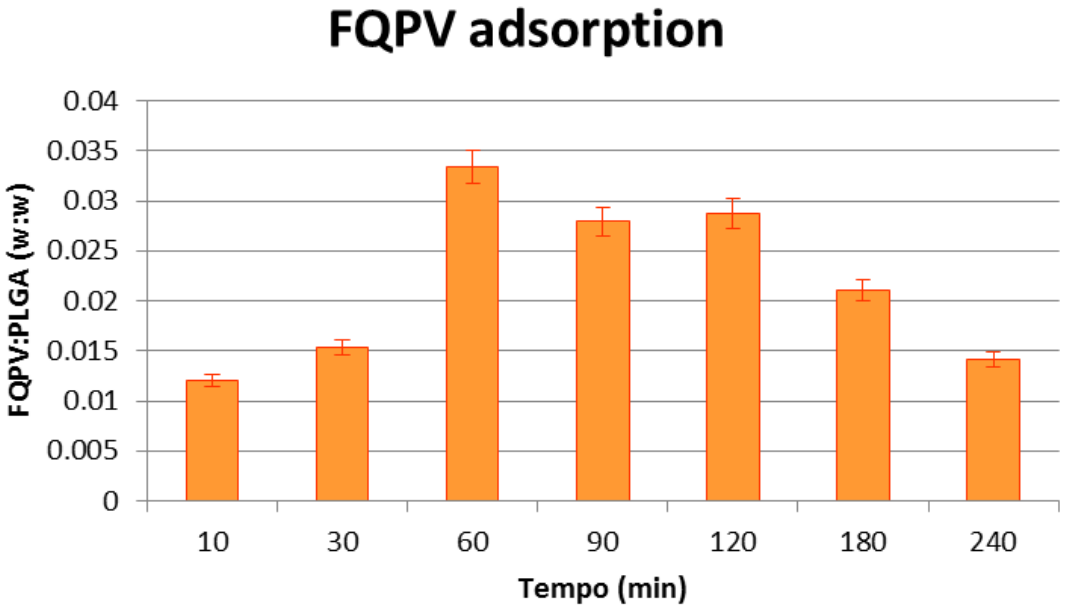

Figure 25: Adsorption of FQPV on PLGA NP surface. The results are expressed as the weight ratio between FQPV adsorbed and PLGA NP at different time points.

We also tried to load model FQPV-PLGA nanoparticles with dexamethasone, a potent steroid drug, used for the treatment of reumathoid. arthritis DXM loaded NPs are prepared either by nanoprecipitation and "hybrid method". Considering the results of EE% and drug content (Table 2), the "hybrid method" is selected as the proper DXM loading method for FQPV-PLGA NPs.

Table 3: DXM loaded FQPV-PLGA nanoparticles characterization

Batch #	Solvent	DXM:polymer ratio p:p	Diameter (nm ± ds)	PI	EE (% p/p w:w)	Drug content (mg_{DXM}/mg_{NP})
#7	DMSO	1:10	154.0±5.4	0.130	0.31±0.02	0.0013
#8	CH_2Cl_2:Acetone	1:10	403.6±173.6	0.185	32.60±1.11	0.033

Results and methods obtained with model FQPV-polymer resulted to be only partially reproducible with GE11 functionalized PLGA, mainly due to the different solubility shown by the two compounds.

In the case of GE11-PLGA, NPs were prepared using a pure nanoprecipitation protocol. Peptide-polymer constructs were dissolved in DMSO and then slowly added to an aqueous

solution of PVA kept under strong magnetical stirring for 4h. The solution was centrifuged for 2 hours, the supernatant removed and the resulting pellet re-suspended in a solvent suitable for the subsequent analysis (Scheme 5).

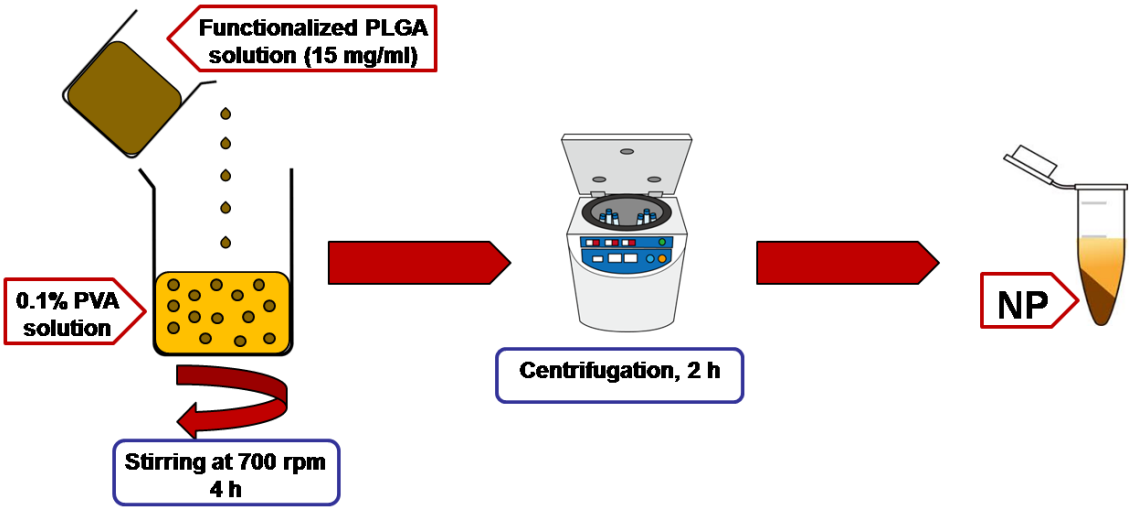

Scheme 5: preparation of GE11-PLGA nanoparticles

Two different nanoparticles batches were prepared and analyzed: one made only with the GE11-PLGA conjugate and the other made with a mixture of GE11-PLGA and PEG-PLGA.

Placebo GE11-PLGA nanoparticles showed homogeneous size distribution and suitable dimensions (254.5±81.8, PI 0.150) (Table 3). Zeta potential was -0.06 mV, different respect to bare PLGA nanoparticles (Table 3#1). NPs prepared with the addition of PEGylated polymer demonstrated good dimension too (Table 3 #3,#4).

Table 4: GE11-PLGA nanoparticles characterization

#	Polymer composition	Conc. (mg/ml)	Conc. PVA (%, w/v)	Polym.:PVA ratio v:v	Curing Time (h)	Dim. (nm ± ds)	PI	Zeta Potential (mV)	Process yield (% w/w)
1	PLGA	15	1	1:2	4	140.8±54.4	0.150	-3.55	57.5
2	GE11-PLGA	15	1	1:2	4	254.5±81.8	0.150	-0.06	59.1
3	PLGA/PEG-PLGA (1:1 w:w)	15	1	1:2	4	158.4±38.3	0.059	-0.60	47.5
4	GE11-PLGA/PEG-PLGA (1:1 w:w)	15	1	1:2	4	159.6±38.8	0.059	-0.45	40.8

TEM micrographs confirmed the results of dimensional analysis and showed a good round shape for all the NPs batches considered (Figure 26).

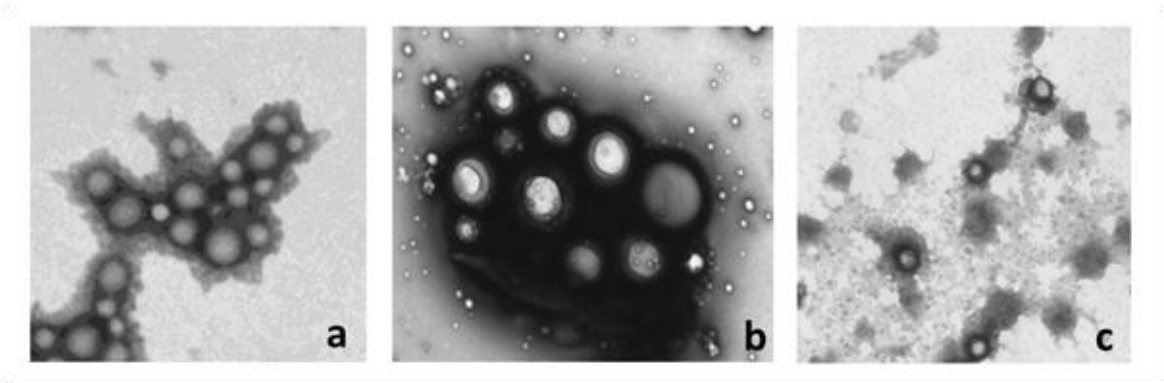

Figure 26: images of PLGA NPs (a), GE11-PLGA NPs (b) and GE11-PLGA/PEG-PLGA NP (c).

3.2.3.1. Cytotoxicity Evaluation

GE11-PLGA nanoparticles cytotoxicity was evaluated using the so called MTS test: this assay measures the reducing potential of the cell using a colorimetric reaction in which (3-(4,5-dimethylthiazol-2-yl)-5-(3-carboxymethoxyphenyl)-2-(4-sulfophenyl)-2H-tetrazolium) (in brief MTS) is reduced to the corresponding formazan by viable cell. After incubation with the substance of interest (NPs in our case) a change in absorbance in respect to a negative control indicates a change in the viability of the cell line.

First of all, two different cellular line, one overexpressing EGFR (A549) the other one chosen as negative control (HUVEC) were treated with a suspension of bare PLGA nanoparticles (Figure 27).

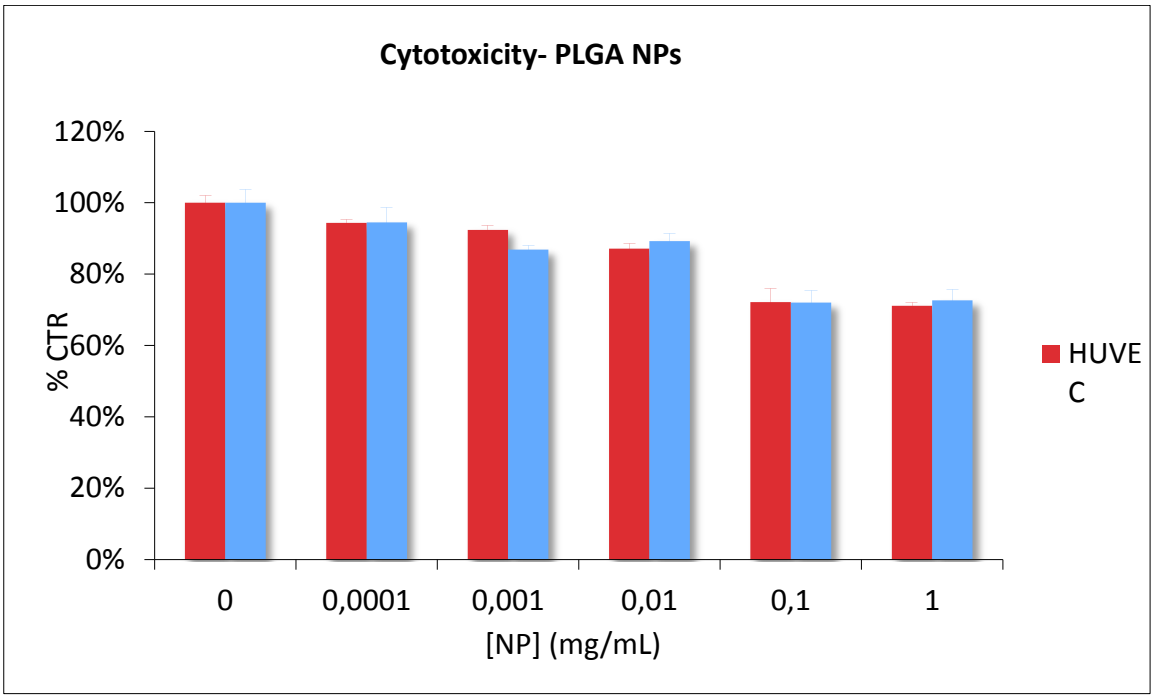

Figure 27: MTS test results for bare PLGA nanoparticles

Then we treated two EGFR overexpressing cellular line, namely A549 and Caki-1 (renal adenocarcinoma), with GE11-PLGA NPs (Figure 28) and with mixed GE11-PLGA /PEG-PLGA nanoparticles (Figure 29).

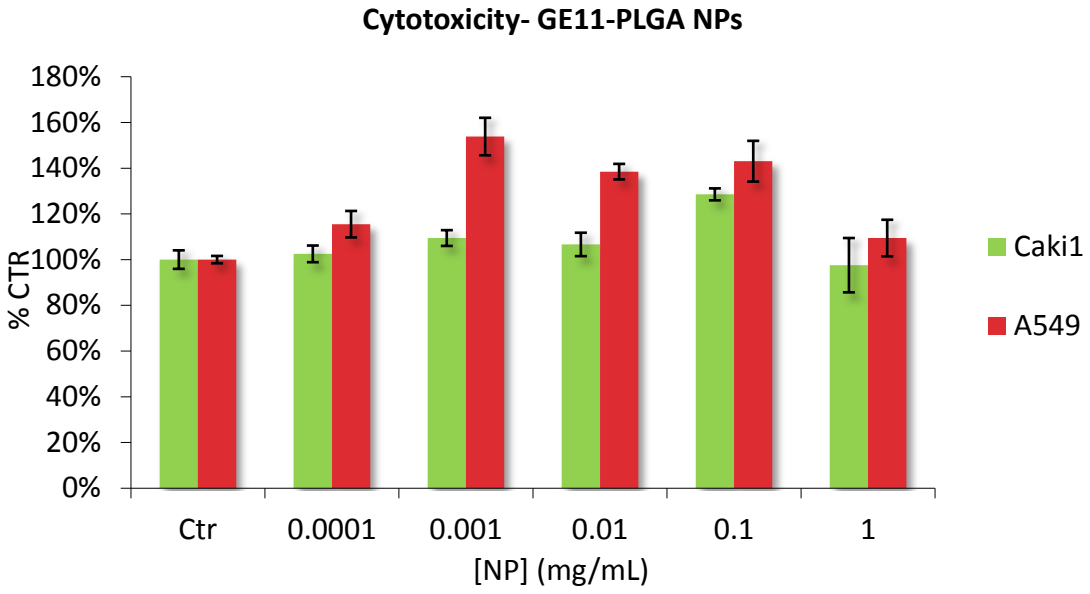

Figure 28: MTS test results for GE11-PLGA nanoparticles

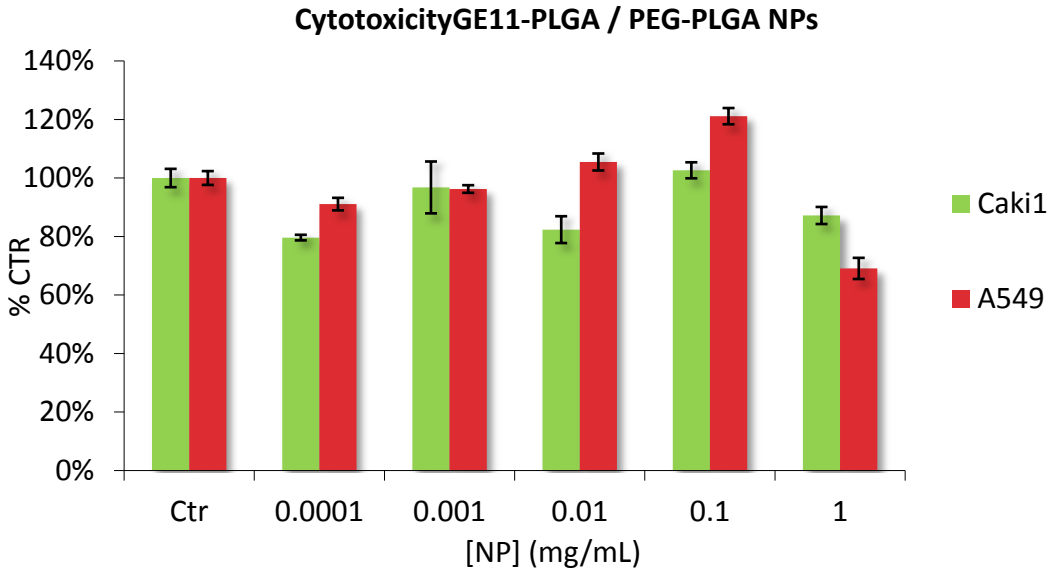

Figure 29: MTS test results for GE11-PLGA /PEG-PLGA nanoparticles

3.3. Studies on poly(γ-glutamic acid) reactivity

Poly(γ-glutamic acid) (γ-PGA) is linear anionic biopolymer synthesized by bacterial fermentation from sustainable resources in which D- and/or L-glutamate is polymerized via γ-amide bonds. Being water soluble, biodegradable, edible and non-toxic to humans and the environment, potential applications of γ-PGA are of interest in a broad range of industrial fields such as food, cosmetics, medicine and bioremediation (Shih, **2001**, **2009**; Poo, **2010**). However, the low stability in moist ambiences and the poor thermal and mechanical properties have hindered its use in widespread areas such as coatings and packaging. Great efforts have been thus made to convert the biopolymer into derivatives endowed with suitable properties for handling and processing at the same time maintaining the biodegradability of γ-PGA (Morillo, **2003**). γ-PGA is produced industrially by fermentation and it is commercially available both as free acid and as sodium salt.

Derivatisation of γ-PGA without affecting the main chain takes advantage of the presence of free α-carboxylic groups on the polymer backbone and the formation of esters or amides is the most commonly used approach to attain its chemical modification.

On the other hand, this is a quite challenging topic, given the peculiarities of γ-PGA, i.e. difficulties in manipulation because of the high viscosity and scarce chemical reactivity of the α-carboxylic side groups which, being directly linked to the polypeptide main chain, are highly hindered and hard to reach by any nucleophilic reagent. A further obstacle is represented by difficulties in the isolation and the purification of the products.

To date, two main methodologies are known for the preparation of γ-PGA derivatives which are depicted in Scheme 6.

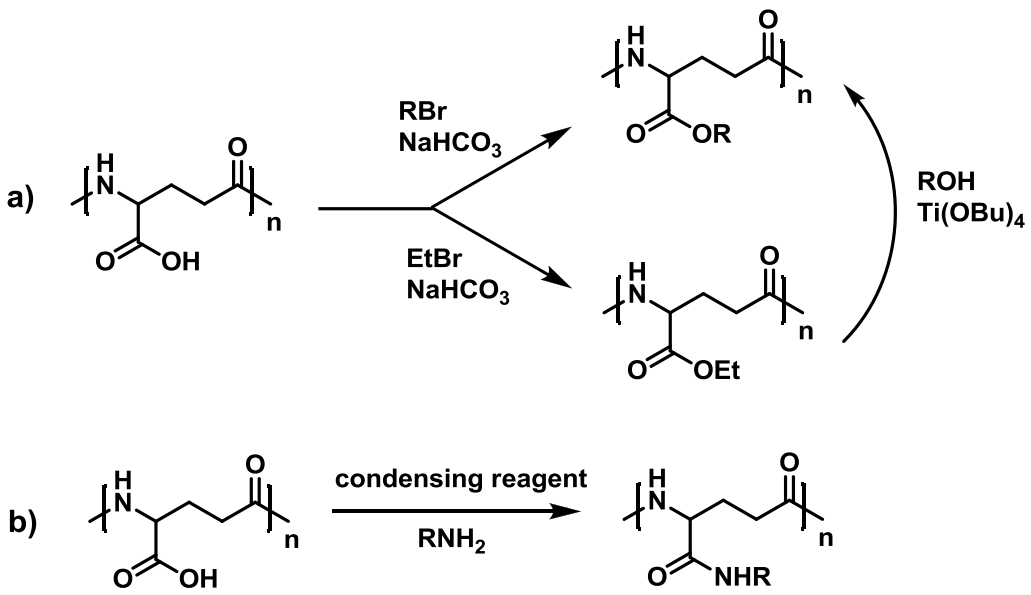

Scheme 6: Chemical modification of γ-PGA

The method a), firstly reported by Kubota and coworkers (Kubota, **1993**, **1995**), consists of the reaction of γ-PGA with alkyl halides in the presence of sodium bicarbonate in organic solvents such as DMF, DMSO or NMP under the appropriate condition of time and temperature. In fact, when γ-PGA is treated with an alcohol in the presence of acid catalyst (Fischer esterification), depolymerization of the resulting ester occurs. Using the Kubota methodology, esterification of γ-PGA with several alkyl halides ranging from methyl up to dodecyl Including dihalogenoalkanes yielding hydrogels with various features (Gonzales, **1996**) was carried out (Muñoz-Guerra, **2013**). The reliability of the method and the esterification yields depend on the size of the alkyl group, with better results obtained with short esters. To achieve a degree of substitution exceeding 50%, the procedure requires dissolving the polymer in a high-boiling solvent such as DMSO and letting it react with alkyl or benzyl halide in basic conditions for periods of time between 5 and 10 days, performing two subsequent derivatizations. Afterwards, the product can be isolated by an often tricky precipitation in cold acidic water. The possibility of a reduction in molecular weight upon prolonged reaction in these conditions has also been reported (Martinez de Ilarduya, **2002**; Melis, **2001**; Morillo, **2001**, **2003**). Such reduction is thought to be due to uncontrolled hydrolysis of the polyamide chain which increases considerably with reaction time and temperature. To overcome this difficulties, a two-step esterification method was developed which was proved to be more efficient for the preparation of poly(γ-glutamate)s with alkyl chain of medium or long size (from 12 to 22 carbon atoms) as well as mono-, di- and triethylene glycols (Pérez-Camero, **2001**; Morillo, **2001**). The method consists in

subjecting the relatively easily accessible poly(α-methyl-γ-glutamate) or poly(α-ethyl-γ-glutamate) obtained by the Kubota method to transesterification with the appropriate alcohol in the presence of $Ti(OBu)_4$ (Scheme 6a). All the alkyl esters of γ-PGA are not soluble in water but only in organic solvent and show thermal stability higher than the biopolymer melting before decomposing.

The second methodology, which is routinely preferred for amide formation (Akagi, **2005a**, **2005b**), makes use of condensing agents, usually a water-soluble carbodiimide such as 1-ethyl-3-(3-dimethylaminopropyl)-carbodiimide (EDC). Experimentally, the polymer is dissolved or suspended in DMSO, and reacted for 24-36 hours in the presence of a base (such as TEA, DiPEA, or Py) and an amine. The product is generally isolated by dialysis against distilled water, followed by lyophilisation. The drawback in this case is the inherent slowness of the dialysis step, and also the difficulty in getting rid of the byproducts of the coupling agent used. Such a method has been widely used to prepare amphiphilic graft copolymers composed of γ-PGA as the hydrophilic polymer and hydrophobic amino acid (HAA) such as L-phenylalanine ethyl/propyl/benzyl esters as the hydrophobic side chains. These amphiphilic γ-PGA derivatives are able to self-assembly in internally structured, biodegradable nanoparticles (Akagi, **2007a**, **2007b**).

Once again the inherent limit in the chemical manipulation and modification of γ-PGA through this methodology lies in its scarce solubility in most organic solvents and in their mixtures which negatively affects yields and strongly narrows down the possible applicable reaction conditions.

Following an effective strategy used in polysaccharide chemistry e.g. to prepare hyaluronic acid derivatives as well as solvent-soluble salts of cellulose sulfate (Bellini, **2011**; Schweiger ,**1972**), we decided to improve the solubility of γ-PGA by exchanging its counterion, in particular by converting its sodium salt into a quaternary ammonium salt[1].

Quaternary ammonium salts are characterized by good solubility in both water and organic solvents, by thermal stability and are commonly used as phase transfer catalysts. With this aim in mind, γ-PGA, in its commercially available sodium salt form, was solubilized in water and the resulting solution percolated through a column filled with a sulphonic resin

[1] All experiments reported in this thesis were carried out on a commercially sample of γ-PGA as sodium salt (Mw XXX determined by SEC-MALS) purchased by Natto Bioscience

in the form of tetrabutylammonium salt (TBA). A cation-exchange resin Dowex 50Wx8 previously activated with an excess of a 40% w/v solution of tertrabutylammonium hydroxide was used. The eluate, containing γ-PGA-TBA salt was collected, freeze-dried and characterized (Scheme 7).

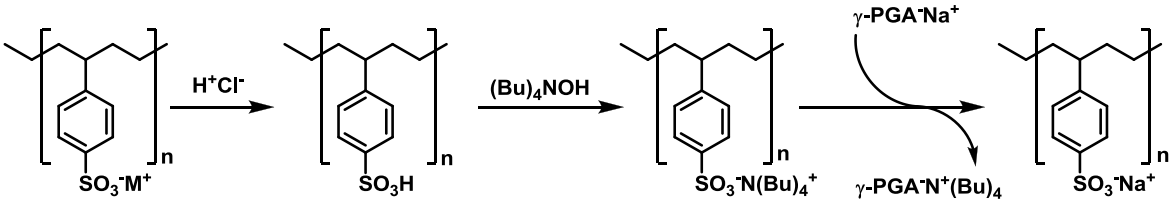

Scheme 7: Preparation of γ-PGA TBA salt

To determine the effect of the counterion exchange, solubility tests were carried out by trying to dissolve a known amount of polymer, in its acid, sodium and tetrabutylammonium salt form, respectively, in an increasing volume of the most commonly used organic solvents (Table 4)

Solvent	2.3 mg γ-PGA Na salt	2 mg γ-PGA Acid form	5 mg γ-PGA TBA salt
MeOH	Not soluble	Not soluble	33.3 mg/mL (X μL)
EtOH	Not soluble	Not soluble	16.7-20 mg/mL
n-PrOH	Not soluble	Not soluble	3.6 mg/mL
i-PrOH	Not soluble	Not soluble	Not solubile
n-BuOH	Not soluble	Not soluble	Scarcely soluble
t-BuOH	Not soluble	Not soluble	Not soluble
BnOH	Not soluble	Not soluble	25 mg/mL
TFE (2,2,2-trifluoroethanol)	Not soluble	Not soluble	16.7 mg/mL
CH_3CN	Not soluble	Not soluble	Scarcely soluble
DMF	Scarcely solubile	Not soluble	50 mg/mL
DMSO	Scarcely soluble	Scarcely soluble	40 mg/mL

Table 5: Solubility of γ-PGA in its acid, sodium and tetrabutylammonium salt form, respectively, in the most common organic solvents. a) Each test was performed by weighting an amount of about 15 μmol of substance (corresponding to 2.3 mg, 2 mg and 5 mg of γ-PGA sodium salt, γ-PGA acid form and γ-PGA TBA salt, respectively) and adding stepwise 50 μL volumes of the selected solvent till complete dissolution or up to 2 ml, under magnetic stirring at room temperature.

The results reported in Table 5 indicated that the presence of the tetrabutylammonium counterion proves to be quite beneficial increasing the solubility of the biopolymer in organic solvents particularly in the case of aprotic polar solvents such as DMF and DMSO and short chain alcohols (MeOH, EtOH, *n*-PrOH). However, γ-PGA TBA salt still remains insoluble in ethers, long chain and branched alcohols. In addition the water solubility of the biopolymer was also increased of about six times.

The next step was to check whether the conversion of γ-PGA into a salt form with improved solubility could facilitate its manipulation and the preparation of derivatives of interest in nanomedicine field such as bioconiugate with peptides. As a first approach, we compared the reactivity of γ-PGA-TBA salt to that of the other available forms of γ-PGA in the esterification reaction using the ethyl ester derivative of γ-PGA as a reference compound. Two methodologies were investigated. The former is the one, described above, proposed by Kubota (Muñoz-Guerra, **2013**), based on carboxylate chemistry which was found to be effective for the sodium salt form of γ-PGA (see Scheme 8 A).

The latter was set up in our laboratories and consists in the *in situ* formation, facilitated by a catalytic amount of DMF, of the acyl chloride of γ-PGA by treatment of with oxalyl chloride, followed by direct esterification with the proper alcohol (see Scheme 8 B). The reaction is carried as a suspension either in an ethereal solvent such as THF, or directly in the alcohol corresponding to the desired ester using γ-PGA in its acidic form as starting material. With respect to the Kubota method our methodology appear advantageous in term of reaction time and ease of recovery of the product which can be isolated by precipitation in a cold alcohol such as methanol and filtration. However the functionalization degree is far to be excellent (see Table 5).

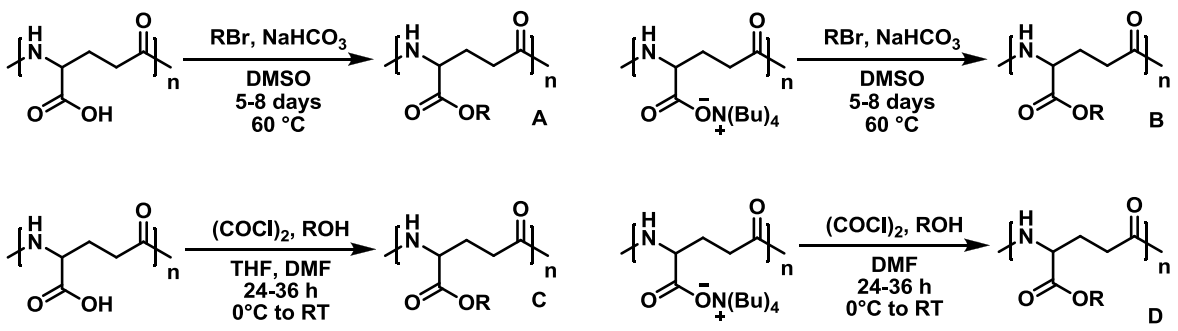

Scheme 8: procedure for the preparation of γ-PGA esters.

Table 6: γ-PGA esterification reactions outcomes; the functionalization degree of γ-PGA esters was determined by ^{1}H NMR by comparison of the NH signals of the ester derivative and of the starting material taking into account that the former is always upfield shifted with respect to the latter (peak at about 8.1-8.2 ppm and 8.2-8.3 pmm, respectively)

Method	R	Recovery %	Functionalization %	T (°C)	Time h
A	Et	28	67	45	192
B	Et	89	85	45	120
C	Et	95	25	25	36
D	Et	66	99	25	36
	Bn	60	80	25	36
	n-Bu	12.5	95	25	36

When the esterification was carried out using γ-PGA-TBA salt as starting material, an overall improvement of the reaction outcome was observed. In the case of Kubota methodology, a higher functionalization degree was obtained with a reduction of the reaction time (120 vs 192 hours); on the other hand, the use of tetrabutylammonium salt of γ-PGA in the procedure *via* acyl chloride seems to exert a strong positive effect on functionalization degree for the same reaction time (which in turn is much shortened with respect to the Kubota strategy) even if reduction in the product recovery occurred.

Since the acyl chloride formation approach gave interesting results for the formation of the ethyl ester of γ-PGA, we also tried this approach by using different alcohols (*n*-BuOH and benzyl alcohol), chosen taking into account the different solubility of the tetrabutylammonium salt of γ-PGA in them. Results obtained with benzyl alcohol in which the starting material is soluble are in good agreement with those obtained for the preparation of γ-PGA ethyl ester. On the contrary the low percent recovery of *n*-butyl ester,

with very high functionalization degree, seems to indicate only the small fraction of starting material dissolved in the alcohol actually reacts and is recovered while most of the not reacted substrate is lost in the precipitation step.

The molecular weight of the γ-PGA derivatives was assessed by Size Exclusion Chromatography using a multi-angle laser light scattering (MALS) absolute detector on-line to a size exclusion chromatographic (SEC or GPC) system to make sure that the procedure adopted for the chemical modification does not induce hydrolysis of the backbone peptide bonds. Results obtained for ester synthesized with method D are summarized in Table 7 which reports the usual averages of the molecular weight (Mn, Mw, Mz), the molecular weight of the peak of the chromatogram (Mp), the dispersity indexes (Mw/Mn and Mz/Mw).

Sample	**Solvent**	**M_p**	**M_n**	**M_w**	**M_z**	**M_w/M_n**	**M_z/M_w**
		kg/mol	**kg/mol**	**kg/mol**	**kg/mol**		
PGA-TBA	Water	47.9	12.6	31.6	47.0	2.5	1.5
PGA-TBA-Et	DMF	23.3	10.9	21.8	34.8	2.0	1.6
PGA-TBA-Bn	DMF	45.2	19.2	39.5	61.7	2.1	1.6
PGA-TBA-nBU	DMF	23.1	14.0	20.8	28.5	1.5	1.4

Table 7: SEC-MALS analysis of PGA derivatives.

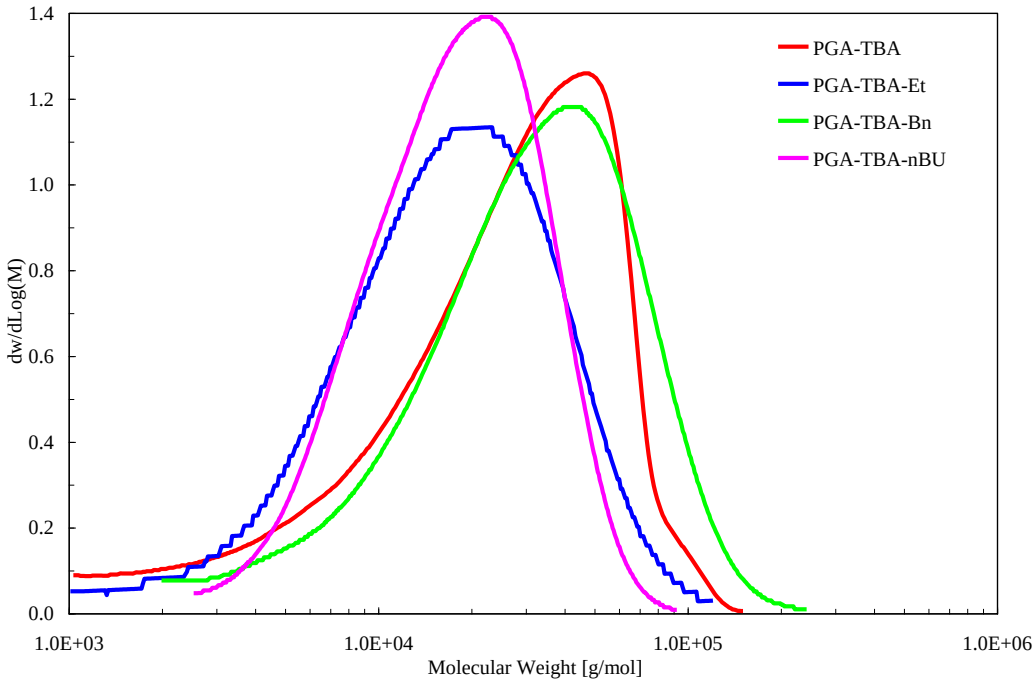

Figure 30: Comparison of Differential MWD of four γ-PGA derivatives

Our data indicate that the esterification procedure *via* acyl-chloride when applied to γ-PGA-TBA salt is a competitive alternative to the Kubota method: the reaction gives good results both in recovery and fuctionalization degree and allows a significant reduction of reaction time. The drawback is that the method is feasible and effective only when the substrate is soluble in the alcohol used for derivatization

Encouraged by these interesting results obtained for the esterification reaction, we decided to use γ-PGA TBA salt also as starting material for the synthesis of amides, with the final goal to find out experimental conditions applicable to an effective and efficient functionalization of the polymer with a peptide, thus creating a material with potential applications in drug-delivery field.

To this aim we thought to use the already described Akagi procedure properly modified taking into account the enhanced solubility of our modified polymer (Scheme 9)

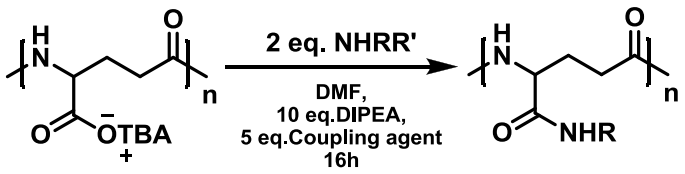

Scheme 9: preparation of γ-PGA amides

In particular, using γ-PGA benzyl amide as reference compound, we tested a number of coupling agents, namely EDC, commonly used by Akagi for amide formation, TFFH, used in literature for the formation of hindered amides, and COMU^{TM}. Obtained results are summarized in Table 8.

Method	Coupling Agent	Recovery %	Functionalization %
A	EDC	82	99
B	TFFH	68	99
C	COMU	81	99

Table 8: comparison of three different coupling agents performance in the preparation of γ-PGA benzyl amide.

Although with all three coupling agents the functionalization was almost complete and the recovery yield very high, NMR analysis revealed that the byproducts deriving from TFFH and COMU were only partially removed in product recovery step while using EDC it is possible to obtain a much more pure amide derivative. So we decide to use EDC as reagent of choice for our amidation reactions.

Following the protocol reported in Scheme 9 all the amides reported in Table 9 were prepared.

Amine	Recovery %	Functionalization %
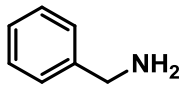	82	99
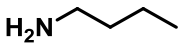	95	80
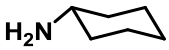	45	75
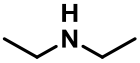	41	70
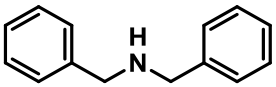	46	45
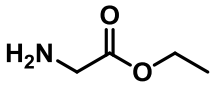	45	33
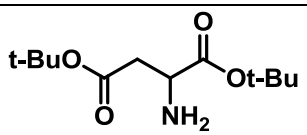	26	65

Table 9: γ-PGA amidation reactions outcomes

The method resulted to be applicable to primary amines with very good results and also quite effective for the preparation of amide derivatives with secondary amines and amino acids. The main problem of the procedure lies in the product recovery step that must be performed using dialysis, thus resulting highly time consuming and detrimental in terms of yield. However any attempt to use an alternative method, for example precipitation followed by centrifugation, was absolutely unsuccessful.

The next step was to use this approach for the synthesis of γ-PGA-peptide conjugates. Some short peptides such as Gly-PheO^tBu, Gly-Asp(O^tBu), Phe-Gly, were tested but unfortunately in all cases we obtained bad results especially with regard to the product recovery.

For this reason, we decided to change strategy taking advantage of solid phase peptide synthesis (SPPS).

Following a standard Fmoc protocol, we prepared some short peptides. After the last amino acid coupling at the end of the sequence but before performing any cleavage from the resin, we condensed γ-PGA-TBA salt to the *N*-terminus of the chain using a combination of HOBt and HBTU as a coupling agents and working at 50°C under MW irradiation (Scheme 10).

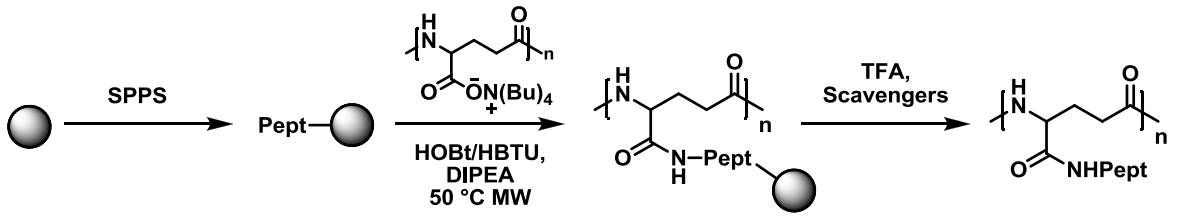

Scheme 10: preparation of γ-PGA peptides conjugates.

Following this strategy we prepared two derivatives (Table 10).

Peptide	Recovery %	Functionalization %
Gly-Phe	30	56
Gly-Tyr-Gly-Arg	35	30

Table 10: outcomes of the coupling reactions of γ-PGA with peptides

Results are still preliminary but very promising and open the way to the set-up of a novel protocol for the preparation of γ-PGA-peptide conjugates.

4. Conclusions

In conclusion, during this PhD thesis the following results were achieved:

1. A micro-wave assisted solid-phase peptide synthesis based on Fmoc strategy of GE11 (a peptide that is known to be a good ligand for EGFR but to have low mitogenic activity) and related fluorescent peptide was carried out.
2. A protocol to conjugate GE11-like peptides to poly(lactic-co-glycolic acid) (PLGA) one of the most successfully developed biodegradable polymers, was established.
3. The resulting PLGA-GE11 conjugates were used to set up a method for the preparation of nanoparticles, that demonstrated to have morphological properties suitable for the intended drug delivery application.
4. Cytocompatibility of PLGA-GE11 nanoparticles was tested and they demonstrated not to have inherent toxicity.

Moreover, intense studies on poly(γ-glutamic acid) (γ-PGA) were performed:

1. A new γ-PGA salt (namely γ-PGA tetrabuthylamonium salt) with enhanced solubility in organic solvents was prepared.
2. Using this material, a new methodolgy for the formation of γ-PGA esters and amides was optimized.
3. A protocol for the derivatization of γ-PGA with peptides , based on γ-PGA-TBA, was set up.
4. Preliminary CD studies to clarify the problem of γ-PGA conformation were performed (see appendix A1).
5. We collected enough clues to reasonably hypothesize that *B. subtilis* GGT, in contrast with other known bacterial GGTs, is evolved to hydrolyze poly(γ-glutamic acid) (see appendix A2).

5. Experimental

5.1. Materials and Methods

γ-PGA was purchased from Natto Bioscience Co. (Japan) as sodium salt (Mw=28,3 kg/mol) or kindly supplied by dr Cinzia Calvio of the Biology and Biotechnology department of the University of Pavia. PLGA was purchased from Laheshore Biomaterials, all other reagents and solvents were purchased from Sigma-Aldrich and/or from VWR International and were used without further purification. All the solvents were of HPLC grade.

Analytical Thin Layer Chromatography TLC was performed on silica gel 60 F254 precoated aluminum sheets (0.2 mm layer; Merck, Darmstadt, Germany); components were detected under an UV lamp (λ 254 nm) and by spraying with a cerium sulfate/ammonium molybdate solution or with a ninhydrin solution (5% (w/v) ninhydrin in ethanol), followed by heating at about 150 °C.

^{1}H NMR spectra were acquired at 400.13 MHz on a Bruker Advance 400 spectrometer (Bruker, Karlsruhe, Germany) interfaced with a workstation running a Windows operating system and equipped with a TOPSPIN software package. ^{1}H chemical shifts (δ) are given inparts per million (ppm) and are referenced to the solvent signals.

Matrix assisted laser desorption/ionization spectra (MALDI TOF) were acquired on a Bruker Microflex LT Spectrometer. Electrospray ionization mass (ESI-MS) spectra were recorded on a Thermo Finnigan LCQ Advantage spectrometer (Hemel Hempstead, Hertfordshire, UK).

For solid phase synthesis a Biotage SP Wave Initiator^{+} synthesizer was used.

SpectraPor3 membranes, MWCO 3500 Da, were used for dialysis.

HPLC were performed using an Amersham pharmacia biotech (P900) liquid chromatographer connected to a UV-vis detector; chromatographic conditions were set as follows: column for analytical HPLC, Jupiter RP-18 (10μm proteo 90A size: 250x4.60 mm, Phenomenex); column for semipreparative HPLC, Jupiter- RP-18 (10 μm,

size:250x10 mm, Phenomenex); detector, λ 226 and 254 nm; mobile phase: A (0,1% TFA (v/v) in water) and B (80% acetonitrile/ 20% water with 0,1% of TFA), gradient elution from 5% to 40% B in 3 column volumes, from 40% to 70% B in 3 cv, from 70% to 100% B in cv and finally 2cv at 100% B.

The characterization of the molecular weight distribution (MWD) of the derivative samples was performed by using a multi-angle laser light scattering (MALS) absolute detector on-line to a size exclusion chromatographic (SEC or GPC) system. The MWD, relative averages and dispersity index of PGA derivatives was obtained by a modular multi-detectors SEC system. The SEC system consisted of an Alliance 2695 separation module from Waters (Milford, MA, USA) equipped with two on-line detectors: a MALS Dawn DSP-F photometer from Wyatt (Santa Barbara, CA, USA) and a 2414 differential refractometer (DRI) from Waters used as concentration detector. The on-line MALS detector furnishes absolute values of the molecular weight of the polymeric samples without external calibration.

5.2. Abbreviations used:

AcOEt: ethyl acetate

BnOH: benzyl alcohol

Boc: *tert*-butoxycarbonyl

BuOH: buthanol

Cbz: carboxybenzyl

COMU: (1-Cyano-2-ethoxy-2-oxoethylidenaminooxy)dimethylamino-morpholino-carbenium hexafluorophosphate

DCM: dichloromethane

DMF: dimethylformamide

DMSO: dimethylsulphoxyde

DIPEA: *N,N*-diisopropylamine

EDC: 1-ethyl-3-(3-dimethylaminopropyl)carbodiimide

EtBr: ethylbromide

EtOEt: diethyl ether

Fmoc: fluorenylmethyloxycarbonyl

HBTU: *O*-benzotriazole-*N,N,N',N'*-tetramethyl-uronium-hexafluoro-phosphate

HOBt: hydroxybenzotriazole

MeOH: methanol

NHS: *N*-hydroxysuccinimide

PLGA: poly(lactic-co-glycolic acid)

TBAOH: tetrabuthylammonium hydroxyde

TFA: trufluoroacetic acid

TFFH: tetramethylfluoroformamidinium hexafluorophosphate

TIPS: triisopropylsilane

Trt: trytil

5.3. Procedures

5.3.1. Preparation of Fmoc-Val-2-Cl-Trityl resin

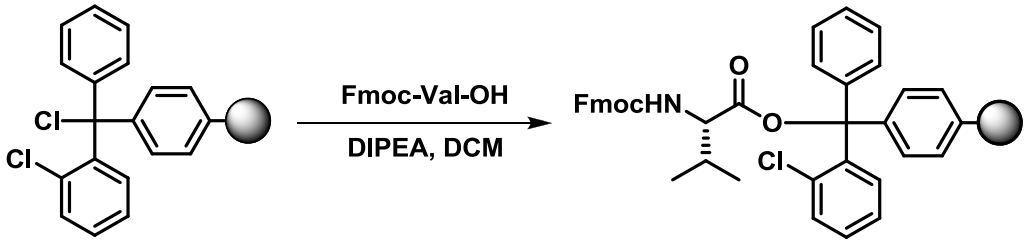

In a plastic syringe equipped with a filter, Cl-(Cl)Trt-resin (320 mg, loading: 1.25 mmol/g) was suspended in anhydrous DCM (3 mL). Fmoc-Val-OH (163 mg, 0.48 mmol) and DIPEA (0.33 mL, 1.92 mmol) were added and the mixture was shaken using an orbital shaker for1.5 hours. Solvent was then removed and resin was washed using a DCM/MeOH/DIPEA (17:2:1) mixture (3 times with 3 mL each), DCM (3 times with 3 mL each), DMF (2 times with 3 mL each) and DCM again (2 times with 3 mL each) and finally dried.

365 mg of dry resin were obtained, corresponding to a Fmoc-Val-OH loading of about 0.45 mmol/g

5.3.2. Preparation of FQPV tetrapeptide

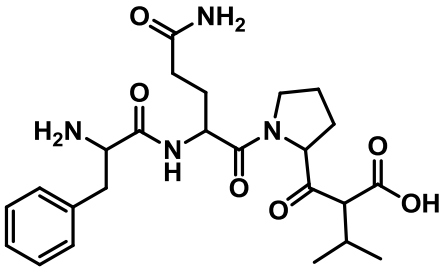

Peptide was obtained by MW assisted solid phase automated synthesis using Fmoc-protocol on a Biotage SP Wave Initiator^{+} synthesizer using a preloaded Fmoc-Val-2-Cl-Trityl resin, swelled using DMF. Synthesis was carried out on 0.2 mmol scale (450 mg of loaded resin).

Each Fmoc deprotection was performed using a 25% pyperidine in DMF solution.

Each coupling reaction was carried out at 50°C in DMF using HOBt (41 mg, 0.60 mmol) and HBTU (114 mg, 0.60 mmol) as coupling agents and DIPEA (0.10 mL, 1.20 mmol) as base; reaction time was 15 minutes.

Each amino acid was used in a 3 fold excess (0.60 mmol):

- 203 mg of Fmoc-Pro-OH
- 367 mg of Fmoc-Gln(Trt)-OH
- 233 mg of Fmoc-Phe-OH

Each amino acid was dissolved, along with coupling agents and DIPEA, in DMF (3 mL) 15 minutes before the reaction

For cleavage a 99% TFA aqueous solution was used: the resin was transferred in a round bottom flask and treated with the cleavage solution for about 1 hour. The solid support was then removed by filtration and the resulting oil was diluted with EtOEt at 0°C. The solvent was removed *in vacuo* and the residue treated with 1:1 hexane:EtOEt mixture and left overnight at -15°C.

Raw product was collected as white solid and purified by HPLC.

78 mg of white solid (1.6 mmol, 80% yield) were obtained.

ESI (*m/z):* 490,4(M+1)

5.3.3. PLGA activation

PLGA (50 mg, 1.67×10^{-3} mmol) was dissolved in anhydrous DCM (2 mL) under nitrogen atmosphere. DIPEA (0.03 mL, 1.67×10^{-1} mmol), EDC×HCl (16.2 mg, 8.35×10^{-2} mmol) and, after 15 minutes NHS (9.6 mg, 8.35×10^{-2} mmol) were added. The reaction mixture was left at RT under magnetical stirring for 24 hours and then washed with water and brine. Organic phase was anidrified using sodium sulphate and dried under reduced pressure.

40 mg of an opaque film were obtained (1.63×10^{-4} mmol, yield: 84%).

5.3.4. PLGA-FQPV

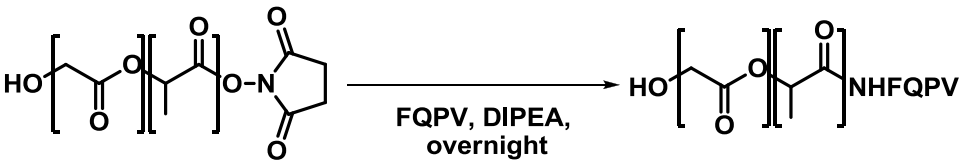

Activated PLGA (50 mg, 2.20×10^{-3} mmol) was dissolved in acetonirtrile (1.5 mL). To the solution FQPV peptide (11 mg, 22×10^{-3} mmol), previously dissolved in acetonitrile (1.5 mL) containing few drops of DIPEA were added, and the mixture was left at RT uneder magnetical stirring for 24 hours. The acetonitrile was removed and the residue was dissolved in of DCM (5 mL) and washed with a NaOH solution (0.5M, 2 times with 3 mL each), water (3 mL) and brine (3 mL). The organic phase was anhydrified using sodium sulphate and dried under reduced pressure.

58 mg of an opaque film were obtained (1.89×10^{-3} mmol) recovery: 86%).

5.3.5. Preparation of Fmoc-Ile-2-Cl-Trityl resin

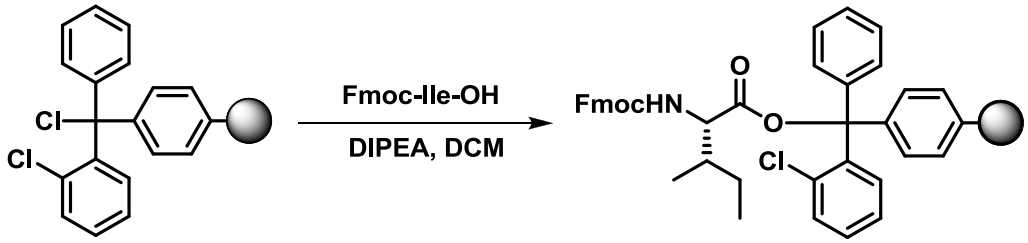

Loading was performed as described in procedure 5.3.1. Fmoc-Ile-OH (170 mg, 0.48 mmol) was used instead of Fmoc-Val-OH

370 mg of dry resin were obtained, corresponding to a Fmoc-Ile-OH loading of about 0.45 mmol/g

5.3.6. Preparation of GE11

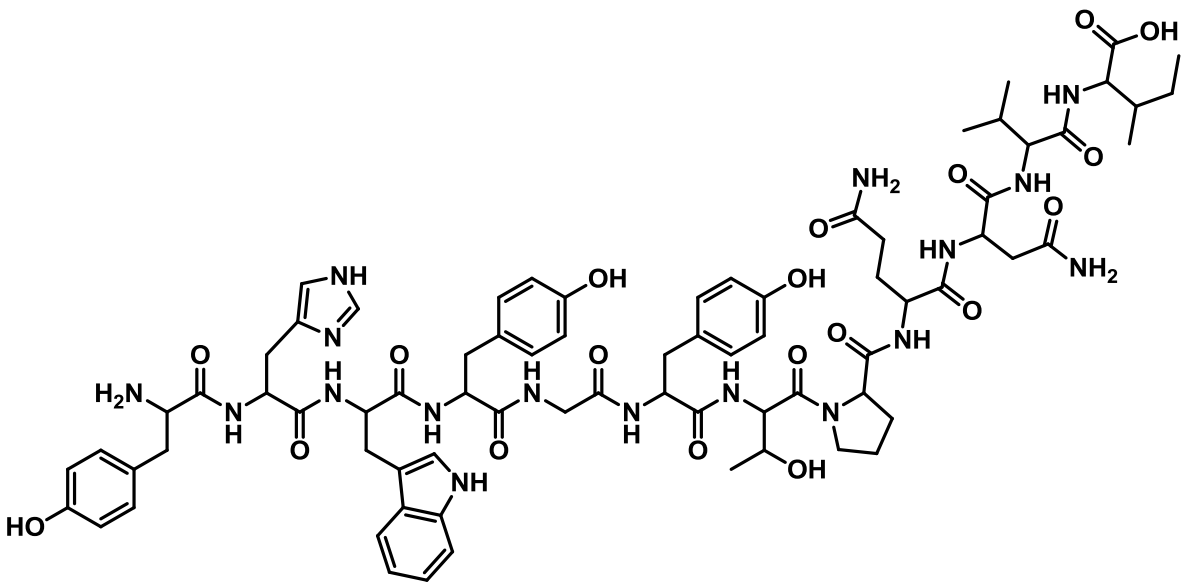

Peptide was obtained by MW assited solid phase automated synthesis using Fmoc-protocol on a Biotage SP wave Initiator^{+} synthesizer using a preloaded Fmoc-Ile-Wang resin, swelled using DMF. Synthesis was carried out on 0.1 mmol scale (220 mg of loaded resin).

Each Fmoc deprotection was performed using a 25% pyperidine in DMF solution.

Each coupling reaction was carried out at 50°C in DMF using HOBt (41 mg, 0.30 mmol) and HBTU (114 mg, 0.30 mmol) as coupling agents and DIPEA (0.10 mL, 0.60 mmol) as base; reaction time was 15 minutes.

Each amino acid was used in a 3 fold excess (0.30 mmol):

- 102 mg di Fmoc-Val-OH
- 179 mg di Fmoc-Asn(Trt)-OH
- 182 mg di Fmoc-Gln(Trt)-OH*
- 101 mg di Fmoc-Pro-OH*
- 119 mg di Fmoc-Thr(tBu)-OH*
- 138 mg di Fmoc-Tyr(tBu)-OH
- 89 mg di Fmoc-Gly-OH
- 138 mg di Fmoc-Tyr(tBu)-OH
- 158 mg di Fmoc-Trp(Boc)-OH*
- 186 mg di Fmoc-His(Trt)-OH*
- 138 mg di Fmoc-Tyr(tBu)-OH*

Each amino acid was dissolved, along with coupling agents and DIPEA, in DMF (3 mL) 15 minutes before the reaction. For amino acids marked with * double coupling protocol was used.

For cleavage a TFA (17,60 ml)/phenol (1.00 g)/H_2O (1.00 ml)/ TIPS (0,40 ml) solution was used: the resin was transferred in a round bottom flask and treated with the cleavage solution for about 1 hour. The solid support was then removed by filtration and the resulting pale yellow oil was treated with EtOEt at 0°C and left overnight at -15°C.

Raw product was collected as white solid and purified by HPLC.

94 mg of white solid (0.06 mmol, 61 % yield) were obtained.

MALDI TOF (m/z): 1541,4 (M+1), 1563 ($M+Na^+$).

5.3.7. Preparation of PLGA-GE11

Activated PLGA (50 mg, 2.20×10^{-3} mmol) was dissolved in acetonitrile (1.5 mL). To the solution were added GE11 peptide (34 mg, 22×10^{-3} mmol), previously dissolved in the minimum amount of water necessary to achieve complete dissolution, and few microliters of DIPEA; the mixture was left at RT uneder magnetical stirring for 24 hours. The acetonitrile was removed and the residue was treated with DCM (5 mL) and washed with a $NaHCO_3$ saturated solution (3 times with 3 mL each), water (3 mL) and brine (3 mL). The organic phase was anhydrified using sodium sulphate and dried under reduced pressure.

48 mg of an opaque film were obtained (1.98×10^{-3} mmol recovery: 90%).

5.3.8. Preparation of 5(6)-carboxyfluorescein succinimidyl ester

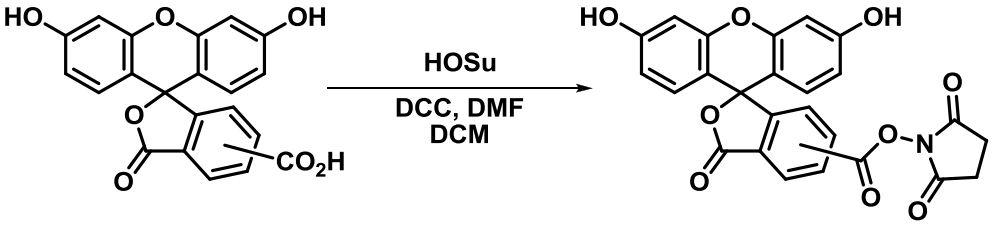

5(6)-carboxyfluoresceine (367 mg, 1.00 mmol) and NHS (149 mg, 1.30 mmol) were dissolved in DCM (12 mL), DMF (3 mL) was added and the mixture cooled to 0°C. DCC (268 mg, 1.30 mmol) was dissolved in DCM (8 mL) and added dropwise to the stirring reaction mixture then was left 5 hours at 0°C and overnight at RT. Reaction mixture was cooled to favour the precipitation of dicyclohexylurea that was filtered. DCM was removed *in vacuo* and the residue was diluted with acetone (15 mL) and phosphate buffer (20 mL, pH=6, 0.1 M); subsequently the solution was extracted with a 2:1 Et_2O/AcOEt mixture (4 times with 15 mL each); reunited organic phases were washed with water and brine, anhydrified with sodium sulphate and the solvent was removed under vacuum. The residue was suspended in Et_2O and filtered.

430 mg of orange solid (3.27 mmol, 91% yield) were obtained.

^{1}H NMR (δ ppm DMSO-d_6): 2.90 (m, 8H, COCH_2CH_2CO); 6.60 (m, 8H, Ar_{Fluo}), 6.69 (br.s, 4H, Ar_{Fluo}), 7,32 (d, *J*=8.0 Hz, 1H, Ar_{Fluo}), 7.64 (s, 1H, Ar_{Fluo}), 8.14 (m, 1H, Ar_{Fluo}), 8.17 (dd, *J*=1.3, 8.0 Hz, 1H, Ar_{Fluo}), 8.41 (d, *J*=1.0 Hz, 1H, Ar_{Fluo})

5.3.9. 6-[Fluorescein-5(6)-carboxyamido]hexanoic acid

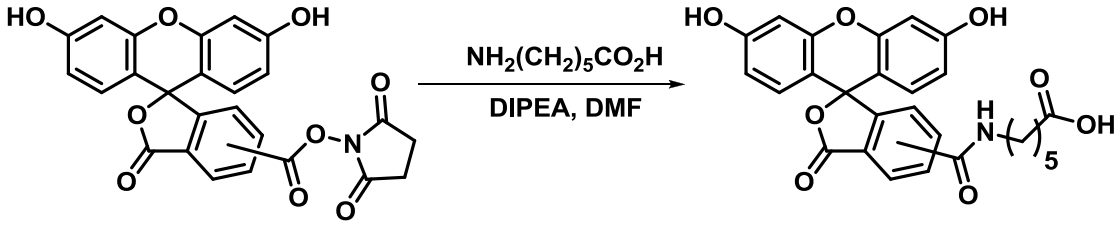

6-aminohexanoic acid (80 mg, 0,61 mmol) was dissolved in anhydrous DMF (4 mL) under nitrogen atmosphere. DIPEA (0.09 mL, 0.51 mmol) and 5(6)-carboxyfluorescein succinimidyl ester (239 mg, 0,51 mmol), previously dissolved in anhydrous DMF (4 mL), were added. The reaction mixture was left at RT under magnetical stirring for 24 hours. The solution was diluted with a saturated bicarbonate solution (12 mL) and washed with AcOEt (2 times with 15 mL each); aqueous phases were acidified to pH=4 with HCl (2M) and then extracted with AcOEt (3 times with 15 mL each). Reunited organic phases were washed with water and brine, anhydrified with sodium sulphate and finally dried under reduced pressure.

153 mg of orange solid (3.29 mmol, yield: 61%) were obtained.

^{1}H NMR (δ ppm MeOD-d_4): 1.30 (m, 2 H, CδH_2), 1.45 (m, 2 H, CγεH_2), 1.56 (m, 2 H, CγεH_2), 2.18 (t, J=7.3 Hz, 2H, CζH_2), 2.23 (t, J=7.76 Hz, 2H, CβH_2), 6.60-(m, 8H, Ar_{Fluo}), 6.67 (br.s, 4H, Ar_{Fluo}), 7.30 (d, J=8.0 Hz, 1H, Ar_{Fluo}), 7.64 (s, 1H, Ar_{Fluo}), 8.10 (m, 1H, Ar_{Fluo}), 8.17 (dd, J=1.3, 8.0 Hz, 1H, Ar_{Fluo}), 8.41 (d, J=1,0 Hz, 1H, Ar_{Fluo}).

5.3.10. Boc-Lys(Z)-OH

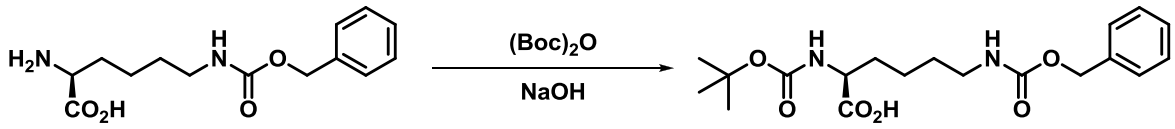

Lys(Cbz)-OH (165 mg, 1.00 mmol) was dissolved in *t*-BuOH:water (1:1, 4 mL) solution. To the mixture were added NaOH (44 mg, 1.00 mmol, pH~12), and, in little portion during 30 minutes, Boc-anhydride (223 mg, 1.00 mmol): a white solid started to precipitate; the solution was left at RT under magnetical stirring overnight. The reaction mixture (pH~8) was washed with *n*-hexane (3 times with 2 mL each); the aqueous phase was acidified to pH~2 using a HCl (0.5 M) solution and extracted with EtOEt (3 times with 2 mL each). Reunited organic phases were washed with water and brine, anhydrified with sodium sulphate and finally dried under reduced pressure.

347 mg of white solid (0.90 mmol, 90% yield) were obtained.

^{1}H NMR (δ ppm MeOD): 1.45 (m, 11H, CβH_2 and $C_{t\text{-}But}CH_3$), 1.55 (m, 2H, CγH_2), 1.80 (m, 2H, CδH_2), 3.20 (m, 2H, CεH_2), 4.35 (m, 1H, CαH), 5.10 (m, 2H, CH_2Ph), 7.35 (m, 5H, Ph).

5.3.11. Boc-Lys-OH

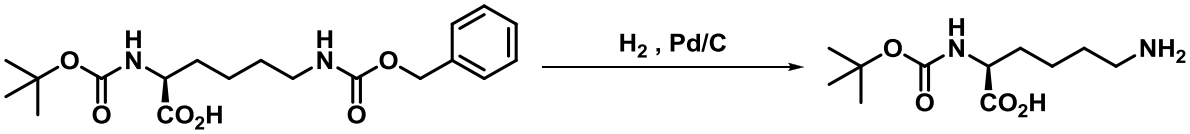

Under argon atmosphere of 10% Pd/C catalyst (335 mg) was suspended in ethanol (5 mL) containing ammonium formate (252 mg, 4.00 mmol). Boc-Lys(Cbz)-OH (347 mg, 1.00 mmol) previously dissolved in ethanol (5 mL) was added and the mixture was refluxed for 5 hours. Catalyst was removed by filtration on celite and the ethanol was removed.

245 mg of white solid (0.99 mmol, 99% yield) were obtained.

^{1}H NMR (δ ppm MeOD): 1.49 (m, 11H, Cβ*H*$_2$ and $C_{t\text{-}But}C$*H*$_3$), 1.75 (m, 4H, Cγ*H*$_2$ and Cδ*H2*), 2.95 (m, 2H, Cε *H*$_2$), 3.95 (m, 1H, Cα*H*).

5.3.12. Boc-Lys(Fmoc)-OH

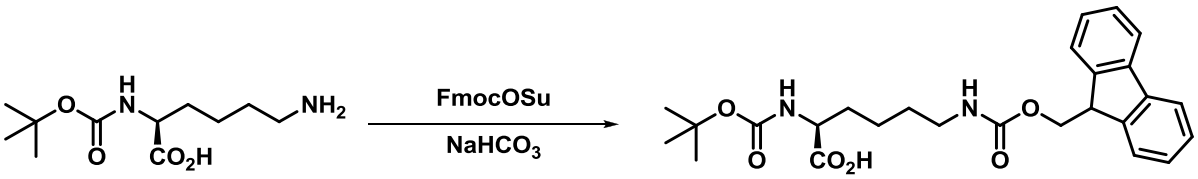

Boc-Lys-OH (343 mg, 0.90 mmol) was dissolved in dioxane:$NaHCO_{3sat}$ (2:1, 15 mL) solution. Working at about 5°C, of Fmoc *N*-hydroxysuccinimide ester (288 mg, 0.85 mmol) was added, in little portion during 40 minutes; after 30 minutes of stirring, reaction mixture were diluted with water and acidified to pH 3 using a solution of $KHSO_4$ (2M). The solution was then extracted using AcOEt (3 times with 5 mL each); reunited organic phases were washed with water and brine, anhydrified with sodium sulphate and finally dried under reduced pressure

395 mg of pale yellow oil were obtained that precipitated by treatment with EtOEt giving 354 mg of white solid (0.76 mmol, 84% yield)

^{1}H NMR (δ ppm DMSO-d_6): 1.35 (m, 13H, CγH_2 C$_\beta H_2$ and $C_{t\text{-}But}CH_3$), 1.60 (m, 2H, CδH_2), 2.95 (m, 2H, Cε H_2), 4.25 (d, 2H, H10), 4.35 (m, 1H, CαH), 4.65 (t, 2H, H9), 7.15 (d, 2H, H1 and H8); 7.40 (dt, 4H, H2 H3 H6 and H7), 7.88 (d, 2H, H4 and H5).

5.3.13. Fmoc-Ile-Wang resin

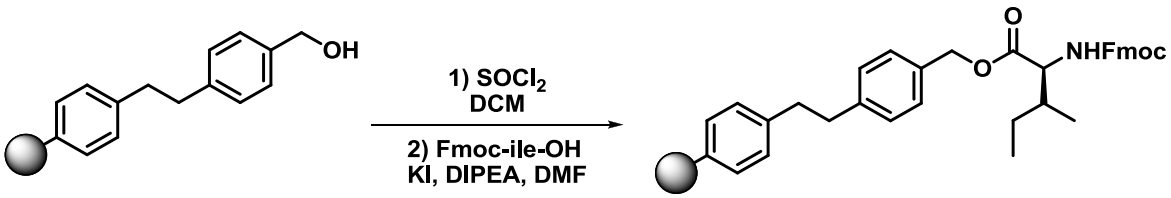

Wang resin (1.50 g, loading 1.21 mmol/g) was suspended in 10 mL of anhydrous DCM under nitrogen atmosphere. Thionyl chloride (0.66 mL, 9.10 mmol) was added and, after 40 minutes, resin was filtered and washed with anhydrous DCM (50 mL) and MeOH (20 mL). The solid was transferred in a round bottom flask containing anhydrous DMF (10 mL) and Fmoc-Ile-OH (1.93 g, 5.50 mmol), KI (92 mg, 0.55 mmol) and, finally, DIPEA (0.96 mL, 5.50 mmol) were added; the mixture was left at RT under magnetical stirring overnight. Resin was filtered, washed with DMF and DCM and then dried.

1.16 g of dry resin was obtained corresponding to a Fmoc-Val-OH loading of about 0.40 mmol/g.

5.3.14. Preparation of Fmoc-6-aminohexanoic acid

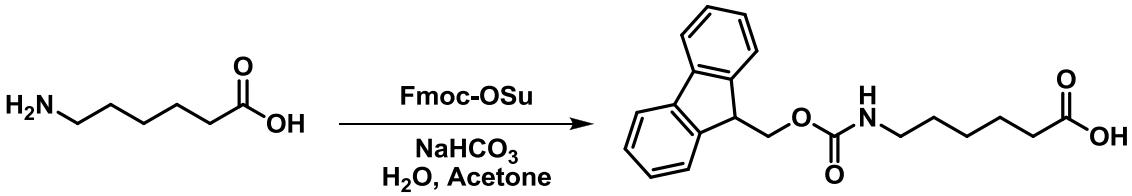

6-hexanoic acid (131 mg, 1.00 mmol) was dissolved in water (8 mL) containing $NaHCO_3$ (168 mg, 2.00 mmol). To the stirred solution Fmoc-OSu (320 mg, 0.95 mmol), previously dissolved in acetone (6 mL), were added dropwise. The reaction mixture was left under stirring at RT for 24 hours. Acetone was then removed under reduced pressure and the resulting solution was washed with EtOEt (2 times with 4 mL each), bring to pH~2 using HCl (0.1 M) solution and finally extracted with DCM (3 times with 20 mL each). Reunited organic phases were washed with water and brine, anhydrified using sodium sulphate and finally dried under reduced pressure. The resulting oil was purified by flash chromatography on silica gel (eluent 5:1 MeOH/DCM).

299 mg of white solid (0.85 mmol, 85% yield) were obtained.

^{1}H NMR (δ ppm MeOD-d_4): 1.36 (m, 2 H, CδH_2), 1.52 (m, 2 H, CγεH_2), 1.68 (m, 2 H, CγεH_2), 2.31 (t, *J*= 7.20 Hz, 2H, CζH_2), 3.15 (q, *J*= 6.49, 12.99 Hz, 2 H, CβH_2), 4.21 (t, *J*= 6.95 Hz, 1 H, CH_{Fmoc}), 4.39 (d, *J*= 6.84 Hz, 2 H, -CH_2Fmoc), 7.21 (dd, 2H, *J*= 7.41, 1.00 Hz Ar_{Fmoc}), 7.33 (t, 2H, *J*= 7.41 Hz Ar_{Fmoc}), 7.62 (d, *J*= 7.66, 2H, Ar_{Fmoc}), 7.80 (d, *J*= 7.66, 2H, Ar_{Fmoc}).

5.3.15. (Fmoc-6-aminohexanoic acid)-2-Cl-Trityl resin

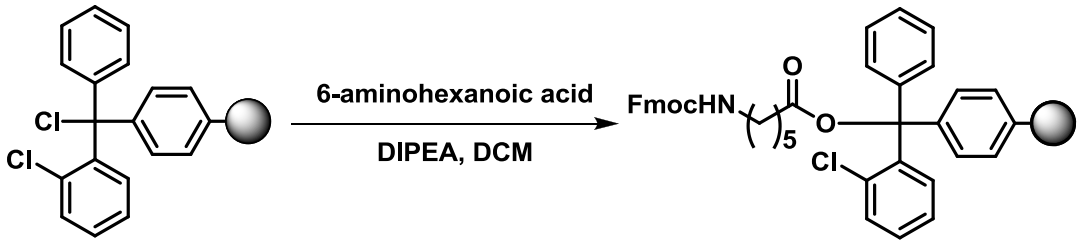

In a plastic syringe equipped with a filter, Cl-(Cl)Trt-resin (1.00 g, functionalization 1.60 mmol/g) were suspended in anhydrous DCM (10 mL). Fmoc-hexanoic acid (555 mg, 1.60 mmol) and DIPEA (1.10 mL, 6.40 mmol) were added and the mixture was shaken using an orbital shaker for1.5 hours. Solvent was removed and resin was washed using a DCM/MeOH/DIPEA (17:2:1) mixture (3 times with 6 mL each), DCM (3 times with 6 mL each), DMF (2 times with 6 mL each) and DCM again (2 times with 6 mL each) and finally dried.

1.357 g of dry resin were obtained corresponding to a Fmoc-hexanoic acid loading of about 0.825 mmol/g.

5.3.16. 6-[Fluoresceine-5(6)-carboxyamido]hexanoic acid

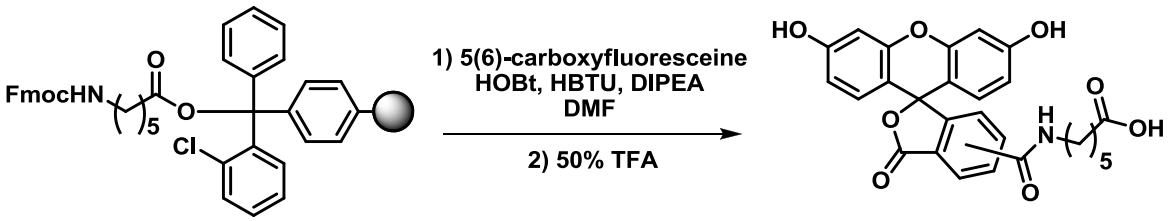

Fmoc-hexanoic acid (340 mg, 0.96 mmol) charged resin (0.28 mmol) was swelled in a plastic syringe with DMF (5 mL). Swelling solvent was removed and the resin was treated with of a DMF (5 mL) solution containing HOBt (130 mg, 0.83 mmol), HBTU (310 mg, 0.83 mmol) and 5(6)-carboxyfluoresceine (310 mg, 0.85 mmol); the reaction mixture was shaken at RT for 5 hours. DMF was removed and resin was washed with DMF (5 times with 5 mL each) and DCM (5 times with 5 mL each).

For cleavage 50% TFA aqueous solution was used: the resin was transferred in a round bottom flask and treated with the cleavage solution for about 1 hour. The solid support was then removed by filtration and the resulting solution was diluted with EtOEt at 0°C. A yellow solid precipitated and was collected by filtration.

90 mg of yellow solid were obtained (1.94 mmol, 93% yield).

^{1}H NMR (δ ppm MeOD-d_4): 1.30 (m, 2 H, CδH_2), 1.45 (m, 2 H, CγεH_2), 1.56 (m, 2 H, CγεH_2), 2.18(t, J=7.35 Hz, 2H, CζH_2), 2.23 (t, J=7.76 Hz, 2H, CβH_2), 6.60 (m, 8H, Ar_{Fluo}), 6.67 (br.s, 4H, Ar_{Fluo}), 7.30 (d, J=8.04 Hz, 1H, Ar_{Fluo}), 7.64 (s, 1H, Ar_{Fluo}), 8.10 (m, 1H, Ar_{Fluo}), 8.17 (dd, J=1.29, 8.01 Hz, 1H, Ar_{Fluo}), 8.41 (d, J=1.00 Hz, 1H, Ar_{Fluo}).

5.3.17. Fluoresceine labelled GE11

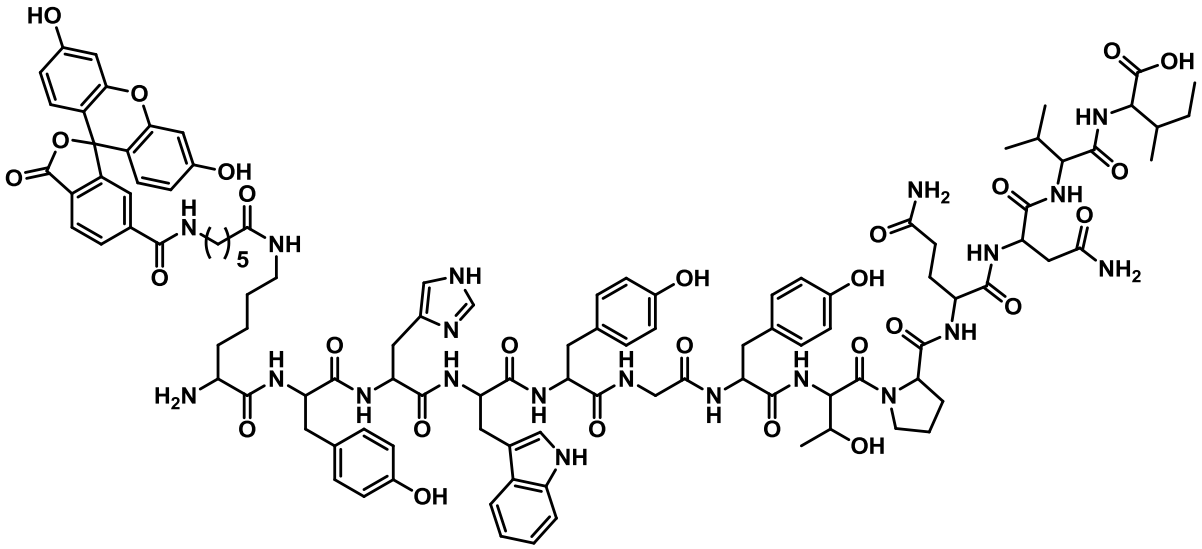

Peptide was obtained by MW assisted solid phase automated synthesis using Fmoc-protocol on a Biotage SP wave Initiator^{+} synthesizer using a preloaded Fmoc-Ile-Wang resin, swelled using DMF. Synthesis was carried out on 0.1 mmol scale (220 mg of loaded resin).

Each Fmoc deprotection was performed using a 25% pyperidine in DMF solution.

Each coupling reaction was carried out at 50°C in DMF using HOBt (41 mg, 0.30 mmol) and HBTU (114 mg, 0.30 mmol) as coupling agents and DIPEA (0.10 mL, 0.60 mmol) as base; reaction time was 15 minutes.

Each amino acid was used in a 3 fold excess (0.30 mmol):

- 102 mg of Fmoc-Val-OH
- 179 mg of Fmoc-Asn(Trt)-OH
- 182 mg of Fmoc-Gln(Trt)-OH*
- 101 mg of Fmoc-Pro-OH*
- 119 mg of Fmoc-Thr(tBu)-OH*
- 138 mg of Fmoc-Tyr(tBu)-OH
- 89 mg of Fmoc-Gly-OH
- 138 mg of Fmoc-Tyr(tBu)-OH
- 158 mg of Fmoc-Trp(Boc)-OH*

- 186 mg of Fmoc-His(trt)-OH*
- 138 mg of Fmoc-Tyr(tBu)-OH*
- 188 mg of Fmoc-Lys(Mtt)-OH*

NB Mtt group was removed treating resin with a DCM/TFA/TIPS (94:1:5) mixture for 5 minutes each; deprotection was repeated until no more color in the cleavage solution could be noticed. After deprotection the resin was washed with DMF (6 times with 3 mL each).

- 245 mg of Fluo-hexanoic acid**

Each amino acid was dissolved, along with coupling agents and DIPEA, in DMF (3 mL) 15 minutes before the reaction.

For amino acids marked with * double coupling protocol. was used.

For coupling marked with ** each reagent was used in 5 fold excess and the reaction was carried out at RT using double coupling protocol.

For cleavage a TFA (17,60 ml)/phenol (1.00 g)/H_2O (1.00 ml)/ TIPS (0,40ml) solution was used: the resin was transferred in a round bottom flask and treated with the cleavage solution for about 1 hour. The solid support was then removed by filtration and the resulting pale yellow oil was treated with EtOEt at 0°C and left overnight at -15°C.

Raw product was collected as yellow solid and purified by HPLC.

108 mg of yellow solid were obtained (0.05 mmol, 50 % yield).

MALDI TOF (m/z): 2157,7 (M+1), 2179.3 ($M+Na^+$).

5.3.18. PLGA-FluoGE12

Activated PLGA (50 mg, 2.20×10^{-3} mmol) was dissolved in acetonitrile (1.5 mL). To the solution were added FluoGE12 peptide (46 mg, 22×10^{-3} mmol), previously dissolved in the minimum amount of water necessary to achieve complete dissolution, and the mixture was left at RT uneder magnetical stirring for 24 hours. The acetonitrile was removed and the residue was treated with DCM (5 mL) and washed with a $NaHCO_3$ saturated solution (3 times with 3 mL each), water (3 mL) and brine (3 mL). The organic phase was anhydrified using sodium sulphate and dried under reduced pressure.

48 mg of an opaque film were obtained (1.98×10^{-3} mmol recovery: 90%).

5.3.19. Preparation of γ-PGA-tetrabutylammonium salt

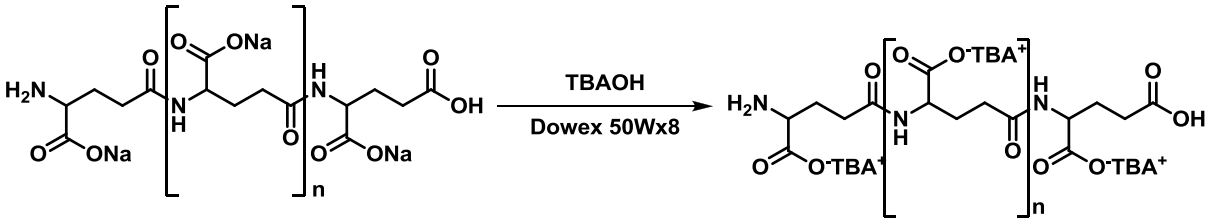

γ-PGA-sodium salt (1,00 g, 6.62 mmol) was dissolved in distilled water (40 ml) and then percolated through a column filled with wet Dowex (3 ml) 50Wx8 ion-exchange sulphonic resin, previously activated for 30 min with an excess of a 40% w/v solution of tertrabutylammonium hydroxide. The resin was subsequently washed 8 times with distilled water. The eluate was collected and lyophilized.

2.20 g of γ-PGA-tetrabutylammonium salt (5.96 mmol, recovery: 90%; ammonium ion exchange degree: 50%) were obtained.

^{1}H NMR (δ ppm DMSO-d_6):0.96 (q, 12H, N($CH_2CH_2CH_2CH_3$)$_4$); 1.32 (m, 8H, N($CH_2CH_2CH_2CH_3$)$_4$); 1.58 [m, 8H, N($CH_2CH_2CH_2CH_3$)$_4$); 1.74 (m, 1H, CβH_2); 1.95 (m, 1H, CβH_2); 2.14 (m, 2H, CγH_2); 3.16 (t, 8H, N($CH_2CH_2CH_2CH_3$)$_4$); 4.07 (s, 1H, Cα*H*); 7.97 (s, 1H, -CON*H*).

5.3.20. Preparation of poly(α-ethyl γ-glutamate), method A

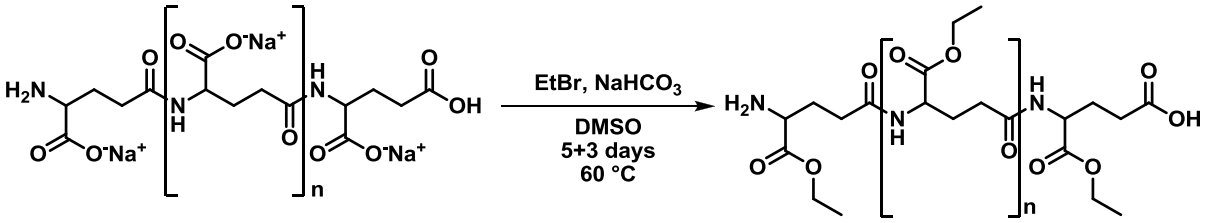

γ-PGA sodium salt (2,00 g 11,83 mmol) was suspended in DMSO (80 ml) and heated, under stirring, to 45 °C. As the solution became homogenous, $NaHCO_3$ (1.99 g, 23,66 mmol) and EtBr (4.38 mL, 59.16 mmol) were added; the reaction was left at 45 °C for 5 days. The solution was cooled to room temperature and then added dropwise to 750 mL of acidic water (pH ~2): a sticky compound precipitated. After filtration, ^{1}H-NMR showed it to be the α-ethyl ester of γ-PGA, with a low (44%) functionalisation degree. The material was again reacted in the same conditions for 3 more days and recovered as already described and residual DMSO traces were removed in high vacuum

525 mg of yellowish powder were obtained (3.33 mmol; Recovery: 28%; functionalisation: 67%).

^{1}H NMR (δ ppm DMSO-d_6): 1.17 (t, 3H, -COOCH$_2$C*H$_3$*); 1.76 [m, 1H, Cβ*H$_2$*); 1.95 (m, 1H, Cβ*H$_2$*); 2.16 (m, 2H, Cγ*H$_2$*); 4.05 (q, 2H, -COOC*H$_2$*CH$_3$); 4.19 (m, 1H, Cα*H*); 8.22 (d, 1H, -CON*H*).

Mw (SEC-MALS): 37.9 kg/mol (first generation), 33.4 kg/mol (second generation).

5.3.21. Preparation of poly(α-ethyl γ-glutamate), method B

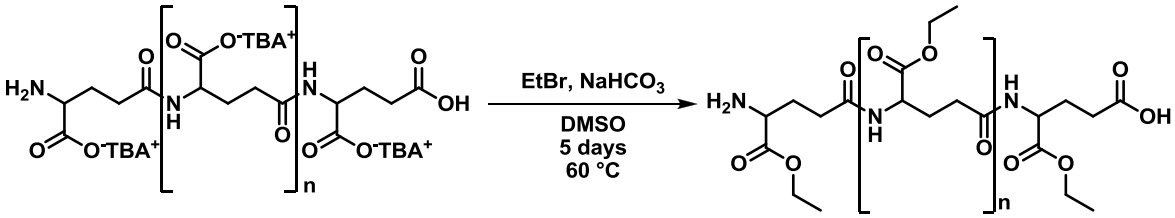

γ-PGA sodium salt (4.37g, 11,83 mmol) was dissolved in DMSO (80 mL) and heated to 45 °C, under magnetic stirring. Then, $NaHCO_3$ (1.99 g, 23,66 mmol) and EtBr (4.38 mL, 59.16 mmol) were added. The reaction was stirred at 45 °C and after 5 days the solution was cooled to room temperature and then added dropwise to 750 mL of acidic water (pH ~2). A sticky compound, that after was recovered by filtration, precipitated. Residual DMSO traces were removed under the high vacuum.

1.987g of brownish powder (10.53 mmol; Recovery: 89.1%; functionalisation: 85%) were obtained.

^{1}H NMR (δ ppm DMSO-d_6): 1.17 (t, 3H, -COOCH$_2$C*H$_3$*); 1.75 [m, 1H, Cβ*H$_2$*); 1.96 (m, 1H, Cβ*H$_2$*); 2.16 (m, 2H, Cγ*H$_2$*); 4.06 (q, 2H, -COOC*H$_2$*CH$_3$); 4.19 (m, 1H, Cα*H*); 8.22 (d, 1H, -CON*H*).

Mw (SEC-MALS): 37.9 kg/mol

5.3.22. Preparation of α-ethyl ester of γ-PGA, method C

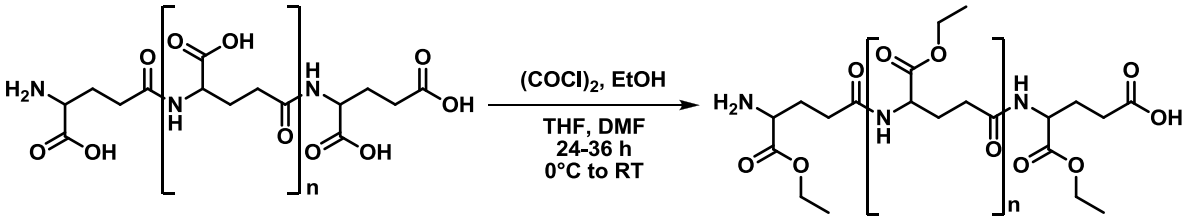

γ-PGA (76 mg, 0.27 mmol) was suspended in anhydrous ethanol (4 mL) and cooled to 0 °C in an ice bath, oxalyl chloride (0.87 mL, 10,20 mmol) and a catalytic amount of anhydrous DMF (~0,1 ml) were then added paying attention not to let the temperature increase above 5 °C. The reaction mixture was left under stirring at RT for 48 hours. The solution was diluted with ethanol (14 ml) and neutralized with saturated $NaHCO_3$ solution (~20 ml). Methanol was removed at the rotary evaporator and formation of a white precipitate was observed. The product was filtered and washed with little portions of distilled water, ethanol and diethyl ether.

101 mg of white powder (x mmol; recovery: 95 %; functionalisation 25%) were collected.

^{1}H NMR (δ ppm DMSO-d_6): 1.18 (t, 3H, -COOCH$_2$C*H$_3$*); 1.77 (m, 1H, Cβ*H$_2$*); 1.97 (m, 1H, Cβ*H$_2$*); 2.18 (m, 2H, Cγ*H$_2$*); 4.05 (q, 2H, -COOC*H$_2$*CH$_3$); 4.20 (m, 1H, Cα*H*); 8.22 (d, 1H, -CON*H*).

Mw (SEC-MALS): 30.0 kg/mol.

5.3.23. General procedure for a synthesis of γ-PGA-esters, method D

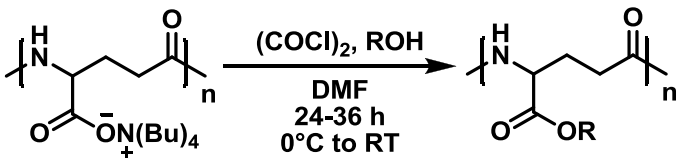

γ-PGA–TBA (100 mg, 0.27 mmol) was suspended in suitable alcohol (3-12 mL), cooled to 0 °C in an ice bath and oxalyl chloride (0.87 mL, 10,20 mmol) and a catalytic amount of anhydrous DMF (~0,1 ml) were then warily added, paying attention not to let the temperature increase above 5 °C. The reaction mixture was left under magnetical stirring at RT for 48 hours. The solution was diluted with ethanol (14 ml) and neutralized with saturated $NaHCO_3$ solution (~20 ml). After removal of methanol at the rotary evaporator, the formation of a white precipitate was observed. The product was filtered and washed with little portions of distilled water, ethanol and diethyl ether.

5.3.23.1. Preparation of α-ethyl ester of γ-PGA

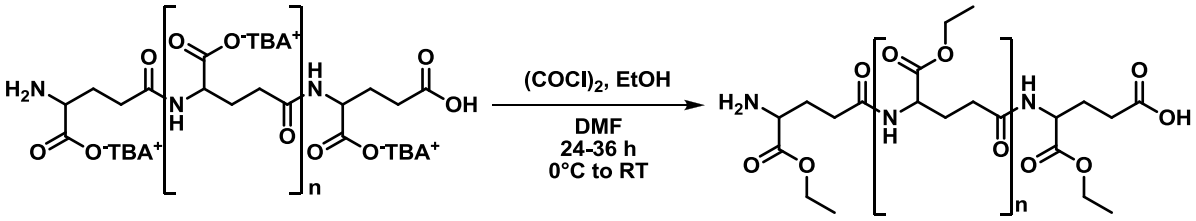

γ-PGA-TBA (100 mg, 0.27 mmol) was suspended in anhydrous ethanol (3 mL) and cooled to 0 °C in an ice bath, oxalyl chloride (0.87 mL, 10,20 mmol) and a catalytic amount of anhydrous DMF (~0,1 ml) were then added. The work-up was done as it is described in general procedure for preparation of γ-PGA-esters (5.3.23).

26.3 mg of white powder (0.18 mmol; recovery: 66 %; functionalisation: 99%) were collected.

^{1}H NMR (δ ppm DMSO-d_6): 1.16 (t, 3H, -COOCH$_2$CH_3); 1.73 (m, 1H, CβH_2); 1.96 (m, 1H, CβH_2); 2.13 (m, 2H, CγH_2); 4.07 (q, 2H, -COOCH_2CH$_3$); 4.17 (m, 1H, CαH); 8.20 (d, 1H, -CONH).

Mw (SEC-MALS): 30.0 kg/mol.

5.3.23.2. Preparation of α-Benzyl ester of γ-PGA

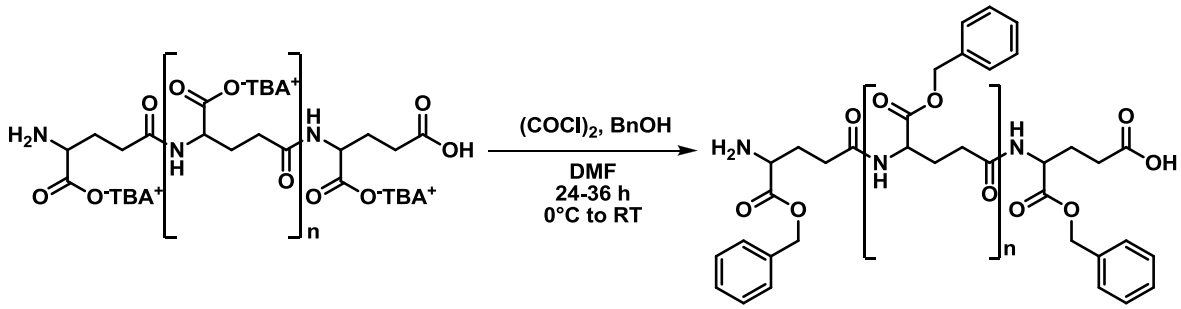

γ-PGA-TBA (100 mg, 0.27 mmol) was suspended in anhydrous ethanol (4 mL) and cooled to 0 °C in an ice bath, oxalyl chloride (0.87 mL, 10,20 mmol) and a catalytic amount of anhydrous DMF (~0,1 ml) were then added. The work-up was done as it is described in general procedure for preparation of γ-PGA-esters (5.3.23).

38 mg of white powder (0.17 mmol; recovery: 63 %; functionalisation 80%) were collected.

^{1}H NMR (δ ppm DMSO-d_6): 1.76 (m, 1H, CβH_2); 1.92 (m, 1H, CβH_2); 2.21 (m, 2H, CγH_2); 4.21 (m, 1H, Cα*H*); 5.11 (s, 2H, -CH_2Ph); 7.37 (s, 5H, Ph); 8.12 (d, 1H, -CON*H*).

5.3.23.3. Preparation of α-*n*-butyl ester of γ-PGA

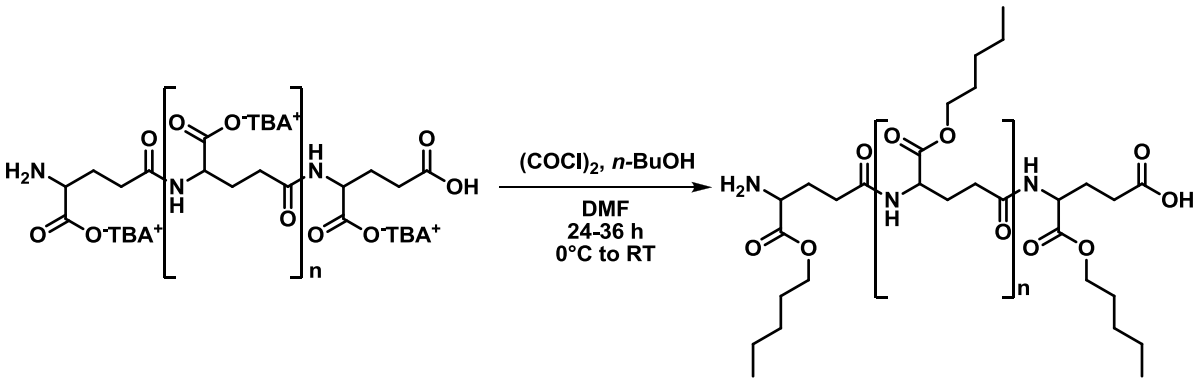

γ-PGA-TBA (100 mg, 0.27 mmol) was suspended in anhydrous *n*-BuOH (12 mL) and cooled to 0 °C in an ice bath, oxalyl chloride (0.87 mL, 10,20 mmol) and a catalytic amount of anhydrous DMF (~0,1 ml) were then added. The work-up was done as it is described in general procedure for preparation of γ-PGA-esters (5.3.23).

23 mg of white powder (0.12 mmol; recovery: 45 %; functionalisation: 95%) were collected.

^{1}H NMR (δ ppm DMSO-d_6): 0.91 (t, 3H, -COO(CH$_2$)$_3$C*H*$_3$); 1.39 (m, 2 H, -O(CH$_2$)$_2$C*H*$_2$CH$_3$); 1.62 (m, 2H, -OCH$_2$C*H*$_2$CH$_2$CH$_3$); 1.74 (m, 1H, Cβ*H*$_2$); 1.97 (m, 1H, Cβ*H*$_2$); 2.21 (m, 2H, Cγ*H*$_2$); 4.05 (m, 2H, -COOCH$_2$(C*H*$_2$)$_2$CH$_3$); 4.17 (m, 1H, Cα*H*); 8,13 (d, 1H, -CON*H*).

5.3.24. Prepraration of γ-PGA benzylamide, method A

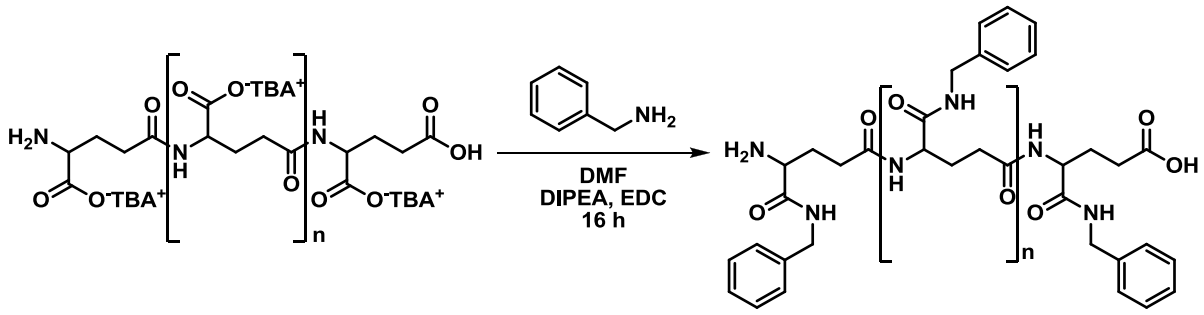

γ-PGA-TBA (100 mg, 0.27 mmol) was dissolved in anhydrous DMF (5 mL) under nitrogen atmosphere. DIPEA (1.72 mL, 10,00 mmol), EDC×HCl (210 mg, 1.35 mmol) and, after complete dissolution, benzylamine (0.06 mL, 0.54 mmol) were added. The reaction mixture was left under magnetical stirring for 16 hours. The solution was transferred in a dialysis tube, dialyzed against distilled water for 48 hours and finally freeze dried.

48 mg of brownish solid (0.22 mmol; recovery: 82%; functionalization: 99%) were recovered.

^{1}H NMR (δ ppm DMSO-d_6): 1.75 (m, 2H, CβH_2); 2.20 (m, 2H, CγH_2); 4.25 (m, 1H, Cα*H*); 4.85 (s, 2H, -CH_2Ph); 7.25 (m, 5H, Ph); 8.15 (m, 1H, -CON*H*); 8.45 (m, 1H, -NHCH$_2$Ph).

5.3.25. Preparation of γ-PGA benzylamide, method B

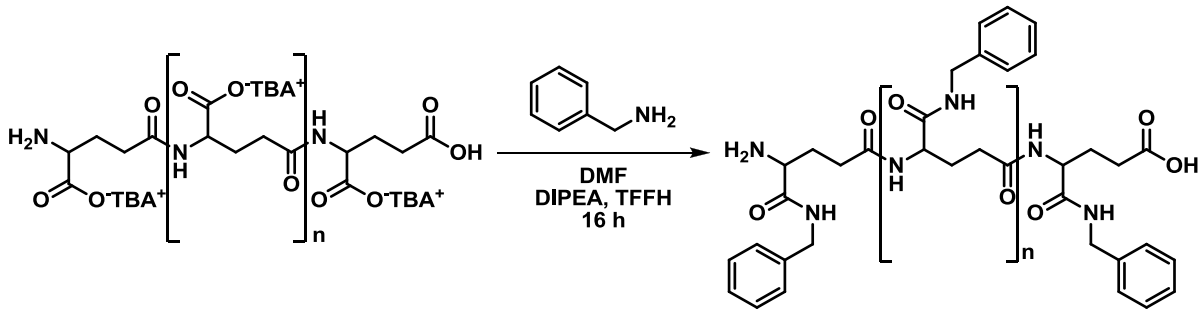

γ-PGA-TBA (100 mg, 0.27 mmol) was dissolved in anhydrous DMF (5 mL) under nitrogen atmosphere. DIPEA (0.47 mL, 1.35 mmol), TFFH (178 mg, 1.35 mmol) and, after complete dissolution, benzylamine (0.06 mL, 0.54 mmol) were added. The reaction mixture was left under magnetical stirring for 16 hours. The solution was transferred in a dialysis tube, dialyzed against distilled water for 48 hours. and finally freeze dried.

40 mg of white solid (0.18 mmol; recovery: 68%, functionalization: 99%) were recovered.

^{1}H NMR (δ ppm DMSO-d_6): 1.74 (m, 2H, CβH_2); 2.23 (m, 2H, CγH_2); 4.26 (m, 1H, CαH); 4.84 (s, 2H, -CH_2Ph); 7.23 (m, 5H, Ph); 8.16 (m, 1H, -CONH); 8.41 (m, 1H, -NHCH$_2$Ph).

5.3.26. Preparation of γ-PGA benzylamide, method C

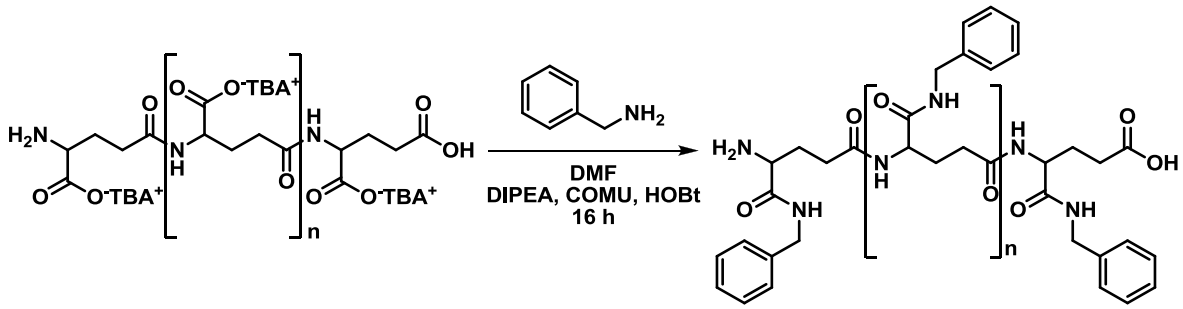

γ-PGA-TBA (100 mg, 0.27 mmol) was dissolved in anhydrous DMF (5 mL) under nitrogen atmosphere. DIPEA (0.86 mL 5,00 mmol), COMU (300 mg, 1.35 mmol), HOBt (91 mg, 1.35 mmol) and, after complete dissolution, benzylamine (0.06 mL, 0.54 mmol) were added. The reaction mixture was left under magnetical stirring for 16 hours. The solution was transferred in a dialysis tube, dialyzed against distilled water for 48 hours. and finally freeze dried.

46 mg of white solid (0.21 mmol; recovery: 81%, functionalization: 99%) were recovered.

^{1}H NMR (δ ppm DMSO-d_6): 1.76 (m, 2H, CβH_2); 2.19 (m, 2H, CγH_2); 4.27 (m, 1H, Cα*H*); 4.83 (s, 2H, -CH_2Ph); 7.23 (m, 5H, Ph); 8.15 (m, 1H, -CON*H*); 8.44 (m, 1H, -NHCH$_2$Ph).

5.3.27. General procedure for preparation of γ-PGA amides

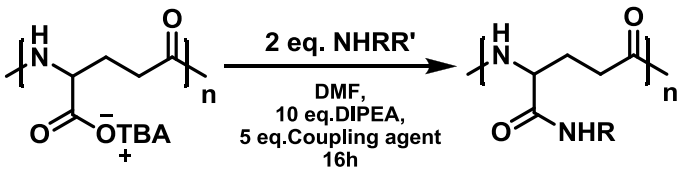

γ-PGA-TBA (100 mg, 0.27 mmol) was dissolved in the minimum quantity of DMF under nitrogen atmosphere. DIPEA (0.94 mL, 2.7 mmol), EDC×HCl (210 mg, 1.35 mmol) and, after complete dissolution, alcohol (0.54 mmol) were added. The reaction mixture was left under magnetical stirring for 16 hours. The solution was transferred in a dialysis tube, dialyzed against distilled water for 48 hours. and finally freeze dried

5.3.27.1. Preparation of γ-PGA n-buthylamide

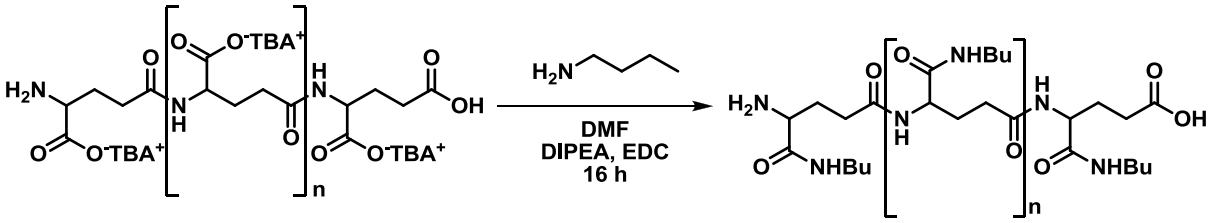

γ-PGA-TBA (100 mg, 0.27 mmol) was dissolved in anhydrous DMF (5 mL) under nitrogen atmosphere. of DIPEA (0.94 mL, 2.7 mmol), EDC×HCl (210 mg, 1.35 mmol) and, after complete dissolution *n*-buthylamine (54 μL, 0.54 mmol) were added. Product was recovered as described in general procedure.

54 mg of white solid (0.25 mmol; recovery: 95%; functionalization: 80%) were recovered.

^{1}H NMR (δ ppm DMSO-d_6): 0.91 (t, 3H, -$(CH_2)_3C\mathit{H}_3$); 1.39 (m, 2H, -$(CH_2)_2C\mathit{H}_2CH_3$); 1.62 (m, 2H, -$CH_2C\mathit{H}_2CH_2CH_3$); 1.85 (m, 2H, Cβ$\mathit{H}_2$); 2.13 (m, 2H, Cγ$\mathit{H}_2$); 4.05 (m, 2H, -$C\mathit{H}_2(CH_2)_2CH_3$); 4.22 (m, 1H, Cα$\mathit{H}_2$); 8.17 (m, 1H, N*H*CO); 8.35 (m, 1H, -N*H*$(CH_2)_3CH_3$).

5.3.27.2. Preparation of γ-PGA cyclohexil amide

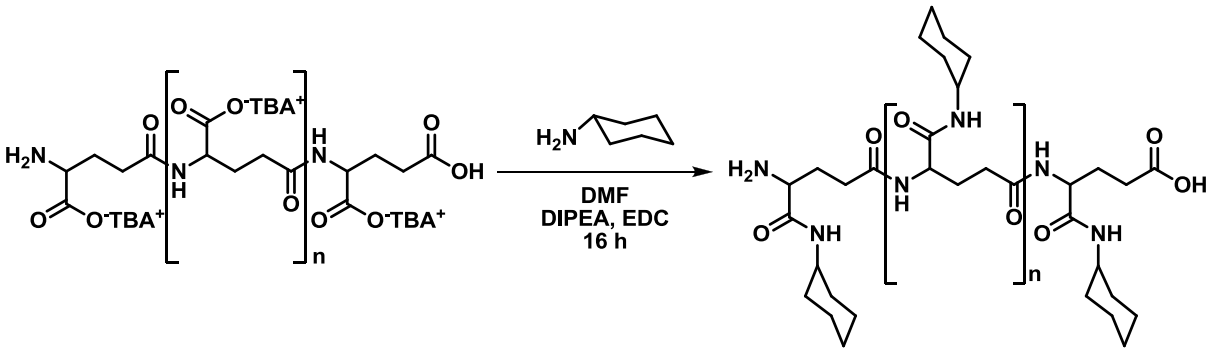

γ-PGA-TBA (100 mg, 0.27 mmol) was dissolved in anhydrous DMF (5 mL) under nitrogen atmosphere. DIPEA (0.94 mL, 2.7 mmol), EDC×HCl (210 mg, 1.35 mmol) and, after complete dissolution, cyclohexylamine (62 μL, 0.54 mmol) were added. Product was recovered as described in general procedure.

45 mg of white solid (0.12 mmol; recovery: 45%; functionalization: 75%) were recovered.

^{1}H NMR (δ ppm DMSO-d_6): 1.12 (m, 5H, *H*ax); 1.92 (m, 7H, CβH_2 + *H*eq); 2.70 (m, 2H, CγH_2); 3.65 (m, 1H, -C*H*NHCO); 4.1 (s, 1H, Cα*H*); 8.15 (m, 1H, -CON*H*).

5.3.27.3. Preparation of γ-PGA dibenzylamide

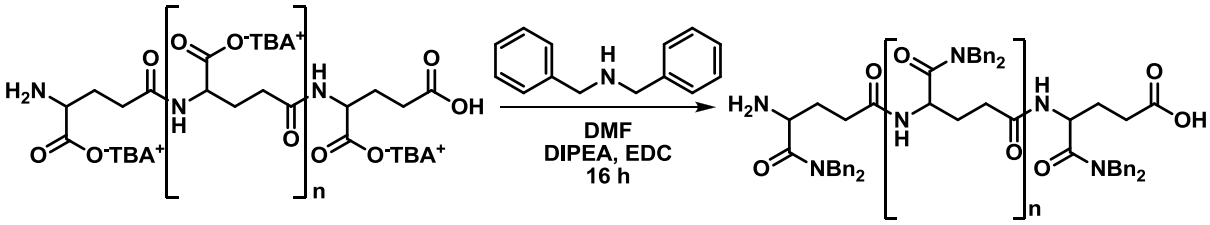

γ-PGA-TBA (100 mg, 0.27 mmol) was dissolved in anhydrous DMF (5 mL) under nitrogen atmosphere. DIPEA (0.94 mL, 2.7 mmol), of EDC×HCl (210 mg, 1.35 mmol) and, after complete dissolution, of dibenzylamine (104 μL, 0.54 mmol) were added. Product was recovered as described in general procedure.

50 mg of white solid (0.125 mmol; recovery: 46%; functionalization: 45%) were recovered.

^{1}H NMR (δ ppm DMSO-d_6): 1.70 (m, 2H, CβH_2); 2.18 (m, 2H, CγH_2); 4.08 (m, 1H, CαH_2); 4.55 (m, 4H, NHCH_2Ph); 7.25(m, 10H, Ph); 8.40 (m, 1H, CONH).

5.3.27.4. Preparation of γ-PGA diethylamide

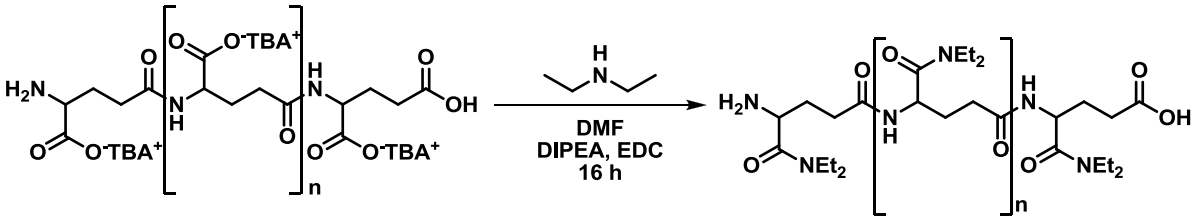

γ-PGA-TBA (100 mg, 0.27 mmol) was dissolved in anhydrous DMF (5 mL) under nitrogen atmosphere. DIPEA (0.94 mL, 2.7 mmol), of EDC×HCl (210 mg, 1.35 mmol) and, after complete dissolution, of dibenzylamine (56 μL, 0.54 mmol) were added. Product was recovered as described in general procedure.

45 mg of white solid (0.11 mmol; recovery: 41%; functionalization: 70%) were recovered.

^{1}H NMR (δ ppm DMSO-d_6): 0.96 (t, 6H, -CH_2CH_3); 1.65 (m, 2H, CβH_2); 2.15 (m, 2H, CγH_2); 4.05 (bq, 4H, -CH_2CH_3); 4.13 (m, 1H, CαH_2); 4.05 (m, 2H, -$CH_2(CH_2)_2CH_3$); 8.18 (m, 1H, N*H*CO); 8.30 (m, 1H, -N*H*$(CH_2)_3CH_3$).

5.3.27.5. Preparation of γ -PGA Gly-OEt

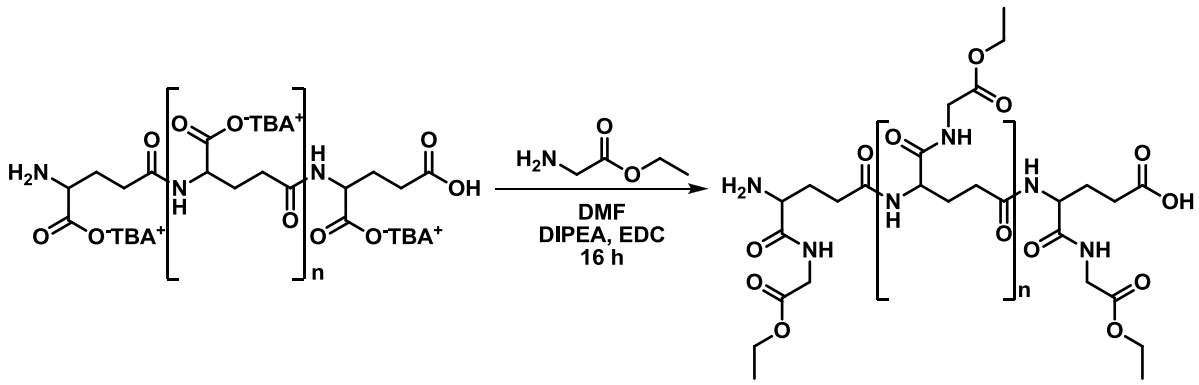

γ-PGA-TBA (100 mg, 0.27 mmol) was dissolved in anhydrous DMF (5 mL) under nitrogen atmosphere. DIPEA (0.94 mL, 2.7 mmol), of EDC×HCl (210 mg, 1.35 mmol) and, after complete dissolution, Gly-OEt*HCl (76 mg, 0.54 mmol) were added. Product was recovered as described in general procedure.

46 mg of white solid (0.12 mmol; recovery: 45%; functionalization: 33%) were recovered.

^{1}H NMR (δ ppm DMSO-d_6): 1.13 (t, 3H, -CH_2CH_3); 1.78 (m, 2H, CβH_2); 2.18 (m, 2H, CγH_2); 3.03 (m, 2H, $C\alpha_{Gly}H_2$); 4.05 (m, 1H, $C\alpha_{Glu}H$); 4.20 (m, -CH_2CH_3).

5.3.27.6. Preparation of γ-PGA H-Asp(O-tBu)$_2$ amide

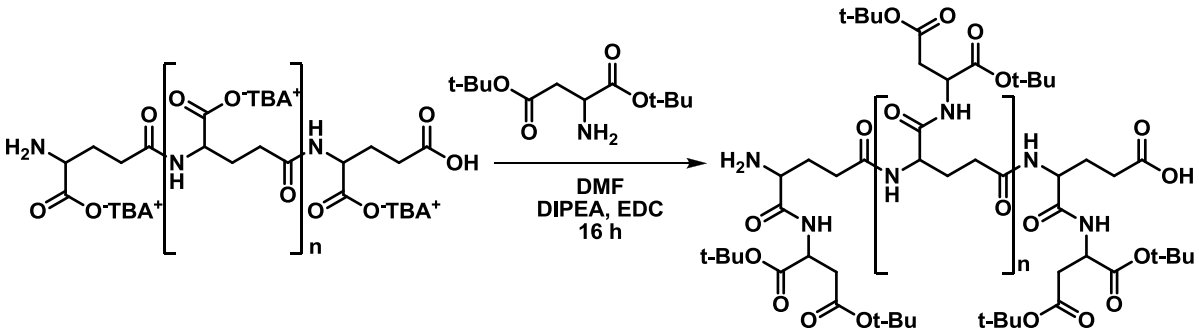

γ-PGA-TBA (100 mg, 0.27 mmol) was dissolved in anhydrous DMF (5 mL) under nitrogen atmosphere. DIPEA (0.94 mL, 2.7 mmol), of EDC×HCl (210 mg, 1.35 mmol) and, after complete dissolution, Asp(O-tBu)$_2$-OH (132 mg, 0.54 mmol) were added. Product was recovered as described in general procedure..

12 mg of oil (0.07 mmol; recovery: 26%; functionalization: 99%) were obtained.

^{1}H NMR (δ ppm DMSO-d_6): 1.40 (s, 18H, -C(C*H*$_3$)$_3$); 1.85 (m, 2H, Cβ*H*$_2$); 2.20 (m, 2H, Cγ*H*$_2$); 2.70 (m, 2H, Cβ$_{Asp}$H$_2$); 4.10 (m, 1H, Cα$_{Glu}$*H*); 4.25 (m, 1H, Cα$_{Asp}$*H*); 8.15 (m, 1H, -CON*H*$_{Glu}$); 8.30 (m, 1H, -CON*H*$_{Asp}$).

5.3.28. Preparation of (γ-PGA)-Gly-Phe

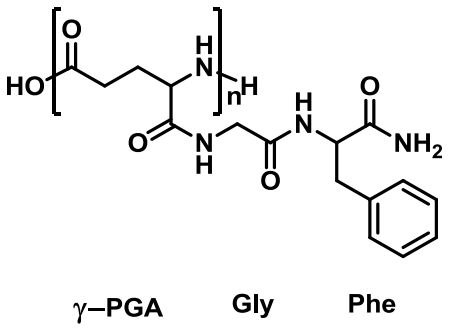

Peptide was obtained by MW assisted solid phase automated synthesis with Fmoc-protocol on a Biotage SPWave initiator+ synthesizer . Synthesis was carried out on 0.1 mmol scale using Rink amide resin (90 mg, loading 1.1 mmol/g), swelled using DMF.

Each Fmoc deprotection was performed using a 25% pyperidine in DMF solution.

Each coupling reaction was carried out at 50°C in DMF using HOBt (41 mg, 0.30 mmol) and HBTU (114 mg, 0.30 mmol) as coupling agents and DIPEA (0.1 mL, 0.60 mmol) as base; reaction time was 15 minutes.

Each amino acid was used in a 3 fold excess (0.30 mmol):

- 116 mg of Fmoc-Phe-OH
- 90 mg of Fmoc-Gly-OH
- 111 mg of γ-PGA-TBA

Each amino acid was dissolved, along with coupling agents and DIPEA, in DMF (3 mL) 15 minutes before the reaction.

For cleavage 80% TFA aqueous solution, containing 1% of thioanisole as scavenger, was used: the resin was transferred in a round bottom flask and treated with the cleavage solution for about 1 hour. The solid support was then removed by filtration and the resulting oil was diluted with EtOEt at 0°C. The solvent was removed *in vacuo* and the residue dissolved in water, dialyzed against distilled water for 48 hours, and finally freeze dried.

10 mg of white solid (0.03 mmol; yield: 30%, functionalization: 56%) were obtained.

^{1}H NMR (δ ppm DMSO-d_6): 1.55 (m, 2H, CβH_2); 2.14 (m, 2H, CγH_2); 3.01 (m, 2H, CH_{2Phe}); 3.91 (d, J=16.4 Hz, 1H, CHH_{Gly}), 3.73 (d, J=16.4 Hz, 1H, CHH_{Gly}); 4.13 (m, 1H, CαH_2); 4.53 (m, 1H, CH_{Phe}), 7.21 (m, 5H, Ar_{Phe}), 8.16 (m, 1H, -CONH_{Glu}); 8.25 (m, 1H, GlyN*H*Phe); 8.31 (m, 1H, GluN*H*Gly).

5.3.29. Preparation of (γ-PGA)-Gly-Tyr-Gly-Arg

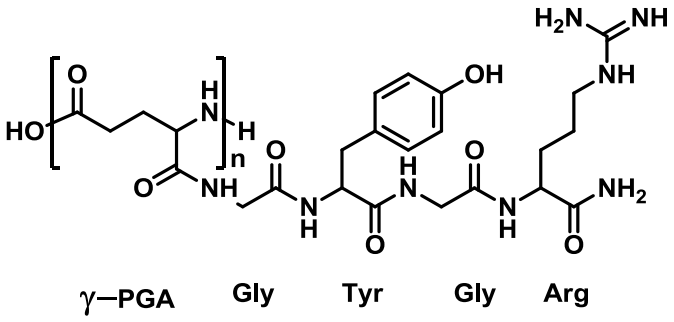

Peptide was obtained by MW assisted solid phase automated synthesis using Fmoc-protocol on a Biotage SPWave initiator+ synthesizer. Synthesis was carried out on 0.1 mmol scale using Rink amide resin (90 mg, loading 1.1 mmol/g), swelled using DMF.

Each Fmoc deprotection was performed using a 25% pyperidine in DMF solution.

Each coupling reaction was carried out at 50°C in DMF using HOBt (41 mg, 0.30 mmol) and HBTU (114 mg, 0.30 mmol) as coupling agents and DIPEA (0.10 mL, 0.60 mmol) as base; reaction time was 15 minutes.

Each amino acid was used in a 3 fold excess (0.30 mmol):

- 195 mg of Fmoc-Arg(Pbf)-OH
- 90 mg of Fmoc-Gly-OH
- 138 mg of Fmoc-Tyr(tBu)-OH
- 90 mg of Fmoc-Gly-OH
- 111 mg of γ-PGA-TBA, NB for this last coupling were used 0.7 mL of DIPEA

Each amino acid was dissolved, along with coupling agents and DIPEA, in DMF (3 mL) 15 minutes before the reaction.

For cleavage a 80% TFA aqueous solution, containing 1% of thioanisole as scavenger, was used: the resin was transferred in a round bottom flask and treated with the cleavage solution for about 1 hour. The solid support was then removed by filtration and the resulting oil was diluted with EtOEt at 0°C. The solvent was removed *in vacuo* and the residue treated with 1:1 hexane:EtOEt mixture and left overnight at -15°C.

20 mg of white solid (0.035 mmol; recovery: 35%, functionalization: 30%) were obtained.

^{1}H NMR (δ ppm DMSO-d_6): 1.60 (m, 4H, Cβ$_{Glu}$*H$_2$*+ Cγ$_{Arg}$*H$_2$*); 2.14 (m, 2H, Cγ*H$_2$*); 2.91 (m, 2H, C*H$_{2Tyr}$*); 3.15 (m, 2H, Cδ$_{Arg}$*H$_2$*); 3.72 (m, 3H, CH*H$_{Gly1}$*+CH*H$_{Gly2}$*+ Cα$_{Arg}$*H*); 3.86 (m, 2H, CH*H$_{Gly1}$*+CH*H$_{Gly2}$*); 4.13 (m, 1H, Cα*H$_2$*); 4.24 (m, 1H, C*H$_{Tyr}$*), 6.71 (d, *J*=8.4 Hz, 2H, Ar$_{Tyr}$); 7.04 (d, *J*=8.4 Hz, 2H, Ar$_{Tyr}$), 8.15 (m, 1H, -CON*H*$_{Glu}$); 8.25 (m, 1H); 8.32 (m, 2H).

Appendix 1:Conformational studies on γ-PGA

A1 1. Introduction

A1 1.1. Background

It is not very clear if and how γ-PGA conformation influence the chemical-physical behavior and the reactivity of the material. A comprehensive study on the subject is still lacking and in literature only fragmentary and sometimes contradictory data and hypothesis are present. All this reports are quite old but all agree in sustaining that the polymer adopts different conformations in solution, depending on factors such as enantiomeric composition, nature of the solvent and degree of ionization.

The first study that gives some information about γ-PGA conformation was published by Rydon (**1964**). In this paper the author suggests, on the basis of optical rotator dispersion (ORD) experiments that in water poly-γ-D-PGA can assume two different form varying its ionization state: the un-ionized polymer assumes an helical conformation while the ionized polymer tends to a random-coil state. Moreover Rydon suggests for the polymer helices a 3_{17} or 3_{19} structure, stabilized by intramolecular hydrogen bonds; this hypothesis has been reinforced in recent years by molecular dynamics and quantum mechanical calculations performed by Zanuy (Zanuy, **1998**; **2001**) that indicated 3_{19} left-handed helix as the most stable conformation for this kind of polymer.

In 1973 Sawa performed viscosimetric, ORD and IR measurements on γ-PGA produced by *B. subtilis* and proposed that the polymer assumes a parallel β-sheet conformation in acidic solution that shifts to a contracted random coil with the rise of pH. In 2000, He (He, **2000**) studied γ-PGA produced by *B.licheniformis* using attenuated total reflectance FT-IR spectroscopy and concluded that its conformation in aqueous solution is affected by pH, ionic strength, and concentration of the polymer itself. For this author observing the shifts of amide I and amide II stretch bands, it is possible to affirm that, at low pH, a low concentrated (0,1 % w/v) γ-PGA solution is in helical conformation. Rising the pH the conformation changes to the β-sheet and then becomes a random coil at high pH values. He observed this transition from helix to β-sheet also increasing the ionic strength and even the concentration of polymer.

A1 1.2. Circular dichroism

Circular dichroism (CD) can be defined as the difference in the absorption of left-handed circularly polarised light (L-CPL) and right-handed circularly polarized light (R-CPL) and occurs when a molecule contains one or more chiral chromophores.

$$\text{Circular dichroism} = \Delta A(\lambda) = A(\lambda)_{LCPL} - A(\lambda)_{RCPL}, \text{ where } \lambda \text{ is the wavelength}$$

Circular dichroism spectroscopy is a spectroscopic technique where the CD of molecules is measured over a range of wavelengths. Defined in this way, the units of CD are the same as absorbance units, i.e. dimensionless. Older definition (related to the above one) is related to the phenomenon of linear polarization becoming elliptical (indeed linear polarization is the sum of in phase S-CPL and R-CPL radiation): ellipticity is $\tan^{-1}$ of the ratio of the minor to the major axis of the ellipse, and thus is given in mdeg.

Since Biot (ca. 1820) it has been known that a solution of chiral molecules exhibits circular birefringence, i.e. L-CPL and D-CPL propagates at different speed. Consequently linearly polarized light, which can be thought as the resultant of the superimposition of two circularly polarized waves, rotates passing through a circularly birefringent medium: this phenomena is known as optical rotation and is measured in polarimetry or in optical rotation dispersion (ORD) spectroscopy as function of wavelength.

ORD is measurable for all samples, CD spectroscopy is applicable only to chiral molecules that contain a chromophore. If CPL is used to excite the chromophore, the two CPL states will be absorbed differently, and this generates a CD signal that could be positive (if L-CDL is absorbed to a greater extent than R-CPL) or negative (in the opposite case). In any case ORD and CD may be related through the so called Kramers-Kronig relation, stating that Optical Rotation at all wavelength is known if the CD of all transitions (or chromophores) is known.

CD is widely used in the conformational analysis of proteins and peptides since the first instrumentation became commercially available in the early 1960s. The reason for this is that the CD spectrum of these molecules is not a mere sum of the contributions of each individual residue, but is greatly influenced by the 3-dimensional structure of the

macromolecule itself. It is so possible to use the technique to identify structural elements and to follow changes in the structure of the macromolecules.

CD spectra of peptides and proteins can be roughly divided into three regions, that can be used to obtain structural information from different types of chromophores. In the far UV region, from 250 nm to the lower limit of measurements (~180 nm), CD signal is mainly due to amide groups and, so, is largely defined by secondary structures. In the near UV, from 250 nm to 300 nm, CD is dominated by aromatic side chains and offers information about protein tertiary structures. Finally, in the proximal near UV, visible and near IR, from ~300 nm to ~1000 nm) CD is significant only in presence of bound chromophores with absorption bands that can be seen in this region and so it is used to monitor ligand binding and conformation.

It can be observed that, for the conformational analysis of peptides, the far UV regions is by far the most interesting; in fact it has been observed that various types of secondary structures have in this region their own characteristics CD patterns, due to the absorption of the peptide chromophore.

In condensed phases (Nielsen, **1967**; Clark, **1995**), where Rydberg transitions are suppressed, the absorption spectra down to ~130 nm of simple amides show signals due only to three excited states:

- The n-π* transition at about 220 nm that is analogous to that of other carbonyl chromophores even if it is weak in absorption (ε_{max}~100 $M^{-1}cm^{-1}$), and thus a weak electric dipole transition moment, it has a large magnetic dipole transition moment (~1 BM = Bohr Magneton) directed along the carbonyl bond and its energy depends on the characteristics (extent and strength) of the hydrogen bonding (λ_{max}~230 nm in nonpolar solvents, ~210 nm in strongly hydrogen-bonding solvents).
- The first π-π* transition (NV_1) has its λ_{max} at 190 nm (for secondary amides) and is characterized by a moderate intensity (ε_{max}~9000 $M^{-1}cm^{-1}$ with a transition moment magnitude $|\mu|$~3 D). It is polarized along the C-N bond direction.
- The second π-π* transition (NV_2) happens near 140 nm; it is less intense than NV_1 and its polarization is approximately orthogonal to that of the NV_1

There the major types of secondary structures, that appear in peptides and proteins, are briefly described (all AA are considered to be L, for D enantiomers all positive bands have to be considered negative and *vice versa*):

α-Helix. Among secondary structures α-helix (Pauling, **1951**) is probably the most abundant and was the first to be characterized by CD (Holzwarth, **1962**; Holzwarth, **1965**): its spectrum is almost insensitive to the side chains and solvents so long that the structure is conserved (Woody, **1997**). The CD spectrum of a typical α-helix, for example the one formed by poly(Glu), has three main bands over 180 nm: a negative band at 222 nm assigned to n-π* transition; a negative band at ~207 (polarized along the helix asses) (forming a negative doublet with the first one) and a positive intense narrow band at ~190 nm (polarized in the plane perpendicular to the axis), the latter two transitions being both due to π-π* (NV_1) transition (Schellman, **1962**; Woody, **1967**; Moffitt, **1956**). Other bands exist below 180 nm, among them the one at 140 nm can be ascribed to π-π* (NV_2) transition (Johnson, **1972**).

3_{10}-Helix. This quite uncommon structure presents a CD spectrum similar to an α-helix one but significantly weaker, especially for n-π* transition (Toniolo, **1996**; Toniolo, **2004**).

β-Sheet. A typical β-sheet gives three CD signals: a negative band at 217 nm (n-π* transition), a positive band near 195 nm and a negative band near 175 nm (exciton splitting of π-π*) (Greenfield, **1969**; Brahms, **1977**). β-Sheet CD spectra show significant variations in absolute and relative magnitude of the bands, probably as a consequence of the intrinsic variability of this secondary structure.

β-Turns. β-turns are quite variable and so they origin several CD patterns (Woody, **1974**). However the two most common types of β-turns (known as types I and II), usually present β-sheet like spectra with bands red-shifted by 5-10 nm.

Unordered polypeptides. Unordered polypeptides (such as poly(Glu) and poly(Lys) at neutral pH) origin CD spectra with a relatively weak positive band at ~217 nm and a strong negative band at ~197 nm. For some authors (Tiffany, **1968**; Tiffany, **1969**) these spectra have a strong resemblance with (or may be even reconducted to) that of poly(Pro)II, the left handed threefold helical form adopted by poly(Pro) in water; on the basis of this consideration they argued that even these structures are not really unordered.

A1 2. Results and discussion

With the aim of getting some insight into the relationship between biopolymer conformation (macrostructure) and enantiomeric composition (microstructure), stereochemically controlled γ-glutamic acid decamer and corresponding polymer were synthesized using a solid phase peptide synthesis protocol and analyzed by electronic CD.

The solid phase synthesis was chosen because of the many advantages it offers over a solution synthetic strategy, as the one published by Sanda (**2001**) and based on the synthesis of γ-glutamic dimers (Scheme A1 1)

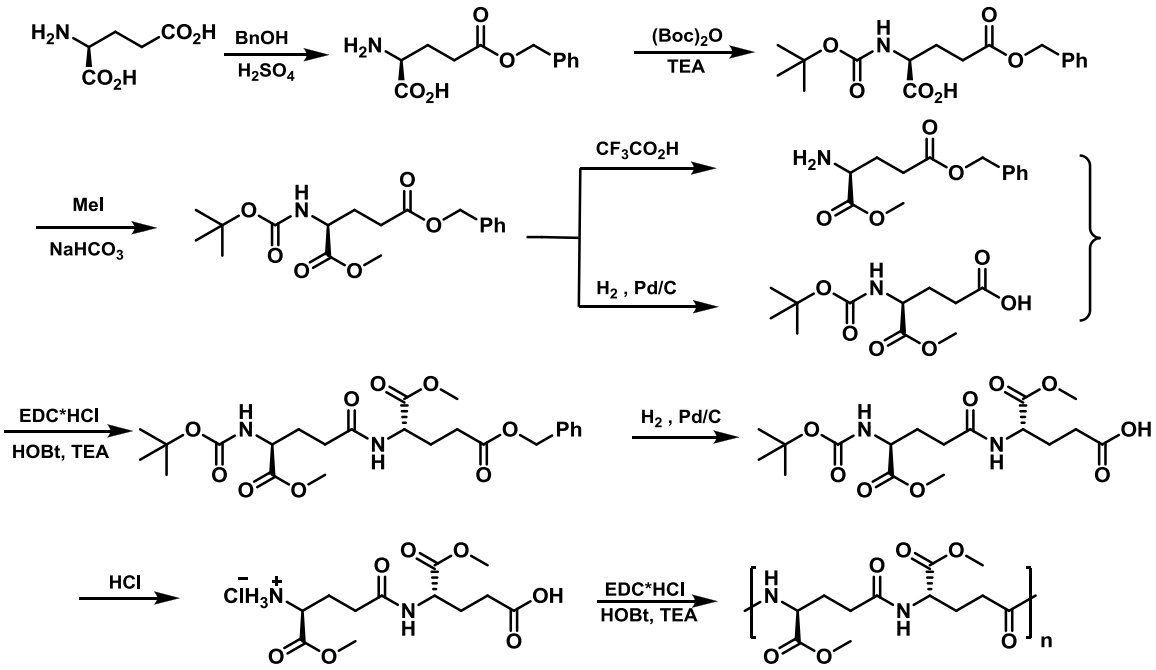

Scheme A1 1: Sanda's strategy for the chemical synthesis of γ-PGA

The major advantage of SPPS on solution strategies is that it offers more stereochemical flexibility: in fact, using the dimer approach, it is only possible to obtain either L-L, or L-D, or D-D oligomer and consequently, the final polymer can only result to homochiral (if the starting dimers are only L-L or D-D), alternated (L-D dimers), or blocky (composed by randomly coupled L-L, D-D and L-D dimers). In contrast using solid phase synthesis is possible to form oligomeric building blocks (in our case, a decamers) which have a more complex structures, and therefore, can originate polymeric products characterized by a larger conformational variety.

For SPPS we followed a standard Fmoc protocol using as monomer the commercially available amino acid Fmoc-Glu-O-*t*Butyl-OH on a very acid labile 2-Cl-Trt resin, chosen because it allows the cleavage of the oligomer without removing the α protecting *t*-butyl group. For the synthesis of the polymer the protected decamer was polycondensed in solution using TFFH as coupling agent and working at high concentration to minimize the possibility of ciclyzation (Scheme A1 2).

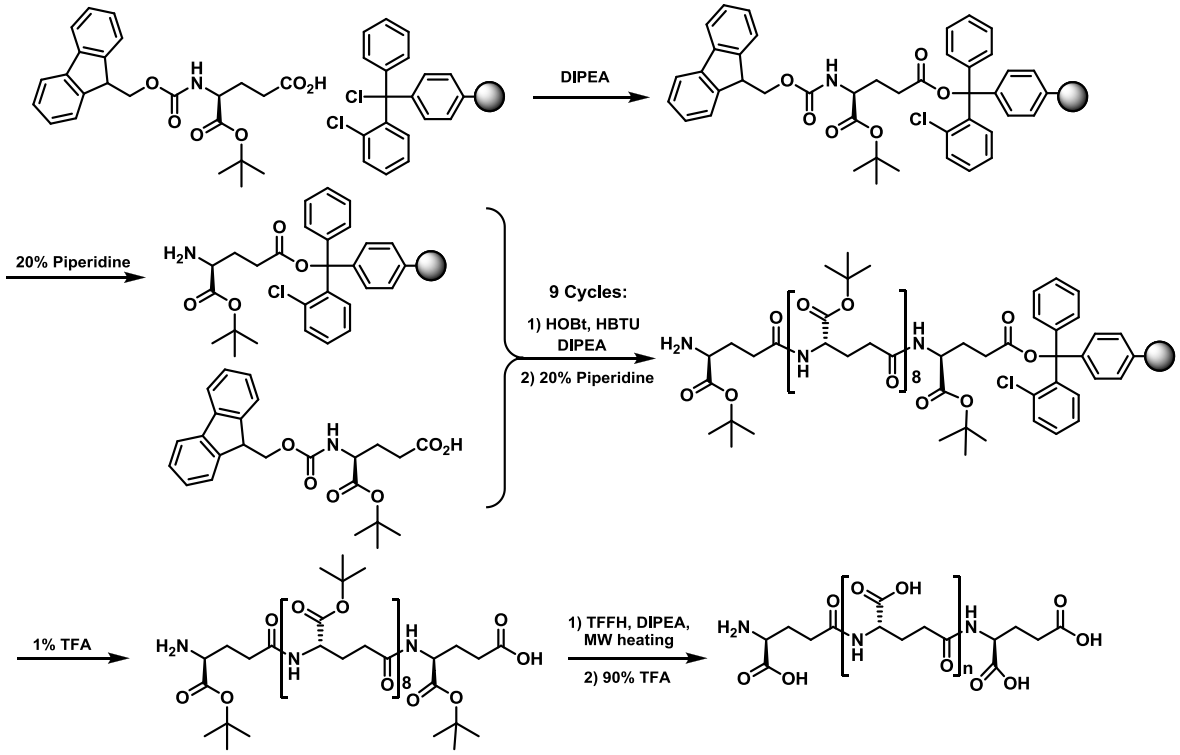

Scheme A1 2: SPPS of γ-PGA oligomers

In figure A1-1 are reported: the CD spectra in the 250-200 nm interval obtained of the L-decamer, of the homochiral L- glutamic acid polymer (MW ~20 KDa) and of two block L-D-cooligomers (sequence LLDDLLDDLL and DDDDDLLLLL respectively).

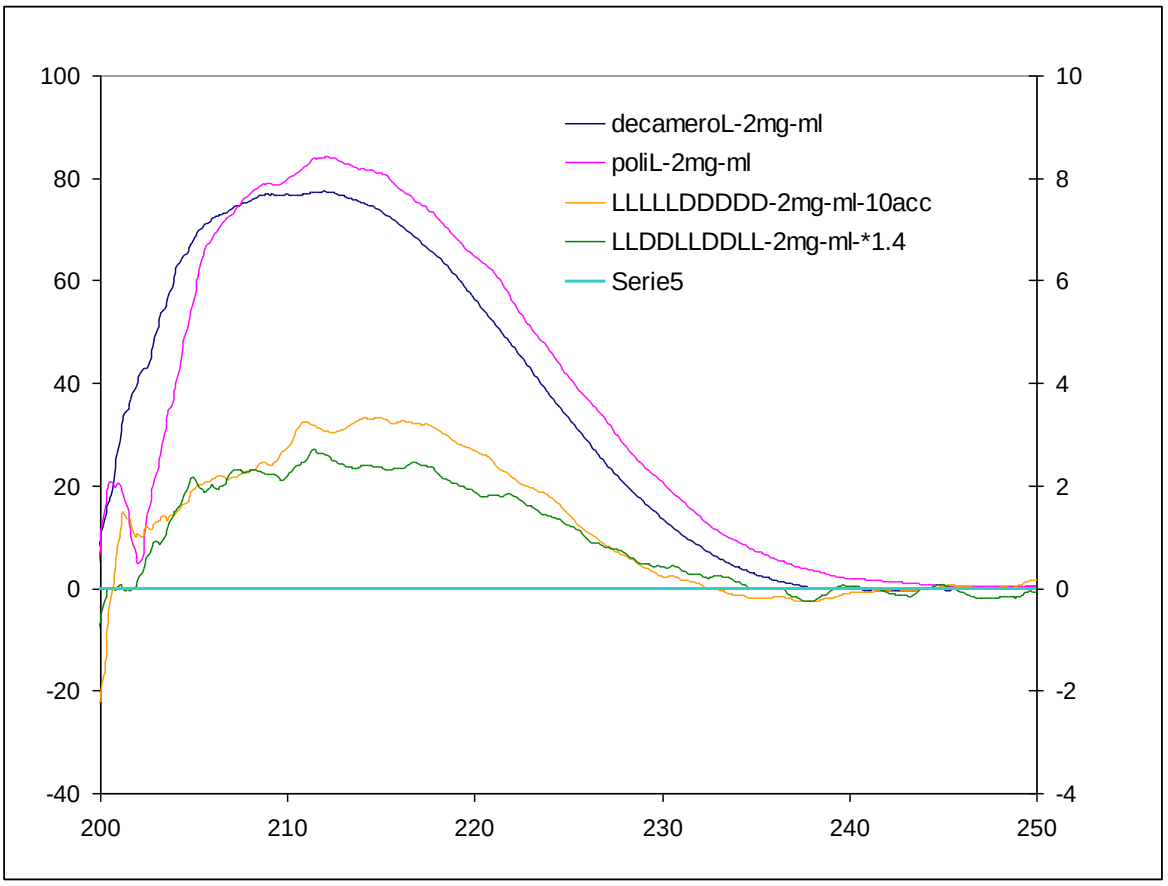

Figure A1 1 CD signal vs wavelength of oligomeric and polymeric γ-PGA samples. Spectra were registered in water at RT, using a 1 mm cell and performing 10 accumulation for each sample. All data were corrected subtracting the signal of pure water.

Analysis of the spectra indicates that the CD signal of L- decamer and L- polymer are almost superimposable (there is just a slight bathochromic shift in the latter case), so a lot of information can be gathered from PGA oligomers, avoiding the troublesome polymerization step necessary to prepare stereochemically controlled polymers (see experimental part). Blocky oligomers give a substantially weaker signal and this indicate that a substantially equilibrated distribution of blocks brings to an almost achiral structure; the weak signal (that is higher for LLLLLDDDDD olygomer) may be due to a slight tendency to form more ordered structure starting from one of the terminus of the peptide sequence; however more experimental data are needed to verify this hypothesis.

We also analyzed the polymer produced by three different bacterial strains (named PB5383, BAST195 and PG11) grown at the University of Pavia by prof. Albertini group. The results are shown in figure A1-2

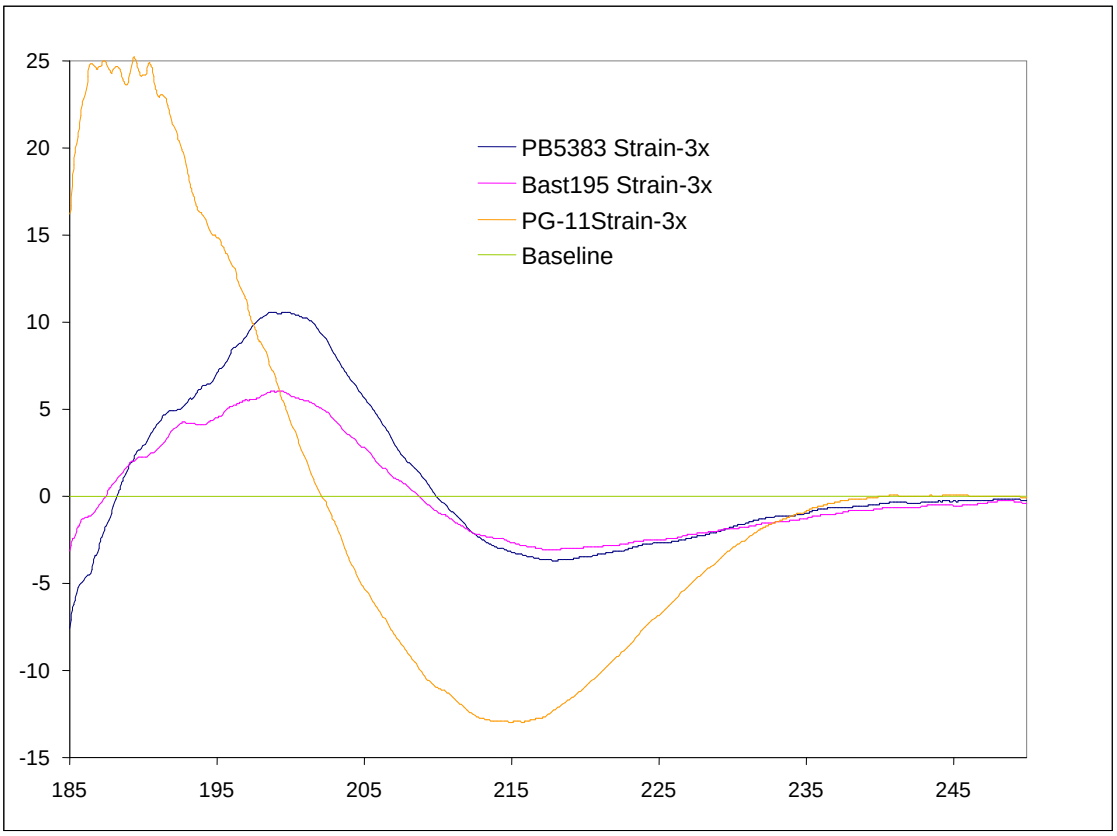

Figure A1 2: CD signal vs wavelength of γ-PGA produced by different bacterial strains developed in Pavia. Spectra were registered in water at RT, using a 1 mm cell and performing 10 accumulation for each sample. All data were corrected subtracting the signal of pure water.

By comparison of these spectra with those of the L-polymer, it is evident how all these three polymers have a high content in D monomers: this observation has been supported by the analysis of the stereochemical composition of the polymer produced by PB5383 strain that resulted to be 84% D/16% L. We can observe that polymer from two of the considered strains give substantially the same signal, while the third, PG11, shows a significant frequency shift. In order to study this behavior, we carried out a series of experiments by varying the pH of the solution and checking if spectral variations can be ascribed to a change in the ionization state of the polymer chain, and, as a consequence, in its conformation. This kind of behavior was already observed in α-PGA by different authors (Finke, **2007**) and also proposed for γ-PGA on the basis of ORD and IR experiments or DFT calculations (Rydon, **1964**; Sawa, **1973**; Zanuy, **1998**; Zanuy, **2001**; He, **2000**).

CD signals registered for synthesized L-γ-glutamic decamer (Figure A1-3), for a commercial sample of γ-PGA (stereochemical composition: 52% L/YY 48% D; Figure A1-4), for PB 5383 produced PGA (Figure A1-5) and for PG11 produced PGA (Figure A1-6).

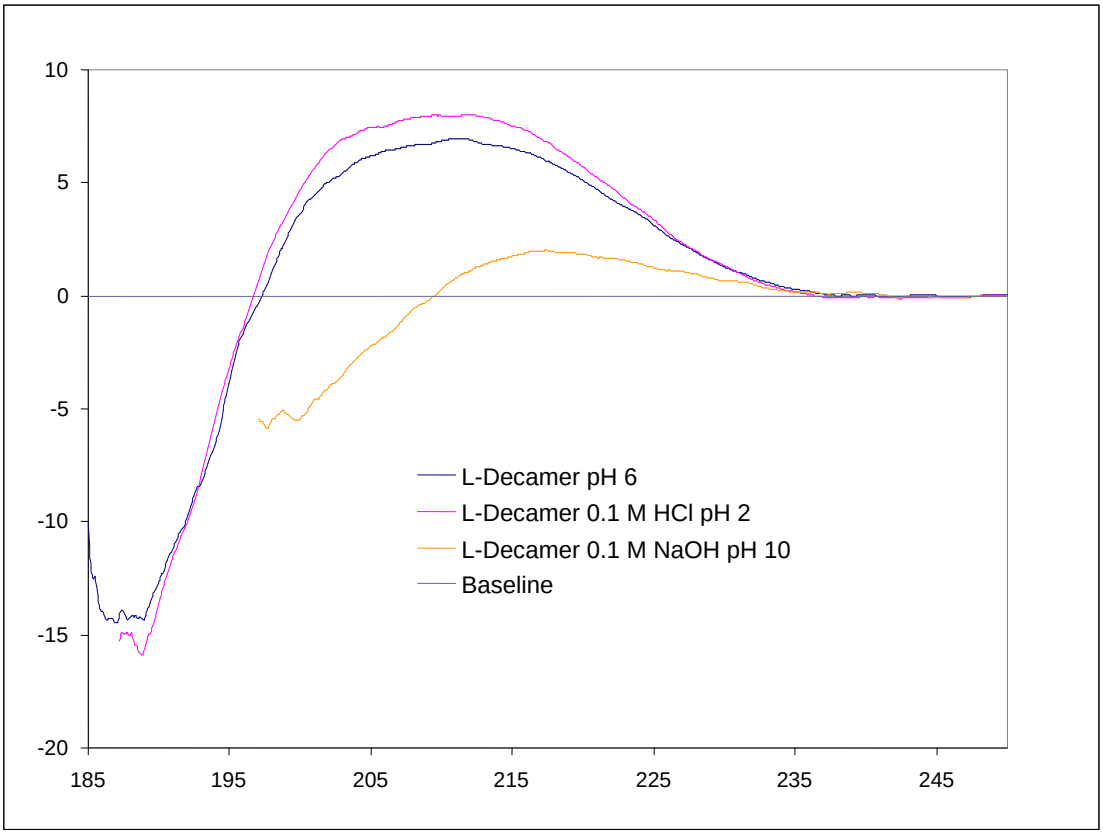

Figure A1 3: CD signal vs wavelength of oligomeric γ-PGA sample (0.6 mg/mL) at different pH. Spectra were registered in water at RT with addition of HCl 0.1M or NaOH 0.1 M to create acidic or basic condition respectively. For the analysis a 0.2 mm cell was used and 10 accumulation was performed for each sample. All data were corrected subtracting the signal of the used solvent.

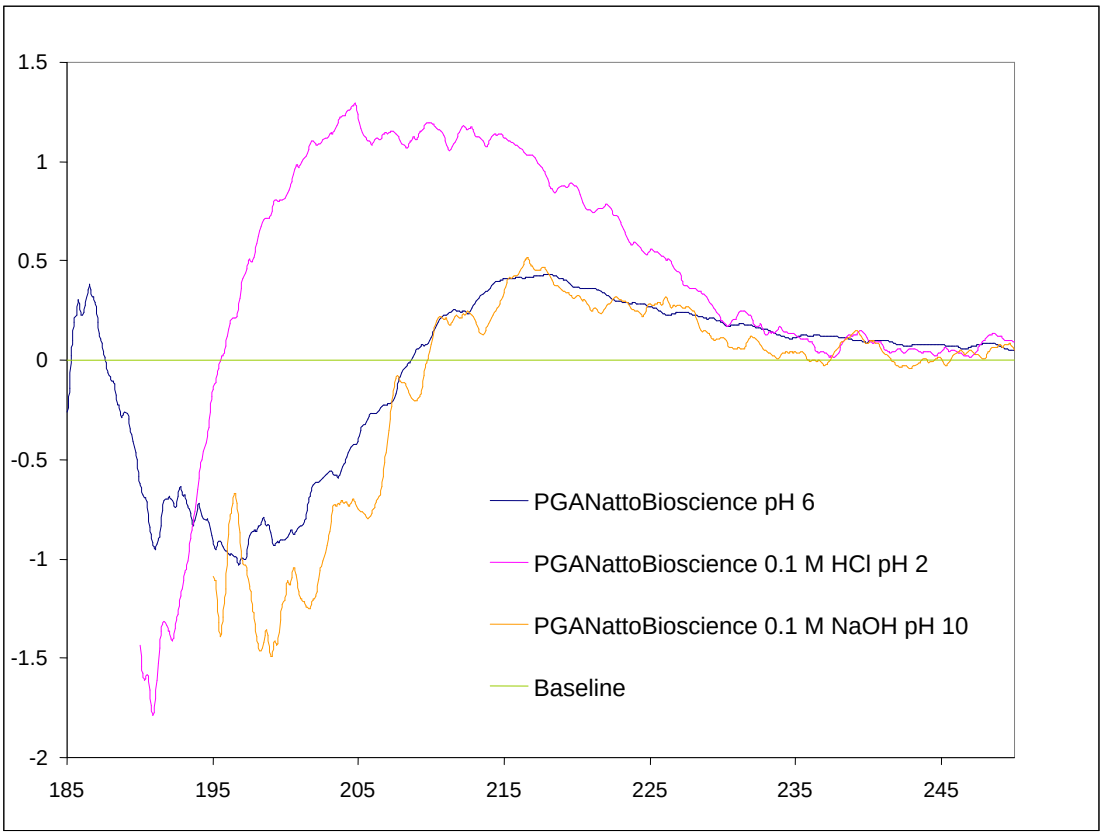

Figure A1 4: CD signal vs wavelength of commercial γ-PGA sample (NattoBioscience) (0.6 mg/mL) at different pH. Spectra were registered in water at RT with addition of HCl 0.1 M or NaOH 0.1 M to create acidic or basic condition respectively. For the analysis a 0.2 mm cell was used and 10 accumulation was performed for each sample. All data were corrected subtracting the signal of the used solvent.

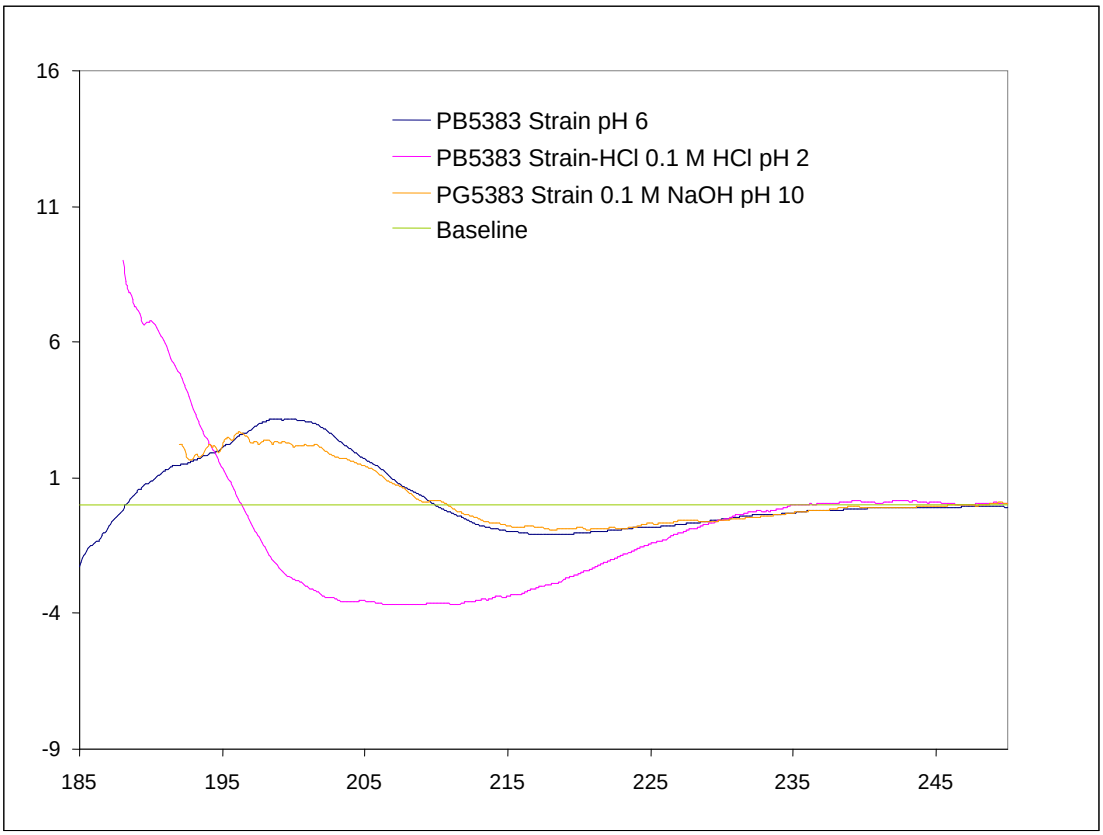

Figure A1 5: CD signal vs wavelength of PB5383 produced γ-PGA sample (0.6 mg/mL) at different pH. Spectra were registered in water at RT with addition of HCl 0.1M or NaOH 0.1 M to create acidic or basic condition respectively. For the analysis a 0.2 mm cell was used and 10 accumulation was performed for each sample. All data were corrected subtracting the signal of the used solvent.

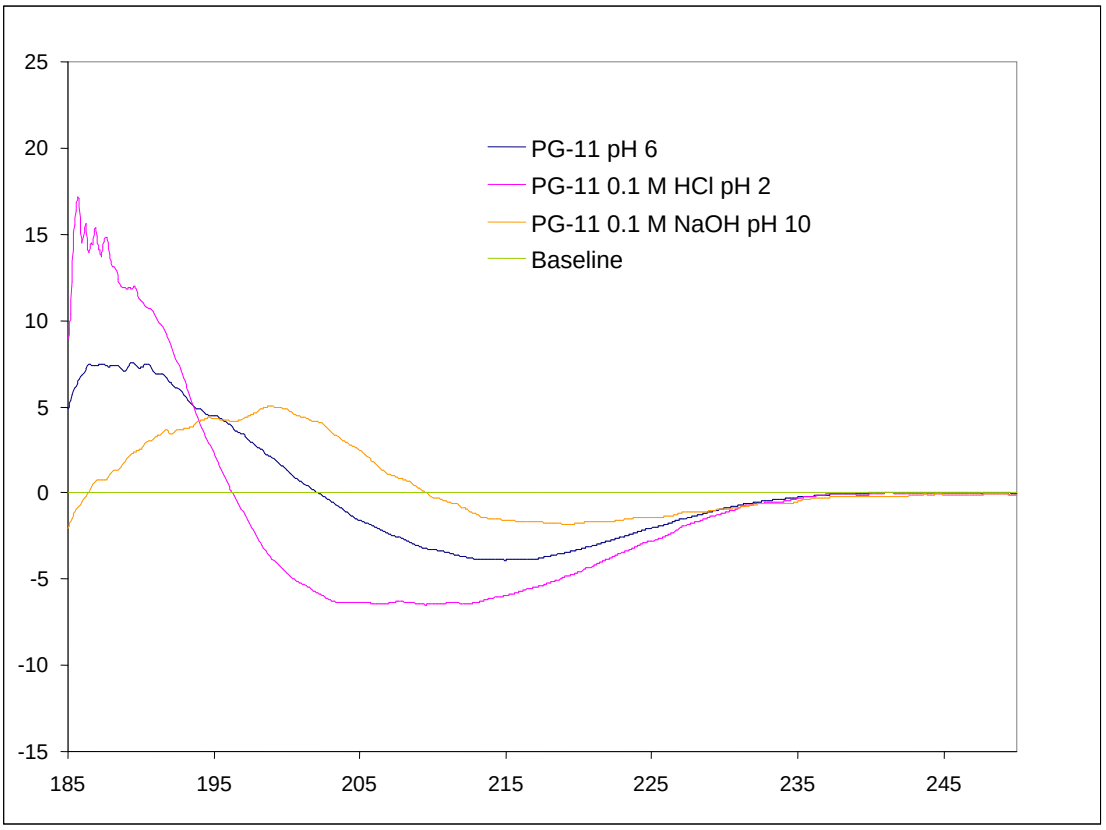

Figure A1 6: CD signal vs wavelength of PG11 produced γ-PGA sample (0.6 mg/mL) at different pH; all the spectra were registered in water at RT with addition of HCl 0.1 M or NaOH 0.1M to create acidic or basic condition respectively. For the analysis a 0.2 mm cell was used and 10 accumulation was performed for each sample. All data were corrected subtracting the signal of the used solvent.

In all analyzed cases we can observe a shift of the CD signal to lower wavelengths in case of low pH values that induce a weaker ionization in polymer chains; this seems to be consistent with what observed by He (He, **2000**) who claimed that γ-PGA chains changed from a helix to a random coil conformation increasing pH. This data also allow to explain the anomaly observed for PG11 strain product: in fact in a more basic or acidic environment the signal of this polymer is absolutely comparable to that of the other strains, only in pure water the pattern is different and this can be ascribed to a different ionization degree of the polymer in his solid form, that can derive from minor differences in the isolation procedures.

A1 3. Experimental

A1 3.1. Materials and Methods

γ-PGA was purchased from Natto Bioscience Co. (Japan) as the sodium salt (Mw=28,3 kg/mol) or kindly supplied by dr Cinzia Calvio of the Biology and Biotechnology department of the University of Pavia. All other reagents and solvents were purchased from Sigma-Aldrich (Milan, Italy) and/or from VWR International and were used without further purification. All the solvents were of HPLC grade.

For solid phase synthesis a Biotage SP Wave Initiator^{+} synthesizer was used.

HPLC were performed using an Amersham pharmacia biotech (P900) liquid chromatographer connected to a UV-vis detector; chromatographic conditions were set as follows: column for analytical HPLC, Jupiter RP-18 (10μm proteo 90A size: 250x4.60 mm, Phenomenex); column for semipreparative HPLC, Jupiter- RP-18 (10 μm, size:250x10 mm, Phenomenex); detector, λ 226 and 254 nm; mobile phase: A (0,1% TFA (v/v) in water) and B (80% acetonitrile/ 20% water with 0,1% of TFA), gradient elution from 5% to 40% B in 3 column volumes, from 40% to 70% B in 3 cv, from 70% to 100% B in cv and finally 2cv at 100% B.

The CD measurements were performed on a Jasco J500 instrument from 250 to 185 nm in 1 or 0.2 mm pathlength quartz cells, and 10 scans for each spectrum were taken. The CD spectrum of the solvent, taken in the same experimental conditions, was subtracted thereafter. All measurements were made at room temperature. UV spectra were also taken on the same solutions, in order to verify that the maximum absorbance was never above the value of 0.8.

A1 3.2. Procedures

A1 3.2.1. Preparation of γ-glutamic acid decamers

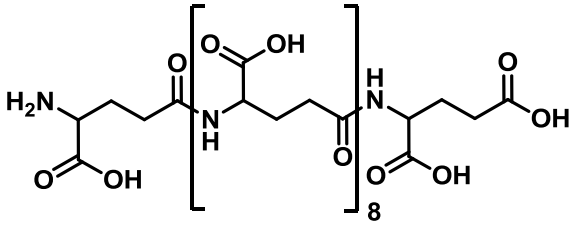

Decamers were obtained by MW assisted solid phase peptide synthesis using Fmoc-protocol working on a Biotage SPWave Initiator+ synthesizer. We chose a 2-Cl-Trt resin preloaded with Fmoc-L-Glu-OtBu and swelled using DMF. Synthesis was carried out on 0.2 mmol scale (220 mg of loaded resin).

Each Fmoc deprotection was performed using a 25% pyperidine in DMF solution.

Each coupling reaction was carried out under MW irradiation at 50°C in DMF using HOBt (68 mg, 0.5 mmol) and HBTU (189 mg, 0.5 mmol) as coupling agents and DIPEA (0.17 mL, 1 mmol) as base; reaction time was set to 15 minutes.

For each coupling, 15 minutes before the reaction, 213 mg of the appropriate enantiomer of Fmoc-Glu-OtBu (0.5 mmol) were dissolved along with coupling agents and DIPEA, in 3 mL of DMF.

For cleavage, resin was transferred in a plastic syringe equipped with a filter, treated with 3 mL of a 1% TFA in DCM solution for 3-4 minutes and then dried collecting the liquid in a flask containing 5 mL of MeOH and 0.3 mL of DIPEA. Process was repeated 10 times collecting the cleavage solution in the same MeOH and DIPEA solution. Resin was then washed with DCM (3 times with 3mL each) and MeOH (3 times with 3mL each); washing solutions were reunited with cleavage solutions and reduced using a rotary evaporator to 5% of the starting volume. A solid precipitated by the addition of 20 mL of water; it was collected and purified.

135 mg of white solid were obtained (72% yield) for L-homochiral decamer.

128 mg of white solid were obtained (68% yield) for DDDDDLLLLL decamer.

116 mg of white solid were obtained (68% yield) for LLDDLLDDLL decamer

MALDI TOF (m/z): 1871 (M+1) for all three samples.

A1 3.2.2. Polymerization

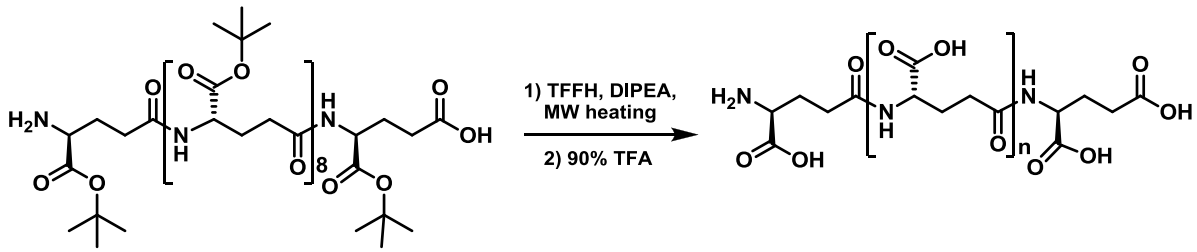

In a glass vial γ-L-glutamic acid decamer (35 mg, 0.02 mmol) was dissolved in 1 mL of DMF. TFFH (25 mg, 0.09 mmol) and DIPEA (17 μL, 0.09 mmol) were added and the solution was reacted for 30 minutes at 75°C under MW irradiation. The reaction mixture was diluted with water (20 mL) and liophylized.

The obtained solid was treated with 50% TFA solution in DCM (10 mL) for 1.5 hours under stirring. The solvent was removed *in vacuo*, and the residue was treated with diethyl ether (20 mL) and, subsequently, *n*-hexane (6 mL) to favor precipitation. After 15 hours at -20 °C the solid precipitate was filtered and washed with cold *n*-hexane.

30 mg of yellowish solid (0.02 mmol, 99% yield) were recovered.

Mw (SEC-MALS): 6530 g/mol.

Appendix 2: Studies on *B. subtilis* GGT

A2 1. Introduction

γ-Glutamyl-transpeptidase (GGT; E.C. 2.2.3.2) are highly conserved enzymes that occur in bacteria, yeast, plants and animals, from nematodes (roundworms) to humans. The enzyme catalyses the removal of the terminal γ-glutamyl moiety from a donor molecule such as glutathione (Elce, **1976**) or another γ-glutamyl compound (Minami, **2003**), forming a γ-glutamyl-enzyme intermediate. The γ-glutamyl moiety could then be transferred to water (hydrolysis) or to an acceptor amino acid or peptide (transpeptidation). Three types of reactions are thus possible depending on the destination of the γ-glutamyl moiety:

- transfer to water, which results in hydrolysis;
- transfer to an 'acceptor' amino acid or peptide, which results in transpeptidation;
- transfer to another molecule of the donor substrate, which results in an auto-transpeptidation reaction.

The three possibilities are shown in figure A2 1:

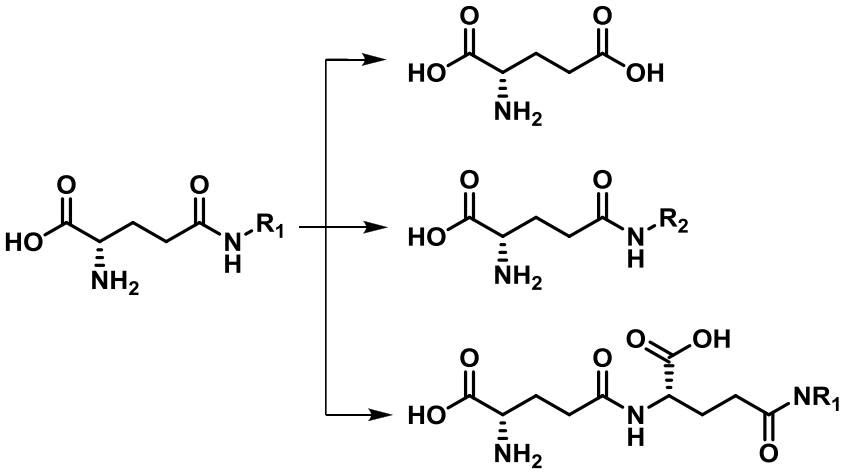

Figure A2 1: Schematic representation of the reactions catalysed by GGT

GGT is a heterodimeric enzyme, which consists of two subunits (large and small), originating after a proteolytic cleavage of a single precursor polypeptide (Suzuki, **1989**)

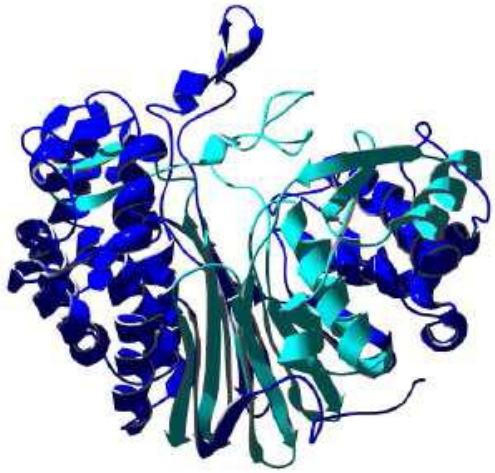

Figure A2 2: Three-dimensional structure of *E. coli* GGT, with the S subunit colored in turquoise and L subunits in blue

A2 1.1. Catalytic mechanism

A2 1.1.1. Active site

Specificity studies support the classification of the active site into three sub-sites. The γ-glutamyl moiety and the leaving group of the donor bind to sub-site 1 and sub-site 2, respectively. The nature of acceptor binding site (sub-site 3) is more ambiguous.

The γ-glutamyl sub-site exhibits broader stereochemical specificity, accepting both L and D isomers of glutamic acid. Both α-amino and α-carboxylic groups of the γ-glutamyl moiety are involved in binding to sub-site 1. However, α-ammonium group appears to be critical as substitution of its nitrogen atom significantly diminishes the affinity. On the contrary, α-carboxylate group tolerates derivatization into uncharged, isosteric or bulkier (e.g., methyl, *t*-butyl) forms (Keillor, **2005**; Cook, **1987**). The presence of a discrete site for the binding of acceptor (sub-site 3) is still inconclusive. Some results tend to indicate that the acceptor binds to the site occupied by the donor leaving group (Taniguchi, **1998**; Thompson, **1977**). The catalytic mechanism in GGT is considered to proceed through a modified ping-pong mechanism (a type of sequential reaction), as there are strong evidences for the presence of a modified enzyme in the form of an acyl-enzyme complex (Tate, **1977**; Smith, **1995**).

A2 1.1.2. Acyl-enzyme intermediate

Formation of γ-glutamyl complex has been demonstrated by chemical, kinetic and crystallographic methods. Treatment with glutamine analogs like 6-diazo-5-oxo-L-norleucine (DON, figure A2 3) (Tate, **1977**) and *O*-diazoacetyl-L-serine (azaserine, figure A2 4) (Smith, **1995**) inactivates the enzyme by covalent and stoichiometric binding to the γ-glutamyl site.

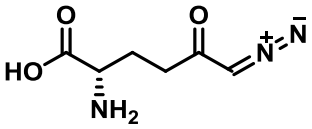

Figure A2 3: 6-diazo-5-oxo-L-norleucine

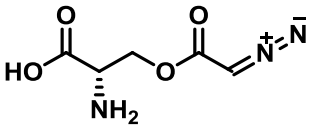

Figure A2 4: azaserine

Thus the reaction is assumed to proceed by nucleophilic attack on the amide bond resulting in a tetrahedral transition state whose collapse leads to the formation of γ-glutamyl-enzyme complex concomitant with the expulsion of the leaving group. The free enzyme is regenerated by the reverse reaction involving a non-enzymic group as the nucleophile.

Catalysis thus proceeds in two steps with an initial 'acylation' step, followed by a 'deacylation' reaction. Formation of an intermediate is additionally supported by stop-flow studies. Under pre-steady state conditions, the activity follows a biphasic pattern that has been interpreted in terms of a fast acylation step followed by a rate-limiting deacylation step. The supposed γ-glutamyl-enzyme intermediate has been observed by crystallographic studies on *E. coli* GGT, wherein γ-glutamylation of the active site was observed for glutathione-soaked crystals (Okada, **2006**).

A2 1.1.3. Catalytic nucleophile

Treatment with labelled DON results in localization of radioactivity in the light chain of the dimeric enzyme molecule, thus mapping the site of covalent attachment (Tate, **1977**). Furthermore, the attachment was found to involve the side chain hydroxyl group of either Ser or Thr. Participation of a critical hydroxyl group is in agreement with the inhibitory effect of serine-borate complex (Tate, **1978**). In borate buffer, the affinity of L-serine for the γ-glutamyl binding site is greatly enhanced and results in competitive inhibition. Borates are known to form reversible complexes with vicinal hydroxyl groups. Therefore, the affinity of L-serine is believed to be due to a borate-bridge between its side chain and a hydroxyl group in the active site. The nucleophilic residue was finally identified by trapping it with the mechanism-based inhibitor 2-amino-4-fluorophosphono-butanoic acid (figure A2 5) (Inoue, **2000**).

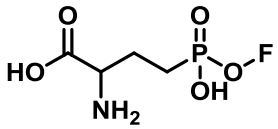

Figure A2 5: 2-amino-4-fluorophosphono-butanoic acid

Phosphonylation occurs at the *N*-terminal Thr residue of the light chain. This residue is conserved in all GGTs. The candidacy of the *N*-terminal threonine is in agreement with the crystal structure of *E. coli* GGT substrate-complex, where a covalent link was observed between the Thr Oγ and the γ-carbon of the glutamyl moiety (Okada, **2006**).

A2 1.1.4. Catalytic mechanism

Insights provided by chemical, kinetic and crystallographic studies allowed elucidation of the mechanism by which GGT promotes hydrolysis and transpeptidation. The activated side chain of the catalytic Thr (-O-) attacks the carbonyl carbon of the scissile bond, thus forming an anionic tetrahedral intermediate. The backbone nitrogen atoms of two Gly residues donate hydrogen bonds to offset the negative charge developed on the carbonyl oxygen of the tetrahedral intermediate, thus acting as the oxyanion hole. C-N bond cleavage occurs with the collapse of the tetrahedral intermediate with the expulsion of the leaving group. The bond breakage occurs concomitantly with the protonation of the amide nitrogen by general acid catalysis (Ménard, **2001**). At the end of the acylation step, the γ-glutamyl moiety is covalently linked to the Thr nucleophile through an ester bond. The free enzyme is regenerated from the esterified nucleophile in a deacylation step by water or by

the free amino group of an acceptor (hydrolysis and transpeptidation, respectively). The catalytic mechanism is schematically represented in figure A2 6.

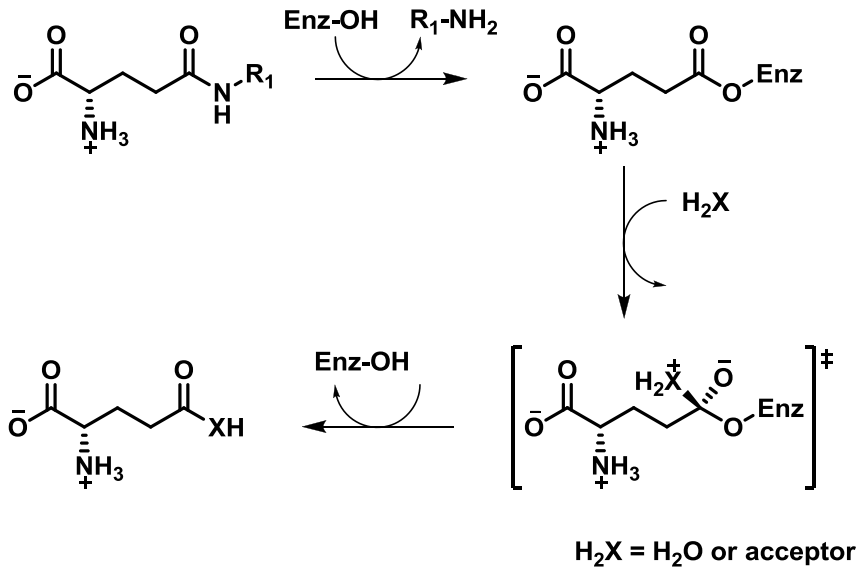

Figure A2 6: Schematic representation of catalytic mechanism of GGT

Alignment of the sequences of GGT from various organisms (e.g. *E. coli*, *B. subtilis*, man, rat, Fig. 7) shows that the residues essential for the activity are substantially conserved. The cataytically active Thr-391 (numeration follows *E. coli* GGT sequence); Thr-409 that forms H-bonds with the O_γ of Thr-391; the Gly-483 and Gly-484 which form the oxyanion hole. This suggests that the mechanism of binding of the substrate and the mechanism of action of the enzyme are almost identical in different species.

On the other hand, the segment of the sequence between Pro-438 and Gly-449 in *E. coli*, corresponding to the loop that extends over the active site, appears to be variable in other GGT (Okada, **2006**), such as *B. subtilis*, whose active site seems to be more open than that of other GGTs.

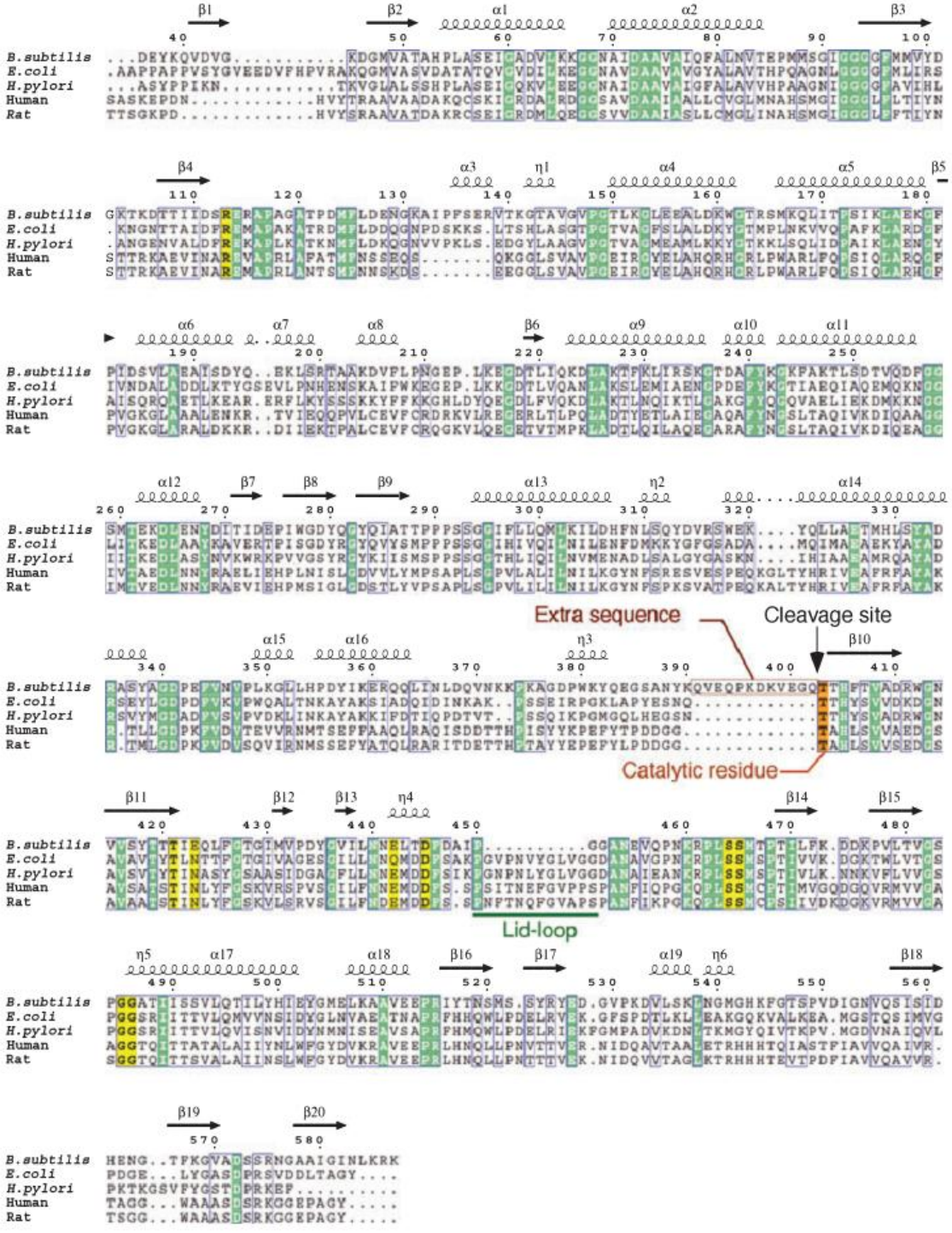

Figure A2 7: multiple sequence alignment of GGTs from several representative organisms. The sequence numbering is shown for *B.subtilis* GGT. Identical residues are highlighted in light green, and similar residues are boxed in blue. The residues of the catalytic nucleophile are highlighted in orange. The residues that participate in hydrogen bonding with glutamate are highlighted in yellow.

***B. subtilis* 168, NCBI accession no.NP_389723; *E. coli* K-12, NP_417904; *H. pylori*, NP_207909; Human, *Homo sapiens*, NM_005265; Pig, *Sus scrofa*, NM_214030; Rat, *Rattus norvegicus*, NM_053840 (Wada, 2010).**

A2 1.2. Prokaryotic and eukaryotic GGTs

Prokaryotic and eukaryotic GGTs differ in both structural and functional aspects. While the prokaryotic GGTs occur as soluble proteins either in the periplasmic or in the extracellular space, the eukaryotic homologues are type II transmembrane proteins. A typical eukaryotic GGT has a large extracellular domain anchored to the membrane by a transmembrane hydrophobic anchor and a short cytoplasmic tail. The large extracellular domain, where the catalytic function is located, can be separated from the membrane by papain treatment (Papain, also known as papaya proteinase I, is a cysteine protease present in papaya and it's used for its proteolytic activity) (Tate, **1985**). The procedure does not affect the enzyme function and is therefore employed in the purification of the enzyme from animal tissues. Furthermore, eukaryotic GGTs have *N*- and *O*-linked glycans whose composition varies in tissue-specific manner. The sugars have no catalytic function, as their removal by enzymatic deglycosylation does not affect the activity (Smith, **1994**). The carbohydrates appear to confer protection against proteases. Furthermore, bacterial and eukaryotic GGTs show marked differences in their kinetic behaviour. Eukaryotic GGTs are catalytically more powerful than their bacterial homologues. The specific activity of rat kidney GGT is nearly 100 fold higher than that of *E. coli* GGT (Ikeda, **1995**). Further differences occur in the nature of the catalyzed reactions. The rate of transpeptidation reactions catalyzed by eukaryotic GGTs can be stimulated up to 100 fold with respect to hydrolysis of the donor in the presence of an acceptor. In contrast, the presence of an acceptor produces marginal change in the transpeptidation reaction rate of prokaryotic GGTs with respect to the hydrolysis.

A2 1.3. Cellular location

Mammalian GGTs occur on the surface of the epithelial cells, mostly in tissues involved in secretion or absorption such as kidneys, bile duct, intestine, pancreas and epididymis (Ikeda, **2005**). The enzyme is located on the cell membrane even in plant cells (Storozhenko, **2002**). On the contrary, the homologue in yeast is located on the inner face of the vacuolar membrane (Mehdi, **2001**). The bacterial homologues are soluble proteins and occur outside the cytoplasm. The enzyme occurs in the periplasmic space of gram-negative bacteria like *Escherichia coli*, *Proteus vulgaris* and *Helicobacter pylori* (Suzuki, **1986**; Nakayama, **1984**; Chevalier., **1999**). In contrast, the homologue in *Neisseria meningitidis* is located in the cytoplasm on the inner face of the inner membrane

(Takahashi, **2004**). The enzyme in gram-positive bacteria like *B. subtilis* is secreted into the extracellular medium (Xu, **1996**).

A2 1.4. Physiological functions

Many lines of evidences point to glutathione as the likely physiological substrate of mammalian GGTs. Glutathione (γ-L-glutamyl-L-cysteinylglycine, GSH, figures A2 8 and 9) is a thiol peptide occurring ubiquitously in eukaryotic cells at levels as high as 0.5-10 Mm (Mesiter, **1983**). The free sulphydryl moiety enables glutathione to function as the major antioxidant to maintain a reducing intracellular environment. Glutathione neutralizes oxidants like peroxides by forming the respective disulphide, while electrophiles are negated by formation of *S*-conjugates (Zhang, **2005**):

$$2\ GSH + H_2O_2 \rightarrow GS\text{-}SG + 2\ H_2O$$

$$GSH + electrophile \rightarrow GS\text{-}conjugate$$

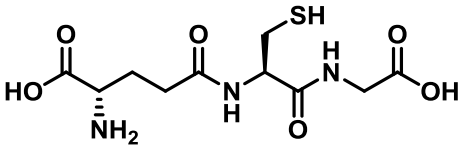

Figure A2 8 glutathione (GSH) reduced

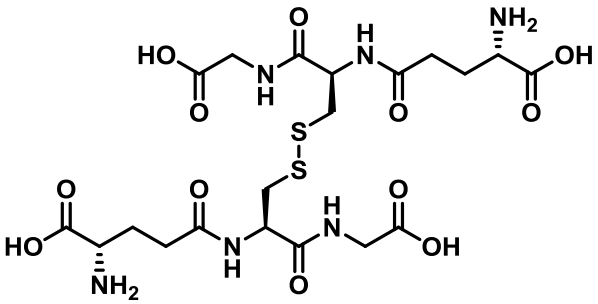

Figure A2 9: glutathione (GSSG) oxidized

The physiological availability of Cys, the critical residue in glutathione, appears to be limited. Mice fed with protein-deficient diet have lower glutathione but higher GGT levels and the digression could be remedied by supplementation with methionine (Whitfield,

2001). These findings demonstrate the dietary importance of sulphur-containing amino acids in maintaining glutathione homeostasis and the reciprocal role of GGT in the process. However, the mechanism by which GGT contributes to glutathione homeostasis is not clear. GGT was proposed to mediate the transmembrane transfer of amino acids by participating in the 'γ- glutamyl cycle' (figure A2 10) (Meister, **1973**).

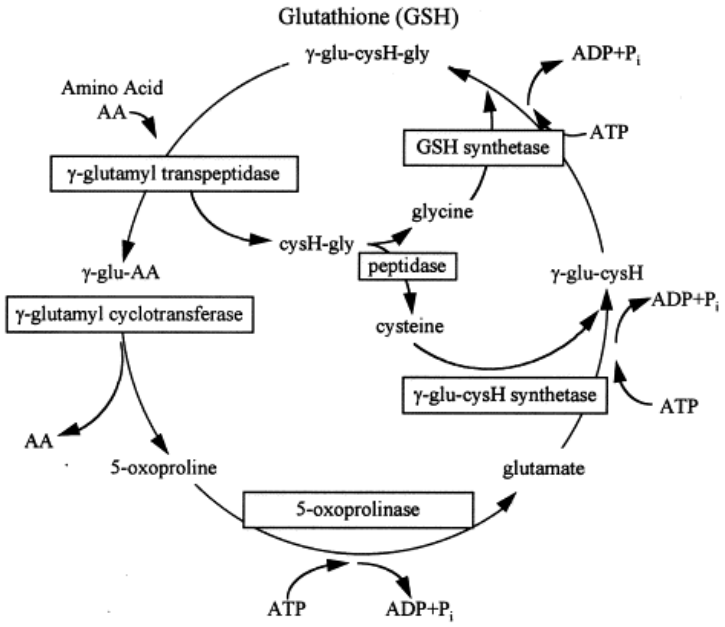

Figure A2 10: γ-glutamyl cycle

The cycle begins with the transfer of γ-L- glutamyl moiety from glutathione to an amino acid (other than proline) to form γ-L-glutamyl-amino acid. It was assumed that the transfer of γ-glutamyl moiety somehow facilitates the transport of the amino acid into the cytoplasm. In this view, glutathione serves as a donor of the vital glutamyl residue. While in the cytoplasm, the glutamylated amino acid forms 5-oxoproline (pyroglutamic acid) with the concomitant release of the amino acid in a reaction catalyzed by a cyclotransferase. Glutamic acid is then reformed from 5-oxoproline for reuse in glutathione synthesis. The predominant localization of GGT in epithelia active in absorptive function apparently supports the putative role in amino acid absorption. However, the hypothesis may not be valid as it is in conflict with the observation of unimpaired amino acid transport in GGT-deficient humans and animals. Furthermore, the 'γ-glutamyl cycle' was proposed on the basis of circumstantial evidences and was not demonstrated by radioactive tracer method. Thus it appears that the primary function of GGT is in the liberation of Cys from glutathione for the salvage pathway.

GGT also appears to be involved in the formation of mercapturic acids (*N*-acetyl *S*-substituted cysteine derivative) from glutathione (Hinchman, **1991**). Mercapturic acid derivatives increase the solubility of the xenobiotics, thus enabling their removal by the excretory system. Biosynthesis of mercapturic acids begins in the cytoplasm of liver cells by conjugation with glutathione, a reaction catalysed by glutathione *S*-transferase. The conjugates are then transported into the extracellular space, where they are converted into cysteine *S*-conjugates by membrane-bound GGT and dipeptidases. These conjugates are then returned to the cytoplasm for acetylation by *N*-acetytransferases.

The role of GGT in plant tissues is still unclear as there is no evidence for the presence of glutamyl cycle in plant tissues (Leustek, **2000**). Furthermore, some plant GGTs have low affinity for glutathione under *in vitro* conditions. The enzyme is speculated to participate in the biosynthesis of γ–glutamyl dipeptides that are formed during fruit ripening and accumulate in storage tissues such as seeds and bulbs in certain plants (Kean, **1980**; Ishikawa, **1967**). In onion, GGT is supposed to catalyse the last step in the formation of precursors of volatile compounds (Martin, **2000**). Studies with suspension cultures of tobacco cells indicate potential participation of GGT in glutathione catabolism (Storozhenko, **2002**).

Among the GGTs present in nature, the more detailed studies have been carried out on the mammals GGT, in particular with regard to that of man and rat and, regarding bacterial GGT, *E.coli*. A number of results and analysis were carried out also on the GGT of *H. pylori* and *B. subtilis*.

A2 1.5. GGT in bacteria

A2 1.5.1. *E. coli* GGT

In *E. coli*, GGT is localized in the periplasmic space and is involved in the hydrolysis of exogenous GSH as a source of cysteine and nitrogen (Suzuki, **1993**); likewise, GGT is involved in the use of various compounds as γ-glutamyl-donor for transpeptidation reactions and as substrates for hydrolysis reactions (Suzuki, **1993**). With reference to its substrate specificity, *E. coli* GGT prefers basic amino acids, especially L-Arg and L-Lys, aromatic amino acids such as L-Phe, and also L-Met.

Amino acids such as L-Ala, L-Cys, L-Glu and L-Ser appear to be bad acceptors, as well as D-type amino acids, which sometimes are not accepted at all by *E.coli* GGT.

The K_M value for γ-glutamyl-donors appears to be quite low, while it is extraordinarily high for the γ-glutamyl acceptors: this evidence suggests that the transpeptidation may not be the main function of this enzyme (Chevalier, **1999**).

The three dimensional structure of the enzyme of *E. coli* K12 has been obtained by X-ray chrystallography: it is a dimer, composed of a large subunit (L, Mr 46,000) and a small one (S, Mr approximately 22,000) (Wada, **2010**).

This enzyme originates from a single precursor protein cut coincident with the peptide bond between Gln-390 and Thr-391 which acts as a nucleophile and becomes the *N*-terminus of the S subunit. Another significant feature of the three-dimensional structure of this enzyme is the presence of a lid that covers the active site. The lid originates after the autoproteolytic cleavage, when the new *C*-terminus (residues 375-390) moves away, allowing the residues 438-449 to cover the binding pocket.

The lid-loop covers the binding pocket, isolating it from the solvent when it is occupied by a substrate or an inhibitor; it also appears to be involved in the recruitment of substrate and it is definitely crucial in the catalytic process (Wada, **2010**). There are two other fundamental differences between mammalian GGT and *E. coli* GGT. The first difference concerns the precursor protein: this protein in *E. coli* has a signal-peptide at the *N*-terminal, which directs the peptide in the periplasmic space, while *N*-terminal region of mammalian GGT allows the association of the enzyme with the plasma membrane. As the second difference, mammalian GGTs are, as already noticed, glycosylated proteins, while the one in *E.coli* is not glycosylated (Okada, **2006**).

A2 1.5.2. *H. pylori* GGT

In *H. pylori* GGT has been identified as a virulence factor, although its precise role is still unknown. It is thought to be associated with the process of colonization of the gastric mucosa, because it was shown that this enzyme induces apoptosis in gastric epithelial cells and inhibits proliferation of T-cells (Morrow, **2007**).

It was also seen that GGT of *H. pylori* is able to degrade glutamine and extracellular GSH, producing glutamic acid, which can be transported inside the bacterium. This hydrolysis of extracellular GSH and Gln, probably coupled with the release of ammonia, can result in damage of the gastric mucosa cells (Morrow, **2007**).

Furthermore, the *H. pylori* enzyme shows a limited transpeptidase activity while using GSH and glutamine as main substrates. It was therefore thought that this enzyme has a function of a generic hydrolase (Lherbert, **2004**). In addition, mutagenesis studies on a particular residue of the lid-loop (Y433A) of *H. pylori* have demonstrated that mutations in this region cause a significant decrease in the catalytic activity of the enzyme, thus giving further evidence for the importance of this region of the enzyme.

A2 1.5.3. *B. subtilis* GGT

GGTs from different strains of *Bacillus*, such as *B. Natto*, *B. subtilis* 168 (Minami, **2003**) or TAM-4 (Abe, **1997**), have been identified and purified. From the analysis of these proteins it was possible to identify some key features that differentiate them from *E. coli* GGT.

The first important feature of the GGT of *B. subtilis* is its extracellular localization. On the contrary, *E. coli* GGT is located in the periplasmic space. This allows the isolation of *B. subtilis* GGT from the culture broth, avoiding the cell disruption step required for *E. coli* GGT. Other interesting characteristics of *B. subtilis* GGT are the absence of the lid-loop and the presence of an extra sequence at the C-terminus of the L subunit.

However, the catalytically active Thr391 and the residues involved in substrate binding appear to be highly conserved. So, unlike the previous two bacterial GGTs described (*E. coli* and *H. pylori*), in which the lid-loop covers the active site when it is busy, in *B. subtilis* there are no segments covering the substrate when it is bound in the catalytic site; therefore the substrate remains exposed to the solvent (Wada, **2010**).

A comparison between the mode of glutamate binding in *B. subtilis* GGT and in *E. coli* GGT is shown in figure A2 11. In both cases the glutamate is bound similarly in the two active sites, with the α-carboxylic and α-amine groups bound to the bottom area of the active site with some hydrogen bonds and salt bridges. In *B. subtilis* (figure A2 11-A) the carboxyl group interacts with Arg113, with the O_γ Ser464 and Ser465, while the amino group interact with Glu442, Glu423 and Asp445 (Wada, **2010**). The carboxyl group in position ε of the glutamate is instead stabilized by hydrogen bonds with the two amino groups of Gly485 and Gly486, which contribute to form the oxyanion hole.

In *E. coli* (figure A2 11-B) all interactions are equal, except for the two residues Glu423 and Glu442, which are replaced by Asn411 and by Gln430, respectively. In conclusion,

B. subtilis GGT does not possess the lid-loop; besides, the *C*-terminal segment of the L subunits, which results from autocatalytic cutting, does not go through any other significant structural change, thus leaving the active site always exposed to the solvent (Wada, **2010**).

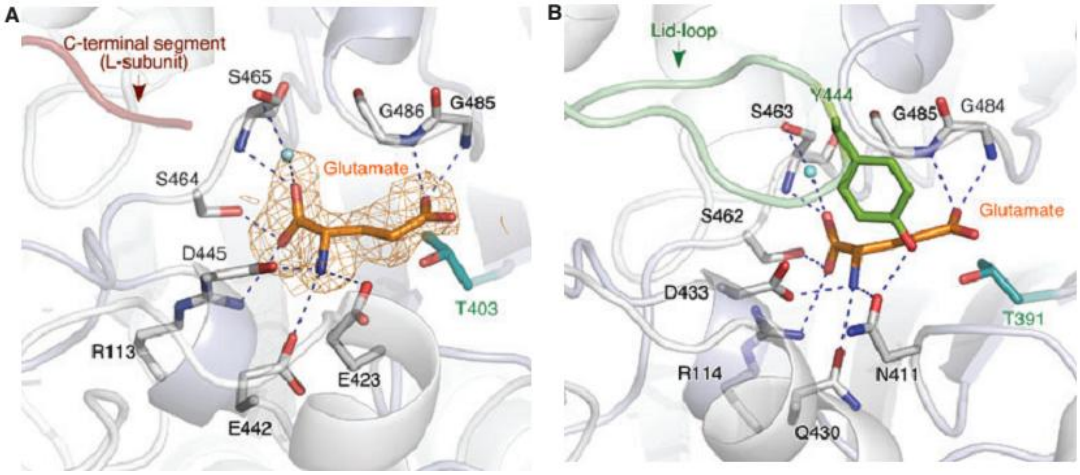

Figure A2 11: A and B: Glutamate binding in the catalytic pocket of GGT. (A) Electron density map for the bound glutamate in *B.subtilis* GGT. (B) The glutamate-binding mode in *E. coli* GGT. The bound glutamate and the catalytic threonines are shown in orange and cyan, respectively (Wada, 2010).

A2 1.6. Correlations between γ-PGA and GGT

It is well known that the γ-glutamyltranspeptidase (GGT) acts as a γ-glutamyl groups-transferring enzyme, and for this reason it has also been defined as γ-glutamyltransferase (GT); this enzyme is excreted into the culture medium also in *B. subtilis* (Kimura, **2004**). It has been shown that certain strains of *B. subtilis* and *B. anthracis* produce a capsule of γ-PGA, whose synthesis is carried out by a series of proteins encoded by operon PgsBCA in *B.subtilis* and CapBCA in *B. anthracis* (Kimura, **2004**). Once the growth conditions no longer require the presence of the γ-PGA capsule, this must be degraded, though probably this process is carried out by different enzymes.

In *B. subtilis* the degradation occurs during the late stationary phase, perhaps through the enzyme whose gene is located in the locus homologous to that of CAPD of *B. anthracis*. Such gene (ywtD) codes for a DL-γ-glutamyl hydrolase and despite the correspondence of the gene loci the two enzymes have no similarity at the level of amino acid sequence.

Afterwards has been discovered that the GGT of *B. subtilis* seems to be able to generate D- and L-glutamic acid monomers from γ-PGA, without any particular regard for the fact that

the terminal residue of the chain was D or L; other studies have shown that this degradation occurs so that bacteria can use these monomers as nitrogen sources.

The γ-PGA hydrolytic activity present in this GGT seems to be absent in *E.coli* and mammalian counterparts: this means that the polymer is a natural substrate only for GGT from *B. subtilis*. However it seems that, before the entire polymer is degraded, it requires to be fragmented through the action of an endo-hydrolase enzyme. Fragments of about $1x10^5$ Da are produced, which seem to be suitable to degradation by the GGT. It seems that the degradation *in vivo* of the γ-PGA capsule leads also to a regulation of the activity of the enzyme itself, *via* feedback inhibition by glutamic acid. This happens to avoid a overdegradation of the polymer and allows to maintain a reserve of glutamate (Kimura, **2004**).

A2 2. Results and discussions

The evaluation of the enzymatic activity of GGTs is typically made through a spectrophotometric assay, monitoring the rate of production of *p*-nitroaniline from γ-glutamyl-*p*-nitroanilide used as the donor compound in an enzyme-catalyzed reaction. However, this method is suited for monitoring the formation of the γ-glutamyl enzyme intermediate, on the assumption that in the presence of a good acceptor the transpeptidation reaction is faster than the hydrolysis of the donor. The actual fate of the γ-glutamyl enzyme intermediate is thus assumed rather than observed. On the contrary, HPLC analyses of the reaction mixtures could allow the observation of all the compounds formed during the reaction.

The first obvious problem is that only a few amino acids presents a chromophoric group and can't be therefore detected without any modification. For this reason, we used a standard pre-column derivatization method for amino acids and peptides HPLC analysis.

The derivatizing agent was dabsyl chloride **(**4-(4-dimethylaminophenylazo)benzenesulfonyl chloride). This compound is able to react quickly and quantitatively with amino groups and allows to identify easily every peptides or amino acids even in nanomolar concentration (Scheme A2 1). The derivatives of dabsyl chloride have a strong absorbance at 436 nm.

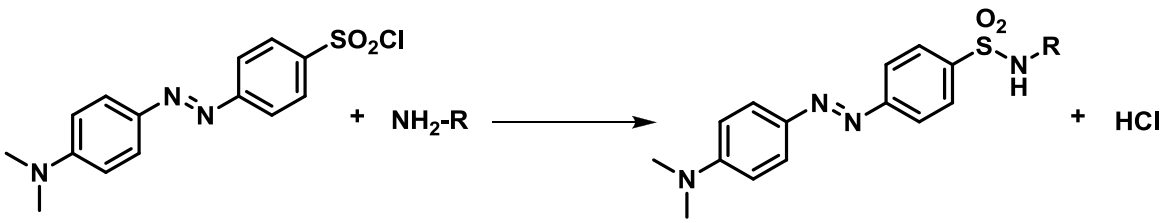

Scheme A2 1: reaction between dabsyl chloride (DBSCl) and amino group.

Dabsyl chloride is a commercial product in the form of small, deep red crystals, which allows derivatization procedure to be achieved quickly in mild reaction conditions at moderate temperature (see experimental).

In all the chromatograms, however, some peaks not assignable to any product from hydrolase and transpeptidase enzyme activity were observed. These peaks can be attributed to by-products of dabsyl chloride. The most intense peak is always present in the

chromatograms (cfr the HPLC-MS chromatograms in the appendix) at 16-17 min retention time and has been attributed to dabsyl acid. By comparison with an authentic sample on purpose prepared, the peak at 27-28 min has been attributed to dabsylamide, arising from reaction of dabsyl chloride with ammonia, originating in turn from the hydrolysis of glutamine during the reactions (Figure A2 1):

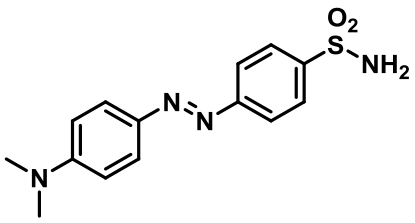

Figure A2 12: Derivate of ammonia, present in all the chromatograms.

A2 2.1. Synthesis of γ-glutamyl derivatives

In order to better understand the behavior of *B. subtilis* GGT, it was necessary to synthesize some γ-glutamyl derivatives to be used as reference compounds. These compounds were used in order to obtain calibration curves for quantitative HPLC evaluations.

The compounds were obtained using a procedure optimized in our laboratories in order to produce, with relative simplicity, γ-glutamyl derivatives. This technique revealed to be very practical: the standard procedure of peptide synthesis, in fact, implies different protection and deprotection steps, which become difficult working on glutamic acid, due to the presence of two acidic carboxylic groups. *N*-phthaloyl L-glutamic acid (**1**) is a commercially available product, but it can also be easily obtained from L-glutamic acid and phthalic anhydride simply by heating the two solids up to 140°C; also this step was optimized in our laboratories.

The procedure takes advantage from the synthesis of a cyclic anhydride of the L-glutamic acid protected on the amino group as phthaloyl derivative (**1**). The cyclization reaction to (**2**) follows in a one-pot procedure with acetic anhydride as dehydrating agent. The *N*-phthaloyl L-glutamic acid anhydride (**2**) can then be used as γ-glutamyl donor in a ring-opening reactions carried out simply by mixing the anhydride (**2**) with the appropriate amino acid (**3**) in DMF at room temperature, with no need of any added catalyst or

additive. The deprotection of the amino group was carried out in a one-pot procedure with an aqueous solution of hydrazine, that releases the amino group producing phthalic hydrazide. The desired γ-glutamyl derivatives usually precipitate during this step and can be recovered by filtration in the form of their hydrazinium salts. Products were then purified by ion exchange chromatography (Scheme A2 2).

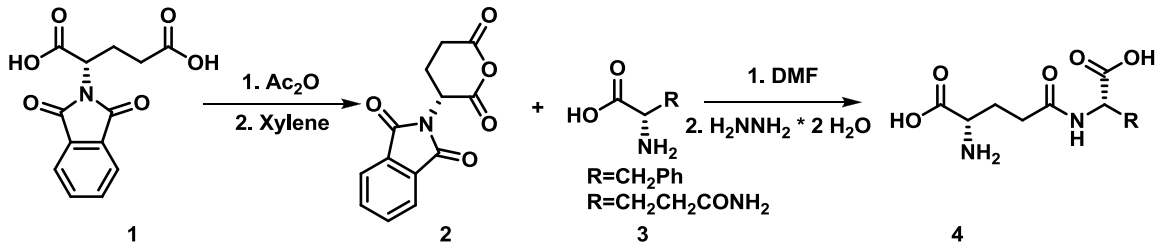

Scheme A2 2: Chemical synthesis of γ-glutamyl derivatives

We observed also that the yields and the reaction times are variable. This can be related to the solubility of the nucleophilic amino acid in DMF. The reaction with the readily soluble Phe, in fact, afforded γ-glutamylphenylalanine within 18 hours reaction time in 86% yield, whereas γ-Glu-Gln was obtained in 34% yield after 48 hours reaction time, due to the low solubility of glutamine.

A2 2.2. GGT hydrolase and transpeptidase activities at different pH

The first target of this work was to evaluate the pH dependence of the GGT activity. For this aim we used the spectrophotometric assay method already used in the literature for the determination of the transpeptidase and hydrolase activities of *B. subtilis* GGT.

The enzyme activity was tested at pH values from 6 to 11, because from the literature it is known that at low pH the GGTs have poor activity in both transpeptidation and hydrolysis. At each pH value, activity was measured both in the presence of an acceptor ("transpeptidation") and in the absence of any added acceptor ("hydrolysis"). The results are summarized in Figure A2 2. Reactions were thus carried out by subjecting γ-gluamyl-p-nitroanilide (γ-GpNA) to the action of the enzyme in the presence of GlyGly ("transpeptidation") and in its absence ("hydrolysis"). Reactions were carried out at 21-22 °C and monitored by measuring the absorbance at 410 nm. In the graph it is reported the reaction rate (average value of three runs) plotted against the pH of the reaction mixture.

From the obtained results it is possible to summarize that at higher pH both hydrolysis and transpeptidation reaction are more efficient. The experiments carried out at pH 6 show that the two reaction rates are nearly superimposable. As the pH value increases, the values of slopes become different. That difference increases more and more, reaching a maximum at pH 10, at which point the rate of reaction carried out in the presence of the acceptor nearly double with respect to the rate of reaction without added acceptor.

At pH 11, finally, a sharp drop was observed for both the reaction rates.

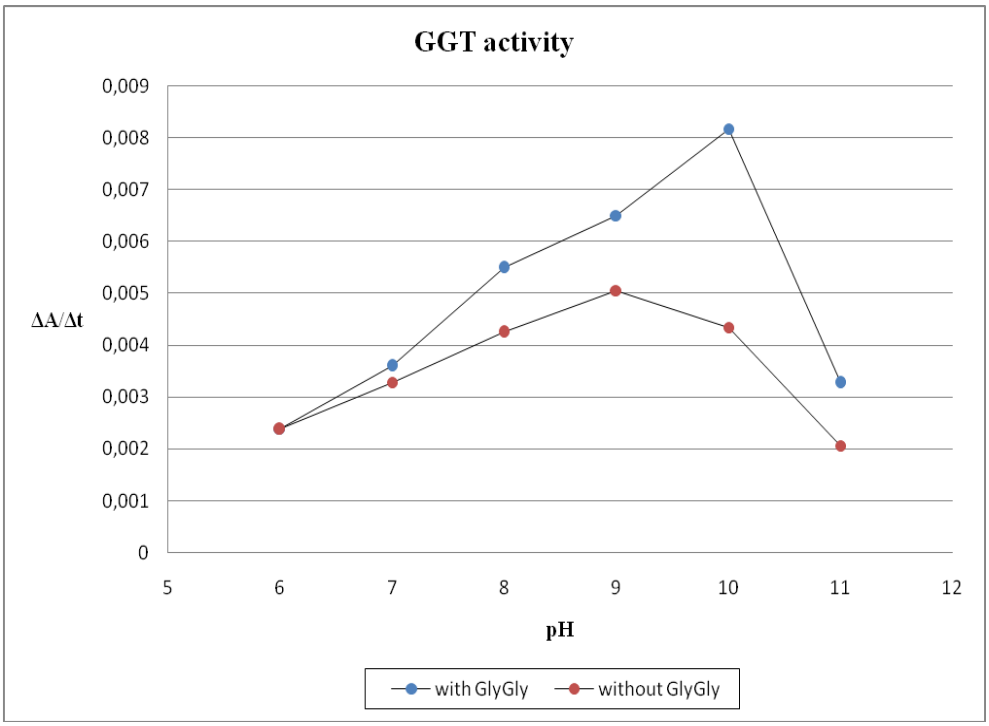

Figure A2 13: pH-dependence of hydrolase and transpeptidase activity of *B. subtilis*.

The descripted behavior of the *B. subtilis* GGT appears to be in contrast with that reported for mammalian GGTs: for these enzymes, in fact, the rate of the transpeptidation reaction in the presence of a good acceptor is up to 180 times higher than the rate of hydrolysis (no acceptor added).

From these evidences it can be concluded that it is very difficult to separate the two activities, due to the low difference between their reaction rates, and that it is also impossible to abolish, when only one of the two reactions is studied, the undesired 'counterpart'.

A2 2.3. Evaluation of pH-dependent glutaminase activity

The glutaminase activity of *B. subtilis* GGT has been already assessed (Minami, **2003**), and its pH-dependence was indagated, albeit in a relative way. We decided therefore to study the GGT-catalyzed conversion of glutamine to glutamic acid quantitatively, in order to establish not only the relative reaction rate, but also the amount of glutamine converted.

Three reactions were carried out at three different pH values (7.4, 8.2 and 9.8) and they were monitored at time intervals by HPLC. The three reactions were carried out with the same amount of enzyme (0.0049 U/mL) and the same quantity of glutamine (1000 µL, 100 mM).

For all the three experiments it's possible to observe a decrease of the glutamine concentration with the time. This is fully coherent with the glutaminase activity of the enzyme. On the other hand, only for the reaction at pH 7.4 an increase of the glutamic acid concentration was observed, which could justify the decrease of glutamine (Figure A2 3). In the reactions carried out at higher pH, in fact, the concentration of glutamic acid was lower than the amount of hydrolyzed Gln.

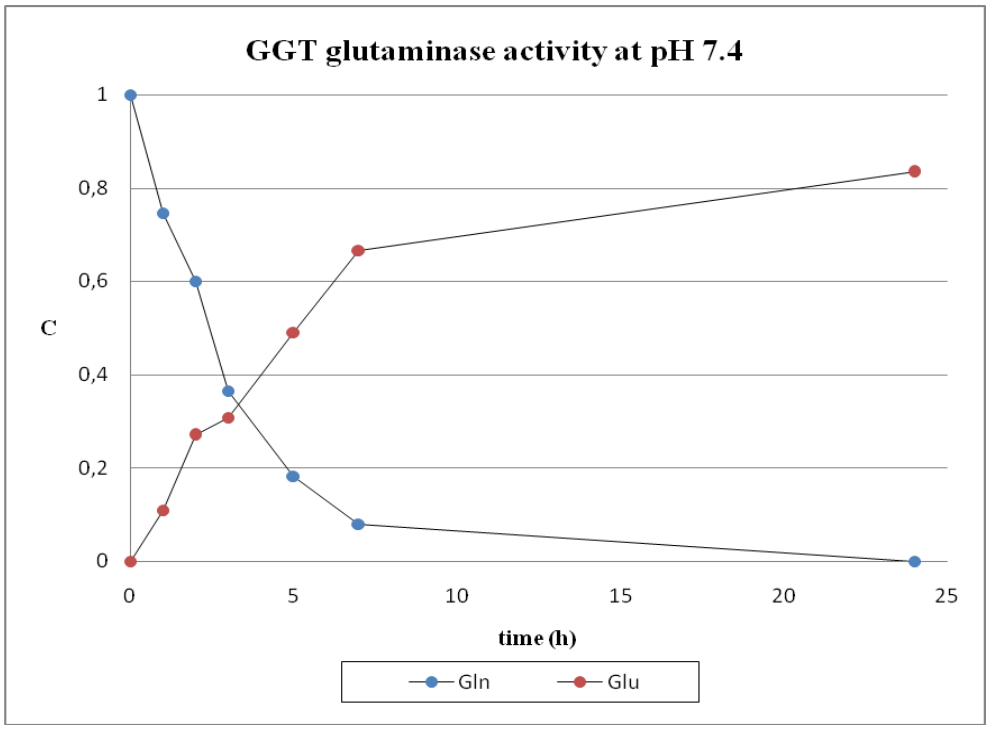

Figure A2 14: Time course of GGT-catalyzed reactions of Gln at pH 7.4.

At pH 8.2 the decrease of Gln concentration was sharper than the increase of glutamic acid concentration (Figure A2 15). In the meantime, a new peak appeared in the

chromatograms. HPLC-MS analysis allowed the attribution of the newly observed peak to γ-glutamyl-glutamine, arising from an auto-transpeptidation reaction. This was also confirmed by comparison with an authentic sample on purpose chemically synthesized.

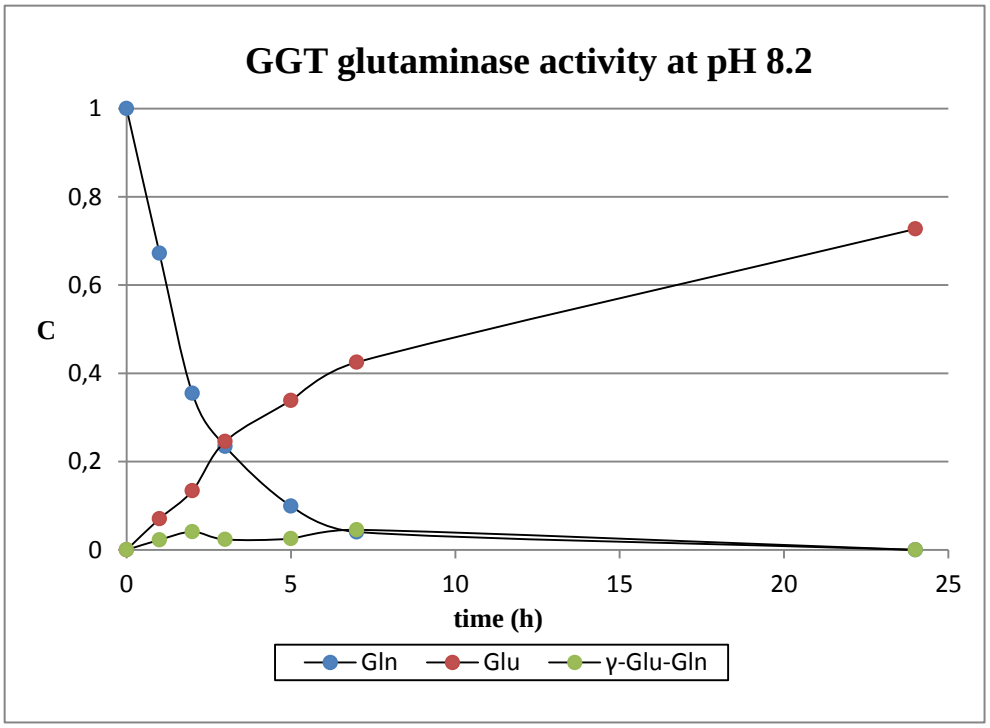

Figure A2 15: Time course of GGT-catalyzed reactions of Gln at pH 8.2.

The formation of this compound was also observed in the reaction carried out at pH 9.8. In this reaction the presence of other products could be observed: the formation of auto-transpeptidation product γ-Glu-Gln was accompanied also by the formation of γ-Glu-Glu (Figure A2 16).

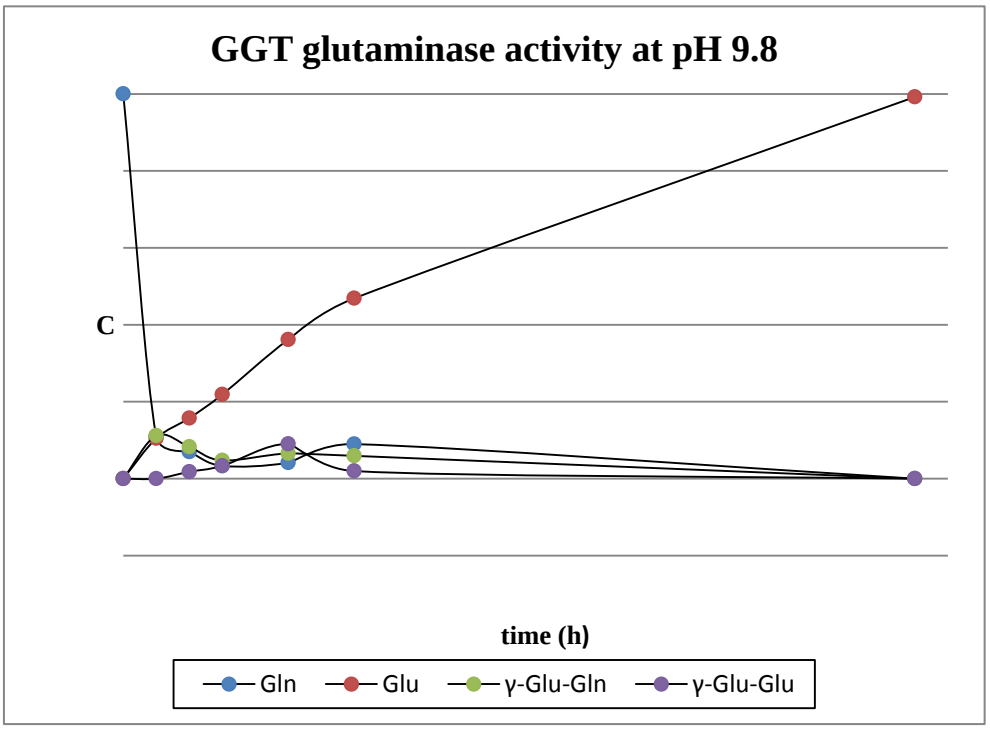

Figure A2 16: Time course of GGT-catalyzed reactions of Gln at pH 9.8.

The sum of the amounts of Glu, γ-Glu-Gln and γ-Glu-Glu formed in the reaction, however, do not reach the amount of Gln disappeared. HPLC-MS analysis of the reaction mixture showed indeed that the process can continue, producing higher γ-glutamyl derivatives, characterized by the presence of also three and four γ-glutamyl residues linked to a single glutamine molecule.

The experiments at pH 9.8 were repeated also using D-Gln. Tests with D amino acid are often omitted (Minami, **2003**) in enzymatic studies, because mammalian GGT and *E. coli* GGT are unable to recognize them as substrates. The trend of the reaction we observed was the same of that with L-Gln.

From this evidences we can affirm that GGT from *B. subtilis*, also in absence of any added acceptor, is able to use glutamine as acceptor in a strongly pH-dependent auto-transpeptidation reaction.

A2 2.4. GGT transpeptidase activity

Glycylglycine was recognized as a very good acceptor for GGT-catalyzed transpeptidation reactions, so it was considered the substrate of choice and the reference compound for such

studies. This behavior was attributed to the low pKa (8.2) of its nucleophilic amino group with respect to those of other amino acids. The low pKa value of the glycylglycine amino group ensures a large proportion of deprotonated, reactive nucleophilic species to be present even at those pH values at which the amino groups of standard amino acids result to be mainly in the protonated, unreactive form.

The reaction was carried out in the presence of equimolar quantities of Gln and GlyGly at pH 8.2, with the same amount of enzyme used in previously described reaction (0.0049 U/mL). Reaction mixtures were analyzed by HPLC with pre-column derivatization.

Figure A2 17 shows the trend of concentrations of reagents and products.

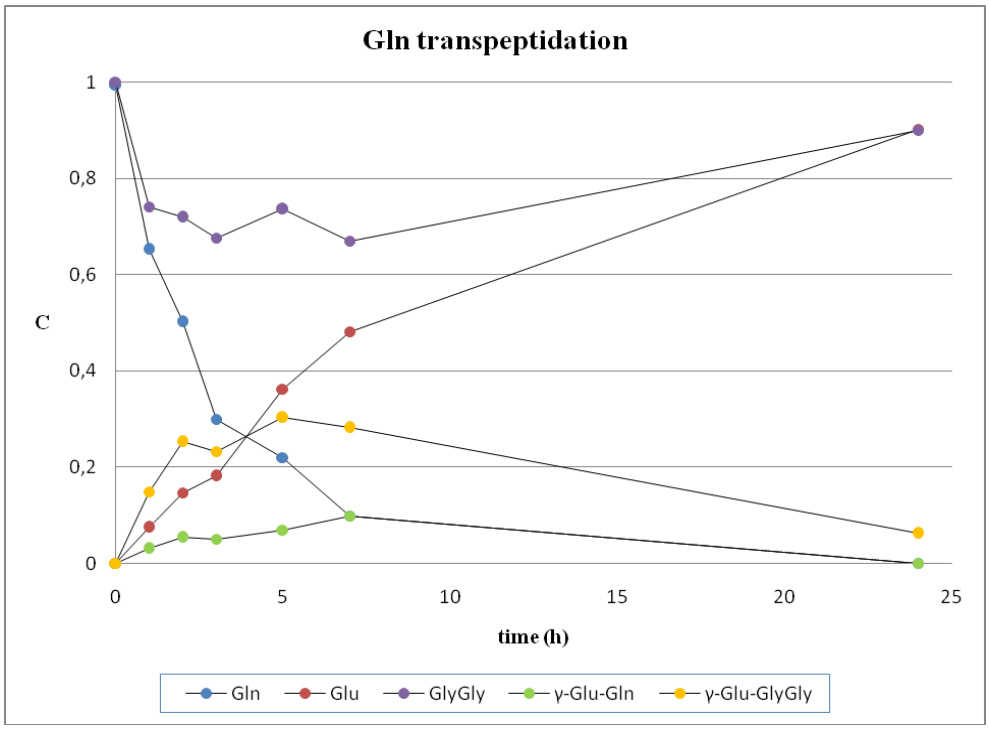

Figure A2 17: Reaction between Gln and GlyGly at pH 8.2; products formation and reagent consumption.

In the course of the reaction a decrease of the glutamine concentration is observed; at the same time it's possible to observe a decrease of the GlyGly concentration during the first 6-7 hours reaction time and a slow increase during the last hours of the reaction. As regards to the product formation, it's possible to observe the formations of both the hydrolysis and transpeptidation products. Glutamic acid concentration increases slowly and the trend of formation of γ-glutamyl-glycylglycine and γ-glutamyl-glutamine increases for the first 5-7 hours and then decreases.

The trend of glycylglycine concentration deserves further analysis: after an initial reduction, the concentration of the acceptor dipeptide stays fairly constant and then it starts to increase, until it reaches almost the starting value. Beyond certain concentrations, the products of the reaction γ-Glu-GlyGly and γ-Glu-Gln become in turn substrates for the GGT-catalyzed hydrolysis. This hydrolytic step is irreversible and thus with prolonged reaction times the only detectable products are glutamic acid and the starting GlyGly.

The graph shows that at pH 8.2 GlyGly is indeed a better glutamyl acceptor than Gln. This can be deduced from the comparison between the trend of the glutamyl products γ-Glu-GlyGly and γ-Glu-Gln: the production of γ-Glu-GlyGly is, in fact, higher than that of γ-Glu-Gln during all the time of the reaction. The enzyme show therefore a preference for GlyGly as the acceptor in a transpeptidation reaction, with respect to glutamine present in the reaction mixture at a similar concentration. This trend, however, will be further analyzed in the following paragraph and a deeper analysis on pH- and acceptor-dependence will be made.

A2 2.5. GGT transpeptidase activity towards amino acids

Transpeptidation reactions between glutamine as the γ-glutamyl donor and selected acceptor amino acids were evaluated at different pH values, ranging from 7.5 to 11.0, in order to assess the degree of transpeptidation with respect to the auto-transpeptidation reaction. 100 mM solutions of glutamine and the acceptor amino acid were incubated in the presence of *B. subtilis* GGT for one hour at 23°C, then aliquots of the reaction mixtures were withdrawn, derivatized with dabsyl chloride and analyzed by HPLC. Only the reaction with phenylalanine as acceptor substrate was carried out at 50 mM concentration, because of solubility reasons.

Candidate amino acids used for this purpose were selected on the basis of the pK_a of their amino group. Glycylglycine was chosen as representative of an acceptor with a low pK_a of the nucleophilic amino group (pK_a 8.2); methionine (pK_a 9.21), phenylalanine (pK_a 9.13) and serine (pK_a 9.15) were selected for having intermediate pK_a similar to each other and to glutamine (pK_a 9.13). Alanine, with a pK_a of the amino group of 9.69, was representative of an acceptor with a slightly higher pK_a.

In the transpeptidation reactions using glycylglycine as acceptor substrate (Figure A2 18), the product concentration appeared to be appreciable even between pH 7.5 and 9.0; after that it increased with increasing pH. However γ-glutamyl-glutamine (not shown in figure),

deriving from the auto-transpeptidation reaction, was also always noticed in the reaction mixtures, albeit in lower concentrations with respect to the desired transpeptidation product. This behavior was however noted also in the previously described transpeptidation assay at pH 8.2 (Figure A2 18).

As the pH of the reaction mixtures approximated the pK_a of the donor glutamine amino group, the concentration of the residual glutamine after 1 h reaction time decreased, due to the auto-transpeptidation reaction. Usually glutamine was hardly detectable after 1 hour in reactions carried out at pH 9.5 and above. HPLC-MS experiments on the crude reaction mixture of the reaction at pH 10.5 demonstrated that, beside in the expected auto-transpeptidation product, γ-glutamyl moiety deriving from the starting glutamine ended up also in γ-glutamyl-γ-glutamyl-glycylglycine and γ-glutamyl-γ-glutamyl-γ-glutamyl-glycylglycine. Also species formed by two γ-glutamyl residues bonded to a single glutamine molecule were identified.

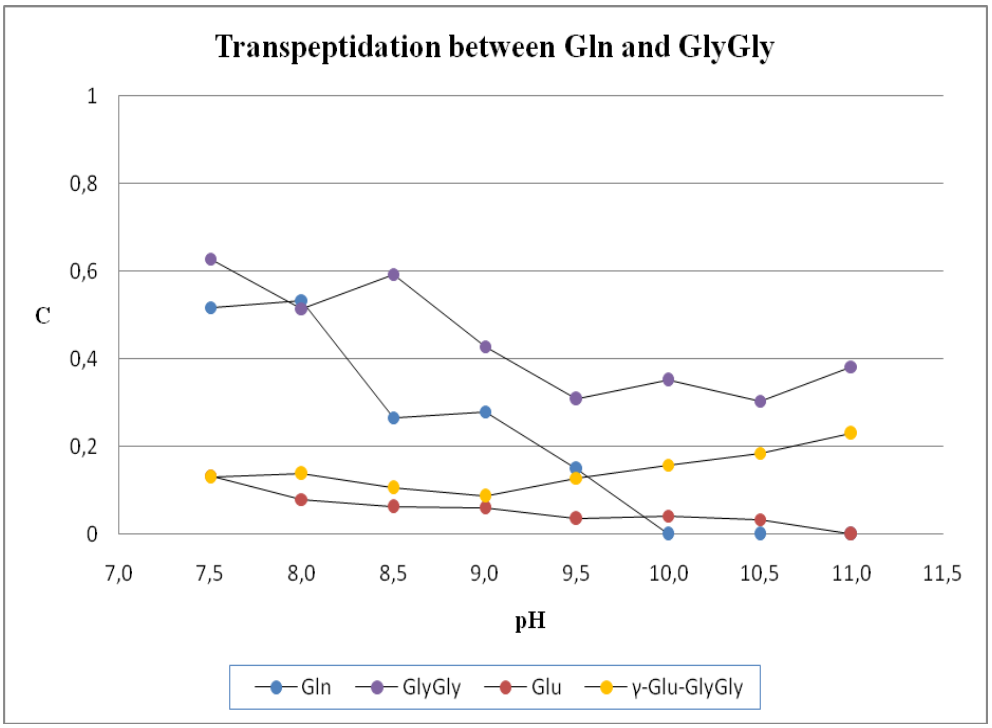

Figure A2 18: Evaluation of GlyGly ability as γ-glutamyl acceptor.

The acceptor activity of GlyGly, therefore, confirms the analysis at pH 8.2 and allows to better understand the pH-dependent behavior.

Reactions in which phenylalanine and methionine were used as acceptors showed, unlike those with GlyGly, low activity at the lower pH values, with a steadily increase of transpeptidation products concentration with pH (Figure A2 19).

Taking the reaction with methionine as an example, HPLC-MS analysis of derivatized reaction mixture after 1 hour reaction time at pH 8.0 confirmed the presence of unreacted methionine and glutamine as the major components. The hydrolysis product glutamic acid, the expected γ-glutamyl-methionine and the auto-transpeptidation product γ-glutamyl-glutamine were present in similar, quite low concentrations. After 1 hour reaction time at pH 10.5, on the other hand, the peak of the transpeptidation product γ-glutamyl-methionine was the most prominent among those of the newly formed compounds. As reported before, glutamine was present in very low concentrations, as did glutamic acid. No peaks attributable to poly(γ-glutamyl)glutamine were detected by HPLC-MS, although small amounts of compounds formed by up to three γ-glutamyl moieties bound to a single methionine residue were identified.

For this reason it can be theorized that the poly(γ-glutamyl)-glutamine derivatives initially formed can act as donor towards methionine in a later stage of the reaction and also that this reaction is favorite considering the absence of derivatives with more than one glutamine but without methionine.

Phenylalanine behaved similarly, and its activity as acceptor substrate was lower with respect to methionine (Figure A2 19). This lower activity can be also observed in HPLC-MS chromatograms: the peak attributable to the γ-glutamyl derivative was always lower for Phe in respect to Met. Furthermore, while in the case of methionine the formation of γ-glutamyl-γ-glutamyl-γ-glutamyl-methionine was observed, for phenylalanine the product with the highest molecular weight was γ-glutamyl-γ-glutamyl-phenylalanine even at the highest pH.

Figure A2 19 also explain the influence of the pK_a of the acceptor amino acid towards the γ-glutamyl derivate formation. GlyGly has the lowest pKa and the production of γ-glutamyl-glycylglycine also at low pH value reflects that value. When the pH of the reaction mixture approximate the pKa of the donor glutamine, auto-transpeptidation reaction become competitive.

On the basis of these results it can be concluded that methionine and phenylalanine compete effectively with glutamine as acceptor substrates, provided the pH of the reaction medium is maintained above the pKa of their nucleophilic amino groups.

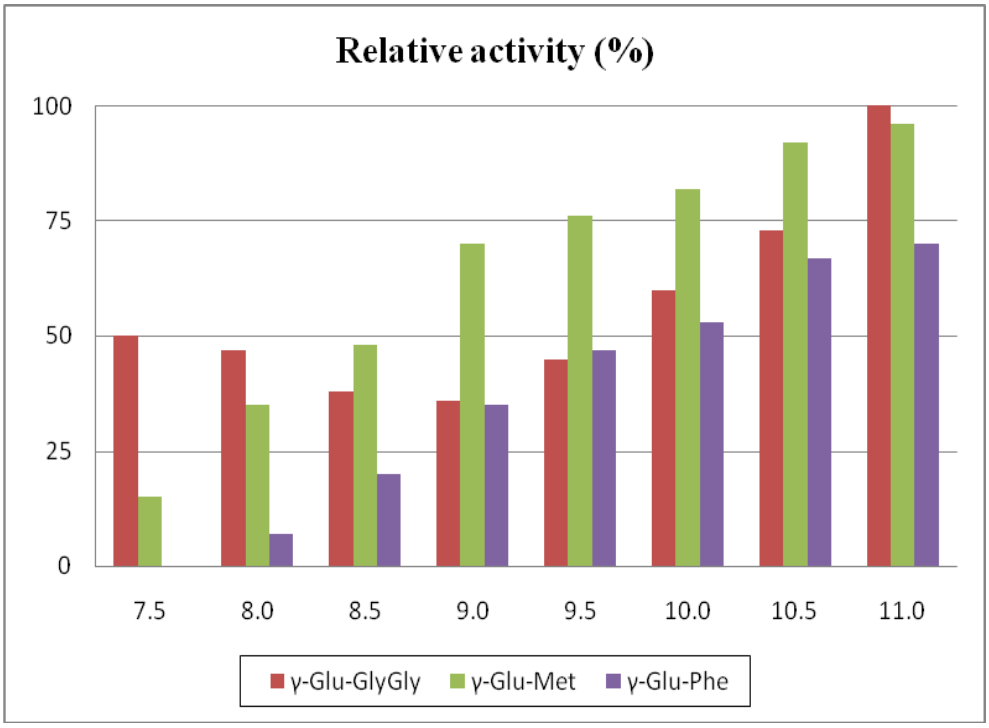

Figure A2 19: Relative activity of Met and Phe as γ-glutamyl acceptor at different pH. Values are related with GlyGly activity.

Moreover, in the presence of a good nucleophile, the hydrolysis reaction is minimized, as demonstrated by the low amount of glutamic acid produced in each reaction.

Serine was also chosen for having a pK_a of the amino group similar to that of glutamine; however its behavior in *B. subtlis* GGT-catalyzed transpeptidation reaction was different. It showed indeed a very low propensity to act as acceptor when compared with methionine and phenylalanine (Figure A2 21). The concentration of the transpeptidation product γ-glutamyl-serine is evident only at relatively high pH values (over 9.5) and, more interesting, the donor substrate glutamine did not disappear even at high pH.

Similar results were obtained using alanine as acceptor substrate. In this case, HPLC-MS of the reaction at pH 10.5, Figure A2 20, showed the presence of only unreacted starting materials and very low amounts of transpeptidation and auto-transpeptidation products, reported in Table A2 1.

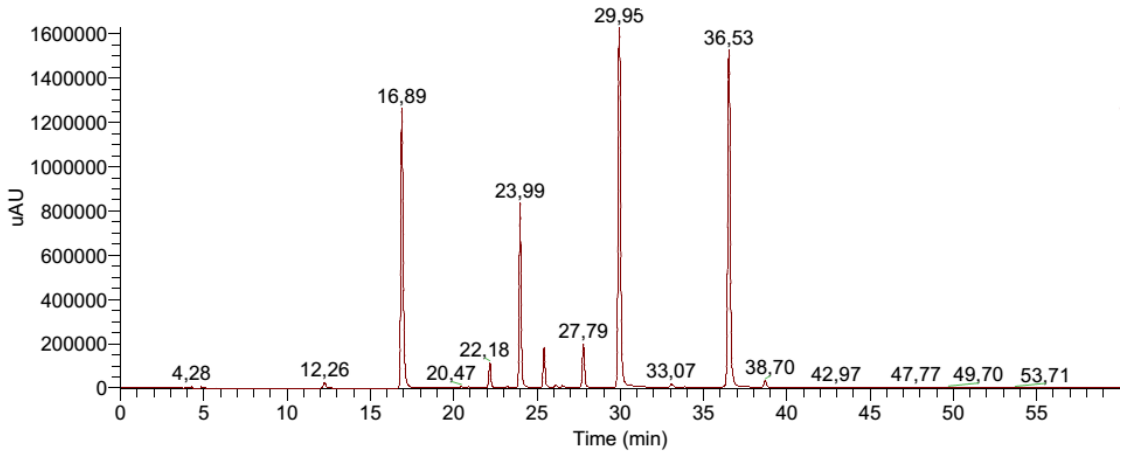

Figure A2 20: Chromatogram of GGT-catalyzed transpeptidation reaction between Gln e Ala at pH 10.5 after 1 hour reaction time. It's possible to observe the peak at 23.99 min corresponding to Gln that is very intense also at high pH.

Retention time (min)	MW	Compound (derivatized)
16.89		DBS
22.18	563.3	γ-Glu-Gln
23.99	434.2	Gln
25.46	506.3	γ-Glu-Ala
27.79	305.3	ammonia
29.95	377.4	Ala
36.53	419.3	Leu

Table A2 1: Peak analysis of GGT-catalyzed transpeptidation reaction between Gln and Ala at pH 10.5 after 1 hour reaction time.

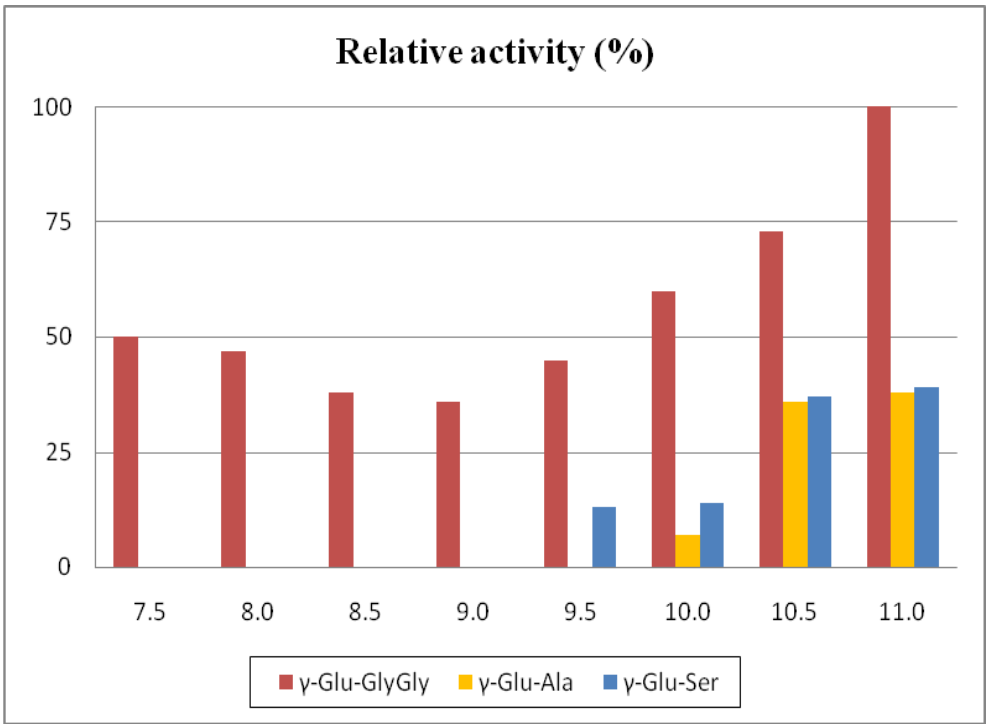

Figure A2 21: relative activity of Ala and Ser as γ-glutamyl acceptor at different pH. Values are related with GlyGly activity.

The poor attitude of serine and alanine to act as acceptor substrates in GGT-catalyzed transpeptidation reactions has been already established for *B. subtilis* 168 GGT (Minami, **2003**) through spectrophotometrically assays, but this assays cannot observe this behavior of lack in the auto-transpeptidation reaction involving glutamine, and so the low concentration of γ-Glu-Gln.

Such a behavior could be indicative of an inhibitory activity of a component of the reaction mixture towards the enzyme. Whether the inhibitory activity is due to the amino acids themselves, or it can arise from the newly formed γ-glutamyl derivatives, will be the subject of further studies in our laboratories.

A2 2.6. Evaluation of auto-transpeptidation products

L-Gln was reported to have a very low γ-glutamyl acceptor activity: 5.4% (Minami, **2003**) of the activity of GlyGly taken as 100%. However this activity was measured using 10 mM acceptor solution and the analysis was carried out in TRIS-HCl buffer at pH 8.73. We have above demonstrated that transpeptidase activity is strictly pH-dependent and the results found for the acceptor ability of Gln must be analyzed in relation with the operative pH. Glutamine has a pKa of 9.13, glycylglycine, instead, has a pK_a of 8.2: working in buffer

with pH 8.73, the amino group of GlyGly is widely deprotonated but that of Gln is not; these variations of protonated/deprotonated state of amino groups lead to variations of the reactivity as acceptor role and it is translates in a low apparent activity for Gln and a corresponding high activity for GlyGly.

For that reasons, we decided to evaluate the acceptor ability of glutamine with a particular method: we chose to use an automatic dispenser in order to dispense, during the reaction time, some amount of Gln 200 mM. In such way it was possible to provide to the enzyme new glutamine every time, preventing the concentration of donor from quickly becoming zero and thus we could observe the formation of auto-transpeptidation products rather than the formation of glutamic acid.

The reaction was monitored after 1.5 hour and after 3 hours during the additions and 1, 2 and 3 hours after the end of the additions; each withdrawal was analyzed with HPLC with pre-column derivatization (Figure A2 22). Furthermore, the withdrawals after three and six hours were analyzed by HPLC-MS. The reaction mixture, after the thermal inactivation of the enzyme by heating at 70°C for 15 minutes was analyzed by MALDI-TOF (Figure A2 23).

The trend for this reaction confirms what we already observed during the previous experiments: Gln, when the pH value overcomes its pK_a, quickly decreases producing γ-glutamyl derivatives with different molecular weight: in HPLC analysis it was possible to follow formation, development and decrease of γ-glutamyl-glutamine and γ-glutamyl-γ-glutamyl-glutamine but in HPLC-MS the peaks of trimers, tetramers, pentamers and also examers (Figure A2 23) were clearly observed. In HPLC-MS chromatogram, also, it is possible to observe a small amount of glutamic acid: the chromatogram, in fact, shows the mixture after six hours reaction time and after three from stopping the glutamine addition. It's also possible to observe a small amount of γ-glutamyl-glutamic acid.

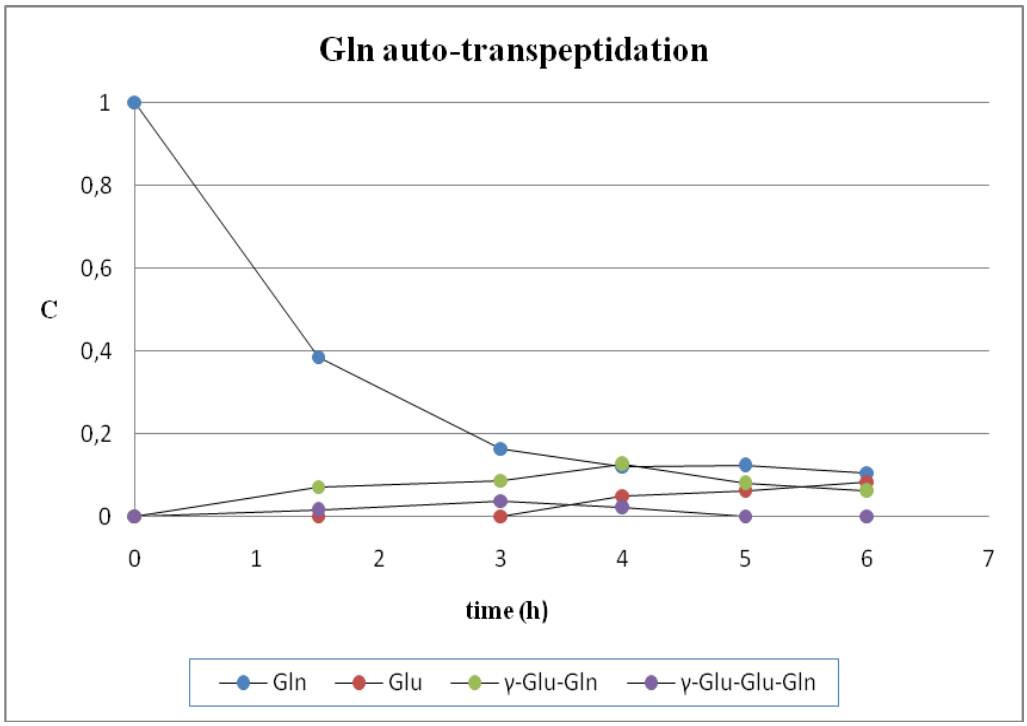

Figure A2 22: Gln auto-transpeptidation carried out with automatic dispenser.

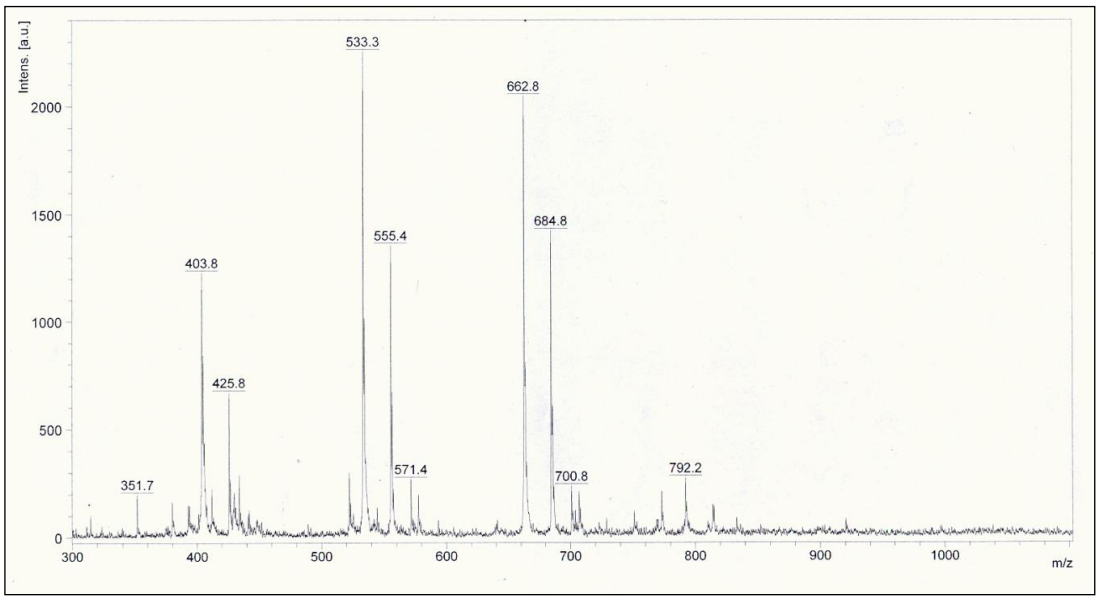

Figure A2 23: MALDI-TOF analysis of reaction mixture not derivatized. Peaks at 403.8, 533.3, 662.8 and 792.2 correspond to γ-glutamyl trimer, tetramer, pentamer and examer. It's possible to observe a minimum peak at 920 corresponding to γ-glutamyl eptamer. The peaks at 425.8, 555.4, 684.8 and 814.2 correspond to $[M+Na]^+$. The peaks at 571.4, 6700.8 and 814.2 correspond to $[M+K]^+$.

In conclusion we can state that the evidence that glutamine was a bad γ-glutamyl acceptor lacks of foundation. Glutamine could become a good γ-glutamyl acceptor at the right pH conditions and also shows a strong tendency towards the auto-transpeptidation in order to form γ-glutamyl derivatives with high molecular weight.

A2 2.7. Synthesis of γ-glutamyl derivatives through GGT-catalyzed transpeptidation

The so far described results suggested that the *B. subtilis* GGT-catalyzed transpeptidation reaction between glutamine as donor and an acceptor amino acid is feasible, provided that the pH of the reaction medium is basic enough to ensure a certain concentration of a deprotonated, nucleophilic amino group of the acceptor molecule. It was also anticipated that at the required basic pH the donor glutamine will disappear rapidly from the reaction mixture, due to the auto-transpeptidation reaction which produces γ-glutamyl-glutamine as major by-product, together with poly-glutamylated glutamines in lower concentrations.

The *B. subtilis* GGT-catalyzed synthesis of γ-glutamyl-methionine, a known naturally occurring flavor enhancer, was chosen in order to test this possibility. GGT-catalyzed synthesis of γ-glutamyl-methionine was carried out at an analytical level (1 mL of 100 mm solution of glutamine and methionine, equal to 0.1 mmol) and monitored by HPLC analysis. This step was used in order to evaluate the best reaction time to use on preparative level, so to stop the reaction at the maximal concentration of the desired product. Results are reported in Figure A2 24.

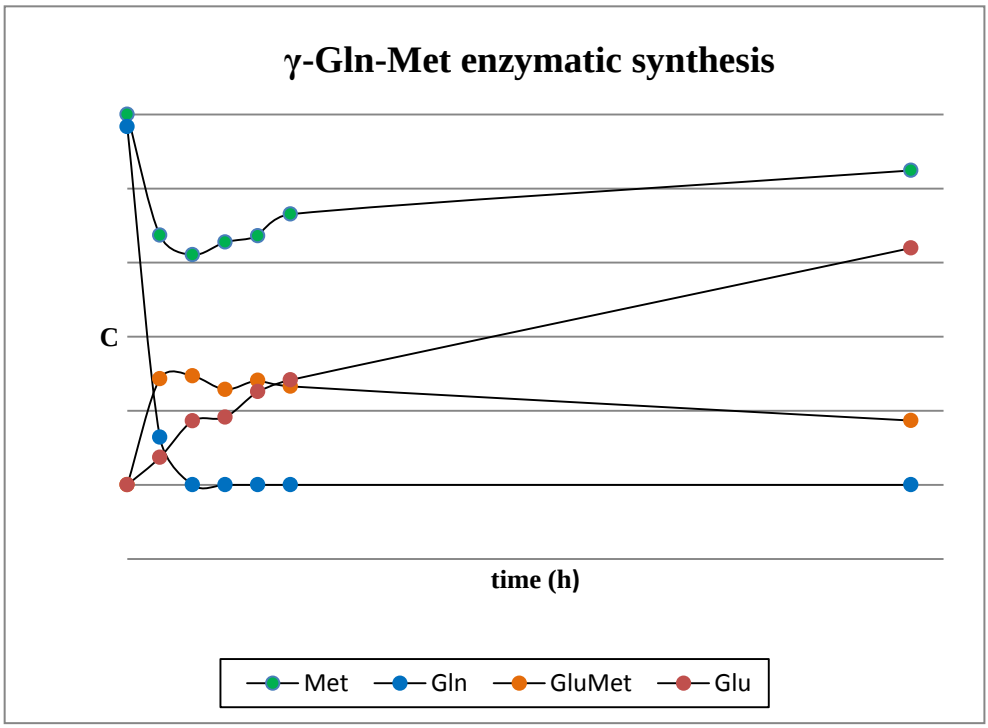

Figure A2 24: reaction trend of GGT-catalyzed transpeptidation between Gln and Met.

The concentration of glutamine dropped rapidly, whereas the decrease in concentration of methionine was accompanied by a parallel increase of γ-glutamyl-methionine up to a calculated concentration of ca 50 mM (50% yield) in the reaction mixture within the first hour reaction time; after that concentrations remained fairly constant up to two hours. The amounts of both glutamic acid and γ-glutamyl-glutamine remained low throughout the reaction. Substantial amounts of glutamic acid and hydrolysis of the formed product γ-glutamyl-methionine became evident only after 24 hours reaction time.

In our opinion the constant concentration of the transpeptidation product even after the disappearance of the donor substrate glutamine can be explained with the early formation of γ-glutamyl-glutamine (not represented in the graph) and other poly-glutamylated species, which became able to function as γ-glutamyl donors in later reaction steps. In this circumstances a complex equilibrium arises, in which auto-transpeptidation and poly-γ-glutamylation reactions of glutamine occurring mainly at the beginning of the reaction, lower the molar concentrations of the donor species, so that the acceptor substrate methionine finds itself in molar excess with respect to the donors. The transfer of the γ-glutamyl moieties from the newly formed donor species to methionine becomes therefore the preferred reaction path up to two hours reaction time.

The reaction was then repeated at one millimole preparative level using 10 mL starting solution (100 mM). After 1.5 hours reaction time, the enzyme was inactivated by heating and the products were isolated by ion exchange chromatography. γ-Glutamyl-methionine was obtained in 46% yield. From the reaction mixture also unreacted methionine (ca 50%) and low amounts of glutamic acid and γ-glutamyl-glutamine (< 10% each) were isolated and identified by NMR.

This reaction, however, even though the desired product was successfully isolated, must be optimized. The product, in fact, was isolated in low yield and an approach which allows to increase that yield must be undertake.

A2 3. Experimental Part

A2 3.1 Matherials and methods

L-glutamine, D-glutamine, L-methionine, L-phenylalanine, L-serine, L-alanine, L-glutamic acid, *N*-phtaloyl-L-glutamic acid, phtalic anhydride, γ-L-glutamyl-*p*-nitroanilide (GPNA), dabsyl chloride (DbsCl) and anhydrous DMF were from Aldrich and were used as received.

Ion exchange chromatography was carried out using a Dowex 1×8 resin 200-400 mesh (Aldrich) in the acetate form. The resin was regenerated by standard methods and equilibrated with 5 volumes of 0.5 M acetic acid prior to use.

Analytical HPLC was performed on a Waters 600 (Millipore) instrument equipped with a Hewlett-Packard diode array detector Series 1050 (Palo Alto, CA) at 436 nm using a 250 × 4.60 mm Gemini column RP C18, 5 μm (Phenomenex Inc., Torrance, CA). Eluents: 0.1% aqueous solution of trifluoroacetic acid (solvent A) and acetonitrile/solvent A 80 : 20 (solvent B).

Elution gradient: 0-5 min isocratic elution using solvent A / solvent B 80 : 20; 5-35 min. linear gradient up to solvent A / solvent B 20 : 80; 35-45 min isocratic elution with solvent A / solvent B 20 : 80. Flow rate: 1.5 mL/min.

^{1}H and ^{13}C NMR spectra were acquired at 400.13 and 100.61 MHz respectively in D_2O or in DMSO-d_6 on a Bruker Advance 400 spectrometer (Bruker, Karlsruhe, Germany) interfaced with a workstation running Windows operating system and equipped with a TopSpin software package. ^{13}C signal multiplicities were based on APT experiments. Chemical shifts are given in ppm (δ) and are referenced to TSP [3-(trimethylsilyl)propionic-2,2,3,3-d_4 acid sodium salt, δ_{Me} 0.00 ppm] as external standard or to DMSO signal as internal standard (δ_H DMSO 2.50 ppm; δ_C DMSO 39.52 ppm).

Electrospray ionization mass spectra (ESI-MS) were recorded on a Thermo Finnigan LCQ Advantage spectrometer (Hemel Hempstead, Hertfordshire, U. K.).

UV measurements were carried out with a Jasco V-360 Spectrophotometer (Jasco International Co., Tokyo, Japan).

HPLC-MS were recorded using a Thermo Finnigan Surveyor LC pump equipped with a Thermo Finnigan Surveyor PDA detector and interfaced with the ESI ThermoFinnigan LCQ Advantage spectrometer using column and elution conditions already described for analytical HPLC.

A2 3.2. Synthesis of γ-glutamyl derivatives as reference compounds

A2 3.2.1. Synthesis of *N*-phtaloyl-L-glutamic acid anhydride

A2 3.2.1.1. Method A: from L-glutamic acid and phtalic anhydride

The procedure by Gu (**2004**) was followed, with some modifications. Glutamic acid (4.44 g, 30.0 mmol) and phtalic anhydride (4.41 g, 30.0 mmol) were ground together in a mortar and transferred into a 25 mL round-bottom flask. The flask was warmed at 140 °C while rotating by means of a Kugelrohr distillation apparatus until evolution of water ceased and an oily mass was formed (ca 30 - 40 min). The mass was cooled to ca 100 °C, acetic anhydride was added (10 mL) and the resulting mixture was stirred at 105 °C in a pre-warmed oil bath for 10 min after complete dissolution (total reaction time 20 - 25 min). The oil bath was removed and xylene (10 mL) was added with stirring to the hot mixture. The clear solution was allowed to cool slowly to room temperature without stirring and then placed at 4 °C overnight. The formed colorless crystals were collected by filtration, washed in succession with small volumes of cold, dry ethanol and ethyl ether and dried under reduced pressure. Colorless crystals, 4.08 g (52% yield). $[\alpha]_D$ = –43.1 (c 1.02, 1,4-dioxane) Lit. –44.7 (c 3, 1,4-dioxane) (Gu, **2004**).

A2 3.2.1.2. Method B: from *N*-phtaloyl-L-glutamic acid

N-phtaloyl-L-glutamic acid (1.386 g, 5 mmol) was suspended in acetic anhydride (4.5 mL) and the suspension was slowly warmed up to 70 °C in an oil bath with stirring, until complete dissolution of the starting material. Warming was continued for further 10 min, then the oil bath was removed and xylene (5 mL) was added with stirring. The mixture was allowed to stand without stirring until it reached room temperature, then the flask was placed at 4 °C overnight. Crystals were collected as in method A. Colorless crystals, 0.960 g (72% yield). $[\alpha]_D$ = –43.6 (c 1.00, 1,4-dioxane) Lit. –44.7 (c 3, 1,4-dioxane) [3].

A2 3.3. Synthesis of γ-glutamyl derivatives of amino acids

A2 3.3.1.General procedure

To a well stirred suspension of the appropriate amino acid (1.05 eq.) in dry DMF (2 mL/mmol of amino acid) under a stream of nitrogen, *N*-phtaloyl-L-glutamic acid anhydride (1.00 eq.) was added in one portion. The mixture was stirred at room temperature for 18-48 h, during which time most of the suspended material dissolves. The reaction mixture was diluted with water (5 % of the DMF by volume) and hydrazine hydrate was added (3.5 eq). Stirring was continued for 4 h. The formed thick precipitate was resuspended by addition of ethanol (half a reaction mixture volume) and the suspension was stirred for additional 2 h at 0 °C. The precipitate was collected by filtration and washed with cold ethanol and ethyl acetate. The dried solid was suspended with water in order to dissolve the hydrazinium salt of the expected product and the suspension was filtered; the pH of the clear solution was adjusted to ca 9 with 1M NaOH and the solution was charged onto a column of Dowex 1 × 8 100-200 mesh ion exchange resin in the acetate form. The resin was eluted with water until negative assay for hydrazine (2% *N*,*N*-dimethylaminobenzaldehyde in 10% HCl solution). Usually six column volumes of water are required. The pad of resin was then eluted with four column volumes of 1.5 M AcOH and the eluate was collected in fractions. Fractions containing the product were combined on the basis of TLC analysis and lyophilized. The obtained products were recrystallized from aqueous ethanol.

Using the general procedure, the following compounds were synthesized.

γ-L-glutamyl-L-glutamine. Obtained from L-glutamine and *N*-phtaloyl-L-glutamic acid anhydride in 50% yield after 48 h reaction time.

^{1}H-NMR (400 MHz; D_2O): δ, 1.86-2.03 (m, 3H, $H\beta_b$ Gln and Hβ Glu); 2.09-2.17 (m, 1H, $H\beta_a$ Gln); 2.30-2.36 (m, 2H, Hγ Gln); 2.37-2.41 (m, 2H, Hγ Glu); 3.41 (t, 1H, *J* = 6.2 Hz, Hγ Glu); 4.18 (dd, 1H, *J* = 8.9, 4.7 Hz, Hα Gln).

^{13}C-NMR (101 MHz; D_2O): δ 27.79 (Cβ Gln); 29.81 (Cβ Glu); 31.80 (Cγ Gln); 32.38 (Cγ Glu); 54.74 (Cα Gln); 55.39 (Cα Glu); 175.26, 178.36, 178.69, 180.33 (COO and CONH).

γ-L-glutamylglycylclycine. Obtained from glycylglycine and *N*-phtaloyl-L-glutamic acid anhydride in 65% yield after 18 h reaction time.

^{1}H-NMR (400 MHz; D_2O): δ 2.20 (broad q, 2H, *J* = 7.0 Hz, Hβ Glu); 2.49-2.62 (m, 2H, Hγ Glu); 3.87 (t, 1H *J* = 6.3 Hz, Hα-Glu); 3.99 (s, 2H, CH_2 Gly); 4.01 (s, 2H, CH_2 Gly).

^{13}C-NMR (101 MHz; D_2O): δ 25.86 (Cβ Glu); 31.10 (Cγ Glu); 41.29 (CH_2 Gly); 42.41 (CH_2 Gly); 53.68 (Cα Glu); 172.01, 175.26, 173.71, 173.42 (COO and CONH).

γ-L-glutamyl-L-methionine. Obtained from L-methionine and *N*-phtaloyl-L-glutamic acid anhydride in 79% yield after 18 h reaction time.

^{1}H-NMR and ^{13}C-NMR: as in ref. (Speranza, **2012**)

γ-L-glutamyl-L-phenylalanine. Obtained from L-phenylalanine and *N*-phtaloyl-L-glutamic acid anhydride in 86% yield after 24 h reaction time.

^{1}H-NMR (400 MHz; DMSO-d_6): δ 1.75-1.89 (m, 2H, Hβ Glu); 2.15-2.29 (m, 2H, Hγ Glu); 2.84 (dd, 1H, J = 13.8, 9.9 Hz, $H\beta_b$ Phe); 3.05 (dd, 1H, J = 13.8, 4.7 Hz, $H\beta_a$ Phe); 3.36 (t, 1H, J = 6.3 Hz, Hα Glu); 4.37 (ddd, 1H, J = 9.6, 8.1, 4.6 Hz, Hα Phe); 7.17-7.28 (m, 5H, aromatic H), 8.50 (d, 1H, J = 8.0 Hz, NH).

^{13}C-NMR (101 MHz; DMSO-d_6): δ 26.88 (Cβ Glu); 31.46 (Cγ Glu); 36.76 (Cβ Phe); 53.10 (Cα Phe); 53.94 (Cα Glu); 126.33, 128.13, 129.07, 137.94 (aromatic C); 170.31, 171.68, 173.27 (COO and CONH).

γ-L-glutamyl-L-serine. Obtained from L-serine and *N*-phtaloyl-L-glutamic acid anhydride in 75% yield after 24 h reaction time.

^{1}H-NMR (400 MHz; DMSO-d_6): δ 1.83-1.97 (m, 2H, Hβ Glu), 2.26-2.40 (m, 2H, Hγ Glu); 3.37 (t, 1H, *J* = 6.4 Hz, Hα Glu); 3.61 (dd, 1H, *J* = 11.1, 4.0 Hz, $H\beta_b$ Ser); 3.68 (dd, 1H, *J* = 11.0, 5.6 Hz, $H\beta_a$ Ser); 4.19 (ddd, 1H, *J* = 7.5, 5.4, 4.3 Hz, Hα Ser); 8.48 (d, 1H, *J* = 7.6 Hz, NH).

^{13}C-NMR (101 MHz; DMSO-d_6): δ 27.14 (Cβ Glu); 31.73 (Cγ Glu); 53.35 (Cα Ser); 55.25 (Cα Glu); 61.32 (Cβ Ser); 170.79, 171.91, 172.25, (COO and CONH).

A2 3.4. Enzyme activity determination

γ-glutamyl-transferase activity was measured by a standard spectrofotometric assay method; this assay uses γ-glutamyl-*p*-nitroanilide as a starting material ad measures the amount of *p*-nitroaniline released by the enzyme. One enzymatic unit (U) was defined as the amount of enzyme that released 1 µmol of *p*-nitroaniline per minute from γ-glutamyl-*p*-nitroanilide (γ-GpNA) through the transpeptidation reaction using GlyGly as the acceptor compound at pH 8.2 and 23°C.

For this purpose the following solutions were used:

- 20 mM GlyGly in 0.1 M $NaHCO_3$ buffer at pH 8.2;
- 2.5 mM γ-GpNA in 0.1 M $NaHCO_3$ buffer at pH 8.2;
- 0.1 M $NaHCO_3$ buffer at pH 8.2.

Before any measure, a calibration curve of *p*-nitroaniline at increasing concentrations was constructed. The concentrations of the solutions used for the calibration curve were 150, 100, 50, 25, 12.5 and 6.25 µM. The absorbance values obtained were related with the corresponding concentration in the calibration curve.

The transpeptidation reaction was carried out in the cuvette for the spectrophotometric measurement. 200 µL of γ-GpNA 2.5 mM in $NaHCO_3$ buffer, 200 µL of GlyGly 20 mM in $NaHCO_3$ buffer and 1580 µL of $NaHCO_3$ 0.1 M were put in the cuvette and the blank was measured; after that 20 µL of diluted enzyme A, GGT WT 10/11, B, GGT WT 5/12 or C, GGT REC 1/3 (0.00041 U/mL) was added and the reaction was monitored at room temperature for 30 minutes. In this time interval the response was found to be linear. The analysis were carried out recording the absorbance of each sample at 410 nm every 20 sec. The activities found, express in enzymatic unit per mL of enzyme solution (U/mL), for the three enzyme were:

- enzyme A, GGT WT 10/11: 0.49 U/mL;
- enzyme B, GGT WT 5/12: 16.98 U/mL;
- enzyme C, GGT REC 1/3: 0.89 U/mL.

A2 3.5. GGT hydrolase and transpectidase activities at different pH

The activity of enzyme B, GGT WT 5/12, was evaluated in dependence of pH variations; for this purpose different assay were conducted in the 6-11 pH interval.

The activity was measured both for transpeptidase (Scheme A2 3) and hydrolase (Scheme A2 4) reaction.

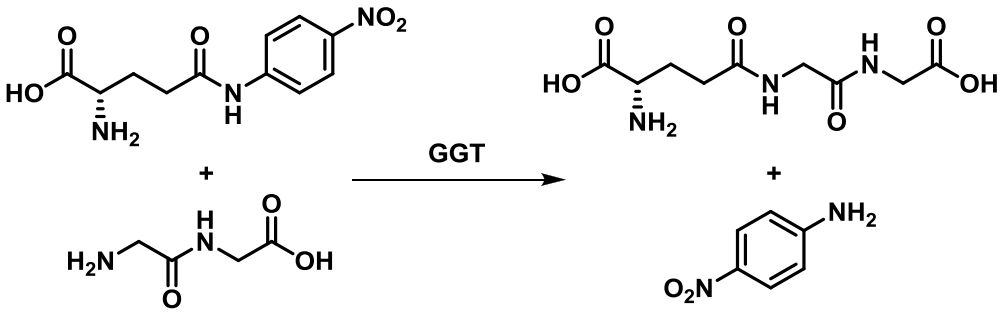

Scheme A2 3: Transpeptidation between γ-GpNA and GlyGly.

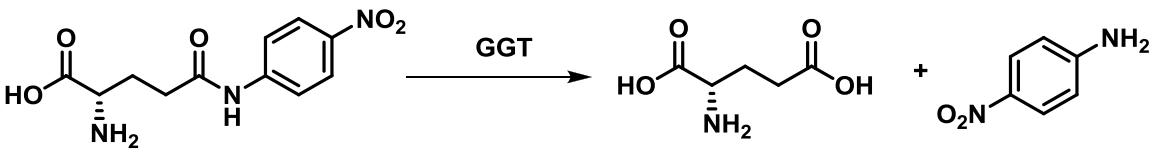

Scheme A2 4: Hydrolysis of γ-GpNA.

For these reactions the following solutions were used:

- 20 mM GlyGly in $NaHCO_3$ buffer at pH 8.2 ;
- 2.5 mM γ-GpNA in six different buffers;
- six different buffers reported in the following table.

pH buffer	Component A	Component B	mL A	mL B
6	Na_2HPO_4 0.2 M	NaH_2PO_4 0.2 M	12	88
7	Na_2HPO_4 0.2 M	NaH_2PO_4 0.2 M	61	39
8	Na_2HPO_4 0.2 M	NaH_2PO_4 0.2 M	97	3
9	Na_2CO_3 0.1 M	$NaHCO_3$ 0.1 M	10	90
10	Na_2CO_3 0.1 M	$NaHCO_3$ 0.1 M	55	45
11	Na_2CO_3 0.1 M	-	100	0

Table A2 2: Buffers used for hydrolase and transpeptidase evaluation.

Each transpeptidation reaction was carried out placing directly 200 µL of γ-GpNA 2.5 mM at each pH, 200 µL of GlyGly 20 mM in $NaHCO_3$ buffer and 1580 µL of buffer at each pH value in the cuvette; each hydrolase reaction was carried out placing 200 µL of γ-GpNA 2.5 mM at each pH, and 1780 µL of buffer at each pH in the cuvette. To each cuvette were added 20 µL of diluted enzyme B, GGT WT 5/12 (0.00041 U/mL) and the reactions were carried out at room temperature and monitored for five minutes measuring the absorbance every 20 sec at 410 nm.

A2 3.6 Pre column derivatization

The following derivatization protocol has been developed so that the derivatization agent, dabsyl chloride, was 2-2.5 times in excess than the analytes. The pH of the analytes solutions was kept between 8.5 and 9.

The derivatization was performed in a pyrex tube with screw cap and pierceable septum; the temperature of the derivatization was controlled by a water bath set to 70°C.

The following solutions have been used:

- 10 mM dabsyl chloride in acetone used as derivatizing solution;
- 0.1 M $NaHCO_3$ buffer at pH 8.2;
- 50 mM leucine in $NaHCO_3$ buffer at pH 8.2 used as internal standard;
- 0.1 % TFA in water.

100 µL of the mixture to be derivatized are withdrawn and placed in a 1.5 mL eppendorf. 100 µL of internal standard solution and 800 µL of $NaHCO_3$ buffer were added. From this solution, 100 µL were taken and put in a pyrex tube with screw cap and pierceable septum. 400 µL of $NaHCO_3$ buffer and 500 µL of dabsyl chloride solution were added. Instantly the solution became deep red with a flocculate precipitate. The tube was capped and was put in a water bath at 70°C for 10 minutes; the solution changed color from red to orange and the precipitate disappeared during the heating. After that the cap was pierced with a needle and the tube was kept in the bath for 5 additional minutes. After being heated the tube was cooled and 500 µL of the mixture was taken and diluted with 500 µL of 0.1% TFA solution. The solution can be analyzed by HPLC at 436 nm. The solutions are stable at low temperature for 12 months and are kept at -20°C.

A2 3.7. Evaluation of pH-dependent glutaminase activity

The activity of GGT was evaluated through the analysis of a 24 hours long reaction and was evaluated with three reactions at different pH: 7.4, 8.2 and 9.8.

The following solutions have been used:

- 150 mM Gln in three different buffers;
- three different buffers at pH 7.4, 8.2 and 9.8, respectively.

pH buffer	Component A	Component B	mL A	mL B
7.4	Na_2HPO_4 0.2 M	NaH_2PO_4 0.2 M	75	25
8.2	$NaHCO_3$ 0.1 M	-	100	0
9.8	Na_2CO_3 0.1 M	$NaHCO_3$ 0.1 M	50	50

Table A2 3: Table 4: buffer used for HPLC evaluation.

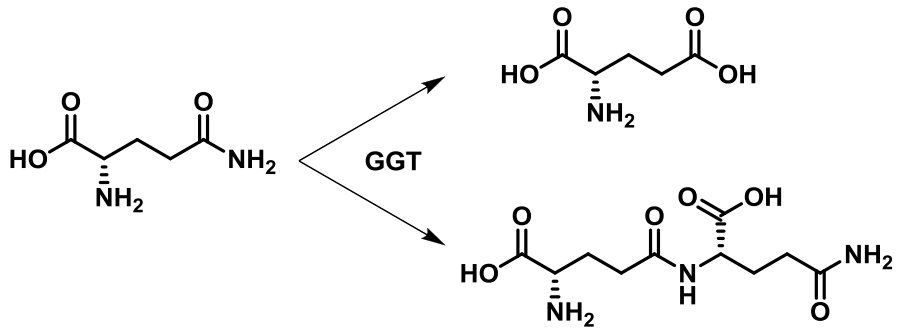

Scheme A2 5: GGT activity; hydrolysis and transpeptidation reactions.

The reactions were carried out putting 667 µL of L-glutamine 150 mM at different pH, 233 µL of buffer at different pH and an entire aliquot of enzyme A, GGT WT 10/11 not diluted (0.0049 U/mL), into a 1.5 mL eppendorf. The mixture was kept at room temperature for 24 hours and was monitored at the following times: start, after 1 hour, after 2, 3, 5, 7, and 24 hours. Each control was derivatized with the previously reported procedure and analyzed by HPLC.

The same procedure was also applied to a solution of D-glutamine 150 mM at pH 9.8 with no difference in the treatment.

A2 3.8 Evaluation of GGT transpeptidase activity

The transpeptidase activity was evaluated through the analysis of a 24 hours long reaction (Scheme 6).

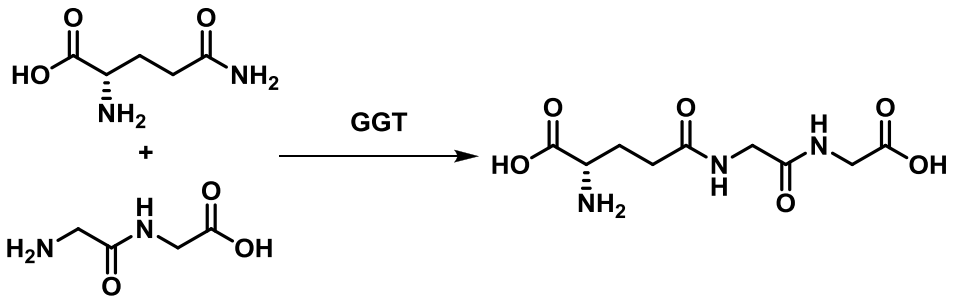

Scheme A2 6: GGT-catalyzed transpeptidation between Gln and GlyGly.

The reaction was carried out putting 667 µL of L-glutamine 150 mM and glycylglycine 150 mM at pH 8.2, 233 µL of $NaHCO_3$ buffer at pH 8.2 and an entire aliquot of enzyme A, GGT WT 10/11 not diluted (0.0049 U/mL) into a 1.5 mL eppendorf. The mixture was kept at room temperature for 24 hours and was monitored at the following times: start, after 1 hour, after 2, 3, 5, 7, and 24 hours. Each control was derivatized with the previous procedure and analyzed by HPLC.

a) Evaluation of the activity in the acceptor role of some amino acids and peptides

For this reactions eight glutamine solution with different pH were prepared: each solution was prepared with Na_2CO_3/ $NaHCO_3$ buffer.

The reaction was conducted with the same procedure for different amino acids (Scheme 7).

The reaction was carried out using 1 mL of a solution of glutamine 100 mM and acceptor amino acid 100 mM at different pH (7.5, 8.0, 8.5, 9.0, 9.5, 10.0, 10.5,11.0), 50 µL of enzyme B, GGT WT 5/12 previously diluted with a 0.1 M $NaHCO_3$ solution (0.0048 U/mL).

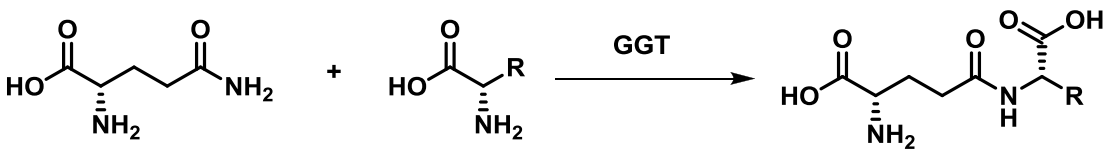

Scheme A2 7: GGT-catalyzed transpeptidation between Gln and generic amino acid.

The reaction was carried out at room temperature for one hour and subsequently analyzed following the previously reported procedure. The amino acids used were: methionine, serine, alanine, phenylalanine and also glycylglycine. For the phenylalanine a 50 mM solution of glutamine and acceptor was used.

The samples at pH 10.5 and 8.0 were afterwards analyzed also with HPLC-MS and the chromatograms were reported in appendix.

b) Evaluation of the auto-transpeptidase activity

The auto-transpeptidase activity was evaluated through the analysis of a reaction conducted with Burette 1S 86 12.

The reaction was carried out putting 50 µL of diluted enzyme B, GGT WT 5/12 (0.0048 U/mL) into a 15 mL falcon; after that a 200 mM L-glutamine solution at pH 10 was added at time intervals following the parameters reported in the table.

Flow	40 µL/min
Start addition	1 mL
Number of additions	12
Time interval between additions	15 min
Volume per addition	250 µL

Table A2 4: burette 1S parameters.

The mixture was kept at room temperature for 6 hours under stirring with orbital shaker and was monitored at the following times: start, after 1.5 hour and after 3 hours during the additions and also 1, 2 and 3 hours after the end of the additions. Each control was derivatized with the previous procedure and analyzed by HPLC.

A2 3.9 Enzymatic synthesis of γ-glutamyl-methionine

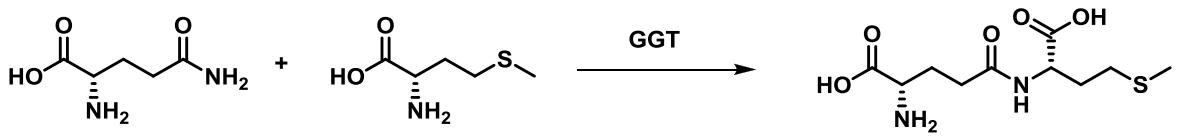

The following reaction was conducted two times with analogous procedures: the first reaction, at analytical level, was used to develop the second one on preparative level.

At analytical level, to 1 mL 100 mM (0.1 mmol) of a L-glutamine and L-methionine at pH 10 were added 50 µL of enzyme B, GGT WT 5/12 enzyme previously diluted with a 0.1 M $NaHCO_3$ solution (0.0048 U/mL). The reaction was carried out and monitored after 1, 2, 3, 4 and 5 hours; each control was derivatized with the previously described procedure and analyzed by HPLC.

At preparative level, to 10 mL 100 mM (1 mmol) of a L-glutamine and L-methionine at pH 10 were added 60 µL of enzyme B, GGT WT 5/12 enzyme (0.102 U/mL). The reaction was carried out under stirring with orbital shaker for 90 minutes at 23°C; after that the enzyme was inactivated by heating up to 70°C for 20 minutes. The mixture was frozen and lyophilized. The solid product obtained was dissolved in water and the pH of the solution obtained was adjusted to 9.0-9.5 with 0.1 M NaOH and the solution was loaded into a

DOWEX 1x8 column. The column was eluted with 5 volumes of H_2O. The product was eluted with 0.5, 1 and 2 M acetic acid solution and collected in fractions which were analyzed by TLC. The fractions containing products were collected, frozen and lyophilized.

Four fractions were obtained and ^1H NMR analysis allowed to identify the corresponding products. γ-glutamyl-methionine was recognized to be in fraction C.

Yield: 33% (97 mg, 0.33 mmol)

^1H NMR (400MHz, D_2O): δ 1.77 (m, 1 H, C*H*$_2$CH$_2$SCH$_3$); 1.85 (m, 2 H, CH(NH$_2$)CH$_2$C*H*$_2$); 2.00 (m, 1 H, C*H*$_2$CH$_2$SCH$_3$); 2.03 (s, 3 H, SC*H*$_3$); 2.26 (t, 2H, CH(NH$_2$)C*H*$_2$CH$_2$); 2.49 (m, 2 H, C*H*$_2$SCH$_3$); 3.17 (dd, 1 H, C*H*NH$_2$, J = 4.4); 4.20 (t, 1 H, C*H*COOH, J = 6.8).

References

- Abe K., Ito Y, Ohmachi T., Asada Y., *Biosci. Biotech. Biochem.*, **1997**, 61, 1621.
- Adams M.L., Lavasanifar A., Kwon G.S., *J. Pharm. Sci.*, **2003**, 92, 1343.
- Aerthon E., Sheppard R.C., *Solid phase peptide synthesis, a practical approach*, IRL PRESS, **1989.**
- Aftabrouchard D., Dorlker E., *STP Pharma. Sci.*, **1992**, 2, 365.
- Akagi T., Higashi M., Kaneko T., Kida T., Akashi M., *Macromol. Biosci.*, **2005a**, 5, 598.
- Akagi T., Kaneko T., Kida T., Akashi M., *J. Control. Release*, **2005b**, 108, 226.
- Akagi, T., Baba, M., Akashi, M., *Polymer*, **2007a**, 48, 6729.
- Akagi, T., Wang, X., Uto, T., Baba, M., Akashi, M., *Biomaterials*, **2007b**, 3427.
- Al-Jamal W.T., Kostarelos K., *Acc. Chem. Res.*, **2011**, 44, 1094.
- Allémann E., Leroux J.C., Gurny R., *Adv. Drug Deliv. Rev.*, **1998**, 34, 171.
- Anderson J.M., Shive M.S., *Adv. Drug. Deliv. Rev.*, **1997**, 28, 5.
- Ashiuchi M., in Amino-Acid Homopolymers Occurring in Nature, Hamano Y. ed, Springer, Berlin, **2010**, pp.77-93
- Azemar M., Schmidt M., Arlt F., Kennel P., Brandt B., Papadimitriou A., et al., *Int. J. Cancer*, **2000**, 86, 269.
- Bajaj I., Singhal R., Bioresour. *Technol*., **2011**, 102, 5551.
- Barichello J.M., Morishita M., Takayama K., Nagai T., *Drug. Dev. Ind. Pharm.*, **1999**, 25, 471.
- Bawa R., Bawa S.R., Maebius S.B., Flynn T., Wei C., *Nanomed. Nanotech. Biol. Med.*, **2005**, 1, 150.
- Bellini D., Topai A., Patent WO2000001733 A1 PCT/IB1999/001254, **2011**
- Bianco R., Melisi D., Ciardiello F., Tortora G., *Eur. J. Cancer*, **2006**, 42, 290.
- Bodmeier R., Chen H., *J. Control. Release*, **1990**, 12, 223.
- Bovarnich M., *J. Biol. Chem.*, **1942**, 16, 265.
- Brahms S., Brahms J., Spach G., Brack A., *Proc. Natl. Acad. Sci. USA*, **1977**, 74, 3208.
- Brambilla D., Le Droumaguet B., Nicolas J., Hashemi S.H., Wu L.P., Moghimi S.M., Couvreur P., Andrieux K., *Nanomedicine*, **2011**, 7, 521.
- Brigger I., Dubernet C., Couvreur P., *Adv. Drug Delivery Rev.*, **2002**, 54, 631.
- Buescher J.M., Margaritis A., *Crit. Rev. Biotechnol.*, **2007**, 27, 1.

- Candela T., Fouet. A., *Mol. Microbiol.*, **2006**, 60, 1091.
- Carpenter G., *Annu. Rev. Biochem.*, **1979**, 48, 193.
- Carpenter G., *Annu. Rev. Biochem.*, **1987**, 56, 881.
- Carpenter G., Wahl M.I., *Handb. Exp. Pharmacol.*, **1990**, 951, 69.
- Carpino L.A., Han G.Y., *J. Am. Chem. Soc.*, **1970**, 92, 5748.
- Chan J.M., Zhang L.E., Yuet K.P., et al., *Biomaterials*., **2009**, 30, 1627.
- Chevalier C., Thiberge J.M., Ferrero R.L., Labigne A., *Mol. Microbiol*., **1999**, 31, 1359.
- Ciardiello F., Caputo R., Troiani T., Borriello G., Kandimalla E.R., Agrawal S., et al., *Int. J. Cancer*, **2001**, 93, 172.
- Citri A., Yarden Y., *Nat. Rev. Mol. Cell Biol.*, **2006**, 7, 505.
- Clark L.B., *J. Am. Chem. Soc.*, **1995**, 117, 7974.
- Cohen S., *J. Biol. Chem.*, **1962**, 237, 1555.
- Cook N.D., Upperton K.P., Challis B.C., Peters T.J., *Biochim. Biophys. Acta*, **1987**, 914, 240.
- Couvreur P., Dubernet C., Puisieux F., *Eur. J. Pharm. Biopharm.*, **1995**, 41, 2.
- Couvreur P., Barrat G., Fattal E., Legrand P., Vauthier C., *Crit. Rev. Ther. Drug. Carrier Syst.*, **2002**, 19, 99..
- Daub H., Weiss F.U., Wallasch C., Ullrich A., *Nature*, **1996**, 379, 557.
- Davis M.E., Chen Z.G., Shin D.M., *Nat. Rev. Drug Discov.*, **2008**, 7, 771.
- de Larco J.E., Todaro G.J., *J Cell Physiol*, **1978**, 94, 335.
- Discher B.M., Won Y.Y., Ege D.S., Lee J.C.M., Bates F.S., Discher D.E., Hammer D.A., *Science*, **1999**, 284, 1143.
- Dreher M.R., Liu W., Michelich C.R., Dewhirst M.W., Yuan F., Chilkoti A., *J. Natl. Cancer Inst.*, **2006**, 98, 335.
- Earp H.S., Dawson T.L., Li X., Yu H., *Breast Cancer Res Treat*, **1995**, 35, 115.
- Elce J.S., Broxmeyer B., *Biochem. J.*, **1976**, 153, 223.
- Elsabahy M., Wooley K.L., *Chem. Soc. Rev.*, **2012**, 41, 2545.
- El-Samaligy M.S., Rohdewald P., Mahmoud H.A., *J. Pharm. Pharmacol.*, **1986**, 38, 216.
- Farokhzad O.C., Langer R., *ACS Nano*, **2009**, 3, 16.
- Finke J.M., Jennings P.A., Lee J.C., Onuchic J.N., Winkler J.R., Biopolymers, **2007**, 86, 193.

- Franovic A., Gunaratnam L., Smith K., Robert I., Patten D., Lee S., *Proc Natl Acad Sci USA*, **2007**, 104, 13092.
- Gabizon A., Catane R., Uziely B., Kaufman B., Safra T., Cohen R., Martin F., Huang A., Barenholz Y., *Cancer Res.*, **1994**, 54, 987.
- Garrett T.P., McKern N.M., Lou M., Elleman T.C., Adams T.E., Lovrecz G.O., et al., *Cell*, **2002**; 110, 763.
- Gindy M.E., Ji S., Hoye T.R., Panagiotopoulos A.Z., Prud'homme R.K., *Biomacromol.*, **2008**, 9, 2705.
- Goldmacher V., Blättler W., Lambert J., Chari R.J.; In: *Biomed aspect drug target*, Muzykantov V., Torchilin V. editors, Springer, **2002**. pp. 291-309
- Gonzales D., Fan K., Sevoian M., *J. Poly. Sci. A: Pol. Chem.*, **1996**, 34, 2019.
- Greene T.W., Wuts P.G.M., *Protective Groups in Organic Synthesis, Third edition*, John Wiley & Sons, Inc., **1999.**
- Greenfield N.J., Fasman G.D., *Biochemistry*, **1969**, 8, 4108.
- Gref R., Minamitake Y., Peracchia M.T., Trubetskoy V., Torchilin V., Langer R., *Science*, **1994**, 263, 1600.
- Gref R., Babak B., Bouillot P., Lukina I., Bodorev M., Dellacherie E., *Colloids Surf A Physicochem Eng Asp*., **1998,** 143, 413.
- Greish K., *J. Drug Targeting*, **2007**, 15, 457.
- Gu H., Jiang Y.A., *Org. Prep. Proc. Int.*, **2004**, 36, 479.
- Gullotti E., Yeo Y., *Mol. Pharmaceutics*, **2009**, 6, 1041.
- Gurny R., Peppas N.A., Harrington D.D., Banker G.S., *Drug. Dev. Ind. Pharm.*, **1981**, 7, 1.
- Harmia-Pulkkinen T., Tuomi A., Kristoffersson E., *J. Microencapsul.*, **1989**, 6, 87.
- He L.M., Neu M.P., Vanderberg L.A., *Environ. Sci. Technol.*, **2000**, 34, 1694.
- Herbst R.S., Shin D.M., *Cancer*, **2002**, 94, 1593.
- Hillaireau H., Couvreur P., in *Polymers in Drug Delivery*, Uchegbu I.F., Schätzlein A.G. ed., Taylor & Francis, New York, **2006**, pp. 101.
- Hinchman C.A., Matsumoto H., Simmons T.W., Ballatori N., *J. Biol. Chem*., **1991**, 266, 22179.
- Holzwarth G., Doty P., Gratzer W.B., *J. Am. Chem. Soc.*, **1962**, 84, 3194.
- Holzwarth Hu S., Shively L., Raubitschek A., Sherman M., Williams L.E., Wong J.Y., et al., *Cancer Res.* **1996**, 56, 3055.

- Hu C.M.J., Zhang L., Aryal S., Cheung C., Fang R.H., Zhang L., *Proc Natl Acad Sci USA*, **2011**, 108, 10980.
- Hubert B., Atkinson J., Guerret M., Hoffman M., Devissaguet J.P., Maincent P., *Pharm. Res.*, **1991**, 8, 734.
- Hynes N.E., MacDonald G., *Current Opinion in Cell Biology*, **2009**, 21, 177.
- Ikeda Y., Fujii J., Taniguchi N., Meister A., *Proc. Natl. Acad. Sci. USA*, **1995**, 92, 126.
- Ikeda Y., Anderson F.J., Anderson M.E. et al., *J. Biol. Chem.*, **1995b**, 270, 22223.
- Ikeda Y., Taniguchi N., *Methods Enzymol.*, **2005**, 401, 408.
- Inoue M., Hiratake J., Suzuki H. et al., *Biochemistry*, **2000**, 39, 7764.
- Ishikawa T., *Agric. Biol. Chem.*, **1967**, 31, 490.
- Iyer A.K., Khaled G., Fang J., Maeda H., *Drug Discov. Today*, **2006**, 11, 812.
- Jaiswal J., Gupta S.K., Kreuter J., *J. Control. Release*, **2004**, 96, 169.
- Johnson W.C., Tinoco I., *J. Am. Chem. Soc.*, **1972**, 94, 4389.
- Jule E., Nagasaki Y., Kataoka K., *Biocon. Chem.*, **2003**, 14, 177.
- Kamaly N., Xiao Z., Valencia P.M., Radovic-Moreno A.F., Farokhzad O.C., *Chem. Soc. Rev.*, **2012**, 41, 2971.
- Kashima N., Furuta K., Tanabe I., United States Patent 20060025346, **2006**.
- Kean E.A., Hare E.R., *Phytochemistry*, **1980**, 19, 194.
- Keillor J.W., Castonguay R., Lherbet C., *Methods Enzymol.*, **2005**, 401, 449.
- Kimmerlin T., Sebach D., *J. Peptide Res.*, **2005**, 65, 229.
- Kimura K., Phan Tra L-S., Uchida I., Itoh Y., *Microbiology*, **2004**, 150, 4115.
- Klein P., Mattoon D., Lemmon M.A., Schlessinger J., *Proc Natl Acad Sci USA*, **2004**, 101, 929-934
- Kreuter J., in: *Specialized drug delivery system*, Tyle P ed., Marcel Dekker, New York, **1990**, pp. 257-66.
- Kreuter J., *J. Control. Release*, **1991**, 16, 169.
- Kubota H., Nambu Y., Endo T., *J. Poly. Sci. A: Pol. Chem.*, **1993**, 31, 2877.
- Kubota H., Nambu Y., Endo T., *J. Poly. Sci. A: Pol. Chem.*, **1995**, 33, 85.
- Kunioka M., *Macromol. Biosci.*, **2004**, 4, 324.
- Lee D.E., Koo H., Sun I.C., Ryu J.H., Kim K., Kwon I.C., *Chem. Soc. Rev.*, **2012**, 41, 2656.

- Lenferink A.E., Pinkas-Kramarski R., van de Poll M.L., et al., *Embo J.*, **1998**, 17, 3385.
- Lemmon M.A., Schlessinger J., *Cell*, **2010**, 141, 1117.
- Letchford K., Burt H., *Eur. J. Pharm. Biopharm.*, **2007**, 65, 259.
- Leustek T., Martin M.N., Bick J.A., Davies J.P., *Ann. Rev. Plant. Physiol. Plant. Mol. Biol*., **2000**, 51, 141.
- Li Z., Zhao R., Wu X.S., Sun Y., Yao M., Li J., Xu Y., Gu J., *The FASEB J.*, **2005**, 19, 1978.
- Liu J., Xiao Y., Allen C., *J. Pharm. Sci.*, **2004**, 93, 132.
- LoPresti C., Lomas H., Massignani M., Smart T., Battaglia G., *J. Mater. Chem.*, **2009**, 19, 3576.
- Lowe P.J., Temple C.S., *J. Pharm. Pharmacol.*, **1994**, 46, 547.
- Maeda H., Wu J., Sawa T., Matsumura Y., Hori K., *J. Control. Release*, **2000**, 65, 271.
- Martin M.N., Slovin J.P., *Plant Physiol*., **2000**, 122, 1417.
- Martínez de Ilarduya A., Ittobane N., Bermúdez M., Alla A., El Idrissi M., Muñoz-Guerra S., *Biomacromolecules*, **2002**, 3, 1078.
- Mc Cune B., Earp H., J Biol Chem, **1989**, 264, 15501.
- Mehdi K., Thierie J., Penninckx M.J., *Biochemistry J*., **2001**, *359*, 631.
- Meister A., *Science*, **1973**, 6, 33.
- Melis J., Morillo M., Martínez de Ilarduya A., Muñoz-Guerra S., *Polymer*, **2001**, 42, 9319.
- Ménard A., Castonguay R., Lherbet C. et al., *Biochemistry*, **2001**, 40, 12678.
- Meng F., Hiemstra C., Engbers G.H.M., Feijen J., *Macromolecules*, **2003**, 36, 3004.
- Merrifield R.B., *J. Amer. Chem. Soc.*, **1963**, 85, 2149.
- Mesiter A., Anderson M.E., *Ann. Rev. Biochem.*, **1983**, 52, 711.
- Mill C.P., Chester J.A., Riese D.J., *Breast Cancer Targets Ther*, **2009**, 2009.
- Miller W.E., Raab-Traub N., *Trends Microbiol*, **1999**, 7, 453.
- Minami H., Suzuki H, Kumagai H., *FEMS Microbiol. Lett.*, **2003**, 224, 169.
- Mishra D., Kang H.C., Bae Y.H., *Biomaterials*., **2011**, 32, 3845.
- Moffitt W., *J. Chem. Phys.*, **1956**, 25, 467.
- Mori H., Iwata M., Ito S., Endo T., *Polymer*, **2007**, 48, 5867.

- Morillo M., Martínez de Ilarduya A., Muñoz-Guerra S., *Macromolecules*, **2001**, 34, 7868.
- Morillo M., Martínez de Ilarduya A., Muñoz-Guerra S., *Polymer*, **2003**, 44, 7557.
- Morrow A.L., Williams K., Sand A., Boanca G., Barycki J.J., *Biochemistry*, **2007**, 46, 13407.
- Muller R.H., Keck C.M., *J. Biotechnol.*, **2004**, 113, 151.
- Muñoz-Guerra S., Garcia-Alvarez M., Portilla-Arias J.A., *J. Renew. Mat.*, **2013**, 1, 42.
- Nair L.S., Laurencin C.T., *Prog. Polym Sci.*, **2007**, 32, 762.
- Nakayama R., Kumagai H., Tochikura T., *J. Bacteriol.*, **1984**, 160, 1031.
- Nam Y.S., Kang H.S., Park T.G., Han S.H., Chang I.S., *Biomaterials*, **2003**, 24, 2053.
- Némati F., Dubernet C., Fessi H., Verdière A.C., Poupon M.F., Puisieux F., et al., *Int. J. Pharm.*, **1996**, 138, 237.
- Nicolas J., Mura S., Brambilla D., Mackiewicz N., Couvreur P., *Chem. Soc. Rev.*, **2013**, 42, 1147.
- Nielsen E.B:, Schellman J.A., *J. Phys. Chem.*, **1967**, 71, 2297.
- Nobs L., Buchegger F., Gurny R., Allémann E., *J. Pharm. Sci.*, **2004**, 93, 1980.
- Oerlemans C., Bult W., Bos M., Storm G., Nijsen J., Hennink W., *Pharm. Res.*, **2010**, 27, 2569.
- Ogiso H., Ishitani R., Nureki O., Fukai S., Yamanaka M., Kim J.H., et al., *Cell*, **2002**, 110, 775.
- Okada T., Suzuki H., Wada K., Kumagai H. and Fukuyama K., *Proc. Natl. Acad. Sci. USA*, **2006**, 103, 6471.
- Oppermann-Sanio F.B., Steinbüchel A., *Naturwissenschaften*, **2002**, 89, 11.
- Orth J.D., Krueger E.W., Weller S.G., McNiven M.A., *Cancer Res*, **2006**, 66, 3603.
- Otani Y., Tabata Y., Ikada Y., *J. Biomed. Mater. Res.*, **1996**, 31, 157.
- Otani Y., Tabata Y., Ikada Y., *Biomaterials*, **1998a**, 19, 2091.
- Otani Y., Tabata Y., Ikada Y., *Biomaterials*, **1998b**, 19, 2167.
- Passerini N., Craig D.Q.M., *J. Control. Release*, **2001**, 73, 111.
- Patil Y.B., Toti U.S., Khdair A., Ma L., Panyam J., *Biomaterials*, **2009**, 30, 859.
- Pauling L., Corey L.B:, Branson H.R., *Proc. Natl. Acad. Sci.* USA, **1951**, 37, 205.

- Peer D., Karp J.M., Hong S., Farokhzad O.C., Margalit R., Langer R., *Nat. Nanotechnol.*, **2007**, 2, 751.
- Pérez-Camero G., Vázquez B., Muñoz-Guerra S., *J. Applied Polymer Science*, **2001**, 82, 2027.
- Perez C., Sánchez A., Putnam D., Ting D., Langer R., Alonso M.J., *J. Control Release*, **2001**, 75, 211.
- Pinto Reis C., Neufeld R.J., Ribeiro A.J., Veiga F., *Nanomed.*, **2006**, 2, 8.
- Poo H., Park C., Kwak M.-S., Choi D.-Y., Hong S.-P., Lee I.-H., Taik Lim Y.T., Choi Y.K., Bae S.R., Uyama H., Kim C.J., Sung M.H., *Chem. Biodiv.*, **2010**, 1555.
- Quintanar-Guerrero D., Allémann E., Fessi H., Doelker E., *Drug. Dev. Ind. Pharm.*, **1998**, 24, 1113.
- Raju B., Kogan T.P., *Tet. Lett.* **1997**, 38, 4965.
- Riehemann K., Schneider S.W., Luger T.A., Godin B., Ferrari M., Fuchs H., *Angew. Chem., Int. Ed.*, **2009**, 48, 872.
- Riese II D.J., Stern D.F., *Bioessays*,**1998**, 20, 41.
- Rydon H.N., *J. Chem.* Soc., **1964**, 1328.
- Sah H., Thoma L.A., Desu H.R., Sah E., Wood G.C., *Int. J. Nanomed.*, **2013**, 8, 747.
- Sanda F., Fukiyama T., Endo T., *J. Polym. Sci. Pol. Chem.* , **2001**, 39, 732.
- Sandhya K., Ravindranath B., *Tet. Lett.*, **2008**, 49, 2435.
- Sanhai W.R., Sakamoto J.H., Canady R., Ferrari M., *Nat. Nanotechnol.*, **2008**, 3, 242.
- Sawa S., Murakawa T., Watanabe T., Murao S., Omata S., *Nippon Nögeikagaku Kaishi*, **1973**, 47, 159.
- Schellman J.A., Oriel P., *J. Chem. Phys.*, **1962**, 37, 2114.
- Sigismund S., Woelk T., Puri C., Maspero E., Tacchetti C., Transidico P., et al., *Proc. Natl. Acad. Sci. USA*, **2005**, 102, 2760.
- Singer J.W., DeVries P., Bhatt R., Tulinsky J., Klein P., Li C., Milas L., Lewis R.A., Wallace S., *Ann. NY Acad. Sci.*, **2000**, 922, 136.
- Sizeland A.M., Burgess A.W., *Mol Biol Cell*, **1992**, 3, 1235.
- Schulze W.X., Deng L., Mann M., *Mol Syst Biol*, **2005**, 1.
- Schweiger R.G., US 3637520 A, **1972**.
- Shi J., Xiao Z., Kamaly N., Farokhzad O.C., *Acc. Chem. Res.*, **2011**, 44, 1123.

- Shih I.L., Van Y.T., *Bioresour. Technol.*, **2001**, 79, 207.
- Shih I.L., Wu J.-Y., in Microbial Production of Biopolymers and Polymer Precursors, Rehm B.H.A. ed., Wiley, **2009**, pp.101-143
- Smith T. K., Mesiter A., *FASEB J.*, **1994**, 8, 661.
- Smith T.K., Ikeda Y., Fuji, J., et al., *Proc. Natl. Acad. Sci.USA*, **1995**, 92, 2360.
- Sorkin A., Mazzotti M., Sorkina T., Scotto L., Beguinot L., *J. Biol. Chem.*, **1996**, 271, 13377.
- Speranza G., Morelli C.F., *J. Mol. Catal. B: Enzymatic*, **2012**, 84, 65.
- Storozhenko S., Belles-Boix E., Babiychuk E., et al., *Plant. Physiol*., **2002**, 128, 1109.
- Sundvall M., Iljin K., Kilpinen S., Sara H., Kallioniemi O-P., Elenius K., *J Mammary Gland Biol Neoplasia*, **2008**, 13, 259.
- Sung M., Park C., Kim C.J., Poo H., Soda K., Ashiuchi M., *Chem. Rec.*, **2005**, 5, 352.
- Suo Z., Risberg B., Karlsson M.G., Villman K., Skovlund E., Nesland J.M., *Int J Surg Pathol*, **2002**, 10, 91.
- Suzuki H., Kumagai H., Tochikura T., *J. Bacteriol*., **1986**, 168, 1332.
- Suzuki H., Kumagai H., Echigo T., Tochikura T., *J. Bacteriol*, **1989**, 171, 5169.
- Suzuki H., Hashimoto W., Kumagai H., *J. Bacteriol*., **1993**, 175, 6038.
- Takahashi H., Watanabe H., *FEMS Microbiol. Lett*., **2004**, 234, 27.
- Taniguchi N., Proc. Intl. Conf. Prod. Eng. Tokyo, Part II, Japan Society of Precision Engineering, **1974**.
- Taniguchi N., Ikeda Y., *Adv. Enzymol. Relat. Areas Mol. Biol.*, **1998**, 72, 239.
- Taniguchi M., Kato K., Matsui O., Ping X., Nakayama H., Usuki Y., Ichimura A., Fujita K., Tanaka T., Tarui Y., Hirasawa E., *J. Biosci. Bioeng.*, **2005a**, 99, 130.
- Taniguchi M., Kato K., Shimauchi A., Ping X., Nakayama H., Fujita K., TanakaT., Tarui Y., Hirasawa E., *J. Biosci. Bioeng.*, **2005b**, 99, 245.
- Taniguchi M., Kato K., Shimauchi A., Xu P., Fujita K., Tanaka T., Tarui Y., Hirasawa E., *J. Biosci. Bioeng.*, **2005c**, 100, 207.
- Tanimoto H., Mori M., Motoki M., Torii K., Kadowaki M., Noguchi T., *Biosci. Biotechnol. Biochem.*, **2001**, 65, 5516.
- Tate S.S., Meister A., *Proc. Natl. Acad. Sci. USA*, **1977**, 74, 931.
- Tate S.S., Meister A., *Proc. Natl. Acad. Sci. USA*, **1978**, 75, 4806.

- Tate S.S., Meister A., *Methods Enzymol.*, **1985**, 113, 400.
- Thompson G.A., Mesiter A., *J. Biol. Chem.*, **1977**, 252, 6792.
- Tice T.R., Gilley R.M., *J. Control. Release*, **1985**, 2, 343.
- Tiffany M.L., Krimm S., *Biopolymers*, **1968**, 6, 1379.
- Tiffany M.L., Krimm S., *Biopolymers*, **1969**, 8, 347.
- Tobío M., Gref R., Sánchez A., Langer R., Alonso M.J., *Pharm. Res.*, **1998**, 15, 270.
- Toniolo C., Polese A., Formaggio F., Crisma M., Kamphuis J., *J. Am. Chem. Soc.*, **1996**, 118, 2744.
- Toniolo C., Formaggio F., Tognon S., Broxterman Q.B., Kaptein B., huang R., Setnicka V., Keiderling T.A., McColl I.H., Hecht L., Barron L.D., *Biopolymers*, **2004**, 75, 32.
- Torchilin V., *Pharm. Res.*, **2007**, 24, 1.
- Tzahar E, Moyer J.D., Waterman H., et al., *Embo J.*,**1998**, 17, 5948.
- Ueda H., Kreuter J., *J. Microencapsul.*, **1997**, 14, 593.
- Ullrich A., Schlessinger J., *Cell*,**1990**, 61, 203.
- Ulrich K.E., Cannizzaro S.M., Langer R.S., Shakesheff K.M., *Chem Rev.*, **1999**, 99, 3181.
- Verrecchia T., Spenlehauer G., Bazile D.V., Murry-Brelier A., Archimbaud Y., Veillard M., *J Control Release*, **1995,** 36, 49.
- Vigenaud V., Ressler C., Swann J.M., Roberts C.W., Katsojannis P.G., *J. Amer. Chem. Soc.*, **1954**, 76, 3115.
- Vonarbourg A., Passirani C., saulnier P., Benoit J.P., *Biomaterials*, **2006**, 27, 4356.
- Wada T., Qian X., Greene M.I., *Cell*, **1990**, 61, 1339.
- Wada K., Ire M., Suzuki H., Fukuyama K., *FEBS J.*, **2010**, 277.
- Wang F., Ishiguro M., Mutsukado M., Fujita K.-I., Tanaka T., *J. Agric. Food Chem.*, **2008**, 56, 4225.
- Watnasirichaikul S., Davies N.M., Rades T., Tucker I.G., *Pharm. Res.*, **2000**, 17, 684.
- Wells A., *Int J Biochem Cell Biol*,**1999**, 31, 637.
- Whitfield J.B., *Crit. Rev. Clin. Lab. Sci.*, **2001**, 38, 263.
- Wilson K.J., Gilmore J.L., Foley J., Lemmon M.A., Riese II D.J., *Pharmacol Ther*, **2009**, 122, 1.

- Woody R.W., Tinoco I., *J. Chem. Phys.*, **1967**, 46, 4927.
- Woody R.W., in *Peptides, Polypeptides, and Proteins*, Blout E.R., Bovey F.A., Goodman M., Lotan N. eds., New York, John Wiley & Sons, **1974**, pp. 338-350.
- Woody R.W., *J. Polym. Sci., Part D: Macromol. Rev.*, **1997**, 12, 181.
- Xu K., Strauch M.A., *J. Bacteriol*., **1996**, 178, 4319.
- Yamamoto Y., Nagasaki Y., Kato Y., Sugiyama Y., Kataoka K., *J Control Release*., **2001**, 77, 27–38.
- Yamazaki T., Zaal K., Hailey D., Presley J., Lippincott-Schwartz J., Samelson L.E., *J Cell Sci*., **2002**, 115, 1791.
- Yarden Y., Kelman Z., *Curr. Opin. Struct. Biol.*, **1991**, 1, 582.
- Yarden Y., *European Journal of Cancer*, **2001a**, 37, S3.
- Yarden Y., Sliwkowski M.X., *Nat Rev Mol Cell Biol*, **2001b**, 2, 127.
- Yasugi K., Nagasaki Y., Kato M., Kataoka K., *J. Control. Release*, **1999**, 62, 89.
- Yoo H.S., Oh J.E., Lee K.H., Park T.G., *Pharm. Res.*, **1999**, 16, 1114.
- Zanuy D., Alemán C., Muñoz-Guerra S., *Int. J. Biol. Macromol.*, **1998**, 23, 175.
- Zanuy D., Alemán C., *Biomacromolecules*, **2001,** 2, 651.
- Zeng F., Lee H., Allen C., *Bioconjugate Chem.*, **2006**, 17, 399.
- Zhang H., Forman H.J., Choi J., *Methods Enzymol*., **2005**, 401, 468.
- Zhang L., Chan J.M., Gu F.X., et al., *ACS Nano*, **2008**, 2, 1696.
- Zhang L., Zhang L., *Nano Life*, **2010**, 1, 163.